Presynaptic mechanisms determining the dynamic range of neurotransmitter release in the Lateral Amygdala

Inauguraldissertation

Zur Erlangung der Würde eines Doktors der Philosophie

Vorgelegt der

Philosophisch-Naturwissenschaftlichen Fakultät

Der Universität Basel

Von

Elodie Fourcaudot

Aus Livry-Gargan, Frankreich

UNIVERSITE LOUIS PASTEUR DE STRASBOURG I

Ecole Doctorale des Sciences de la Vie et de la Santé

THESE

Discipline : Sciences du vivant

Spécialité : Aspects moléculaires et cellulaires de la biologie

Présentée par

Elodie Fourcaudot

en vue d'obtenir le grade de Docteur des Universités
Louis Pasteur de Strasbourg et Basel Universität, Suisse

Presynaptic mechanisms determining the dynamic range of neurotransmitter release in the Lateral Amygdala

Soutenue publiquement le 19 Décembre 2007 devant le jury composé de :

Rapporteur interne :
Mr le Pr. Rémy Schlichter*, Professeur de l'Université Louis Pasteur de Strasbourg*

Rapporteurs externes :
Mr le Pr Kaspar Vogt, *Professeur de Basel Universität, Suisse*
Mr le Dr. Jean-Christophe Poncer*, Chargé de recherche INSERM, HDR*

Directeurs de thèse :
Mr le Dr. Bernard Poulain*, Directeur de Recherche CNRS, HDR*
Mr le Pr. Andreas Lüthi*, Professeur de Basel Universität, Suisse*

Genehmigt von der Philosophisch-Naturwissenschaftlichen Fakultät

Auf Antrag von

Prof. Dr. Andreas Lüthi, Prof. Dr. Kaspar Vogt

Basel, den 11.12.2007

Dekan

Prof. Dr. Hans-Peter Hauri

THESIS ACKNOWLEDGEMENT

This thesis would not have been possible without the help and support of many people.

First of all I would like to express my gratitude to my two supervisors, Bernard Poulain (Strasbourg) and Andreas Lüthi (Basel). Both were always present whenever I needed some help, a piece of advice or simply to discuss about science.

I gratefully acknowledge Yann Humeau for his advice and supervision in a daily manner. He triggered the development of a collaboration between the two labs, and he helped me a lot with the development of my project. When Yann went back to Strasbourg, we kept on discussing very regularly on the technical aspect of my experiments as well as more general ideas.

Guillaume Casassus was also a great help for daily discussion about my results, science in general, rugby… His support and friendship were extremely precious some days.

I am very grateful to Bernard Poulain, Yann Humeau, Frederic Doussau and all the members of my examination jury for their assistance on editing my thesis writing.

In general, I would like to thanks all the members of the two labs for all the discussions and the great atmosphere that reigned in the two labs. In particular, I will not forget the raclettes, the barbecues and the bowling parties in Basel and in Bischwiller.

More specifically, I would like to thank Renaud Thiebaut, my climbing teacher, with which I spent so many evenings and travels, Emeline Umbrecht-Jenck, my “writing partner” who was always present whenever I needed to talk (and I talk a lot!), Frédéric Gambino, Lynda Demmou and Philippe Gastrein, you all three arrived quite recently but I enjoy a lot the time spent in your company.

Finally, I owe special gratitude to my boyfriend Yannik and to my parents for the constant support, understanding and love that I received from them during the past years.

ABBREVIATIONS

AC: adenylyl cyclase

AKAP: A kinase anchoring protein

AMPA: α-Amino-3-hydroxy-5-Methyl-4-isoxazolepropionique acid

AMPAR: AMPA receptor

aPKC: atypical protein kinase C

BA: basal nucleus of the amygdala

BLA: basolateral complex of the amygdala

CA1: zone if the hippocampus

CA3: zone of the hippocampus

CaMKII: calcium/calmodulin-dependent protein kinase II

cAMP: cyclic AMP

CaN: calcineurin

CAZ: cytomatrix at the active zone

CE: central nuclei of the amygdala

CG: central grey

CNS: central nervous system

cPKC: conventional protein kinase C

CS: conditioned stimulus

DAG: diacylglycerol

DHPs: dihydropyridines

Doc2 : double C2-domain protein

DSI: Depolarization-induced suppression of inhibition

EAAT: excitatory amino acid transporters

E-LTP: early LTP

EPSC: excitatory post-synaptic current

EPSP: excitatory post-synaptic potential

HVA: high voltage-activated channels

iGluR: inotropic glutamate receptor

ITC: intercalated cells of the amygdala

KO: knockout

LA: lateral nucleus of the amydala

LH: lateral hypothalamus

L-LTP: late LTP

LVA: low voltage-activated channels

MAPK: mitogen-activated protein kinase

mEPSC: miniature EPSC

mfLTP: Mossy fiber LTP

mGluR: metabotropic glutamate receptor

n and N: number of release sites

NBQX: 2,3-dihydroxy-6-nitro-7-sulphamoyl-benzo(f)quinoxaline, AMPAR antagonist

NMDA: N-methyl-D-aspartatic acid

NMDAR: NMDA receptor

NO: nitric oxide

nPKC: novel protein kinase C

NT: neurotransmitter

p and P: probability of release

PDE: phosphodiesterases

PKA: protein kinase A

PKC: protein kinase C

PPF: paired-pulse facilitation

PSD: postsynaptic density

PTP: post-tetanic potentiation

PVN: paraventricular hypothalamus

q and Q: quantum

RIM: Rab3 Interacting Molecule

RIM-BP: RIM binding proteins

RRP: readily-releasable pool

SH3: Src homology 3 domain

STD: Short-Term Depression

STDP: Spike-Timing Dependent Plasticity

STP: Short-Term-Potentiation

SV: synaptic vesicle

synprint: synaptic protein interaction site, on the intracellular loop L_{II-III} of VDCCs

TBOA: D,L-threo-β-benzyloxyaspartate, glutamate uptake blocker

US: unconditioned stimulus

VDCC: voltage-dependent calcium channel

TABLE OF CONTENTS

PREAMBLE

In the amygdala, and more generally in the central nervous system (CNS), the excitatory and the inhibitory networks are intertwined and control each other. At the synapses between cortical and thalamic afferents and the principal neurons of the lateral amygdala, which are the synapses I am interested in, the excitatory neurotransmitter is glutamate. For that reason I will focus this manuscript on excitatory glutamatergic neurotransmission.

The manuscript opens with a general introduction, containing a description of the amygdala and long-term plasticity. The following sections concern the results I obtained during my thesis on synaptic plasticity at the cortico-amygdala presynapse. For each chapter I wrote a small introduction to the concept(s) studied, the experimental results and the conclusions derived. A general discussion concludes the manuscript.

To avoid many digressions in the general introduction, I provided insights on glutamatergic synapse and synaptic vesicle cycle in two sections placed at the end of the manuscript (see appendixes A and B). A third appendix covers two papers I contributed to at the beginning of my PhD studies. The first one concerns another form of Hebbian plasticity described in the lateral amygdala, at the cortico-lateral amygdala synapse as well. The long-term potentiation (LTP) described is induced postsynaptically: The second paper is a study of synaptic organization in cerebellar organotypic slices cultures.

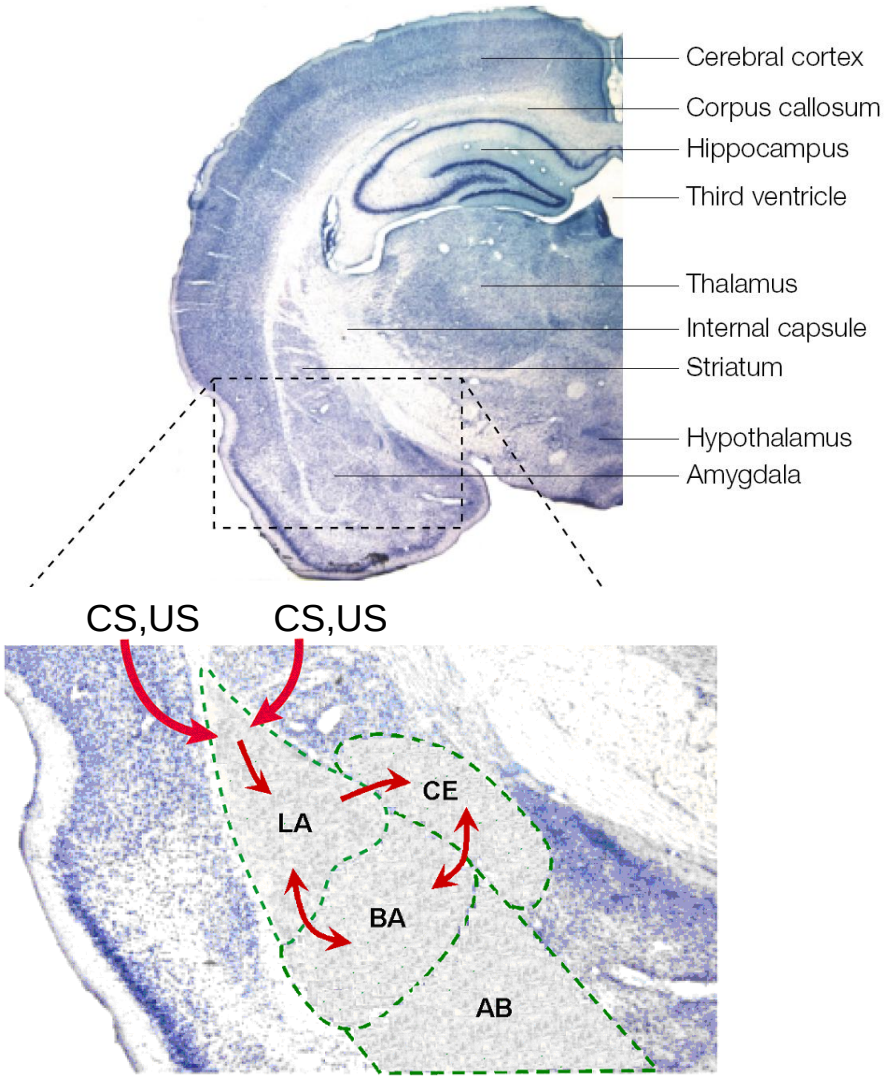

Figure 1: Amygdala structure and connectivity. A, An example of the amygdala region (Nissl staining) **B,** The area of the amygdala is enlarged to show the four main subdivisions of the amygdala: LA (lateral nucleus), BA (basal nucleus), CE (central nucleus) and AB (accessory basal nucleus). The CS (conditioned stimulus) and US (unconditioned stimulus) converge on single cells in the LA. From LA stimuli signal conveyed to CE and BA. Reciprocal connections connect BA with LA, and BA with CE. (Adapted from (Medina et al., 2002))

I) GENERAL INTRODUCTION

A) The amygdala

1) Discovery of the amygdala's role in emotional processes

In 1937, James Papez discovered that several structures from the medial part of the brain were interconnected, and proposed that this circuit, also-termed "Papez circuit" is the anatomical site where emotions are processed (Papez, 1937). The amygdala was not included in this first circuit. At the same time, Klüver and Bucy described a phenomenon called "psychic blindeness" or Klüver-Bucy syndrome. After bilateral temporal lobectomy, monkeys are dulled, less fearful and unable to recognize familiar objets (Klüver and Bucy, 1937). Weiskrantz was the first to show that bilateral lesions of the amygdala is sufficient to induce the Klüver–Bucy syndrome (Weiskrantz, 1956). The removal of the amygdala also permanently disrupt the social behavior of monkeys, usually resulting in a fall in social standing (Rosvold and Delgado, 1956) whereas its electrical stimulation induces fearful reactions (Delgado et al., 1956). This line of research established the significant role of the amygdala in memory formation.

2) Structure

The amygdala receives sensory information from very diverse regions of the central nervous system. In particular, it is highly connected to structures related with memory systems, such as the hippocampus or the medial temporal lobe, and it receives inputs from structures which relay sensory informations, such as thalamus and sensory cortex.

a) Position in the central nervous system

The amygdala is a central brain structure, located deeply within the medial temporal lobe, medial to the hypothalamus and ventral to the hippocampus (Figure 1). It is a non-layered structure, containing around 13 nuclei. These are further subdivided in subnuclei, which are distinguished on the basis of cytoarchitecture, histochemistry, and the connections they make (Krettek and Price, 1978; Pitkänen, 2000).

b) Internal structure

Amygdala nuclei are divided into three groups (Figure 1):

- the deep or basolateral complex (BLA), which is constituted of the lateral nucleus (LA), the basal nucleus (BA), and the accessory basal nucleus (AB)
- the superficial or cortical-like group, which is the closest from the surface of the brain. It includes for example the cortical nuclei and the nucleus of the lateral olfactory tract
- the centromedial group composed of the medial and central nuclei (CE).

Finally, there is a separate set of nuclei that cannot easily be classified as belonging to any of these three groups and are listed separately. These include the intercalated cell masses and the amygdalohippocampal area. (Sah et al., 2003).

c) Excitatory and inhibitory networks

Several ways to classify neurons coexist and are overlapping. The three main criteria are the morphology, the electrophysiological properties and immunocytochemical content of the neurons.

The morphology can be determined by Golgi-staining. Two main morphological types of neurons were described in the basolateral amygdala: spiny neurons, which possess dendrites covered by numerous spines (pyramidal neurons or class I); and small aspiny neurons (class II) (McDonald, 1982). Further detailed analysis revealed the existence of other aspiny neurons in the basolateral amygdala such as extended neurons, cone cells, chandelier cells and neurogliaform cells (for review, Sah et al., 2003).

On the basis of their electrophysiological properties, two classes of neurons were initially described: pyramidal-like cells with broad action potentials which fire trains of action potentials showing spike frequency adaptation in response to a prolonged current injection (Faber et al., 2001); and a second cell type with faster action potentials and almost no spike frequency adaptation (Mahanty and Sah, 1998). This last category is thought to represent local GABAergic interneurons (McDonald and Augustine, 1993; Pare and Smith, 1993). However, neurons with intermediate features were also described in the amygdala (Lopez de Armentia and Sah, 2004; Martina et al., 1999; Rainnie et al., 1993; Schiess et al., 1993; Washburn and Moises, 1992).

A third way to classify neurons is based on their immunocytochemical content of calcium-binding proteins (such as parvalbumin or calbindin) and neuropeptides (such as somatostatin or cholecystokinin) (Mascagni and McDonald, 2003; McDonald and Mascagni, 2001; McDonald and Pearson, 1989). Recently, another classification method has been used in the amygdala, based on the method of cluster analysis, discriminating cell populations

through the compilation of electrophysiological and molecular parameters (Sosulina et al., 2006).

From those different studies, it appears that projection neurons (class I neurons) represent the largest population of neurons in the amygdala, from 75 to 93% (Mahanty and Sah, 1998; McDonald and Augustine, 1993). They are large spiny cells, with low firing rates, frequency adaptation and expression of the vesicular glutamate transporter (VGLUT1). Their dendrites cover a large part of the lateral amygdala. Two classes were distinguished on the basis of electrotonic properties and the presence (IB) or absence (IA) of vasointestinal peptide (VIP).

Four classes of glutamate decarboxylase (GAD67) containing interneurons were also described. They displayed smaller somata and spine-sparse dendrites. Class III neurons reflected "classical" interneurons, generating fast spikes with no frequency adaptation. Class II neurons generated fast spikes with early frequency adaptation and differed from class III neurons by the presence of VIP and the relatively rare presence of neuropeptide Y (NPY) and somatostatin (SOM). Class IV and V were not clearly separated by molecular markers, but by membrane potential values and spike patterns (Sosulina et al., 2006).

3) Connectivity

a) Connections of the amygdala to other brain regions

The BLA receives connections from cortical and thalamic areas. Cortical inputs provide information about highly processed visual, somatic sensory, visceral sensory, and auditory stimuli. Thalamic areas receive afferents from the spino-thalamic tract. Thus, the LA is the integration site for auditory and somatosensory inputs. This is confirmed by the fact that coupling auditory and nociceptive stimuli enhances the auditory evoked responses recorded *in vivo* in the LA (Quirk et al., 1997; Rogan et al., 1997; Rosenkranz and Grace, 2002).

The medial part of the LA is innervated by axons coming from structures related with memory systems, including the prefrontal and perirhinal cortical areas, and the hippocampal formation. The CE receives relatively unprocessed visceral sensory inputs directly from some thalamic nuclei, the olfactory bulb, and the nucleus of the solitary tract in the brainstem. CE neurons project to central grey (CG), lateral hypothalamus (LH) and paraventricular hypothalamus (PVN) (for review, Medina et al., 2002; Pitkänen et al., 1997; Purves et al., 2001). Thus, at a very rough level of analysis, we can say that the amygdala links cortical regions which process sensory information with hypothalamic and brainstem effector systems.

b) Connections within the amygdala

Projections from various brain areas to the amygdala terminate in different amygdala subnuclei. For example, projections from the entorhinal cortex terminate most heavily in the basal nucleus, but also sparsely in the central and lateral nuclei, and projections from the hypothalamus terminate in the central, medial, basal and accessory basal nuclei (for review, Pitkänen et al., 1997) Thus, intra-amygdala processing through internucleus connections is necessary to integrate the information. Tract tracing studies have revealed that amygdala nuclei have extensive intranuclear and internuclear connectivity (Krettek and Price, 1978; Pitkänen, 2000).

Intra-amygdala axons originate mostly in the LA and project to the CE both directly and through the BA. The BA also sends direct projections to other amygdala nuclei such as the CE, which is the major output nucleus for amygdala axons projecting to the brainstem and hypothalamus. Interestingly, inputs from the different subnuclei are spatially segregated in the CE. However, intra-amygdala connections are not always descending (from LA to BA and CE), internuclei connections are often reciprocal. It allows thus a negative feed-back loop from downstream amygdala nuclei which could control LA inputs. As explained by Pitkänen (Pitkänen et al., 1997), "an alternative hypothesis is that reciprocal connections might be the way through which extra-amygdala regions providing afferents to these areas can influence the early stages of amygdala processing of sensory information at the level of the lateral nucleus, i.e. they might set the 'strength of the filter' within the lateral nucleus."

c) Lateral amygdala connections

The excitatory projections to the LA are spatially segregated: cortical and thalamic axons constitute respectively the external and internal capsules. Each LA principal neuron receive monosynaptic cortical and thalamic contacts. With the help of two-photon imaging, based on the detection of calcium flow through NMDAR, Yann Humeau from the lab demonstrated that cortical and thalamic spines are present on dendrites at the same average distance from the soma. They can even be found on the same dendritic portions, sometimes spaced by less than 5µm (Humeau et al., 2005).

Electron-microscopical studies have shown that the axons coming from LA principal neurons form numerous contacts with dendritic spines belonging to other LA principal neurons (Smith and Pare, 1994). Unfortunately, the demonstration that these putative contacts are functional is very difficult because the connectivity rate for randomly chosen pairs of neurons is very low (Nicola Kamp, Guillaume Casassus and Philippe Gastrein personal

communications). This apparent low connectivity suggests a selective organization of the intra-amygdala connections, which is still to be determined.

4) Role of the amygdala in emotional memory

a) Classical fear conditioning as a simple Pavlovian learning paradigm

Fear conditioning is a simple Pavlovian learning process in which a neutral stimulus (called conditioned stimulus or CS), such as a tone or a light, is coupled with an aversive stimulus (the unconditioned stimulus or US), typically a footshock. After several CS-US pairings, the CS itself becomes aversive and the animal expresses a high fear level in the presence of the CS alone. The conditioned fear response which is measured is usually a freezing reaction (a cessation of movement), it is also associated with sweating and changes in heart rate and blood pressure. This learned behavior is rapidly acquired and long lasting.

b) Description of the neuronal circuit of fear learning

A large body of evidence from lesion, pharmacological and neurophysiological studies placed the amygdala at the center of fear conditioning (Davis, 1997; Fendt and Fanselow, 1999; Lavond et al., 1993; LeDoux, 1996). It is generally accepted that sensory information enters the amygdala through its basal and lateral nuclei (BLA) (Aggleton, 2000; LeDoux, 1996; but for an alternative view see Pare et al., 2004) where CS–US association (or fear memory trace) formation is believed to take place. These nuclei are interconnected with the central nucleus (CeA), which is thought to be the main amygdala output structure sending projections to various regions involved in fear responses. (for review, Kim and Jung, 2006; LeDoux, 2000; Maren and Quirk, 2004).

5) From fear learning to long-term potentiation

a) *In vivo* long-term potentiation

The idea that long-term potentiation (LTP) of synaptic strength is the brain mechanism supporting memory formation and maintenance exists since several decades. The first notion came from the publication in 1949 by Donald Hebb of his postulate indicating that the coincident and repetitive activation of two connected neurons will give rise to the reinforcement on a long-term basis of their synaptic contact. During the following years, the *in vivo* study of memory formation and the *in vitro* study of this new phenomenon called LTP

were done in parallel. Evidence implicating LTP in the amygdala in the acquisition of Pavlovian learning was described, as well as insights into the underlying molecular mechanism (for review, Maren, 1999). For example, infusion of NMDAR antagonists in the BLA, which blocks some forms of synaptic potentiation, also prevented fear memory formation.

Another way to link LTP to fear memory formation was to perform *ex vivo* experiments, consisting of *in vivo* conditionings preceding the sacrifice of the animals and the *in vitro* study of neuronal properties. The authors could then compare those parameters with datas obtained during classical LTP experiments (McKernan and Shinnick-Gallagher, 1997; Rogan et al., 1997). Recently, Whitlock et al succeeded to draw a clear link between LTP and memory formation by inducing LTP *in vivo*, through stimulating electrodes implanted directly in the hippocampus. Another supporting piece of evidence is that *in vivo* LTP was occluded by a previous behavioral training (Pastalkova et al., 2006; Whitlock et al., 2006).

b) NMDAR and fear learning

NMDA receptors (NMDARs) are known to be necessary for LTP formation in the CA1 region of the hippocampus *in vitro* (for review, Bliss and Collingridge, 1993; Malenka and Nicoll, 1999). NMDAR are described since the middle of the 80's to be necessary as well for *in vivo* memory formation in the hippocampus: Morris et al were the first to demonstrate that the intra-ventricular infusion of D-APV, a blocker of NMDAR, impaired the subsequent hippocampus-dependent spatial learning, in the Morris water maze. Behavioral experiments testing the importance of NMDAR in hippocampal-related learning were extensively done (for review, Martin et al., 2000; Riedel et al., 2003).

However, one disadvantage of spatial learning paradigms is the fact that stimulus control is difficult to achieve. It is not yet clear which clues actually guide the behavior and it is therefore impossible to switch them on or off at a defined time point. Better stimulus control is possible in fear conditioning. In the middle of the 90's, Miserendino et al directly applied D-APV in the BLA *in vivo*, prior to light-shock pairings. As a result, they observed one week later a complete block of conditioned fear-potentiated startle. However, the same injection done after the training procedure and before the startle testing had no effect, demonstrating first that the effect was due to the block of NMDAR and not to a damage to the amygdala, and second that the expression of the conditioned fear-potentiated startle does not depend on NMDAR activity (Miserendino et al., 1990).

Similarly, NMDARs in the amygdala are involved in second-order fear conditioning. Second-order conditioning is a two-step training protocol involving 2 conditioned stimuli (or

CS): first, CS1 is paired with the unconditioned stimulus. Once this has been achieved, pairings of CS1 with CS2 will generate a transfer of informative state from CS1 to CS2, resulting in the fact that CS2 alone evokes an unconditioned response. Intra-amygdala infusion of APV during CS1/CS2 associations prevented second-order fear conditioning (for review, Riedel et al., 2003; Walker and Davis, 2002). Inhibitory and active avoidance, two conditioning procedures in which the animal learns to avoid a punishment by doing (active avoidance) or abstaining of doing a specific action (inhibitory avoidance) and both depending on the amygdala, are also dependent on NMDAR activity (Roesler et al., 2003; Savonenko et al., 2003).

With respect to auditory fear conditioning, intra-amygdala infusion of APV blocked the acquisition, the expression and the extinction of conditioned fear. These finding confirmed the hypothesis that fear acquisition and extinction are two forms of learning which share at least partially the same mechanism (for review, Rodrigues et al., 2004; Walker and Davis, 2002).

c) GABAR and fear learning

- $GABA_A$ receptors

Principal cells in the LA receive a high inhibitory modulation *in vivo* (Pare et al., 2004) as well as *in vitro* (Loretan et al., 2004). Even though the inhibitory circuit is composed by a small fraction of the overall neuron number, the *in vivo* and *in vitro* stimulation of afferent systems to the amygdala lead to predominance of the inhibitory responses in the recordings of synaptic activities (Bissiere et al., 2003; Lang and Pare, 1997). The strength of the inhibitory circuit is thus susceptible to prevent the induction of associative plasticity, as described by Hebb's rules, in the amygdala. Thus a possibility arises that endogenous modulations of the inhibitory system are triggered by the fear learning. Several lines of evidences argue in favor of such a possibility: the fear reaction of the animal is correlated with the $GABA_A$ receptor expression level in the amygdala (Caldji et al., 2004), and more specifically their decrease in the LA (Chhatwal et al., 2005). These changes cannot precisely control the induction level for associative plasticity in the amygdala, and are completed by the activation of numerous neuromodulators, which could potentially be fast modulators of the GABA system:

- *dopamine*: behavioral and *in vitro* experiments demonstrated that dopaminergic fibers are activated in conditions similar to those leading to fear conditioning: dopamine is released in the amygdala during stress episodes (Inglis and Moghaddam, 1999), and a pharmacological blockade of dopaminergic receptors also blocks the acquisition of fear

conditioning (Guarraci et al., 2000; Guarraci et al., 1999). *In vitro*, dopamine binding to D2 receptors reduces the induction of associative plasticity by suppressing the feedforward inhibition (Bissiere et al., 2003).

- *opiates*: opiate receptors have multiple functions in the CNS, in the amygdala they are known to regulate stress, anxiety and nociception (Vaccarino et al., 1999). They are involved as well in the modulation of fear level (Good and Westbrook, 1995) and in the consolidation of aversive fear, probably by controlling the noradrenergic, cholinergic and GABAergic systems (McGaugh, 1989). *In vitro*, the application of the selective agonist of μ receptors DAMGO specifically decreases GABA release (Sugita and North, 1993).

- *norepinephrine*: similarly to dopamine, norepinephrine suppresses GABAergic inhibition onto principal neurons and the subsequent decrease of the network activity allows LTP induction in the absence of $GABA_A$ receptor blockers (Tully et al., 2007).

- *endocannabinoids*: depolarization-induced suppression of inhibition (DSI) is a very efficient way to quickly suppress GABA release. This retrograde control is triggered by postsynaptic depolarization which triggers dendritic release of endocannabinoids. The endocannabinoids diffuse in the synaptic cleft and activate presynaptic CB1 receptors, which decrease the probability of release of GABA vesicles (Wilson and Nicoll, 2001; for review, Diana and Marty, 2004; Lovinger, 2007). Such a depolarization of the principal neurons was recorded *in vivo* during fear conditioning experiments (Rosenkranz and Grace, 2003), and CB1 receptors are highly dense in the BLA (Katona et al., 2001), which is in favor of endocannabinoid modulation. Moreover, perturbing the endocannabinoid system decreases the extinction of fear conditioning and acquisition of associative plasticity in the amygdala (Azad et al., 2004; Marsicano et al., 2002).

- *$GABA_B$ receptors*

$GABA_B$ receptors are also present in the amygdala (Bischoff et al., 1999; McDonald et al., 2004) and can be activated by excitatory fiber stimulation *in vivo* (Lang and Pare, 1997; Sugita et al., 1992) and *in vitro* (personal observation). They are present and functionally important at the presynaptic level as well as at the postsynaptic side: Indeed tetanic stimulation (1.5s, 30Hz) of cortical fibers does not trigger long-term potentiation (LTP) in control conditions. However, using the same stimulation in presence of $GABA_B$ antagonists can induce a presynaptic form of homosynaptic LTP (Shaban et al., 2006). This experiment shows that $GABA_B$ receptors are essential in order to prevent the induction of homosynaptic LTP at cortical synapses. This mechanism seems to be crucial for amygdala function: mice lacking the $GABA_{B(1A)}$ subunit, a mouse model in which the induction of homosynaptic LTP was possible *in vitro*, also displayed no ability to discriminate between the tone paired with

the US (CS+) and a non-paired tone (CS-) and expressed a fear reaction in the presence of the two tones. Hence, it seems that $GABA_B$ receptors helps to prevent the generalization of fear conditioning (Shaban et al., 2006).

B) Long-term plasticity

The efficacy of synaptic transmission can be changed, sometimes over long periods of time. This notion is termed 'synaptic plasticity'. As early as in 1973, the concept that linked the LTP phenomenon to learning processes was set (Bliss and Lomo, 1973). The study of synaptic plasticity became an important issue.

The concept of LTP can cover very different kinds of potentiation, depending whether experiments are performed *in vivo* or *in vitro*: an experiment is considered to be long-lasting if the potentiation last for more than 30 minutes for patch-clamp recording *in vitro*, and for several days *in vivo*. Even more, *in vitro* LTP induction can give rise to different forms of LTP, initially called early LTP (or E-LTP) and late LTP (or L-LTP), and now separated in three different mechanisms: LTP1, the equivalent to E-LTP, a rapidly decaying protein synthesis-independent mechanism; LTP2, an intermediate phase of L-LTP that requires protein synthesis but is independent of gene transcription; and LTP3, which represents the durable, translation- and transcription-dependent component of L-LTP (Abraham and Otani, 1991). In this manuscript, I will exclusively talk about *in vitro* recordings of LTP1.

1) Associative plasticity and spike-timing dependent plasticity

Long-term potentiation (LTP) and depression (LTD) can involve different mechanisms, depending on the CNS area, the cell type, the developmental stage and the induction protocol used (for review, Bliss et al., 2003; Lynch, 2004; Malenka and Bear, 2004).

Donald Hebb postulated that memories are formed in the brain by synaptic modification that strengthens connections between two neurons when presynaptic activity correlates with postsynaptic firing (Hebb, 1949). However, 'Hebbian' modification alone would not be sufficient, there must also exist a synaptic basis leading to the weakening of synaptic connections, otherwise brain circuits should reach at one point their maximal activity and should not be able to undergo any further potentiation. In agreement with this model, Stent proposed the idea that the strength of synaptic connections can weaken when

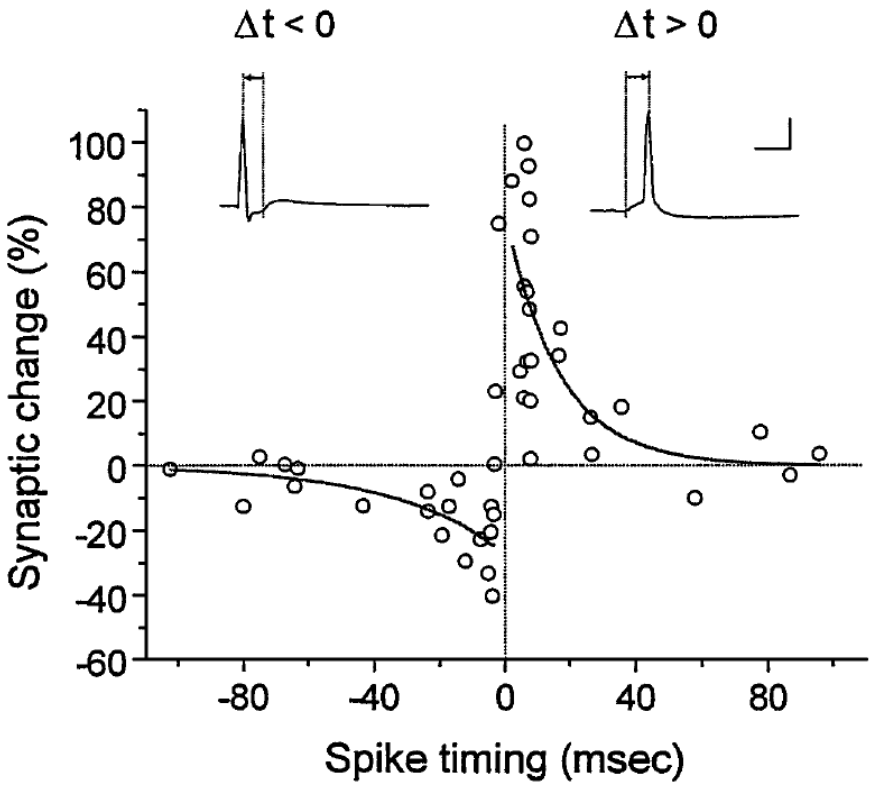

Figure 2: Critical window for synaptic modifications. Long-term potentiation (LTP) or Long-term depression (LTD) were induced by correlated pre-and postsynaptic spiking at synapses between hippocampal glutamatergic neurons in culture. The percentage change in the excitatory postsynaptic current (EPSC) amplitude at 20-30 min after repetitive correlated spiking (pulses at 1 Hz) was plotted against spike timing, which is defined as the time interval (Δt) between the onset of the EPSP and the peak of the postsynaptic action potential during each pair of correlated spikingm as illustrated by the traces above. Scales 50mV and 10ms. (adapted from (Bi and Poo, 1998)

presynaptic terminals are inactive at the same time that the postynaptic neuron is active (Stent, 1973). According to this way of thinking, postsynaptic activity, driven by a set of well-correlated inputs, initiates the physiological processes that lead to the potentiation of the active synapses and the depression of the inactive ones, giving rise to the concept of LTD.

In 1983, Levy & Steward studied in more detail the temporal specificity in associative synaptic modifications. Stimulating a weak and a strong input from the entorhinal cortex to the dentate gyrus of hippocampus, led to LTP of the weak input. This associative induction is heterosynaptic, because it requests the activation of a second group of synapses in order to potentiate the response at the first input. Moreover, they discovered that associative induction of LTP does not require perfectly synchronous co-activation of the two pathways, but the temporal order of their activity is crucial. Indeed LTP of the weak input could be induced when the strong input was following the activation of the weak input by 0 to as much as 20 ms (Levy and Steward, 1983). When the temporal order was reversed, LTD was induced instead of LTP. This, and other early studies (Gustafsson and Wigstrom, 1986; Kelso and Brown, 1986), revealed the existence of a temporal specificity in activity-induced synaptic modification.

LTP can also be induced in the hippocampus and in different cortical areas by coupling low-frequency stimulation with postsynaptic depolarization, as hypothesized by Hebb (Kelso et al., 1986; Malenka and Nicoll, 1999; Sastry et al., 1986; Wigstrom et al., 1986). This form of LTP is also called homosynaptic, because the potentiated synapses are the ones which receive the induction protocol. One of the possible mechanisms is that the postsynaptic depolarization triggers action potentials which can back-propagate as calcium spikes into the dendrites (Buzsaki et al., 1996; Hoffman et al., 1997; Stuart and Sakmann, 1994). This concept, called Spike-Timing Dependent Plasticity (STDP), lies on the relative timing between the arrival of back-propagating spikes and the onset of the EPSPs at a postsynaptic spine is the key element to trigger LTP or LTD at the studied synapse (Markram et al., 1997) (Figure 2). A critical window for plasticity has been described in cell culture (Bi and Poo, 1998), LTP and LTD can be induced if the EPSP occurs at maximum 40ms before or after the postsynaptic spike trigger, respectively.

Presynaptic induction of LTP is also described, but more rarely. Until recently, it was thought to be a pure non-hebbian mechanism (i.e. non associative). However, Humeau et al (Humeau et al., 2003) discovered a presynaptic form of LTP that is heterosynaptic and associative. I will provide further details about it in section B4 from the chapter I.

2) Mechanisms underlying long-term depression

Low frequency stimulation of glutamatergic fibers during several minutes generally give rise to LTD in the CNS. The induction mechanism implicates mGluR and NMDAR activation. Most of the time, the requirement for NMDA and mGluR activation is mutually exclusive (for review, Kemp and Bashir, 2001).

- mGluRs: they have different roles in LTD induction depending on the brain area studied. At some synapses, as for example in the cerebellum at the parallel fiber to Purkinje cell synapse, mGluRs are activated postsynaptically. This leads to the activation of PKC, a central element for LTD induction at this synapse, release of calcium from intracellular stores and activation of NO intracellular pathway (for review, Anwyl, 1999). Presynaptic mGluRs can also trigger LTD. At mossy fiber to CA3 principal cell synapse in the hippocampus, their activation decreases cyclic AMP (cAMP) production and protein kinase A (PKA) activity (Tzounopoulos et al., 1998). An increase in calcium concentration is also required and activates CAMKII (Kobayashi et al., 1999). Various other mechanisms coupling activation of mGluRs to intracellular effectors exist, as for example the recruitment of phospholipase or other kinases (Kahn et al., 2001; Otani et al., 1999; Otani et al., 2002).

- NMDAR: NMDAR-dependent induction of LTD was the first form of LTD studied. Since its initial description at the Schaffer collateral to CA1 principal neuron synapse in the hippocampus (Dudek and Bear, 1993; Fujii et al., 1991; Mulkey et al., 1994), postsynaptic NMDAR-induced LTD has been demonstrated in several other brain areas (for review, Kemp and Bashir, 2001). NMDAR opening gives rise to a massive and quick calcium influx and triggers LTP induction. It is interesting to note that LTP induction involves a calcium influx as well, which is of smaller amplitude but over a much longer periode of time (Yang et al., 1999). Calcium-dependent phosphatase are then activated, which in turn allows the dis-inhibition of the phosphatase PP1 (Mulkey et al., 1994).

In several brain structures such as in basal ganglia, in the hippocampus or in the amygdala, LTD is also mediated by endocanabinoids (Gerdeman and Lovinger, 2003). Moreover, presynaptic NMDAR seem to be involved in an endocannabinoid-dependent LTD in layer 5 (Sjostrom et al., 2003). As endocannabinoid release is induced by postsynaptic activity, the convergence of NMDAR and endocannabinoid signals at the presynaptic terminal could be an efficient detector for synchronized pre- and postsynaptic activity, thus leading to LTD expression.

The postsynaptic expression mechanisms of LTD involve regulations of AMPARs, either through dephosphorylations (Kameyama et al., 1998; Lee et al., 1998), endocytosis of

AMPAR (Man et al., 2000; Wang and Linden, 2000) or the expression of different AMPAR subtypes (Mameli et al., 2007). Presynaptic expression mechanisms of LTD are yet to be elucidated. In accumbens nucleus, presynaptic mGluRs seem to decrease glutamate release through an inhibition of VDCCs (Robbe et al., 2002).

3) Mechanisms of long-term potentiation

The notion of LTP exists since more that 30 years: it was first described at the end of the 60's (Bliss and Lomo, 1970; Lomo, 1966) and was confirmed by two papers few years after (Bliss and Gardner-Medwin, 1973; Bliss and Lomo, 1973).

In order to celebrate the anniversary of this discover, a full issue of the Philosophical transactions of the Royal Society was dedicated to LTP (Morris, 2003).

a) Postsynaptic mechanisms

Most of the LTP studies concern postsynaptic LTP. It is induced by repetitive presynaptic stimulations at high frequency, pairing of two inputs, or pairing presynaptic stimulation with postsynaptic firing but with a very precise time window (see SDTP).

The induction mechanism which is very often described involves the activation of postsynaptic NMDAR. This is the case, for example, at the synapse between by Schaffer collaterals and CA1 pyramidal neurons of the hippocampus. NMDAR activation leads to calcium influx, which in turn activates several kinases. The most important one is the calcium/calmodulin-dependent protein kinase II (CaMKII) (for review, Malenka and Nicoll, 1999). Once activated, CAMKII phosphorylates the AMPA receptor subunit GluR1 (Benke et al., 1998) and/or leads to an increase in the number of postsynaptic AMPARs (Shi et al., 1999). To a less extent, postsynaptic protein kinase C (PKC), A (PKA) or mitogen-activated protein kinase (MAPK) are also involved (for review, Malenka and Bear, 2004; Malenka and Nicoll, 1999).

b) Presynaptic mechanisms

Presynaptic induction of LTP also occurs in several brain areas. Mossy fiber LTP has been coined from the reference synapse, which is the synapse formed by mossy fibers to principal neurons in the CA3 area of the hippocampus. Mossy fiber LTP (mfLTP) was initially described by Higashima and Yamamoto (Higashima and Yamamoto, 1985). It is independent of NMDAR activation (Harris and Cotman, 1986; Nicoll and Malenka, 1995; Zalutsky and Nicoll, 1990) and its induction threshold is thought to be modulated by

presynaptic kainate GluR5 receptors (for review, Bortolotto et al., 2003, but see Castillo et al., 1994).

In addition, it was shown that mfLTP requires the presence of calcium, not in the postsynaptic cell but presynaptically (Castillo et al., 1994; Zalutsky and Nicoll, 1990). Moreover, changes in postsynaptic membrane potential were also demonstrated playing no role in mfLTP. In the mean time, a competiting group claimed that a postsynaptic calcium rise is necessary to get mfLTP (Jaffe and Johnston, 1990; Johnston et al., 1992; Yeckel et al., 1999). The main reason for those differences was that concentration of postsynaptic BAPTA used by Johnston group was much higher than what is classically used in order to block a postsynaptic signal, therefore BAPTA could have an side effect which was not related to the block of a putative postsynaptic calcium entry in the spines. The initial postulate of a purely presynaptic LTP was confirmed over years by other groups for example (Katsuki et al., 1991; Langdon et al., 1995; Mellor and Nicoll, 2001).

Calcium entry in the presynapse induces the activation of calcium-dependent adenylyl cyclase and a downstream recruitment of PKA (Nicoll and Malenka, 1995). The consequence of this is a large increase in the probability of release *P* proposed to be the expression mechanism for mfLTP (Weisskopf and Nicoll, 1995). Additionally, mfLTP can also involve an increase in the number of active release sites *N*, meaning it can activate some presynaptically silent synapses (Reid et al., 2004).

Other forms of presynaptic LTP exist. One is present at the synapse formed in the cerebellum by parallel fibers on Purkinje cells and at cortico-thalamic synapses. Both are independent of NMDAR, and involve presynaptic calcium influx and ensuing PKA activation (Castro-Alamancos and Calcagnotto, 1999; Linden and Ahn, 1999; Salin et al., 1996).

In order to understand induction mechanism of presynaptic LTP, one had to understand what protein is phosphorylated by PKA, leading to the enhancement of *P* and/or *N* at the studied synapses. The most studied synaptic proteins that are PKA substrates were the synapsins, however double knockout (KO) mice for synapsin I and II exhibit normal LTP (Spillane et al., 1995). On the reverse, The Rab3A GTPase, which is not phosphorylated by PKA, appears to be essential for presynaptic LTP (Castillo et al., 1997). This apparent paradoxe is resolved by the fact that several binding partners of Rab3A, such as Rabphilin or *RIM1*α, harbour a consensus sequence motif for PKA (Sudhof, 2004). Mice lacking rabphilin exhibit normal mfLTP (Schluter et al., 1999). On the contrary, *RIM1*α-deficient mice lack mfLTP and parallel-fiber-LTP in the cerebellum. This indicates that *RIM1*α is likeky a PKA substrate needed for expression of different forms of presynaptic LTP. The rescue of mfLTP by the transfection of a copy of *RIM1*α is possible provided the gene is not mutated on one of

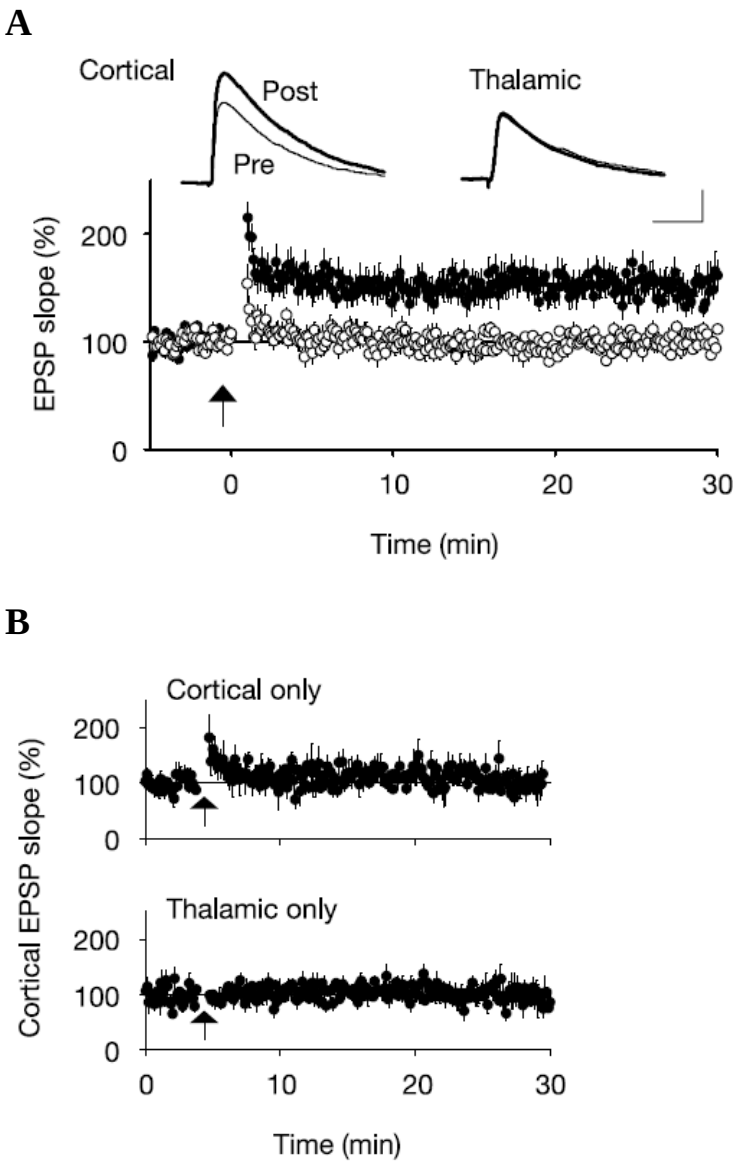

Figure 3: Induction of LTPHA at cortical, but not at thalamic, afferent synapses. A, Time course of synaptic changes after simultaneous Poisson-train stimulation (arrow) of cortical (filled circles) and thalamic (open circles) afferents. Scale bars, 2mV and 50ms. **B,** Time course of synaptic changes occurring at cortical afferent synapses upon Poisson-train stimulation (arrow) of either cortical or thalamic afferents alone. (Humeau et al., 2003)

the two consensus sequences for PKA in *RIM1α* (Castillo et al., 2002; Lonart et al., 2003). The lack of LTP in Rab3A-deficient mice could imply that Rab3A is necessary to get *RIM1α* in a ready-to-be-phosphorylated state.

c) LTP integrating presynaptic and postsynaptic mechanisms

LTP is not strictly following a unique rule: LTP can be induced postsynaptically and have a presynaptic expression, either by changing *P* or *N*. In this case, it requires a retrograde messenger, which might consists of NO or endocannabinoids.

In the case of mfLTP, there are some debate on its site of induction (see paragraph above): indeed, recent studies suggest that concerted postsynaptic and presynaptic signaling is required for the induction and expression of mfLTP (Contractor et al., 2002). The authors demonstrate the presence of a retrograde signaling cascade, involving ephrins and their receptors, which links postsynaptic calcium influx with the increase in transmitter release by presynaptic mossy fiber boutons.

4) Presynaptic LTP in the amygdala: heterosynaptic associative LTP

The deciphering of LTP mechanisms in the LA has led to the identification of a new form of presynaptic LTP (Humeau et al., 2003). The authors showed that the simultaneous stimulation of thalamic and cortical afferents by randomly-distributed train stimuli at an average frequency of 30Hz induced LTP at cortical, but not thalamic, afferent synapses. LTP induction required the association of cortical and thalamic stimuli, a train of stimuli at one or the other pathway being not sufficient for inducing LTP (Figure 3). Classical associative LTP is homosynaptic, with its induction involving the coupling of presynaptic and postsynaptic activity. Here, this novel form of LTP was fully presynaptic and associative, thus the authors termed it heterosynaptic associative LTP (abbreviated as LTP_{HA}). This heterosynaptic LTP is reminiscent of heterosynaptic facilitation (Kandel and Tauc, 1964). By applying the glutamate uptake blocker TBOA (D,L-threo-β-benzyloxyaspartate), Humeau et al were able to induce LTP at cortical afferents using a single cortical stimulus train. Thus the induction of homosynaptic LTP by cortical glutamate release was impossible to trigger because of rapid clearance of glutamate by uptake mechanisms, and thalamic costimulation should allow to overflow the glutamate uptake system. They showed that LTP_{HA} is dependent on NMDAR activity but not on postsynaptic calcium influx. This led to two possibilities: either NMDARs were postsynaptic but involved in a calcium-independent way, or alternatively NMDAR were located on presynaptic cortical boutons. Using MK-801 in the patch pipette in order to

selectively block postsynaptic NMDARs, they were able to induce LTP_{HA}. Bath application of BAPTA-AM, a membrane-permeant calcium chelator, prevented LTP_{HA}, indicating that LTP_{HA} was calcium-dependent. They hypothesized that the induction of this associative LTP was dependent on presynaptic NMDARs and presynaptic calcium influx. However the question whether the NMDAR involved were located on presynaptic cortical afferents or on other neurons in the LA remained open. To examine this question, the authors blocked network activity by the application of the AMPAR antagonist NBQX (2,3-dihydroxy-6-nitro-7-sulphamoyl-benzo(f)quinoxaline). Even in the presence of NBQX they were still able to induce LTP_{HA} (by recording NMDAR-mediated EPSCs), meaning that the required NMDAR are not located on other neurons from the network. Hence they confirmed their hypothesis that LTP_{HA} was triggered by the activation of NMDARs on cortical presynaptic boutons.

Several sets of data support the presynaptic nature of LTP_{HA}. Indeed, it is associated with a persistent decrease in paired-pulse facilitation (PPF). Assuming that an increase in neurotransmitter release due to a rise in *P* is correlated with paired-pulse ratio (PPR) changes, the decrease in PPF is an indication of an increase in *P* as an expression mechanism. Analysis of the fluctuations in the postsynaptic response amplitude before and after LTP induction allows to determine the $1/(c.v.)^2$ (where c.v. is the coefficient of variation) plotted against the mean response amplitude. It indicated that LTP_{HA} expression is presynaptic, probably involving an increase in *P* and not in *N*. Lack of changes in the amplitude of the quantal size *Q* was further confirmed by the determination of the unchanged amplitude of miniature EPSCs obtained from the asynchronously released quanta in the presence of strontium ions.

Moreover, postsynaptic manipulations, such as voltage-clamping the postsynaptic neuron at -70 mV or perfusing the postsynaptic neuron with a Ca^{2+} chelator or an NMDA receptor antagonist, all manipulations that are well known to block the induction of postsynaptic, NMDA receptor-dependent forms of LTP, did not interfere with the induction of LTP_{HA} (Humeau et al., 2003). Thus, expression of LTP_{HA} is likely to be mediated by an overall increase in the probability of release *P*.

In conclusion, this study first revealed the existence of a new form of LTP, which is dependent on the activation of presynaptic NMDAR, requires heterosynaptic stimulation and is induced and expressed presynaptically.

C) The aim of this study

Several form of PKA-dependent presynaptic plasticity have been identified in the hippocampus and in the cerebellum. PKA was also pointed out in some studies *in vivo* as a molecule necessary for memory formation in several structures, including the amygdala. Another molecule which appears to be important for synaptic plasticity in the hippocampus and the cerebellum is *RIM1*α. The molecular pathway involved in LTP was partially addressed in the amygdala as well, where the authors showed that a postsynaptically-induced LTP at the cortico-amygdala synapse is dependent on the recruitment of Rab3A (Huang et al., 2005). However, the molecular cascade which is implicated in synaptic plasticity was never addressed in its entirety in the amygdala. Another point which seems important to address is the physiological role of *RIM1*α in presynaptic LTP, meaning by which mechanism can it affect neurotransmitter release on a long-term scale.

This work tries to answer those questions in the context of the synaptic plasticity at the cortico-amygdala presynapse. More specifically, I will focus a part of this manuscript on the analysis of molecular mechanisms implicated in the formation and the maintenance of LTP_{HA} downstream of NMDAR activation.

II) LTP_{HA} AND PAIRED-PULSE RATIO

My first goal was to reproduce LTP_{HA}, by combining cortical and thalamic stimulus trains (Humeau et al., 2003). In order to confirm that the LTP_{HA} was presynaptic, I studied the change in paired-pulse plasticity during LTP_{HA}.

A) Introduction on the paired-pulse plasticity

Paired-pulse plasticity, one of the forms of short term plasticity, is generated by twin stimuli separated by a short time interval (from tens of millisecond to several seconds). Depending of the type of synapse and the physiological conditions, paired-pulse plasticity can be seen as paired-pulse facilitation (PPF) or paired-pulse depression (PPD). PPF/PPD represents an increase/decrease in the synaptic strength at the second stimulus. In its simplest view, PPF is believed to result from an increase in the probability of release during the second stimulus, arising from an accumulation of residual Ca^{2+} near release sites that occurs after the first stimulus (Katz and Miledi, 1968, for review, Zucker and Regehr, 2002). Concerning PPD, though several mechanisms have been proposed and are still debated (Bellingham and Walmsley, 1999; Chen et al., 2004; Hsu et al., 1996), is generally attributed to a depletion of the readily-releasable pool (RRP) (Singer and Diamond, 2006; Zucker and Regehr, 2002) that occurs after the first stimulus. Because both mechanisms underlying PPF and PPD coexist at the same synapse, the paired-pulse ratio (PPR) reflects a balance between an increase in the probability of release and a depletion of the RRP. Finally, based on the fact that the depletion of the RRP is controlled by the probability of release, paired-pulse experiments are usually performed to probe a change in presynaptic mechanisms and more precisely a change in the probability of release after a treatment that affect the functioning of the synapse.

Nevertheless, it should be noted that postsynaptic mechanisms can also be involved in short-term plasticity. The first possibility is that neurotransmitters released during the first stimulation already saturate postsynaptic receptors. Thus the putative increase in neurotransmitter that may occur during the second stimulation would not be detected at the postsynaptic side. The inactivation of the postsynaptic receptors can also be a reason for PPD (for review, Jones and Westbrook, 1996). The receptors can turn into a non-responsive state that may last from few milliseconds to several minutes.

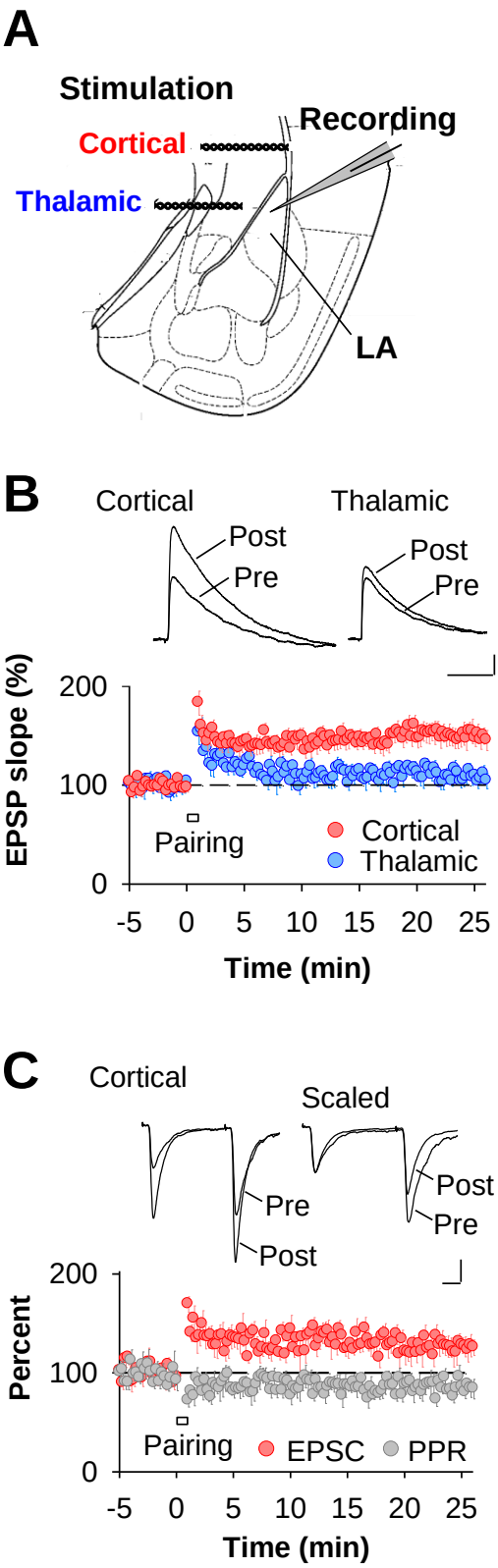

Figure 4 Presynaptic LTP at cortico-LA synapses (LTP_{HA}) is associated with a persistent decrease in the paired-pulse ratio (PPR). (A) Placement of stimulating and recording electrodes. **(B)** Pathway-specific LTP induction. Simultaneous Poisson-train stimulation of the thalamo-LA and cortico-LA pathways induces specific potentiation of cortico-LA synapses (n = 14 for both pathways, $p < 0.05$ for cortical pathway; thalamic pathway: n.s.). Scale bars: 1 mV and 50 ms. **(C)** Cortico-LA LTP is associated with a persistent decrease in the paired-pulse ratio (PPR) (n = 11, $p < 0.05$). Scale bars: 50 pA and 10 ms.

B) Results

1) Paired-pulse ratio

Whole-cell current clamp recordings from projection neurons showing spike frequency adaptation upon depolarizing current injection were obtained in the dorsal subdivision of the LA (Bissiere et al., 2003; Weisskopf et al., 1999). Stimulation of afferent fibers from the internal capsule, containing thalamic afferents (Weisskopf et al., 1999), or from the external capsule, containing cortical afferents (Huang and Kandel, 1998) (Figure 4A) elicited monosynaptic EPSPs of similar amplitudes and slopes at both inputs. As previously described (Humeau et al., 2003), simultaneous stimulation of cortical and thalamic afferents with a single Poisson-train (45 stimuli at an average frequency of 30 Hz) resulted in the pathway-specific induction of associative LTP at cortico-LA synapses called LTP_{HA} (cortical: 151 ± 9% of baseline, n = 14, $p < 0.01$; thalamic: 108 ± 4%, n = 14, n.s.)(Figure 4B). LTP_{HA} was associated with a decrease in the paired-pulse ratio (PPR)(86 ± 3% of baseline, n = 11, $p < 0.01$)(Figure 4C) suggesting a presynaptic expression mechanism.

A previous paper from the lab showed that LTP_{HA} is likely to be mediated by an overall increase in the probability of release *P* (Humeau et al., 2003) (see p15 of this chapter). An increased *P* might be mediated by several mechanisms such as an increased number of release sites or releasable vesicles, or an increase in the probability of release of single synaptic vesicles.

2) Multivesicular release

An overall increase in *P* at a population of synapses could involve several mechanisms including an increased probability that the release of a single vesicle occurs at a given synapse, or an increased number of released vesicles per synapse (i.e. a change in multi-vesicular release). Multivesicular release is the simultaneous or near-simultaneous exocytosis of multiple vesicles at the same active zone, which induce an increase of the glutamate concentration in the synaptic cleft. To examine possible changes in multi-vesicular release, I used the low-affinity AMPA receptor antagonist γ-D-glutamyl-glycine (γ-DGG), which can be used to probe for changes in synaptic glutamate (Christie and Jahr, 2006): when the glutamate concentration is low, γ-DGG binds AMPAR and efficiently blocks AMPA response; at a high glutamate concentration however, γ-DGG has a too low affinity to compete with glutamate binding, thus leading to a reduction in the AMPA block. Comparing the effect of γ-DGG application (2.5 mM) before and after LTP induction revealed no significant difference in the fractional block of AMPA EPSCs (baseline: 64 ± 7%, n = 8; LTP:

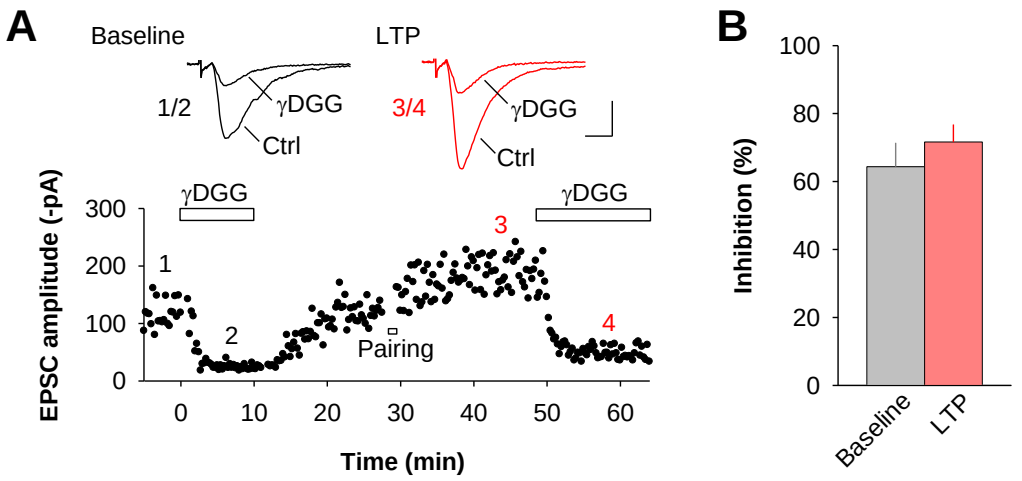

Figure 5: Presynaptic LTP does not involve an increased probability of multi-vesicular release. (A) Time course of an example experiment illustrating γ-DGG-mediated inhibition of synaptic transmission before and after induction of LTP (pairing). Depicted traces were taken at the time points indicated by the numbers. Scale bars: 50 pA and 5 ms. **(B)** There was no difference in the fractional block of synaptic transmission induced by γ-DGG (2.5 mM) before and after LTP induction (n = 8, n.s.).

71 ± 5%, n = 8; n.s.) (Figure 5). This indicates that LTP_{HA} does not involve changes in multi-vesicular release, but is rather mediated by a modulation of the release process itself.

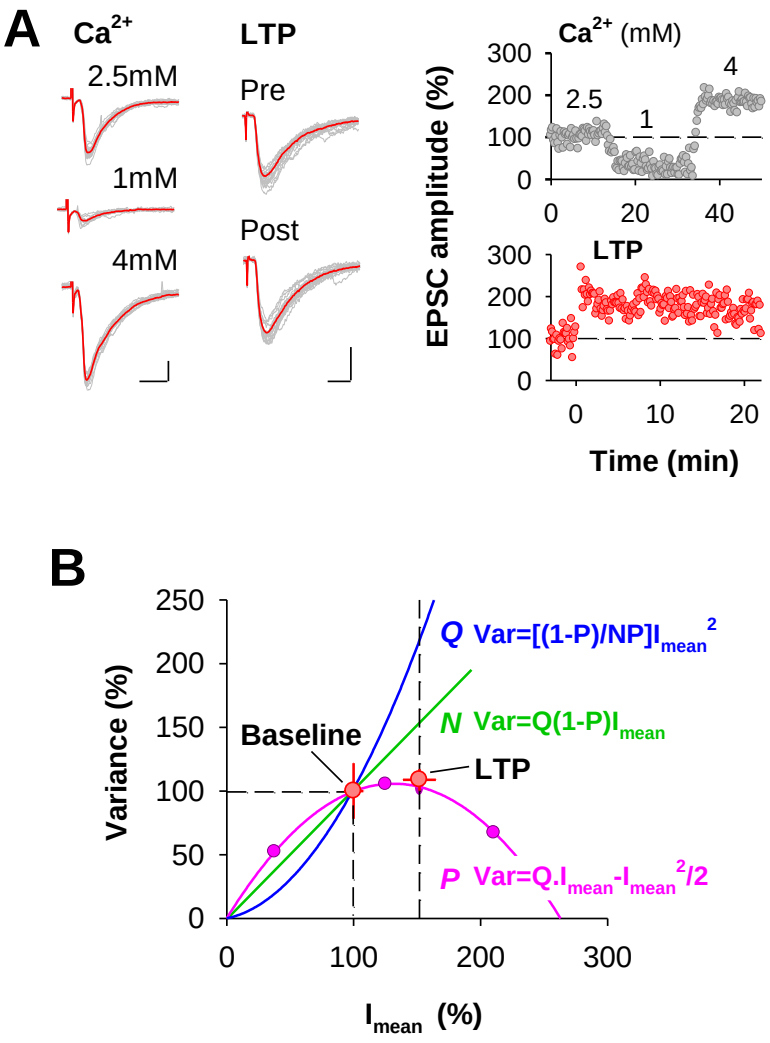

Figure 6: LTP_{HA} is mediated by a persistent increase in the probability of release. (A) Variance-mean analysis indicates that LTP at cortico-amygdala synapses involves an increase in P. Left, sample traces illustrating the EPSC variance recorded at different Ca^{2+} concentrations and before and after LTP induction. Scale bars: 50 pA and 10 ms. Right, example time courses of EPSC amplitude variations recorded at different Ca^{2+} concentrations and before and after LTP induction. Scale bars: 50 pA and 10 ms. **(B)** Scaling EPSC variance and mean amplitude before and after LTP induction (red symbols, n = 7) to the variance-mean plot obtained using different Ca^{2+} concentrations (n = 9) reveals an almost exclusive increase in *P* after LTP. Green and blue lines indicate the expected increase in variance upon changes in *N* and *Q*, respectively. Error bars, ± SEM.

III) QUANTAL PARAMETERS CHANGED BY LTP_{HA}

In electrophysiological experiments, synaptic transmission is measured postsynaptically, by recording the variations of the postsynaptic membrane potential or current induced by the release of neurotransmitter (NT) from synaptic vesicles (SV), the opening of the postsynaptic receptors and the ion fluxes induced. The current recorded is a function of the neurotransmitter release. Consistent with the quantal hypothesis of neurotransmitter release, evoked postsynaptic responses can be described as a stochastic, quantal process defined by three parameters:

- *Q*, the amplitude of the quantal size
- *P*, the output probability that a ready-to-release SV fuses with plasma membrane upon an increased calcium concentration in the presynaptic terminal.
- *N*, the number of independent release sites

A variation in PPR gives an indication for a change in *P*. However, changes in *Q* or *N*, which can be involved as well, are not detectable with this analysis method. In order to precisely determine which of the quantal parameter is affected by LTP induction, I used a method called fluctuation analysis, or variance-mean analysis, which is based on the fact that evoked transmitter release follows the rules of a binomial distribution. It consists on the analysis of the variance of the signal recorded at different probabilities of release, and allows a graphical distinction between changes in the different quantal parameters.

A) Variance-mean analysis

The variance-mean technique is a well-established method, which allows for distinguishing between changes in the quantal parameters (*N*, *P* or *Q*) by analysing the EPSC variance as a function of the mean amplitude under conditions of different release probabilities, or Var = *f*(Imean) (Clements, 2003; Foster and Regehr, 2004; Humeau et al., 2001; Humeau et al., 2002; Reid and Clements, 1999; Scheuss et al., 2002; Silver, 2003; Silver et al., 1998) (for more informations, see the material and method part).

When measured at increasing probabilities of release, EPSC variance plotted vs. the mean amplitude follows a parabolic function. I first estimated the baseline quantal parameters of synaptic transmission at cortico-LA synapses at different Ca^{2+} concentrations (P_1 = 0.14 ± 0.02, $P_{2.5}$ = 0. 47 ± 0.08, P_4 = 0. 80 ± 0.01, Q = –7.8 ± 0.9 pA, N = 33 ± 6, n = 9, Figure 6A,B). In a second set of experiments the average baseline variance at 2 mM external Ca^{2+}

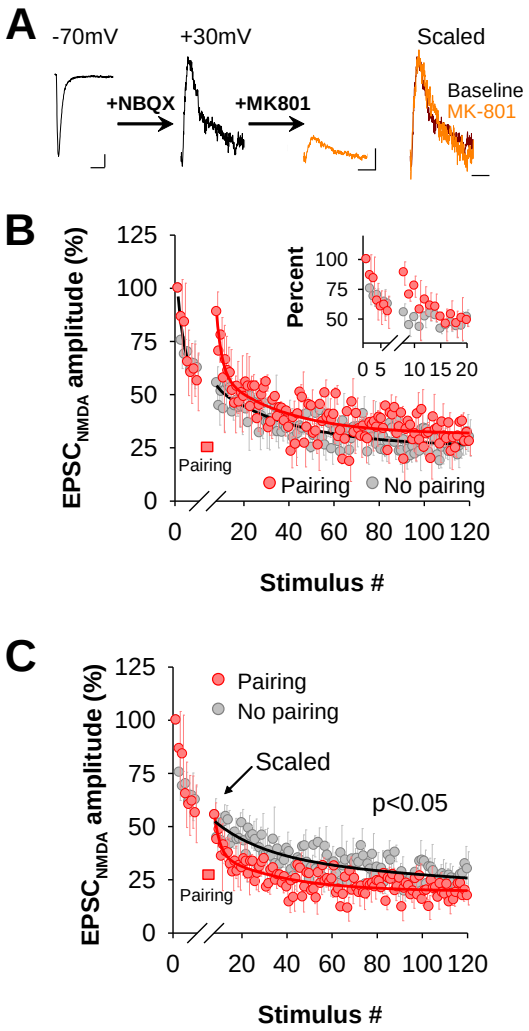

Figure 7: Intracellular perfusion with the use-dependent NMDA receptor antagonist MK-801 (1 mM) confirm an increase in P_r upon LTP induction. (A) After recording EPSCs at -70 mV, AMPA receptors were blocked by bath application of NBQX (20 μM) and NMDA receptor-mediated EPSCs recorded at +30 mV. After 100 stimulations, MK-801-induced a large decline of evoked NMDA receptor-mediated EPSCs. Scale bars: 20 pA and 20 ms (left) and 10 pA and 20 ms (middle). **(B,C)** Average MK-801-induced decay of NMDA receptor-mediated EPSCs before and after LTP induction. After 7 stimulations at +30 mV neurons were re-polarized to -70 mV and LTP was induced by pairing thalamic and cortical afferent stimulation. Resuming stimulation at +30 mV revealed a significantly faster decay after pairing **(B)** Superimposed and **(C)** Scaled traces. Scale bar: 10 ms. ($n = 5$; $p < 0.05$).

was normalized to the parabola obtained from the control experiments (n = 7, Figure 6B). Subsequently LTP was induced and the change in variance measured after LTP induction was plotted against the increased mean EPSC amplitude. These experiments revealed that LTP_{HA} can entirely be accounted for by an increase in *P* ($P_{baseline}$ = 0.38 ± 0.03; P_{LTP} = 0.58 ± 0.05; n = 7; $p < 0.05$)(Figure 6B).

B) Postsynaptic MK801 infusion

To confirm the results involving an increase in the probability of release *P*, I used a third method. As LTP_{HA} seems to be purely presynaptic, and LTP_{HA} depends on presynaptic, but not postsynaptic, NMDA receptors (Humeau et al., 2003), I used the activity-dependent block of NMDARs by the open-channel blocker MK-801 as a more direct read-out of possible changes in the release probability (Rosenmund et al., 1993). MK-801 (1 mM) was applied to the postsynaptic neuron intracellularly via the patch-pipette (Humeau et al., 2003). The stimulation intensity was adjusted (while holding the cells at -70 mV) to evoke postsynaptic AMPA receptor-mediated EPSCs of similar amplitudes as in the control LTP experiments. Subsequently, the AMPA receptor antagonist NBQX (20 µM) was washed in, the cells were depolarized to +30 mV, and stimulation was resumed to monitor pharmacologically isolated NMDA receptor-mediated EPSCs.

In control experiments, this resulted in a gradual decay of the amplitude of NMDA-EPSCs (Figure 7A,B). The time-course of the decay was biphasic and could be fitted with a bi-exponential function (τ_{fast} = 2.3 ± 0.4 stimulations; τ_{slow} = 29.5 ± 8.1 stimulations; n = 5)(Figure 7B)) indicating that the total population of stimulated synapses could be divided in (at least) two sub-populations with different *P*. In a second set of experiments, stimulation was stopped after 7 stimuli, the cell was repolarized to -70 mV, in order to stay in the same induction conditions as for classical LTP_{HA} induction, and the cortico-LA and thalamo-LA pathways were co-stimulated with the same protocol used for LTP induction. Subsequently, single-shock stimulation was resumed at +30 mV. Delivery of an LTP induction protocol resulted in the potentiation of the NMDA EPSC relative to the last stimulation before induction (158 ± 15%; n = 5; Figure 7B). Moreover, LTP induction was associated with the re-appearance of the fast-decaying component, which had entirely disappeared after the first 7 stimulations (Figure 7B,C). While in the control group the decay of the NMDA EPSC amplitude from stimulation 8 on was following a mono-exponential time-course, the decay after LTP induction again followed a bi-exponential time-course (τ_{fast} = 2.1 ± 0.4 stimulations; τ_{slow} = 30.2 ± 4.3 stimulations; n = 5). The fast component in the LTP group was significantly

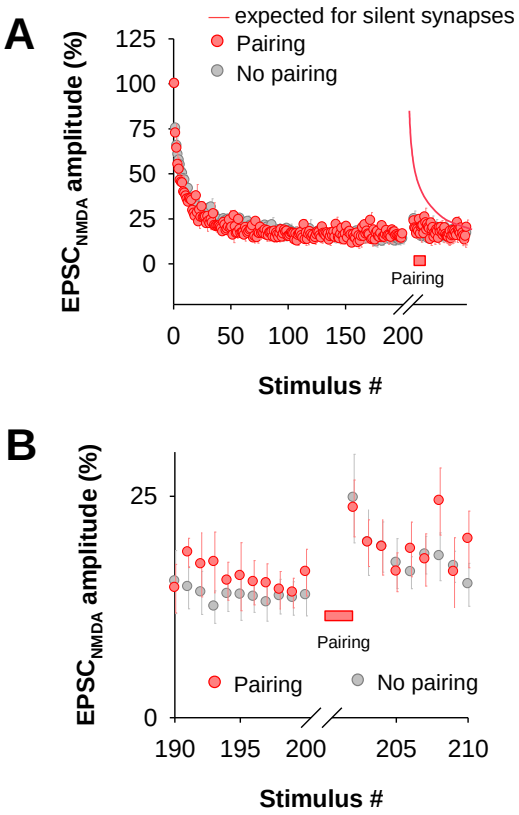

Figure 8: LTP_{HA} does not activate silent synapses. (A) Average MK-801-induced decay of NMDA receptor-mediated EPSCs before and after LTP induction. After 200 stimulations at +30 mV neurons were repolarized to -70 mV and LTP was induced by pairing thalamic and cortical afferent stimulation. Resuming stimulation at +30 mV revealed a significantly faster decay after pairing. Line: expected NMDA decay in case of an activation of silent synapses. **(B)** Same as in (A) at an enlarged scale. Resuming stimulation at +30 mV revealed no difference after pairing compared to control condition (control n = 8; LTP n = 7; $p > 0.05$).

different from the slow time-constant in the control group (n = 5; $p < 0.05$) and did not significantly differ from the initial fast component in the control group (n = 5). These experiments directly demonstrate that *P* at cortico-LA synapses is heterogeneous, and that induction of LTP_{HA} induces a selective increase in P at a subset of synapses

However, it is still possible that LTP_{HA} induction protocol triggers the activation of previously silent synapses which have a high *P*. As shown in the control condition in the previous MK801 experiment (Figure 7B,C), the probability of release is not uniform among the cortico-LA synapses. One can postulate that some of the putative silent synapses could express a high probability of release, which would correspond to the fast component in the control experiment of the figure 7. Therefore a second set of MK801 experiments were performed, with a higher MK801 concentration (4 mM), and an increased stimulation intensity. After 200 stimulations at +30 mV, the cell was repolarized to -70 mV, in the presence of the absence of LTP induction. In order to avoid the short-term potentiation which is also triggered by the induction protocol, I waited for 5 minutes before resuming NMDA-recordings at +30 mV (Figure 8). Due to the presence of AMPAR blockers in the bath and of NMDAR blockers in the patch-clamp pipette, LTP_{HA} expression cannot be registered. However, a previous set of experiments allowed me to control that LTP_{HA} is inducible more than 30 minutes after the opening of the cell. The NMDA EPSCs were not different between the two conditions (control: 26 ± 5 % of the initial NMDA EPSC, n = 8; LTP induction 24 ± 3 %, n = 7, $p > 0.05$), leading to the conclusion that LTP_{HA} induction recruited only synapses which were previously active and fully blocked by MK801. The component which reappears both in control and in LTP conditions probably reflects the recovery of the NMDA response by spontaneous removal of MK-801 from NMDARs and/or by lateral diffusion of unblocked NMDARs into the synapse.

From all these experiments, we can conclude that cortico-amygdala LTP is exclusively due to an increase in the probability of release at already active synapses; with no change in *N* or the activation of silent synapses.

IV) KINASE INVOLVEMENT IN LTP INDUCTION

A) Introduction

Kinases are one of the most common classes of signaling molecules involved in synaptic plasticity. The intracellular pathways involving the protein kinase C (PKC) pathway, or the adenylyl cyclase/protein kinase A (AC/PKA) have been particularly well studied in synaptic plasticity.

1) Protein kinase C

a) Description

Protein kinase C (PKC) is a calcium activated serine/threonine kinase. This family of kinases consists of ~10 isozymes, which are splitted up into three subfamilies according to the second messenger associated with their regulatory region: conventional (or classical), novel, and atypical PKC:

- Conventional (c) PKCs require calcium ions diacylglycerol (DAG), and a phospholipid such as phosphatidylcholine for activation.
- Novel (n) PKCs require DAG, but do not require calcium ions for activation.
- Atypical (a) PKCs (including protein kinase Mζ) require neither calcium nor DAG for activation.

The structure of all PKCs consists of a regulatory domain and a catalytic domain tethered together by a hinge region. The catalytic region is highly conserved among the different isoforms. It consists of a bilobal structure with a β sheet comprising the N-terminal lobe and an α helix constituting the C-terminal lobe. The cleft formed by these two lobes contains the ATP- and substrate-binding sites, and it is also the place where the pseudosubstrate domain of the regulatory region binds. The pseudosubstrate region is a small sequence of amino acids mimicking the substrates. This domain keeps the enzyme inactive when it binds to the substrate-binding cavity in the catalytic domain.

PKC catalytic sites are active only in the phosphorylated form. The conventional and novel PKCs have three phosphorylation sites, the atypical PKCs are phosphorylated only on two sites. The 3-phosphoinositide-dependent protein kinase-1 (PDK1) is the upstream kinase

responsible for initiating the process by phosphorylation of the activation loop (Balendran et al., 2000).

The regulatory domain of the all PKCs contains a C1 domain that contains a binding site for DAG and phorbol esters (non-hydrolysable and non-physiological analogues of DAG). The C1 domain is only functional in c- and nPKCs. Those two subtypes also contain a C2 domain, which acts as a calcium sensor for cPKC but is not functional for nPKCs. The binding of DAG and calcium to C1 and C2 domains respectively induce the recruitment of PKC to the membrane. This leads to the release of the pseudosubstrate from the catalytic site and the activation of the enzyme.

b) Role in synaptic plasticity

In the 90's, several studies pointed out the importance of PKC, and notably of the atypical PKC isoenzyme PKM zeta, in LTP in the hippocampal CA1 area (Hrabetova and Sacktor, 1996; Ling et al., 2002). PKC activation was shown to be specifically enhanced in CA1 during the induction and maintenance phases of LTP (Klann et al., 1993; Sacktor et al., 1993). PKC may act in LTP by enhancing a NMDA-evoked current via the activation of the non-receptor tyrosine kinase (Src) signaling cascade (Lu et al., 1999).

An involvement of PKC in the induction of non-NMDAR-LTD was demonstrated in several brain areas. For example, it has been shown that postsynaptic injection of PKC inhibitory peptide or PKC inhibitors blocked synaptically stimulated LTD in CA1, dentate gyrus, cerebellum and ventral tegmental area. (for review, Anwyl, 2006). PKC can also act in LTD by phosphorylating AMPAR subunits. In the cerebellum the phosphorylation of the C-terminal region of the AMPAR GluR2 subunit by PKC induces the dissociation of GluR2 from GRIP, a postsynaptic density protein important for AMPAR clustering. This leads to clathrin-mediated endocytosis of AMPAR that finally underlies LTD (Chung et al., 2003; Matsuda et al., 2000). PKC has also been involved presynaptically by increasing the readily releasable pool or reducing the quantal size. PKC probably acts by phosphorylating several presynaptic proteins such as synaptotagmin, syntaxin or SNAP25 that are involved in synaptic vesicle release (for review, Barclay et al., 2005).

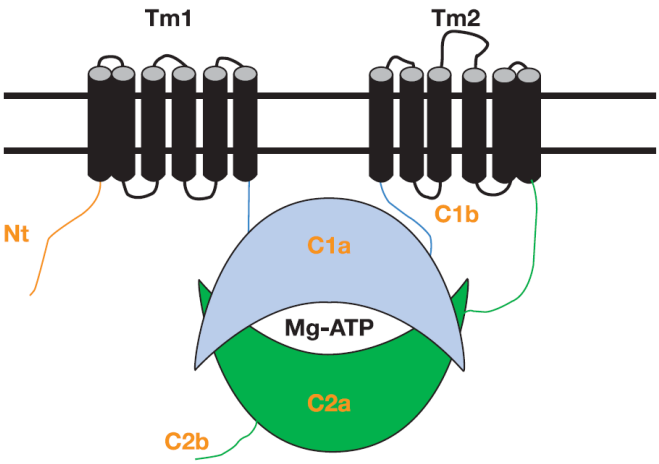

Figure 9: Structure of adenylyl cyclase (AC). ACs can be divided into 5 major domains: The N-terminus (Nt); the first transmembrane cluster (Tm1), the fisrt cytoplasmic loop (C1), the second Tm cluster (Tm2) and the second cytoplasmic loop (C2). The C2 and C2 regions are further subdivided into the highly conserved catalytic C1a and C2a regions, which dimerize to form the catalytic site, and the less conserved C1b and C2b domains (Cooper, 2003).

2) The adenylyl cyclase / protein kinase A pathway

a) The Adenylyl cyclase

- Description

Adenylyl cyclase (AC) catalyzes the conversion of ATP to pyrophosphate and cAMP, an important second messenger in eukaryotic cells. In mammals, there are ten known ACs. Their difference resides mainly in their regulation by calcium/calmodulin and G proteins. Tissue distribution of ACs is also isoform-specific. Except sAC which is soluble, all other ACs are transmembrane proteins, with 12 transmembrane domains. Their structure can be divided into five major domains (Figure 9) (Cooper, 2003):

- the N-terminus, cytoplasmic
- a first cluster of 6 transmembrane domains (Tm1)
- a first cytoplasmic loop, C1, constituted by two catalytic domains C1a and C1b
- the second cluster of 6 transmembrane domains (Tm2)
- the second cytoplasmic loop, C2, formed as well by two catalytic domains C2a and C2b

C1a and C2a dimerize to form the catalytic site of the enzyme.

- regulations and clustering

With the exception of AC9, all known isoforms of mammalian AC are stimulated by Forskolin. Other modulators, such as α- and βγ-subunits of G proteins, calcium/calmodulin, PKC and PKA, are specifically acting on certain AC isoforms, either by stimulating or inhibiting them (for review, Sunahara and Taussig, 2002). Based on their amino-acid sequences and their functional regulation, ACs can be divided into five distinct families. The first family that comprises AC1, AC3, and AC8 corresponds to calcium-calmodulin sensitive ACs. The second family constituted by AC2, AC4, and AC7 is stimulated by Gβγ. AC5 and AC6 that form the third family are distinguished by their inhibition by both calcium and Gαi isoforms. Both AC9 and sAC form a separate family on their own.

This specificity in the regulation raised the question of the subcellular distribution of AC subtypes in the cell. Isoforms AC3, AC5, AC6 and AC8 are found enriched in lipid raft fractions, where numerous ion channels (including Kv1.4, Kv1.5, Kv4.2, L-type calcium channel and voltage-gated sodium channel) are present (for review, Ostrom and Insel, 2004). Surprisingly, AC incorporation in lipid rafts is not due to their hydrophobic TM-domains, but rather involves their cytosolic domain, probably through protein-protein interactions (Crossthwaite et al., 2005).

In addition to the spatial clustering of AC, the very rapid activation of phosphodiesterases (PDE) can lead to transient and localized cAMP response. Targets of cAMP should be also present in close vicinity, as shown for AC in HEK-293 cells (Willoughby et al., 2005). Cyclic AMP that escapes degradation by PDE slowly accumulates in the cytosol.

- Role in synaptic plasticity

In the brain, only calcium-calmodulin sensitive forms of AC are expressed (i.e. AC1, AC3 and AC8). Calcium-inhibited form AC3 is present in the main olfactory epithelium and seems to be involved in the detection of odorants. Calcium-activated forms AC1 and AC8 are expressed in various parts of the brain and notably in the cortex, the hippocampus and the cerebellum. Interestingly, AC1 stimulation requires the simultaneous presence of α- subunit of G-proteins and a high calcium concentration (Wayman et al., 1994). Therefore, AC1 functions as a coincidence detector to integrate calcium and G-protein-coupled receptor activation. The second calcium-stimulated AC, AC8, is five times less sensitive to calcium than AC1 and not regulated by G-proteins. Thus AC8 is considered to be a strict low-affinity calcium detector (for review, Ferguson and Storm, 2004; Wang and Storm, 2003).

In order to study their involvement in long-term memory, knockout (KO) mice for AC1 and /or AC8 were generated. AC1 and AC8 are not required for the survival of mice since all three homozygous KO mice were viable. AC1 KO mice showed a severe impairment in presynaptic LTP at mossy fiber to CA3 synapses in the hippocampus as well as at parallel fiber to Purkinje cell synapses in the cerebellum, two forms of LTP which are known to be dependent on PKA (Nicoll and Malenka, 1995; Salin et al., 1996). This deficit in PKA-dependent LTP was rescued by forskolin application, indicating that AC acts upstream to PKA activation (Villacres et al., 1998). Moreover, AC1-AC8 double knockout mice exhibit deficits in the hippocampal NMDAR-dependent LTP expressed in the CA1 area (Wong et al., 1999). *In vivo*, a lack of ACs induces a robust impairment in several forms of long-term memory such as passive-avoidance memory, which again can be rescued by forskolin injections in the hippocampus (Wong et al., 1999). Thus the hypothesis that a direct recruitment of neuronal ACs by calcium leads to PKA activation seems to be confirmed, at least in the hippocampus (for review, Ferguson and Storm, 2004; Wang and Storm, 2003).

b) Protein kinase A

- Description

Protein kinase A (PKA), also known as cAMP-dependent protein kinase or A kinase, is an enzyme which phosphorylates proteins at serine or threonine residues. PKA is a holoenzyme that requires the presence of a cofactor, cAMP, to be activated.

PKA consists of two regulatory domains, containing cAMP binding sites, and two catalytic subunits. The regulatory domains contain an auto-inhibitory domain which acts as a pseudosubstrate for the catalytic subunit when the enzyme is inactive. Cyclic AMP binding leads to a conformational change that finally induces the release of the catalytic subunits. The activity of the catalytic subunits activity can be directly regulated by phosphorylation. The activity of PKA is also modulated by a group of proteins called protein kinase inhibitors. These molecules often act as pseudosubstrates for the catalytic subunit, competing with real phosphorylation targets. The mammalian PKA family is constituted by four regulatory subunits (RIα, RIβ, RIIα, RIIβ) and three catalytic subunits (Cα, Cβ, Cγ). Two major isozymes of PKA are called type I (with RIa and RIb dimers) and type II (with RIIa and RIIb dimers).

- Regulations and spatial segregation

PKA is capable to auto-regulate its activity; a sustained activity can be maintained by a selective degradation of regulatory subunits or by their phosphorylation by the catalytic subunits, which decreases their affinity to the catalytic subunits. The different regulatory subunits possess also different sensitivities to cAMP, leading to a modulation of the PKA activation profile (Nguyen and Woo, 2003).

Protein kinase A often acts at very discrete domains within the cell. The subcellular localization of PKA results from the interaction of regulatory subunits with proteins called A kinase anchoring proteins (AKAPs). A large number of AKAPs have been identified and all target PKA to specific substrates including ion channels, cytoskeletal elements and centrosomes (for review, Tasken and Aandahl, 2004), but also to their activator, cAMP (Willoughby et al., 2005).

- Role in synaptic plasticity

The importance of PKA activity in memory formation was first discovered in *Aplysia*, where this enzyme plays a role in the molecular mechanisms underlying the gill-withdrawal reflex. Stimulation of the snails' siphon coupled with a noxious tail shock causes the animal to withdraw its gill. This form of conditioning leads to sensitization so that further siphon

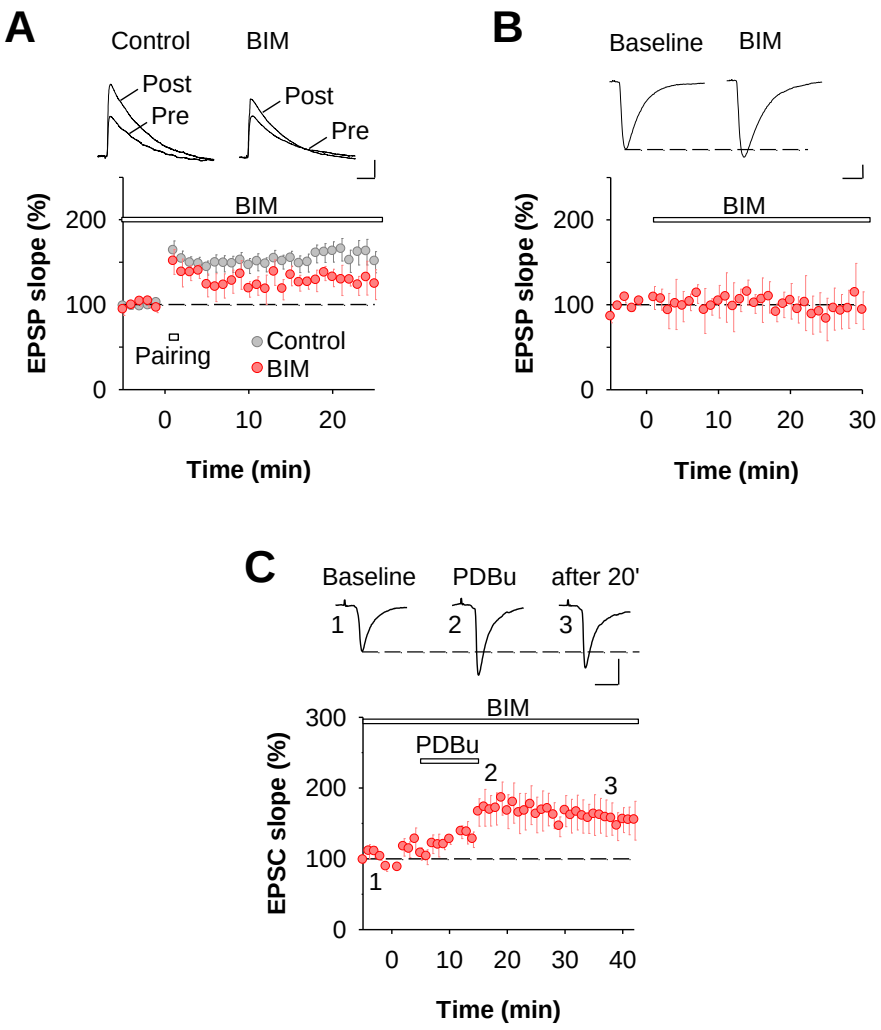

Figure 10 PKC pathway is partially involved in LTP_{HA} expression mechanism. (A) PKC antagonist Bisindolylmaleimide II (BIM; 200 nM) partially reduces LTP_{HA} expression ($n = 6$, $p < 0.05$) at cortico-amygdala synapses. Scale bars: 2 mV and 50 ms. **(B)** Application of Bisindolylmaleimide II does not change basal neurotransmission. Scale bars: 20 pA and 10 ms. **(C)** PDBu-potentiation of synaptic transmission is independent from PKC pathway (PDBu 1 µM ,n=4). Scale bars: 50 pA and 10 ms.

stimulation results in gill withdrawal. This memory can last for several days, and requires AC recruitment via the stimulation of serotonergic receptors as well as PKA activation through the increase in cAMP levels. The importance of cAMP signaling in learning and memory formation was also demonstrated in *Drosophila* (for review, Abel and Kandel, 1998).

PKA involvement in mammalian plasticity was studied mainly in hippocampal LTP (see part B3b from the chapter I). Knockout mice for the PKA subunits Cβ1 or RIβ showed a decreased mfLTP (Huang et al., 1995; Qi et al., 1996). However, total PKA activity was unchanged in whole-brain or hippocampal extracts derived from these mutant mouse lines, suggesting the existence of a compensatory mechanism: the defect in mfLTP could be due to the disruption of the balance in the activities of intracellular signalling pathways. Tetanization of Schaffer collaterals induced LTP which can occlude a form of potentiation induced by the application of exogenous cAMP (Sp-cAMPS) and potentially blocked by PKA inhibitors. However, this blockade is dependent of the paradigm of stimulation used to induce LTP: using different tetanic train stimulations, Woo et al (Woo et al., 2003) were able to elicit a form of LTP insensitive to PKA inhibitors.

In the amygdala, several studies demonstrated that PKA signaling is essential for memory formation. *In vivo*, the injection of PKA inhibitors into the basal and lateral amygdala immediately after fear conditioning blocked the consolidation of fear memory (Schafe and LeDoux, 2000). PKA inhibitors altered as well long-term memory formation in a conditioned taste-aversion task, which is also dependent on the amygdala. Furthermore, KO mice for the regulatory subunit RIIb, which is highly expressed in the amygdala, showed deficits in long-term memory of a taste-aversion task. Therefore, several studies suggested that PKA activity is important for memory formation in the amygdala (for review, Arnsten et al., 2005). Moreover, *in vitro* experiments at cortico-LA synapses demonstrated that postsynaptically induced LTP is PKA-dependent (Huang and Kandel, 1998).

B) Results

1) PKC pathway

I first tested the influence of PKC on LTP_{HA}. The application of the PKC inhibitor Bisindolylmaleimide II (BIM, 200 nM) partially blocked the induction of LTP_{HA} (control 155 ± 10% of baseline, n = 18, $p < 0.05$; BIM 125 ± 11%, n = 6, $p < 0.05$, Figure 10A) whereas it has no effect on basal neurotransmission (BIM 97 ± 3% of baseline, ns, Figure 10B). I then tried to stimulate PKC activity in order to study a putative occlusion with LTP_{HA}. The

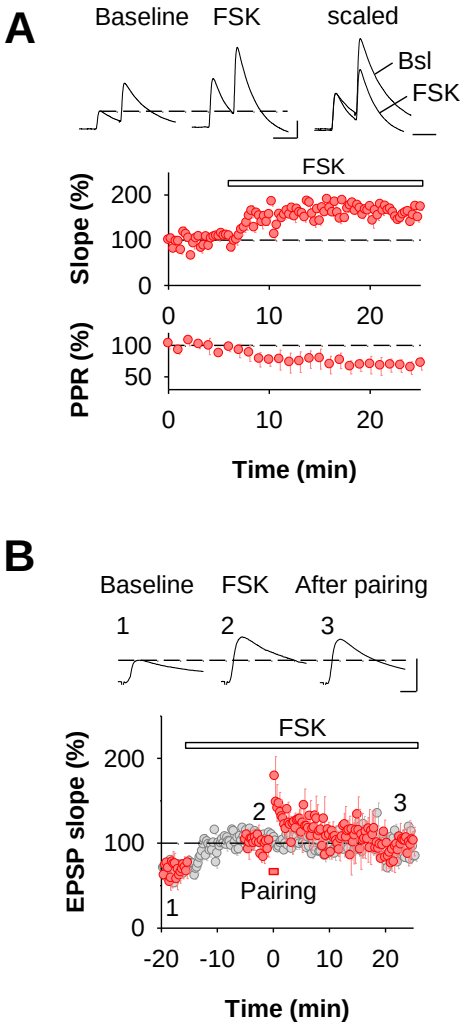

Figure 11: Forskolin-LTP and LTP_{HA} share a common pathway. (A) Forskolin (FSK; 50 µM) enhances synaptic transmission (n = 5, $p < 0.01$) and decreases PPR (n = 5, $p < 0.05$) at cortico-amygdala synapses. Scale bars: 5 mV and 50 ms. **(B)** FSK-induced potentiation of synaptic transmission occludes the induction of LTP_{HA} (n = 5, $p < 0.01$). Grey symbols represent FSK-potentiation of synaptic transmission in the absence of LTP induction (same data as in panel A). Averaged sample traces were taken at the time points indicated by the numbers. Scale bars: 5 mV and 10 ms.

methods currently used to chemically stimulate PKC activity involves the use of phorbol-ester called Phorbol 12.13-Dibutyrate (or PDBu). PDBu binds the C1 domain of the conventional and novel PKC regulatory subunit, allowing the activation of the catalytic subunit. However the presynaptic protein Munc13-1, importantly involved in synaptic vesicle priming, contains a C1 domain which can binds PDBu as well (Betz et al 1998, 2001). A preliminary experiment showed that PDBu-potentiation (1 μM) is not blocked by Bisindolylmaleimide II, signifying that at least a part of PDBu potentiation is not mediated by PKC, and could potentially be due to Munc13-1 activation (Figure 10C).

2) AC/PKA pathway

Given the well established role for cAMP/PKA signaling in presynaptic forms of LTP in other brain areas (Weisskopf and Nicoll, 1994; Salin et al., 1996), and the demonstration that postsynaptically induced LTP at cortico-LA synapses is also PKA-dependent (Huang and Kandel, 1998), we tested whether cAMP/PKA signaling would also be required for the presynaptic induction of LTP_{HA}. We first applied the adenylate cyclase (AC) activator forskolin (FSK; 50 μM). FSK application increased excitatory synaptic transmission at cortical afferents (160 ± 8% of pre-drug baseline, $n = 5$, $p < 0.05$)(Figure 11A). Consistent with a FSK-induced increase in P, the increase in EPSP amplitude was associated with a decrease in PPR (69 ± 11% of pre-drug baseline, $n = 5$, $p < 0.05$)(Figure 11A).

Forskolin-induced potentiation of synaptic transmission completely occluded any further induction of LTP_{HA} by co-stimulation of thalamo- and cortico-LA afferents (95 ± 13% of baseline, n =5, Figure 11B), suggesting a rise in presynaptic cAMP during LTP induction.

To directly test this idea, I applied the non-hydrolysable cAMP analog Rp-cAMPS (100 μM), which blocks the cAMP-dependent pathways. As Rp-cAMPS slowly pass cellular membrane, slices were pre-treated at least for 45 min. with Rp-cAMPS. This long incubation time prevented me to test the influence of Rp-cAMPS on basal release. However, baseline recordings in the presence of Rp-cAMPS were stable over more than 30 minutes (data not shown). In slices pretreated with Rp-cAMPS, LTP_{HA} could not be induced (control: 160 ± 15% of baseline, $n = 18$, $p < 0.05$; Rp-cAMPS: 101 ± 12% of baseline, $n = 6$, n.s., Figure 12A). This indicates that a rise in presynaptic cAMP is both necessary and sufficient for LTP induction at cortico-LA synapses.

To assess whether the Rp-cAMPS effect was due to the blockade of PKA I tested if the PKA inhibitor H-89 (20 μM) blocked forskolin-induced potentiation and LTP_{HA}. In the

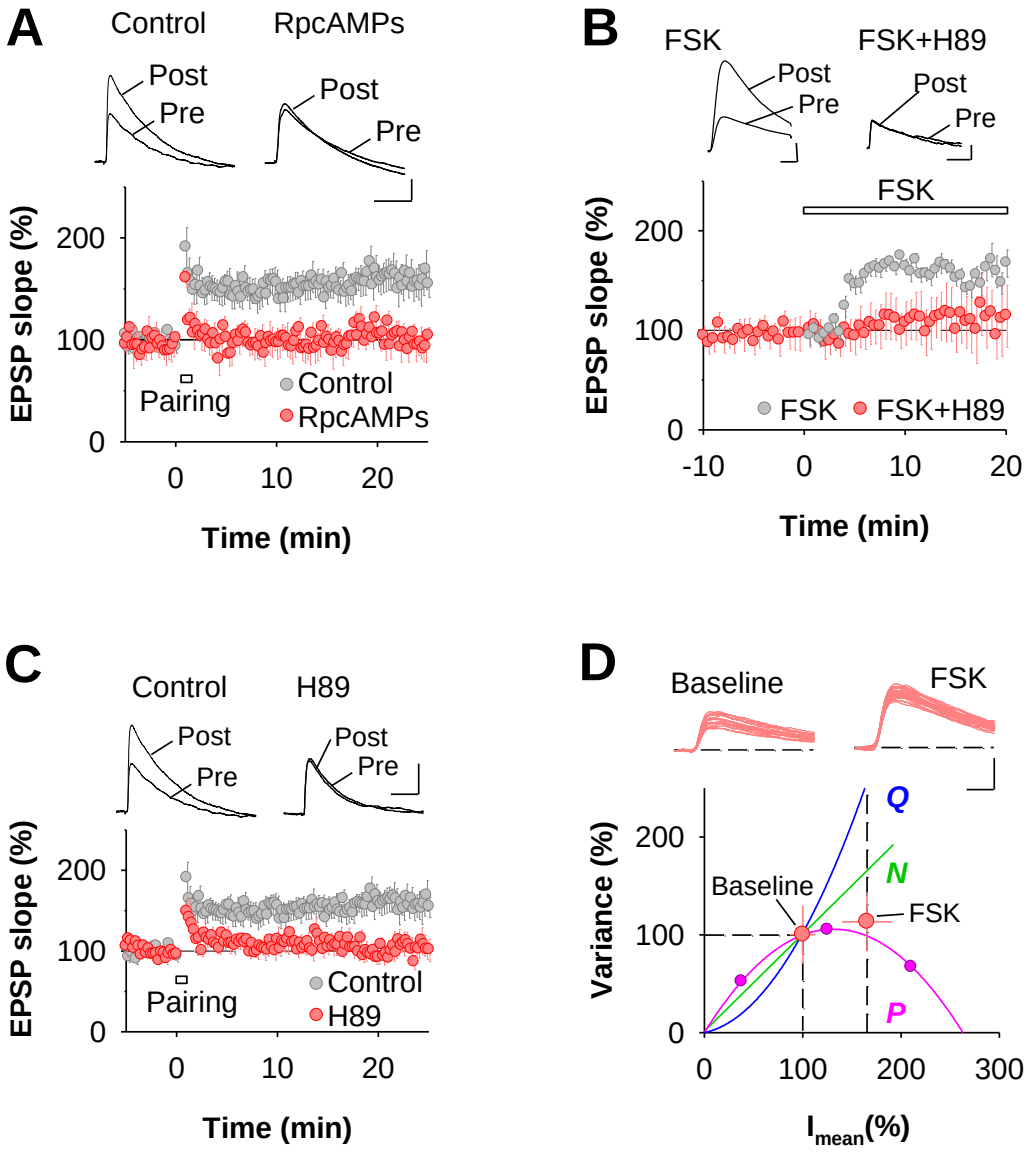

Figure 12 : Activation of the cAMP/PKA pathway is necessary and sufficient for presynaptic LTP. (A) LTP induction is blocked by the non-hydrolyzable cAMP analog Rp-cAMPS (100 µM)(control, n = 18; Rp-cAMPS, n = 6; $p < 0.05$). Scale bars: 2 mV and 50 ms. **(B)** FSK-potentiation of synaptic transmission requires activation of PKA. Bath application of the PKA antagonist H-89 (20 µM) completely abolishes the effect of FSK on synaptic transmission (control: n = 5; H-89: n = 5; $p < 0.05$). Scale bars: 2 mV and 50 ms. **(C)** Induction of LTP at cortico-LA synapses is blocked by the PKA antagonist H-89 (20 µM)(control: n = 18; H-89: n = 8, $p < 0.05$). Scale bars: 2 mV and 50 ms. **(D)** Variance-mean analysis shows that FSK-potentiation is associated with an increase in *P*. Top, single experiment illustrating FSK-induced increase in synaptic transmission and representative traces before and during FSK (50 µM) application. Scale bars: 2 mV and 10 ms. Bottom, scaling EPSC variance and mean amplitude before and after FSK application (red symbols, n = 19) to the variance-mean plot obtained using different Ca^{2+} concentrations (same data as in figure 11B) reveals an almost exclusive increase in *P*. Green and blue lines indicate the expected increase in variance upon changes in *N* and *Q*, respectively.

presence of H-89 both forskolin-induced potentiation (control: 162 ± 14% of baseline, n = 5, $p < 0.05$; H-89: 111 ± 29% of baseline, n = 5, n.s.)(Figure 12B) and LTP_{HA} were completely abolished (control: 160 ± 15% of baseline, n = 18, $p < 0.05$; H-89: 103 ± 11% of baseline, n = 8, n.s., Figure 12C). These results demonstrate that the increase in the probability of release during LTP_{HA} requires the activation of presynaptic AC and PKA, and that cAMP/PKA signaling is necessary and sufficient for LTP induction.

If electrically induced LTP_{HA} and forskolin-induced potentiation of synaptic transmission are one and the same, then forskolin-potentiation, like LTP, should be mediated exclusively by an increase in *P*. Therefore, we used variance-mean analysis, to examine changes in the quantal parameters *N*, *P* and *Q* upon forskolin application. Very similar to the results obtained after LTP induction, we found that forskolin-potentiation almost exclusively involved an increase in *P* ($P_{initial}$ = 0.38 ± 0.05, P_{LTP} = 0.63 ± 0.1) (Figure 12D). Taken together, these results indicate that forskolin-potentiation relies on the same induction machinery and involves the same expression mechanisms as LTP induced by co-stimulation of thalamo- and cortico-LA afferents.

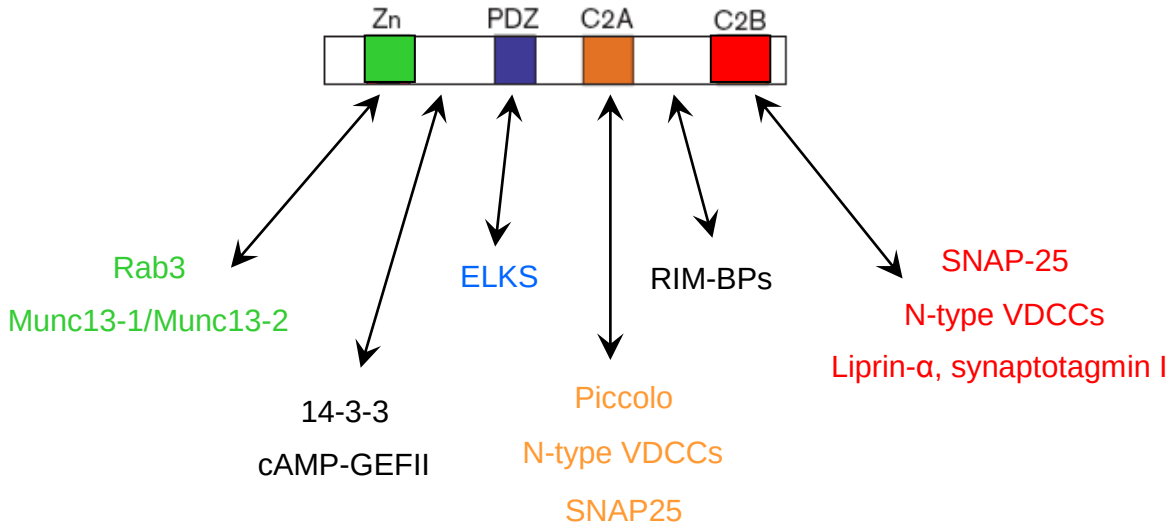

Figure 18: RIM1α structure and interacting partners RIM1α contains a single amino-terminal zinc finger domain, a PDZ domain and two C2 domains. These domains share limited homology with the analogous domains in Piccolo/Aczonin. Adapted from (Garner et al., 2000)

V) RIM1 ALPHA

Next, I addressed the mechanisms and components of LTP expression downstream of PKA recruitment. Several proteins involved in the vesicular cycle are phosphorylated by PKA. Studies of KO mice showed that the presence of rabphilin, synapsin I and synapsin II that are all substrates of PKA is not necessary for mfLTP (Schluter et al., 1999; Spillane et al., 1995). At the contrary, the presence of Rab3A, a monomeric G protein which is not phosphorylated by PKA, was shown to be necessary for the expression of mfLTP (Castillo et al., 1997). Therefore, to identify the target of PKA in mfLTP, the studies focused on binding partners of Rab3A which are PKA substrates. One candidate was *RIM1*α, a central component of the active zone.

A) Introduction

1) Description

RIMs constitute a family of multidomain proteins that were initially discovered as putative effectors for the synaptic vesicle protein Rab3 (Wang et al., 1997). In vertebrates, RIMs are encoded by four different genes that generate several isoforms by alternative splicing (Wang and Sudhof, 2003). *RIM1*α, the best studied isoform, is located at the active zone of presynaptic terminals and forms a scaffolding protein interacting with key molecules.

- Structure of the protein

*RIM1*α consists of a N-terminal zinc finger domain, a central PDZ, a short proline-rich motif and two C2 domains, a central C2A and a C-terminal C2B domain (Figure 13).

The prolin-rich region is known to bind proteins containing a SH3 (Src homology 3 domain) domain, which is a domain present in highly interacting proteins. The PDZ domain is a common structural domain of 80-90 amino acids found in signaling proteins. PDZ is an acronym combining the first letters of the three proteins which were first discovered to possess this domain: post synaptic density protein (PSD95), Drosophila disc large tumor suppressor (DlgA), and zonula occuldens-1 protein (zo-1). These domains help anchoring transmembrane proteins to the cytoskeleton and helding together signaling complexes.

The zinc finger domain confers to *RIM1*α its ability to bind DNA. A zinc finger consists of about 30 amino acid residues creating two antiparallel β sheets, and an α helix. The zinc ion which holds the β sheets and the α helix together is crucial for the stability of this

domain. The binding specificity for 3 to 4 DNA base pairs is conferred by a short stretch of amino acid residues in the α-helix.

A C2 domain is a calcium-dependent membrane-targeting module found in many cellular proteins involved in signal transduction or membrane trafficking. It is composed of 8 β-sheets, forming a beta-sandwich motif and has a high affinity for calcium ions. The C2 domain is thought to be involved in calcium-dependent phospholipid binding and in membrane targetting processes such as subcellular localization. The *RIM1*α C2 domain does not contain the consensus calcium binding sites that were defined in the synaptotagmin C2 domains (Sudhof and Rizo, 1996) and are necessary for calcium-binding. Thus calcium binding to *RIM1*α is still questionable (Sudhof and Rizo, 1996; Wang et al., 1997). Thanks to those four domains, *RIM1*α can bind several proteins, all important for vesicular neurotransmitter release.

- Interacting partners

The first partner of *RIM1*α is the protein at the origin of its name, Rab3A. Surprisingly, *RIM1*α interacts with Rab3A via its zinc finger domain, which is in principle devoted to DNA-binding. This binding happens only when Rab3A is in the GTP-bound configuration (Wang et al., 1997) (Figure 13).

The *RIM1*α zinc finger domain also binds Munc13-1, a protein involved in synaptic vesicle priming (Betz et al., 2001). These authors demonstrated that Munc13-1 and Rab3A bind the same amino-acid sequence, in a competitive and mutually exclusive manner. Based on their observations, Betz et al suggested that *RIM1*α contributes to vesicle tethering via its binding to Rab3A and creates a physical link between the tethering and priming apparatus by interacting with Munc13-1. Another possibility is that *RIM1*α directly regulates the priming activity of Munc13-1.

*RIM1*α PDZ domain interacts with the active zone proteins ERCs, ERCs being the acronym of the various names those proteins have in the literature (i.e. ELKS, Rab6-interacting protein 2, and CAST) (Ohtsuka et al., 2002; Wang et al., 2002).

Via their C-terminal C2B-domain, *RIM*s interact with α-liprins and in a calcium-dependent manner with synaptotagmin 1 (Schoch et al., 2002). Furthermore, *RIM*s have been shown to bind *in vitro* to cAMP-GEFII (guanine nucleotide-exchange factor) (Ozaki et al., 2000), SNAP-25 (25-kDa synaptosome-associated protein (Coppola et al., 2001), N-type calcium channels (Coppola et al., 2001), and 14-3-3 adaptor proteins (Simsek-Duran et al., 2004; Sun et al., 2003).

Finally, *RIM1*α indirectly interacts with L-type calcium channels through *RIM* binding proteins (RIM-BP) through the proline-rich region located between the C2 domains (Hibino et al., 2002, for review, Dresbach et al., 2001; Li and Chin, 2003).

In conclusion, thanks to its multiple binding partners, *RIM1*α occupies a central position in the presynapse and can participate to one or several steps of synaptic vesicle cycle, and coordinates the necessary proteins in time and space.

2) Role in transmission

- Presynaptic LTP

As a putative target of PKA, *RIM1*α could be involved in the expression of mfLTP. Castillo et al (Castillo et al., 2002) showed that in *RIM1*$\alpha^{-/-}$ mice, mfLTP in completely absent in the CA3 area of the hippocampus and in the cerebellum. Moreover, they showed that forkolin-induced potentiation is also abolished at CA3 synapse. As the synaptic responses elicited in mutant synapses were comparable in amplitude to those obtained in wild-type synapses, they concluded that *RIM1*α effect is specific to presynaptic LTP mechanisms, and that *RIM1*α acts downstream of PKA activation.

- Phosphorylation by PKA

Because presynaptic LTP is dependent on PKA and *RIM1*α, determining whether *RIM1*α is directly phosphorylated by PKA was important. *RIM1*α contains two consensus sites for PKA phosphorylation which are highly conserved among vertebrate species, one between the N-terminal zinc finger and the central PDZ domain (residues 410 to 413) and the second at the C-terminus (residues 1545 to 1548). In a very interesting study, Lonart et al (Lonart et al., 2003) showed that in primary cultures of cerebellar neurons from *RIM1*$\alpha^{-/-}$ mice presynaptic LTP was rescued by transfecting neurons with a wildtype (WT) copy of the *RIM1*α gene. Moreover, they could induce an LTP-like phenomenon by directly stimulating PKA with a cAMP analog, thereby bypassing the initial steps of the induction, in WT and "rescued" slices but not in *RIM1*$\alpha^{-/-}$ slices. This confirmed the fact that *RIM1*α is downstream of the AC/PKA pathway in the molecular cascade triggered by LTP induction. In order to address the question of PKA phosphorylation, they performed the same recue experiments with copies of *RIM1*α gene containing substitutions in the putative phosphorylation sites. As a point mutation at the serine 413 (and not at the serine 1548) blocked the rescue phenomenon, the authors concluded that phosphorylation of *RIM1*α at a single site, serine 413, by PKA is

required for presynaptic LTP of neurotransmitter release at cerebellar parallel fiber synapses, and probably more generally for mfLTP.

- Role in short-term changes

Schoch et al (Schoch et al., 2002) were the first group to compare the effects of *RIM1*α knockout (KO), Rab3A homozygous and Munc13-1 heterozygous KO mice on short-term plasticity at the Schaffer collateral to CA1 principal neuron synapse. First, these authors confirmed that *RIM1*α KO did not induce any upregulation in RIM2α expression. The only change in expression levels concerned a decrease by about 60% in Munc13-1 expression, probably because Munc13-1 binds to *RIM1*α (Betz et al., 2001) and become destabilized in the absence of *RIM1*α. *RIM1*$\alpha^{-/-}$ and Rab3A$^{-/-}$ mice presented a similar large increase in PPF at short interstimulus intervals (50ms) at excitatory synapses, while Munc13-1 heterozygous mice have no alterations in PPF. In contrast, in *RIM1*$\alpha^{-/-}$ inhibitory synapses (stratum radiatum to pyramidal neurons in CA1 area) the paired-pulse ratio was decreased, indicating that *RIM1*α might have different functions at excitatory and inhibitory synapses.

Longer lasting forms of short-term synaptic plasticity were also altered at excitatory synapses in *RIM1*$\alpha^{-/-}$ mice. PTP was increased and there was less depression at moderate stimulation frequencies as compared to WT controls. This suggests that *RIM1*α acts as a regulator of *P*. These data are similar to those obtained in Rab3A$^{-/-}$ mice, Munc13-1$^{+/-}$ mice being similar to WT. These results confirmed that *RIM1*α is linked to Rab3A and mediates its effects on synaptic transmission.

Calakos et al (Calakos et al., 2004) investigated the step of the synaptic vesicle cycle during which *RIM1*α is involved. To this aim, they recorded EPSCs in autaptic hippocampal neurons prepared from *RIM1*$\alpha^{-/-}$ and WT mice. They found a reduction in the EPSC charge for *RIM1*$\alpha^{-/-}$ neurons, associated with a 50% reduction in the RRP of synaptic vesicles measured upon stimulation with hypertonic solution. Interestingly, Calakos et al found a normal vesicular release probability, which means that primed vesicles in the remaining RRP undergo normal exocytosis. The remaining RRP is independent as well on RIM2α, absent in hippocampal cultures. Those findings revealed a role for *RIM1*α as an enhancer of neurotransmitter release through the potentiation of synaptic vesicle priming.

After the arrival of an action potential at an excitatory synapse, neurotransmitter release displays two components (Goda and Stevens, 1994): a fast and synchronous component triggered by synaptotagmin I (Fernandez-Chacon et al., 2002), and a slow, asynchronous component which is also calcium-dependent but not well understood. Calakos et al showed finally that *RIM1*α participates to about 50% of the asynchronous calcium-

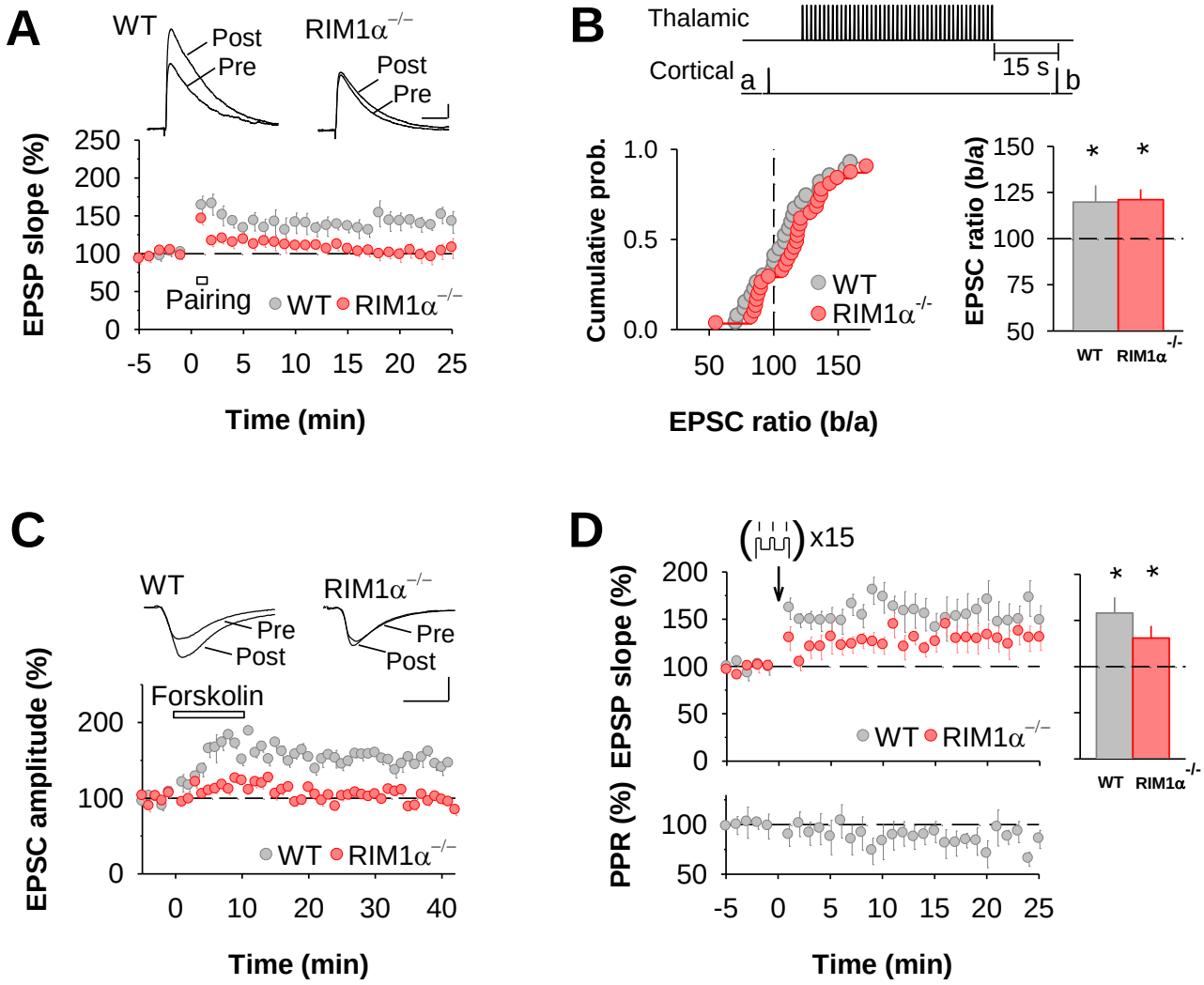

Figure 14 The PKA target RIM1α is necessary for the induction of presynaptic LTP. (A) Cortico-amygdala LTP is absent in *RIM1α*$^{-/-}$- mice (wild-type littermates: n = 5; *RIM1α*$^{-/-}$**:** n = 9; $p < 0.01$). Scale bars: 1 mV and 50 ms. **(B)** Heterosynaptic facilitation of cortico-LA synapses by tetanic stimulation of thalamic afferents is not altered in *RIM1α*$^{-/-}$ mice. (Top) Stimulation protocol used to assess cortico-LA PPR before and after tetanic stimulation (45 stim. at 30 Hz) of thalamo-LA afferents. (Bottom) Cumulative distribution of PPR values after tetanic stimulation of thalamo-LA afferents in *RIM1α*$^{-/-}$ mice (n = 33) and wild-type littermates (n = 28). (Right) *RIM1α*$^{-/-}$ mice and wild-type animals exhibited significant and equal heterosynaptic facilitation ($p < 0.05$ for both genotypes; wild-type vs. *RIM1α*$^{-/-}$: n.s.). *$p < 0.05$. **(C)** FSK-induced potentiation of synaptic transmission is completely abolished in *RIM1α*$^{-/-}$ mice (50 µM FSK; wild-type littermates: n = 16; *RIM1α*$^{-/-}$: n = 10; $p < 0.05$). Scale bars: 100 pA and 10 ms.**(D)** Expression of LTP at cortical afferents by pairing presynaptic stimulation with sustained postsynaptic depolarization, correlated with a decrease in PPR in wild-type mice (bottom), is partially reduced in *RIM1α*$^{-/-}$ mice (n = 5, $p < 0.05$).

triggered release, which implicates *RIM1α* in a post-priming step related to calcium-triggered fusion.

- Role in vivo

The fact that *RIM1α*$^{-/-}$ mice exhibit a deficit in short- and long-term synaptic plasticity in the hippocampus raises the question whether a deficit in *RIM1α* expression affects learning and memory in living mice. Powell et al performed a broad behavioral analysis in *RIM1α* deficient mice (Powell et al., 2004). They first tested emotional learning and memory, in a context-dependent fear conditioning paradigm, which requires both hippocampus and amygdala, and in a cue-dependent fear conditioning paradigm, which is strictly dependent on the amygdala. *RIM1α*$^{-/-}$ mice were significantly impaired in both context- and cue-dependent fear conditioning. *RIM1α*$^{-/-}$ mice also poorly performed in the Morris water maze, revealing a deficit in spatial learning, as well as in their locomotor response to novelty. On the other hand, *RIM1α*$^{-/-}$ mice exhibited normal coordination and anxiety-like behaviors. Taken together, these results showed that the hippocampus, but not the cerebellum, is affected by the mutation. Surprisingly, the authors neglected the putative involvement of the amygdala in those results.

B) Results

To address the role of *RIM1α* in presynaptically induced and expressed LTP_{HA} I compared LTP in *RIM1α*-deficient mice (*RIM1α*$^{-/-}$) and wild-type littermate controls. LTP was completely absent in *RIM1α*$^{-/-}$ mice (littermate controls: 143 ± 10%, n = 5, $p < 0.05$; *RIM1α*$^{-/-}$: 102 ± 10%, n = 9, n.s., Figure 14A). The observed deficit in LTP in *RIM1α*$^{-/-}$ mice could have been caused by a diminished glutamate release from thalamo-LA synapses, and therefore by a lack of NMDA receptor activation on cortico-LA terminals. To control for this I measured heterosynaptic interactions between thalamo- and cortico-LA synapses. Tetanic stimulation of thalamo-LA afferents leads to a heterosynaptic, NMDA receptor-dependent increase in the probability of release at cortico-LA synapses (Humeau et al., 2003). This heterosynaptic facilitation was not affected in *RIM1α*$^{-/-}$ mice (wild-type: 120 ± 9% of EPSC ratio; *RIM1α*$^{-/-}$: 121 ± 5 of EPSC ratio, Figure 14B). Therefore I can conclude that the absence of LTP in *RIM1α*$^{-/-}$ mice was due to a failure of LTP induction and/or expression at cortico-LA synapses.

In accordance with the lack of LTP, forskolin-potentiation was completely abolished in *RIM1α*$^{-/-}$ mice (littermate controls: 155 ± 4%, n = 16, $p < 0.05$; *RIM1α*$^{-/-}$: 104 ± 4%, n =

10, n.s.; measured 25-30 min after forskolin application)(Figure 14C). Thus, RIM1α is an essential component of the presynaptic machinery underlying LTP induction and/or expression at cortico-LA synapses.

In order to check whether *RIM1α*$^{-/-}$ mice exhibit a general deficit in LTP, or whether the deletion of *RIM1α* gene affects specifically presynaptic LTP, I decided to use a protocol which is known to trigger postsynaptic LTP: Classically, this kind of protocols consist in the pairing of presynaptic firing and postsynaptic depolarization, repeated several times. In the amygdala, pairing 15 bursts of 3 action potentials and 3 EPSPs at 30Hz induces STDP at thalamo-LA synapses, but no change of the synaptic strength at cortico-LA synapse. However, applying additional, sustained depolarization in between the APs during the bursts is sufficient to induce LTP at cortico-LA synapses. (Humeau et al., 2005) (see appendix C). The authors showed that this form of LTP was induced postsynaptically.

With the protocol described by Humeau *et al*, wild-type animals expressed LTP at a comparable level to what was expected (158 ± 17% of baseline, $n = 5$, $p < 0.05$, Figure 14D). *RIM1α*$^{-/-}$ mice exhibited a 50% lower LTP level (131 ± 13% of baseline, $n = 5$, $p < 0.05$). Moreover, sustained depolarization-induced LTP expression in WT mice was correlated with a trend to a decrease in PPR (82 ± 9% of baseline, ns), which is an indication for a presynaptic change. Thus pairing presynaptic firing to postsynaptic depolarization could involve some presynaptic mechanisms, which could explain why *RIM1α*$^{-/-}$ mice exhibit a partial deficit in this form of LTP.

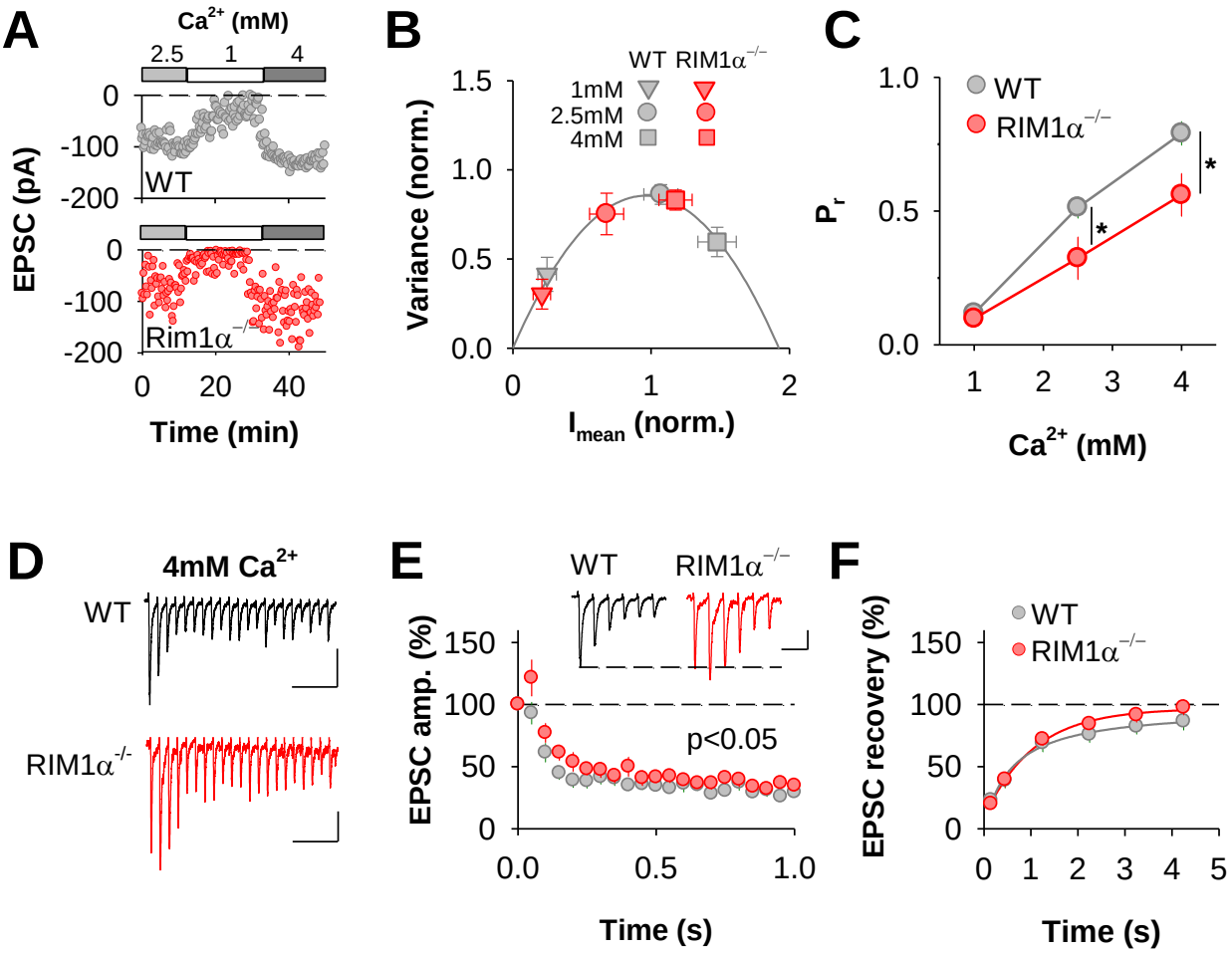

Figure 15: *RIM1α*$^{-/-}$ mice exhibit impaired Ca^{2+}-release coupling and altered short-term plasticity at cortico-LA synapses. (A-C) Variance-mean analysis reveals a significantly lower P at cortico-LA synapses in *RIM1α*$^{-/-}$ mice. **(A)** Representative examples illustrating variance of evoked EPSCs at different Ca^{2+} concentrations in wild-type littermates (top) and *RIM1α*$^{-/-}$ mice (bottom). **(B)** Averaged variance-mean plots for wild-type (n = 9) and *RIM1α*$^{-/-}$ mice (n = 8). Scaled parabolas reveal lower *P* in *RIM1α*$^{-/-}$ mice as compared to wild-type littermates. The effect increases with higher external Ca^{2+} concentrations. **(C)** P in wild-type mice and *RIM1α*$^{-/-}$ mice plotted as a function of external Ca^{2+} concentration. In *RIM1α*$^{-/-}$ mice P is significantly reduced at 2.5 mM ($p < 0.05$) and 4 mM Ca^{2+} ($p < 0.05$). **(D)** Repetitive train stimulation at 20 Hz reveals altered short-term plasticity in *RIM1α*$^{-/-}$ mice. Representative traces from wild-type littermates (top) and *RIM1α*$^{-/-}$ mice (bottom) recorded at 4 mM Ca^{2+}. Scale bars: 250 pA and 50 ms. **(E)** Averaged and normalized time course of EPSC depression during 20 Hz stimulation recorded at 4 mM Ca^{2+}. *RIM1α*$^{-/-}$ mice (n = 10) exhibited an initial facilitation followed by a significantly slower depression (n = 10, $p < 0.05$). Traces illustrate the first 6 EPSCs during 20 Hz train stimulation (same traces as in panel D). Scale bars: 50 pA and 100 ms. **(F)** Recovery from depression was not different between *RIM1α*$^{-/-}$ mice (n = 10) and wild-type littermates (n = 10; n.s.). *$p < 0.05$.

VI) RIM1α AND CALCIUM IONS

Although it seems that *RIM1*α C2 domains are not able to bind calcium ions (Wang et al., 1997), *RIM1*α has several binding partners which are able to bind calcium ions through their own C2 domains (for example, Munc13-1) or which are themselves permeable for calcium (N-type calcium channels, and indirectly to L-type calcium channels through RIM-BP). The involvement of *RIM1*α in calcium-dependent processes is thus an important issue to test.

Although deletion of *RIM1*α completely abolishes presynaptic LTP at a number of synapses, this does not correlate with changes in baseline release properties. For example, at hippocampal mossy fiber terminals, baseline release properties appear normal in *RIM1α*$^{-/-}$ mice, at least as judged by measuring PPR (Castillo et al., 2002). To address whether deficiency of *RIM1*α had an effect on baseline release properties of cortico-LA synapses we analyzed the probability of release at different Ca^{2+} concentrations using variance-mean analysis. Comparing the relation between EPSC variance and mean EPSC amplitude revealed a significantly lower baseline release probability in *RIM1α*$^{-/-}$ mice (n = 9) as compared to littermate control animals (n = 8, Figure 15A-C). The difference in *P* between wild-type and *RIM1α*$^{-/-}$ mice was increasing as a function of the extracellular Ca^{2+} concentration (Figure 15B,C). While at 1 mM external Ca^{2+} there was no significant difference detectable (wild-type: 0.12 ± 0.02, n = 9; *RIM1α*$^{-/-}$: 0.10 ± 0.03, n = 8; n.s.), increasing external Ca^{2+} to 2.5 mM or 4 mM revealed a significant deficit in *P* in *RIM1α*$^{-/-}$ mice (2.5 mM: wild-type: 0.51 ± 0.04, n = 9; *RIM1α*$^{-/-}$: 0.32 ± 0.08, n = 8; $p < 0.05$; 4 mM: wild-type: 0.79 ± 0.04, n = 9; *RIM1α*$^{-/-}$: 0.56 ± 0.08, n = 8; $p < 0.05$, Figure 15C). Thus, although *P* increases in *RIM1α*$^{-/-}$ mice with increasing external Ca^{2+} concentrations, the dependence of *P* on external Ca^{2+} is markedly less steep as compared wild-type controls. The normalization process introduces a loss of information concerning *Q* and *N*. Therefore, *Q* and *N* datas were collected from individual non-normalized parabolas and averaged. No significant difference was observed neither for *Q* (wild-type: 8.5 ± 0.7 pA; *RIM1α*$^{-/-}$: 11,2 ± 1,3 pA, ns) nor for *N* (wild-type: 26.7 ± 4.1 sites; *RIM1α*$^{-/-}$: 28.5 ± 8.5 sites, ns).

The difference in the baseline probability of release and in the Ca^{2+}-dependency of release in *RIM1α*$^{-/-}$ animals predicts that short-term synaptic dynamics might be altered. Therefore I analyzed short-term plasticity of cortico-LA synapses during and after delivering trains of stimuli at 20 Hz. Given that the difference in baseline *P* was most prominent at high Ca^{2+}

concentrations, these experiments were performed in the presence of 4 mM external Ca^{2+}. Analysis of EPSCs during 20 Hz stimulation revealed that *RIM1α*$^{-/-}$ mice exhibited increased short-term facilitation during the initial phase of the stimulation train (wild-type: n = 10; *RIM1α*$^{-/-}$: n = 10; $p < 0.05$)(Figure 15D,E). During the later phase of 20 Hz stimulation (i.e. after 6-7 stimuli) synaptic transmission reached similar levels of steady-state depression in *RIM1α*$^{-/-}$ and wild-type control mice (last 5 stimuli: wild-type: 30 ± 5% of first EPSC, n = 10; *RIM1α*$^{-/-}$: 35 ± 4% of first EPSC, n = 10; n.s.)(Figure 15D).

The level of steady-state depression during train stimulation depends on a number of factors including *P*, the rate of refilling of the readily releasable pool of synaptic vesicles, and the rate of vesicle recycling (Zucker and Regehr, 2002). Indeed, lowering *P* by reducing external Ca^{2+} from 4 mM to 2 mM not only increased facilitation during the first few stimulations, but also reduced the level of steady-state depression (last 5 stimuli: 4 mM: 31 ± 4% of first EPSC, n = 10; 2 mM: 61 ± 5% of first EPSC, n = 15; $p < 0.01$) (Figure S4). Given that the initial P is reduced in *RIM1α*$^{-/-}$ mice, this suggests that during train stimulation either P or the rate of vesicle supply catches up to compensate for the reduced initial P. Since recovery of depression, reflecting the rate of refilling of the readily releasable pool of synaptic vesicles, was normal in *RIM1α*$^{-/-}$ mice (n = 10; n.s.)(Figure 6E), the probability of vesicular fusion is most likely non-stationary during train stimulation in *RIM1α*$^{-/-}$ mice (Calakos et al., 2004).

Taking together the normal rate of refilling of the readily releasable pool and the fact that the difference in initial P is largely Ca^{2+}-dependent, this suggests that the deficit in overall P in *RIM1α*$^{-/-}$ mice is mediated by a reduced probability of vesicular fusion rather than by a deficit in vesicle priming associated with a smaller readily releasable pool. Finally, analysis of steady-state depression levels is consistent with the idea that *RIM1α*$^{-/-}$ mice exhibit differential changes in P during train stimulation. Thus, RIM1α appears to play a central role in regulating the dynamics of Ca^{2+}-release-coupling at cortico-LA synapses.

VII) RIM1α AND PRESYNAPTIC CALCIUM CHANNELS

As *RIM1α*$^{-/-}$ mice exhibit deficits in calcium-dependent release, it was important to examine the role of voltage-dependent calcium channels (VDCCs). *RIM1α* has been reported to directly or indirectly interact with different presynaptic VDCCs.

A) Introduction to presynaptic voltage-dependent calcium channels

1) General description

a) Subunit composition

VDCCs are complex proteins composed of four or five distinct subunits, which are encoded by multiple genes. An intracellular β subunit and a transmembrane, disulfide-linked $\alpha_2\delta$ subunit complex are components of most types of VDCCs, sometimes associated with a γ subunit. The α1 subunit of 190 to 250 kDa is the largest subunit (Figure 16A). It forms the conduction pore, the voltage sensor and the gating apparatus. It is also the site of channel regulation by second messengers, drugs, and toxins. Although these auxiliary subunits modulate the properties of the channel complex, the key factor determining the pharmacological and electrophysiological diversity of VDCCs is the existence of multiple forms of α1 subunits (for review, Ertel et al., 2000).

b) Families

There are at least 6 functionally distinct voltage-dependent calcium channel (VDCC) subtypes described so far in the CNS: L-, N-, P-, Q-, R- and T-type (Catterall, 2000; Tsien et al., 1988).They can be regrouped in 3 families according to their sequence homology (for review, Elmslie, 2003) (Figure 16B):

- Ca_V1 family: it is composed of L-type VDCCs. They are sensitive to dihydropyridines (DHPs). Neurons can express 3 members of this family, CaV1.2, CaV1.3 and CaV1.4.
- Ca_V2 family: it includes P/Q-type (CaV2.1), N-type (CaV2.2) and R-type (CaV2.3). N-type VDCCs are blocked by ω-conotoxins, P/Q-type VDCCs are blocked by ω-agatoxins. R-type VDCCs are defined by the impossibility to specifically block them,

as T-type VDCCs they are sensitive to nickel. However, a subtype of R-type VDCCs is selectively blocked by the toxin SNX-482.

- Ca_V3 family: it consists of T-type VDCCs. All three members of this family are widely expressed in the CNS. They are non-specifically blocked by nickel and are characterized by a low threshold voltage for activation and a fast inactivation.

c) Nomenclature

Initially, VDCCs were separated into two groups. The first group regrouped the low voltage-activated channels (LVA) which are rapidly inactivated channels and are activated by a weak depolarization. The second group corresponded to high voltage-activated channels (HVA), which require a stronger depolarization, and exhibit variable inactivation patterns (Carbone and Lux, 1984). Three different nomenclature were then used simultaneously: a classification in function of the subunit composing the pore of the channel; a classification based on the current recorded (L-, P-…); and the separation in families based on structural homologies, the Ca_V nomenclature (Ertel et al., 2000).

In the following parts, I will use the nomenclature based on the electrophysiological current recordings (Figure 16).

2) Physiology of voltage-dependent calcium channels

a) Activation

The time necessary for VDCC activation is specific for each family of VDCCs, on average it requires approximatively 1 ms for L-, P/Q-, N- and R-type VDCCs. The order of activation is $\alpha1_D > \alpha1_C > \alpha1_A > \alpha1_B > \alpha1_G$ (from faster to slower) (for review, Jones, 2003). The activation of VDCCs is regulated by the $\beta\gamma$ subunits of G proteins, which can slow down the activation of N- and P/Q-type VDCCs as well as increasing the voltage requested for the opening of the channel (for review, Catterall, 2000).

b) Selectivity

Voltage-dependent calcium channels become nonselective for cations in the absence of Ca^{2+} ions. In presence of Ca^{2+} ions, the presence of a glutamate residue in the pore region lead to out all other cations. The glutamate residue is absent in sodium channels,and mutating the corresponding site in sodium channels transform them into a kind of channel sharing many of the features of calcium channels (Heinemann et al., 1992).

c) Inactivation

In general, VDCCs can be inactivated either by calcium- or voltage-dependent mechanisms (Budde et al., 2002; Eckert and Chad, 1984; Hering et al., 2000; Stotz and Zamponi, 2001). Calcium-dependent inactivation is a calmodulin-dependent process, involving sites on the C-terminal domain of the channel (Peterson et al., 1999; Zuhlke et al., 1999) whereas voltage-dependent inactivation depends on the type of VDCC. For example, T-type VDCC tend to inactivate rapidly and almost completely (Perez-Reyes, 2003; Yunker and McEnery, 2003). VDCC activation state can also be modulated by their subunits, by phosphorylation and by G-protein binding (Zamponi and Snutch, 1998). The inactivation site is not clear, a candidate is the loop between domains I–II (Stotz and Zamponi, 2001).

3) Role in neurotransmission

At excitatory synapses, it is generally believed that the entry of Ca^{2+} ions that triggers neurotransmitter release is performed through N- and P/Q type VDCCs. In most systems, N-type channels are responsible for the majority of excitatory transmitter release early in development, whereas P/Q-type VDCCs become more prominent during maturation. There are also evidence for very little coexpression of N-type and P/Q-type VDCCs (for review, Reid et al., 2003). If involvement of N and P/Q channels in transmitter release is the rule, it must be noted some exceptions. R-type VDCCs can contribute to baseline transmission at specific synapses (Gasparini et al., 2001; Iwasaki and Takahashi, 1998; Wu et al., 1998), but their major role concerns synaptic plasticity (Dietrich et al., 2003). L- and T-type VDCCs are usually considered to have no role in neurotransmitter release at the CNS (but see Heidelberger and Matthews, 1992; Jensen and Mody, 2001; Pan et al., 2001).

4) Synaptic localization

a) Spatial distribution

The specific involvement of subtypes of VDCCs in neurotransmitter release can result from their differential localization at the presynaptic active zone. Several putative targeting motifs were identified. The C terminus of N-type VDCCs contains elements that interact with the scaffolding proteins Mint1 and CASK, which are required for both targeting and channel function (Maximov and Bezprozvanny, 2002). Another possible targeting motif is the synaptic protein interaction site, called synprint, found in the intracellular loop L_{II-III} on the α-

subunit of both N-type and P/Q-type VDCCs (Mochida et al., 2003; Spafford and Zamponi, 2003) (see Figure 16A).

b) Synaptic protein binding

At the presynaptic active zone, calcium channels are associated with SNARE proteins. The first proof came from colocalization experiments between high-density clusters of N- or P/Q-type VDCCs and the SNARE protein syntaxin (Westenbroek et al., 1995). More recently, binding experiments showed that the synprint of N- and P/Q-type VDCCs binds specifically to synaptotagmin and to the SNARE proteins SNAP-25 and syntaxin. This binding occurs in a Ca^{2+}-dependent manner (Sheng et al., 1998; Walker and De Waard, 1998, for review, Zamponi, 2003). The specific interaction of VDCCs with SNARE proteins can be explained by the very important role of calcium in synaptic vesicle exocytosis.

N-type VDCCs can also directly bind *RIM1*α C2B domains (Coppola et al., 2001). L-type VDCCs can bind *RIM* binding proteins (RIM-BP), and thus indirectly interact with *RIM1*α (Hibino et al., 2002).

B) Results

Since some VDCCs play an important role in normal release processes and therefore might interfere with LTP induction indirectly by reducing the amount of glutamate released during tetanic stimulation, I first evaluated the effect of VDCC antagonists on forskolin-potentiation, which depends on the same induction and expression mechanisms as LTP. Comparing antagonists against L-type (verapamil, 50 µM), N-ype (ω-conotoxin, 1 µM) and P/Q-type (ω-agatoxin, 0.5 µM) VDCCs revealed a specific role of L-VDCCs in forskolin-potentiation (Figure 17A,B). While forskolin-potentiation was normal in the presence of N-VDCC and P/Q-VDCC antagonists (control: 144 ± 13% of baseline, n = 17; ω-conotoxin: 146 ± 14% of baseline, n = 10, $p < 0.05$; ω-agatoxin: 145 ± 13% of baseline, n = 4, $p < 0.05$, Figure 17B), forskolin-potentiation was completely abolished by the L-VDCC antagonist verapamil (78 ± 13% of baseline, n = 6, n.s., Figure 17A,B). As a control, I applied sequentially the different calcium antagonists on basal transmission (n = 7, Figure 17C): N- and P/Q-type VDCCs were responsible for respectively 37 and 32% of the transmission, although they were not involved in LTP_{HA}. L-type VDCC antagonist blocked 19% of the EPSC amplitude. As forskolin potentiated the EPSC amplitude by 50%, and this potentiation was completely reversed by verapamil, then verapamil effect on forskolin-potentiation could not be explained just by a decrease of basal transmission.

Since verapamil has been reported to interact with other channels in addition to L-VDCCs (e.g. (Aicardi and Schwartzkroin, 1990; Ruschenschmidt et al., 2004), we confirmed the effect on forskolin-potentiation using another L-VDCC antagonist (nimodipine, 10 µM), which also completely blocked forskolin-potentiation (90 ± 15% of baseline, n = 8, n.s., Figure 17B). Since forskolin-potentiation and LTP_{HA} utilize the same molecular machinery we next tested whether L-VDCCs were also necessary for electrically-induced LTP. LTP_{HA} was completely blocked in the presence of verapamil (control: 146 ± 12%, n = 19, $p < 0.05$; verapamil: 95 ± 11%, n = 9, n.s.)(Figure 17D). These experiments show that LTP_{HA} requires the activation of L-VDCCs, and that L-VDCCs, like *RIM1α*, are downstream of PKA in the molecular cascade. Thus, L-VDCCs might contribute to either the induction or expression of presynaptic LTP_{HA}.

VIII) L-TYPE VOLTAGE-DEPENDENT CALCIUM CHANNELS

A) Introduction

1) L-VDCCs in muscles cells

L-type VDCCs are mainly known to couple excitation to contraction in the skeletal, cardiac and smooth muscles. Their coupling to intracellular mechanisms is extremely different in each of those muscle types (for review, Wang et al., 2004).

2) L-VDCCs in hair cells

Presynaptic L-type VDCCs has been reported in hair cells of the auditory pathway. Hair cells are tonically releasing cells and L-type VDCCs are the only subtype required for the continuous transmitter release (Fuchs et al., 1990; Moser and Beutner, 2000; Platzer et al., 2000; Roberts et al., 1990; Spassova et al., 2001). The mechanism underlying the coupling of L-type VDCCs with tonic release is still poorly understood.

3) CNS neurons

a) Basal neurotransmission

Although the general dogma is that L-type calcium channels play no role in neurotransmitter release in the CNS, few works reported the presence of L-type VDCCs in various parts of the CNS, including hippocampus, striatum and thalamus, and their physiological role (Avery and Johnston, 1996; Vergara et al., 2003; Zhuravleva et al., 2001). Interestingly, the current recorded in those experiments showed characteristics of T-type VDCCs as they are activated at a low voltage. On the other hand those currents were partially reduced by the application of dihydropyridines, which is specific to L-VDCCs currents. The explanation of this paradox comes from a bias committed in L-type VDCC characterization studies: they concerned so far only $Ca_V1.2$ subtype, which are high-voltage-activated channels with a high sensitivity to dihydropyridines. On the contrary, $Ca_V1.3$ and $Ca_V1.4$ L-type VDCCs have a low-threshold activation and exhibit only a partial block by dihydropyridines.

This corresponds exactly to the observations by Avery and Johnston, Vergara et al and Zhuravleva et al (for review, Lipscombe et al., 2004).

b) Synaptic plasticity

L-type VDCCs are also involved in synaptic plasticity. Their importance was shown in postsynaptic NMDAR-dependent form of LTP in the CA1 area of the hippocampus (Udagawa et al., 2006; Zakharenko et al., 2001), the striatum (Vergara et al., 2003), the superior colliculus (Zhao et al., 2006) or the amygdala (Bauer et al., 2002). L-type VDCCs were also hypothesized to be the only trigger of LTP in the basolateral amygdala-dentate gyrus pathway (Niikura et al., 2004).

Recently, a group showed that the activation of presynaptically silent synapses in the hippocampus is dependent on L-type VDCCs, PKA and actin polymerization (Yao et al., 2006). These authors reported that the potentiation of miniature EPSC (mEPSC) amplitude, the presynaptic enhancement of mEPSC frequency and the FM staining was blocked by L-type antagonists. Although they did not demonstrate whether L-type VDCCs are pre- or postsynaptic, they discovered of an unconventional presynaptic plasticity.

c) Fear conditioning

In spite of the relatively weak involvement of L-type VDCCs in neurotransmitter release, they seem to play a role *in vivo*, more specifically in fear memory formation. Shinnick-Gallagher et al studied their importance *in vivo* in the amygdala (Shinnick-Gallagher et al., 2003). L-type VDCCs antagonists blocked the expression of fear-potentiated startle in a dose-dependent manner. By comparing the physiology of brain slices coming from naïve and fear-conditioned animals in an *ex vivo* approach, the authors could observe a fear-induced and L-type dependent potentiation of the EPSCs, coupled to a decrease of PPF. This last point in particular is an indication that L-type VDCC involvement in learning and memory could be at least partially dependent on presynaptic mechanisms.

B) Results

To examine whether L-VDCCs contribute to LTP expression I first compared the effect of verapamil on synaptic transmission at naive synapses and at synapses where LTP had been induced. To avoid a possible confound due to a reduction in glutamate release from

thalamo-LA synapses during LTP induction, I used forskolin to potentiate synaptic transmission independent of thalamo-LA afferent stimulation.

In naïve slices bath application of verapamil resulted in a small but significant reduction in synaptic transmission (16 ± 5% inhibition, n = 8, $p < 0.05$, Figure 18A). In contrast, when verapamil was applied after induction of forkolin-potentiation, the impact of verapamil, and thus the contribution of L-VDCCs to synaptic transmission, was markedly increased (38 ± 8% inhibition, n = 11, $p < 0.05$)(Figure 18B,C). In the absence of verapamil, LTP_{FSK} remained stable for the duration of the experiment (Fig. 18B).This indicates that L-VDCCs are necessary for the expression of LTP_{HA}.

To further address this point using an independent measure, I analyzed changes in short-term plasticity induced by forkolin and whether such changes could be reversed by an L-VDCC antagonist. Forkolin-potentiation was associated with a significant shift in short-term synaptic plasticity during repetitive 20 Hz stimulation (Figure 19A). Consistent with the fact that forskolin induces an increase in *P*, forskolin application resulted in a more rapid depression of cortico-LA EPSCs during 20 Hz stimulation (n = 10, $p < 0.05$). Moreover, the steady-state level of depression was lower than in naïve slices (last 5 stimuli: control: 60 ± 5% of the first response amplitude, n = 10; FSK: 40 ± 3% of the first response amplitude, n=10, $p < 0.05$)(Figure 19A), indicating that LTP induction predominantly increases the probability of vesicular release, without any concomitant increase in the rate the readily releasable pool is refilled during repetitive stimulation. Application of the L-VDCC antagonist verapamil completely reversed the forskolin-induced changes in short-term synaptic plasticity (n = 7)(Figure 19B). In the presence of verapamil, both the rate of depression, as well as the steady-state level of depression were not significantly different from control slices (last 5 stimuli: control: 60 ± 5% of the first response amplitude, n = 10; FSK + verapamil: 60 ± 5% of the first response amplitude, n = 7, n.s., Figure 19B). Taken together, these data demonstrate that the expression of presynaptic LTP_{HA} and forskolin-potentiation are almost entirely due to a change in L-VDCCs function.

Since both L-VDCCs and *RIM1*α are required for LTP_{HA} downstream of PKA activation, and because previous reports have demonstrated direct or indirect functional interactions between *RIM1*α and L-VDCCs in other systems, I next examined the contribution of L-VDCCs to synaptic transmission in $RIM1\alpha^{-/-}$ mice. In slices from wild-type and $RIM1\alpha^{-/-}$ mice blockade of L-VDCCs (in 4 mM external Ca^{2+}) resulted in similar levels of inhibition of synaptic transmission (wild-type: 75 ± 11% of baseline, n = 9; $RIM1\alpha^{-/-}$: 74 ± 10%, n = 9, $p < 0.05$, Figure 20A), indicating that L-VDCCs are present at similar levels in $RIM1\alpha^{-/-}$ mice and in control mice..

To address a possible functional alteration in L-VDCC during short-term synaptic plasticity I examined the impact of verapamil on PPR in *RIM1α*$^{-/-}$ mice and littermate controls. While L-VDCC blockade markedly increased PPR in wild-type mice (control: 1.00 ± 0.08, n = 16; verapamil: 1.79 ± 0.59, n = 6, $p < 0.05$), PPR was not significantly affected in *RIM1α*$^{-/-}$ mice (control: 1.34 ± 0.12, n = 17; verapamil: 1.46 ± 0.17, n = 7, n.s., Figure 20B). Thus, while L-VDCCs equally contribute to synaptic release upon single-shock stimulation in wild-type and *RIM1α*$^{-/-}$ mice, the temporal dynamics of L-VDCC contribution to short-term synaptic plasticity is altered in the absence of *RIM1α*. This indicates that *RIM1α* determines the functional coupling of presynaptic L-VDCCs to the release process.

IX) GENERAL DISCUSSION

During my PhD studies, I investigated the molecular mechanism requested for the induction and the expression of LTP_{HA}, a presynaptic LTP described in the lateral amygdala and dependent on cortical presynaptic NMDA receptor. I found that LTP_{HA} is entirely mediated by an increase in the probability of vesicular release. Downstream of the cAMP/PKA pathway, LTP induction and expression depends on the active zone protein *RIM1*α and L-type voltage-dependent Ca^{2+} channels (L-VDCCs). *RIM1*α-deficient mice not only exhibited a lack of presynaptic LTP but also showed reduced Ca^{2+}-sensitivity of evoked synaptic transmission and altered coupling of L-VDCCs to synaptic release.

A) cAMP, adenylyl cyclase and PKA in LTP_{HA}

In this study, I have investigated the molecular mechanisms responsible for presynaptic LTP induction and expression in the LA. My results indicate minor PKC involvement (Figure 10). In addition, I have observed that blocking the AC/PKA pathway prevents the possibility to induce LTP_{HA} (Figure 12); and stimulating this pathway occludes LTP_{HA} (Figure 11). My findings implicate an increase in cAMP underlay LTP_{HA}. This is consistent with a substantial body of evidence implicating that cAMP activates cAMP-dependent protein kinase (PKA) and elicits a long-lasting increase in transmitter release at many central synapses (Chavez-Noriega and Stevens, 1994; Colwell and Levine, 1995; Salin et al., 1996; Weisskopf et al., 1994). This effect is also believed to underlie long-term potentiation of synaptic efficacy and memory consolidation (Bailey et al., 1996).

1) The adenylyl cyclase involved

Almost all the isoforms of AC so far known are expressed in the brain. Five of them are calcium-sensitive: AC1, AC3, AC5, AC6 and AC8. Yann Humeau demonstrated that LTP_{HA} is triggered by a calcium flow through NMDAR located at the presynaptic cortical terminal (Humeau et al., 2003). It is thus tempting to speculate that the calcium transients due to activation of presynaptic NMDARs mediate the AC recruitment necessary for $LTP_{HA.}$ The identity of the AC isoform(s) expressed in the LA and involved in LTP_{HA} remains unknown, however some isoform are unlikely to be involved. For instance, the AC5 and AC6 isoforms

are inhibited by a calcium rise, thereby leading to decrease in the cAMP levels. Hence, by inference, their implication is unlikely. Among the three remaing calcium-calmodulin stimulated AC, two isoforms deserve special consideration: AC1 and AC8 knock-out studies showed that these two AC isoforms are involved in hippocampal-dependent synaptic plasticity and memory formation (for review, Ferguson and Storm, 2004; Wang and Storm, 2003). Moreover, the anterior cingulate cortex expresses a form of LTP that depends mainly on AC1, and maybe on AC8, and requires calcium entry through NMDAR and L-type VDCCs. On the basis of this striking similarity with LTP_{HA} (LTP_{HA} implicates NMDAR (Humeau et al., 2003) and L-type VDCCs (my study)), it is tempting to speculate that calcium-calmodulin dependent AC1 and/or AC8 might be involved in LTP_{HA} induction. Further experiments are needed to verify this possibility.

2) Similarity of the forskolin LTP and LTP_{HA}

In this study, several pieces of evidence converged to the idea that LTP_{HA} and forskolin-LTP are identical in their expression mechanism. First, forskolin-LTP occludes any further induction of LTP_{HA} (Figure 11B). Second, they are both blocked by the application of H89 (Figure 12B). Last, LTP_{HA} and Forskolin-LTP are both mediated by an increase in the probability of vesicular release. Taken together, these results indicate that LTP_{HA} and forskolin-LTP share the same molecular pathway. As Forskolin-LTP directly activates the AC/PKA pathway, any mechanism blocking both forms of presynaptic LTP is necessarily downstream of PKA recruitment.

3) Is PKA the only target of cAMP?

In neurons and other secretory cells such as the pancreatic beta-cells, it has been established that protein kinase A (PKA) is not the only cAMP-binding protein: cAMP can bind to *Epac (Epac1 and Epac2)*, a guanine-nucleotide exchange factor for Rap, which is a small GTPase that has been implicated in long-term ultrastructural synaptic plasticity in hippocampal neurons (Fu et al., 2007). PKA-independent actions of cAMP, likely to be mediated by Epac, enhance the release of transmitters and hormones. For example, at the crayfish neuromuscular junction, cAMP activates presynaptic exchange proteins via the cAMP-Epac pathway and hyperpolarization and cyclic nucleotide-activated (HCN) channels, thereby increasing transmitter release (Beaumont and Zucker, 2000; Zhong and Zucker, 2005). At the calyx of Held, cAMP facilitates transmitter release via activating the *Epac* pathway in the nerve terminal (Kaneko and Takahashi, 2004). In the pancreatic ß-cells *Epac*

couples cAMP production to the stimulation of fast calcium-dependent exocytosis and mediates the cAMP-dependent mobilization of calcium from intracellular calcium stores, thus modulating the efficacy of secretion (Kwan et al., 2007). Similarly, cAMP *Epac*-dependent and protein kinase A-independent signaling cascade have been shown to control neuronal excitability, these effects involve the activation of Rap and p38 MAPK, which then mobilizes intracellular calcium stores (Ster et al., 2007). Moreover, PKA and *Epac* can share common downstream targets: for example in the ß-cells, Epac2 and *RIM2* interact together (Ozaki et al., 2000) and bind to Munc13-1 (Kwan et al., 2007), which is a key actor in the priming of synaptic vesicles (Augustin et al., 2001).

Despite the impressive list of evidence supporting a potential role of *Epac* in mediating increase in neurotransmitter release, we can rule out the possibility that *Epac* plays a role in the LTP_{HA} mechanisms: it is now well established that H89 -the PKA inhibitor I used in my experiments- leaves *Epac* intact (Huang and Hsu, 2006; Kwan et al., 2007; Ster et al., 2007), but similarly as Rp-cAMPs does, H89 blocks the induction of LTP_{HA}. Moreover, H89 blocks Forskolin-LTP, which confirms that Forskolin activates PKA via the stimulation of AC and cAMP production. All together, these findings clearly indicate that PKA is the only cAMP-binding target activated following the increase in cAMP levels. Thus, recruitment of the AC/PKA pathway is likely to mediate LTP_{HA} (induction and/or expression) (Figures 16 and 17).

B) RIM1α in LTP

1) RIM1α is the target of PKA during LTP_{HA}

Many possible targets of PKA are likely being involved in up-regulating neurotransmitter release. This comprises i) the calcium channels (for N-type VDCCs see Yokoyama et al., 1997, for L-type VDCCs, see below) and 2) several proteins of the exocytotic machinery.

Indeed PKA has been reported to phosphorylate the SNARE protein SNAP-25 (Nagy et al., 2004), several proteins interacting with the SNAREs as Snapin and the cyst-string-proteins (reviewed by Evans and Morgan, 2003), and other regulatory proteins of the exocytotic machinery thought to be involved in the priming mechanisms as the synapsins, and the two targets of Rab3-GTPAse: Rabphilin (Lonart and Sudhof, 1998) and *RIM* (including *RIM1α*) (Lonart et al., 2003). Other essential proteins of the release machinery as Munc18 and Munc13 are phophorylated by PKC.

Phosphorylation of SNAP-25 has been reported to regulate the RRP sizes in chromaffin cells following its phosphorylation (Nagy et al., 2004) but this mechanism has never been suspected to play a role in LTP. Synapsins have been found to be not necessary for the induction or expression of postsynaptic LTP at the Schaffer collateral-CA1 synapse,but also for presynaptic LTP at the mossy fiber (mf)-CA3 pyramidal cell synapse in the hippocampus. Furthermore, synapsins play no role in mediating the enhancement in transmitter release elicited by PKA activation (for review, Spillane et al., 1995). Recently, cAMP-dependent tyrosine phosphorylation of Rabphilin has been reported to occur during the late phase of long-lasting LTP in CA1 (Capron et al., 2007). Thus, with the exception of *RIM1*α, none of the mentioned proteins are candidates to be phosphorylated by PKA and to support expression of LTP.

In line with above mentioned finding, I have reported that presence of *RIM1*α is required for LTP_{HA} expression (Figure 14) or Forskolin-LTP. This is highly suggestive that a NMDAR-AC-PKA-*RIM1*α pathway is involved in LTP_{HA}, reminiscent of the presynaptic AC-PKA-*RIM1*α pathway already demonstrated in the hippocampus at the mossy fiber to CA3 pyramidal neuron synapse, and in the cerebellum at the parallel fiber to purkinje cell synapse (Castillo et al., 2002; Castillo et al., 1994; Lonart et al., 2003; Nicoll and Malenka, 1995; Zalutsky and Nicoll, 1990). Intringuingly, a similar NMDAR-AC-PKA-*RIM1*α pathway has been reported to play a role in postsynaptic Late-LTP but not Early-LTP in the hippocampal Schaffer collaterals to CA1 synapse (Huang et al., 2005). Thus, implication of a NMDAR-AC-PKA-*RIM1*α can no longer be considered as pinpointing a presynaptic locus for expression of LTP. Postsynaptic implication of the pathway AC-PKA-*RIM1*α is consistent with the notion that the mechanisms involved in membrane insertion of AMPAR during LTP in CA1 is mediated by an exocytotic machinery very similar to the presynaptic one involved in neurotransmitter release (Lledo et al., 1998).

In addition to the role of *RIM1*α in LTP_{HA} expression, I found that *RIM1*α was partially involved in another form of LTP at cortico-LA synapse, the sustained depolarization-induced LTP (Figure 14D). This LTP, induced by pairing presynaptic firing with postsynaptic depolarizations, was considered to be postsynaptic (Humeau et al., 2005). Interestingly, Huang et al (2005) found as well a LTP depending from post- and presynaptic mechanisms at corticoamygdala pathway, and they observed a partial decrease in LTP expression for *RIM1*$\alpha^{-/-}$ mice. It implies two different possibilities: either *RIM1*α has a postsynaptic role, or sustained depolarization-induced LTP requests some presynaptic mechanisms as well. If *RIM1*α is present at the postsynaptic side, it could have an influence on LTP_{HA} as well.

Several lines of evidence confirm LTP_{HA} expression is purely presynaptic:

- LTP_{HA} is dependent on calcium, and blocking calcium signaling with BAPTA infusion in the postsynapse has no effect on LTP induction (Humeau et al., 2003)
- it is coupled to PPR decrease (Humeau et al., 2003) (Figure 4)
- fluctuation analysis with mean current amplitude plotted against $1/(cv)^2$ (Humeau et al., 2003) or the variance of the signal (Figure 6) both showed that LTP_{HA} induction is correlated with an increase in *P*, and no change in *Q*
- the amplitude of stimulation-induced miniature EPSCs obtained in the presence of strontium is not affected by LTP_{HA} induction; meaning that quantal amplitude *Q* was not changed by LTP_{HA} (Humeau et al., 2003)
- homosynaptic LTP induced by the suppression of $GABA_B$ inhibition on presynaptic cortical afferents is not blocked by postsynaptic infusion of a membrane-impermant form of RpcAMPs (unpublished datas from Hamdy Shaban). Homosynaptic LTP is dependent on AC/PKA pathway and fully occludes with LTP_{HA}, thus demonstrating that these two LTP share the same presynaptic induction pathway.

However, the deletion of a postsynaptic protein could have no influence in the expression of a presynaptic LTP. In wild-type animals, sustained depolarization-induced LTP is coupled with a decreased PPR, which is an indication for an increase in the probability of release. Thus it seems very likely that sustained depolarization-induced LTP is partially due to presynaptic mechanisms and *RIM1*α is only presynaptic. Further experiments on sustained depolarization-induced LTP, such as fluctuation analysis, could be interesting to be performed in order to confirm this hypothesis.

The two forms of presynaptic LTP in the hippocampus and the cerebellum in which the AC-PKA-*RIM1*α pathway has been implicated (for refs see above) are induced in a very different way from LTP_{HA}. Indeed LTP_{HA} needs the activation of NMDAR at the cortical-amygdala presynapse, which is an unusual mechanism. Moreover, NMDAR activation is dependent on the co-stimulation of the cortical and the thalamic afferents. This heterosynaptic associative induction mechanism is unique in the CNS. This raises the question of the role of *RIM1*α in neurotransmitter release and synaptic plasticity, and whether the steps downstream from *RIM* are specific for LTP_{HA} or shared with other forms of LTP.

2) Does *RIM1α* play a role in the SV priming mechanisms?

RIM1α is generally considered as a key molecule involved in the priming mechanism of synaptic vesicles. In *C. elegans* unc-10 mutants lacking *RIM*, normal levels of synaptic vesicles appearing morphologically docked at the release sites have been reported, suggesting

that *RIM* is not involved in the SV traffic or tethering at the release sites. Moreover NT release is reduced fivefold without change in calcium sensitivity of release events (Koushika et al., 2001). On this basis it has been first proposed that *RIM1*α acts during a step downstream from tethering of synaptic vesicles to the release site but before the fusion step. This is likely to correspond to priming, the ensemble of molecular events enabling synaptic vesicles to be ready-to-release. *RIM1*α is associated to plasma membrane and can form a tripartite complex with the SV-associated Rab3 GTPase and protein kinase Munc13 (Dulubova et al., 2005). Indeed, *RIM1*α can recruit Munc13 isoforms at the active zone (Andrews-Zwilling et al., 2006; Betz et al., 2001) and disruption of the *RIM*/Munc13 interaction leads to decrease in the size of the RRP in the calyx of Held synapse (Dulubova et al., 2005). Moreover, this complex may support expression of synaptic plasticity. For example, Munc13 can also form a complex with calmodulin, thereby mediating calcium-dependent modulation of the RRP size in the hippocampus (Junge et al., 2004). However, at mice lacking *RIM1*α, exocytosis still occurs suggesting it is not fully indispensable (or compensated) (Calakos et al., 2004; Schoch et al., 2002), thus *RIM1*α may boost the priming mechanisms.

If these above deductions are right, the priming mechanisms should be slower in nerve terminals taken from mice lacking *RIM1*α. When the stimulation frequency is increased, neurotransmitter release in *RIM1*$\alpha^{-/-}$ synapses should be more susceptible to undergo high-frequency depression because the priming mechanisms are too slow to refill on time the RRP. This should express as faster depletion kinetics, lower level for the plateau reach during depression and slower time constant for recovery of initial level of transmission when the high frequency stimulus is terminated. To my surprise, no significant change in depression and recovery kinetics or plateau level was detected at cortical (Figure 15) and thalamic (not shown) synapses onto the pyramidal cells in the LA taken from *RIM1*$\alpha^{-/-}$ mice. This clearly argues against the possibility that *RIM1*α plays role in priming, but does not negate the possibility that it plays other roles. In this line, I propose (see discussion below) that *RIM1*α functionnally interacts with L-types VDCCs. A careful comparison with previously published results is needed: I observed that during the 20 Hz-induced depression (Figure 15), *RIM1*$\alpha^{-/-}$ slices showed an increase in PPR as compared to WT, pinpointing a decrease in release probability. This is fully consistent with the decreased release probability detected by the Variance to Mean plots (Figure 15). *RIM1*$\alpha^{-/-}$mice expressed an increased PPR compared to WT as well in hippocampal glutamatergic autapses (Calakos et al., 2004) and CA1 synapses (Schoch et al., 2002). Moreover, *RIM1*$\alpha^{-/-}$ has been reported better able to sustain responses

during high-frequency stimulation compared to WT (Calakos et al., 2004; Schoch et al., 2002). This may be due to the decreased release probability: indeed, when the synaptic vesicle demand at each stimulus is reduced, less release sites needs to be refilled. Consistent with my data, Calakos et al (2004) observed that the kinetic of recovery from depression is unaltered, suggesting no change in the refilling kinetics. However, the authors observed that amplitude of hypertonic sucrose-elicited response, generally believed to be an index for the RRP size, is diminished. Note that no data clearly establish that the RRP and the synaptic vesicle pools recruited by hyper-sucrose are identical. Overall, the set of data presented by Calakos et al. (2004), Schoch et al. (2002) and my data are difficult to reconcile with the earliest proposal that *RIM1*α plays a role in the priming mechanisms. However, this difference could be explained by the fact that the synapses studied are very different one from each other.

3) An altered Ca^{2+}-release coupling in RIMα$^{-/-}$ synapses

Two previous studies (Calakos et al., 2004; Schoch et al., 2002) together with my observations clearly demonstrated a decrease in the release probability at the glutamatergic synapses taken from mice lacking *RIM1*α. However, no alteration in Ca^{2+} responsiveness has been been detected in the initial studies performed using the *C. elegans unc-10* mutant (Koushika et al., 2001), as well as in the Calakos et al (2004)'s studies performed on hippocampal neuron autapses. Our findings indicate that the Ca^{2+}-release coupling is diminished at synapses lacking *RIM1*α (Figure 15).

A first possibility implicates *RIM1*α itself as a potential Ca^{2+}-sensor and regulates fusion. Indeed *RIM* proteins have been suggested to bind the SNAREs proteins as SNAP-25 and Syntaxin (Coppola et al., 2001). It also contains several C2 domains homologous to the C2 calcium and lipid binding domains of PKC and synaptotagmins. However, the C2 domains in *RIM1*α are degenerated (Wang et al., 1997) and lack the calcium-binding motif or 'C_2-motif' defined in synaptotagmin (Sudhof and Rizo, 1996). Thus, *RIM1*α is unlikely to serve as a calcium-detector and we cannot explain the decrease in release probability by the loss of such a calcium sensor.

Alternative possibilities comprise the recruitment of a calcium-sensor by *RIM1*α. In the synaptic complex at the active zone, several C2-containing molecules interact directly or indirectly with *RIM1*α. Piccolo/Aczonin, Munc13-1 and synaptotagmin I are three *RIM1*α partners possessing C2 domains and demonstrated to interact directly with *RIM1*α. Piccolo C2-domain binds to calcium with low affinity and it triggers a large conformational change of the protein (Gerber et al., 2001). It can also bind to L-type VDCCs (Shibasaki et al., 2004).

However, the involvement of Piccolo in exocytosis and synaptic plasticity is far from being established. Munc13-1 possesses three C2 domains, one of them being essential for synaptic vesicle priming in the glutamatergic synapses (Rosenmund et al., 2002). The integral synaptic vesicle membrane protein Synaptotagmin has two C2 domains and is believed to be the main calcium-sensor mediating the coupling between calcium-influx and the triggering of exocytosis (for review, Chapman, 2002; Rizo et al., 2006). *RIM1*α and Synaptotagmin have been reported to interact, albeit the identity of the domains of interaction remains controversial (Coppola et al., 2001; Schoch et al., 2002). Anyway, the loss of interaction between these two proteins has been speculated by Schoch et al (2002) as being responsible for a reduced probability that occurs after loss of *RIM1*α. To this long list should be added the indirect interactions of *RIM1*α with Rabphilin-3A and double C2-domain protein (Doc2) which both are synaptic vesicle-associated proteins (Orita et al., 1995; Shirataki et al., 1993) and interact respectively with Rab3 and Munc13, which are themselves *RIM1*α binding partners. Overall, no functional data supports any of the mentioned interactions may be involved in the decrease in Ca^{2+}-release coupling that I observed at both the cortical and thalamic nerve glutamatergic terminals.

Last but not the least, *RIM* proteins have been suggested to bind directly to the α1B (P/Q-type) and α1C (L-type) subunits of VDCCs in dendrites and cell bodies (Coppola et al., 2001).However this direct interaction has been rejected by others (Hibino et al., 2002). *RIM1*α interacts with the *RIM* binding proteins (RIM-BP), which have been found to bind to the α subunit of several VDCCs, including the α1C but not α1D (both are L-types) (Hibino et al., 2002). During my thesis experimental work, I have explored this promising possibility. A set of evidence supports the idea that *RIM1*α may play role in a calcium-dependent step of neurotransmitter release and expression of LTP via the control of the presynaptic L-type VDCCs. Obviously, modulation of the activity of a VDCC should lead to a change in release probability, which is what I have observed. I discuss this important part of my thesis work in the next paragraphs.

4) Functional linkage between L-type calcium channels, PKA and *RIM1*α

I have used a pharmacological approach to determine if a VDCC subtype is involved in expression of LTP_{HA}. N- and P/Q-type calcium channels antagonists do not have significant effect on LTP_{HA} expression: while they effect on baseline release, they do not modify LTP_{HA}. I found a different situation with the L-type VDCCs blockers (verapamil and nimodipine),

which diminish basal release by 25% and completely abolished LTP_{HA}. Moreover these L-type blockers also prevented Forskolin-induced LTP (Figure 17). This latter experiment is important because it rules out the possibility that prevention of induction of LTP_{HA} was due to decrease in glutamate release by the conditioning thalamic nerve endings. Moreover, this experiment clearly demonstrates that L-type VDCCs are involved in a step downstream from PKA activation.

The L-type blockers also prevent the other forskolin-induced mechanisms that we observed at the studied synapses: the extent of synaptic depression (as determined at plateau) induced by 20 hertz stimulus train experiments is increased following forskolin application but this effect is prevented by verapamil application (Figure 19). This demonstrates that the functional linkage between PKA and L-type calcium channel is not specific to LTP_{HA} but to the presynaptic transmitter release modulations involving the PKA-pathway.

No LTP_{HA} can be induced at the cortical-amygdala synapse after genetical ablation of *RIM1*α or pharmacological deletion of L-type VDCCs. Thus, both *RIM1*α and L-type VDCCs are needed for expression of LTP_{HA}. These findings can be interpreted into two manners:

1), they act at distinct unrelated steps; their respective inactivation being mutually occluding. In this first possibility, the pathway downstream from PKA may branch to activate separately *RIM1*α and L-type VDCCs.

2) the NMDAR-AC-PKA-*RIM* pathway converges on the L-type VDCC, the activity of which is regulated by *RIM1*α, possibly by the mean of the *RIM* Binding Proteins. In both cases this raises the question of the role that L-type VDCCs may play in neurotransmitter release, under basal condition or during expression of synaptic plasticity forms.

C) The role of L-type channels in CNS synaptic transmission and plasticity

1) L-type VDCCs in neurotransmitter release in the CNS

Studies on the role in neurotransmitter release of the different types of VDCCs have revealed that the N- and P/Q-types are dominant in triggering transmitter release at most of the synapses. Overall they form a patchwork (reviewed by Reid et al., 2003): at few terminals only N-type contributes to release and in others only P/Q types contributes but in general both types are active in the same nerve endings. This, added with 1) a developmental switch during which predominant N-type VDCCs are replaced in large part by P/Q-, and sometime R-types

channels, and 2) differences in the spatial distribution of the N-, P/Q-, and R-types channels, enable a wide range of specific modulations of transmitter release.

Contribution of L-type channels to neuronal release of transmitters is exceptional. Their involvement in presynaptic transmission release is revealed in neuromuscular junction only after BAPTA loading. A slower rise time in the L- versus the P/Q-type VDCC-mediated endplate potentials suggest that L-type VDCCs are located further from the active zone(Urbano and Uchitel 1999, Urbano et al 2001). L-type VDCCs are primarily responsible for the control of both spontaneous and sound-evoked transmitter release from inner hair cells (Robertson and Paki, 2002).

By contrast with finding at most synapses of the CNS synapses, I have reported a noticeable contribution of the L-type VDCCs to the baseline evoked glutamate release at cortico-amygdala or thalamo-amygdala synapses. Indeed, inhibition of the L-type VDCCs leads to ~25% inhibition of the EPSC amplitude (Figure 17).

2) L-type VDCCs activity tuning by PKA

The activity of voltage gated L-type calcium channels is tuned by PKA. This has been widely studied in the heart because L-type VDCCs are prominent in the control of cardiac rate and muscle fibre contraction. A similar modulation has been described in neuron cells (Gray and Johnston, 1987). The α1-subunit (α1-C or α1-S) of L-type VDCC can be phosphorylated by PKA, for example on serine 1928 of the α1-subunit (for review, Catterall, 2000; Keef et al., 2001); phosphorylation may effect on the ß-subunit as well. Phosphorylation results in the enhancement of L-type current by increasing the opening probability of individual channels (Bean et al., 1984; Yue et al., 1990). Channel phosphorylation and de-phophorylation are facilitated by submembrane targeting of protein kinase A (PKA) -via its regulatory subunits- or calcium/calmodulin-activated phosphatase calcineurin (CaN) through association of L-type VDCC with an A-kinase anchoring protein (AKAP79/150 in neurons) (for example, see Gao et al., 1997; Oliveria et al., 2007). Cotargeting of PKA and CaN to AKAP79/150 confers bidirectional regulation of L-type current amplitude (Oliveria et al., 2007).

We have established that expression of LTP_{HA} is cAMP-PKA-dependent. As the L-types blockers (verapamil, nimodipine) abolish LTP_{HA}, this means that the supplement of glutamate release underlying LTP_{HA} expression is contributed only by the L-types channels. Thus during the course of LTP_{HA} the contribution of L-type channels should be responsible for ~50% of total glutamate release (25% baseline + 100% surplus). Is a direct phosphorylation of the L-type channels by PKA sufficient for explaining such an effect? This

is plausible because in the dendritic spines of CA1 pyramidal neurons, L-type current contributes for 10% of total spine Ca^{2+}-current at rest but, upon stimulation of ß2 adrenergic receptors, PKA is activated and phosphorylates L-type channels leading to a 50% increase in spine calcium current (Hoogland and Saggau, 2004). In this example, the contribution of L-type channels to total calcium current increases from 10% (rest) to 36% after stimulation of ß2 adrenergic receptors.

However, the possibility that *RIM1*α mediates the increased contribution of the L-type current should be also considered. Indeed, as already mentioned above, L-type VDCCs binds to the *RIM*-binding proteins (Hibino et al., 2002). However, we have no idea of whether such an interaction modifies the opening probability, conductance, desensitization of L-type channels or regulates their recruitment to the release sites.

Thus as mentioned above, we are facing two likely possibilities with a clear difficulty in determining which one is the most relevant, namely:

1) PKA phosphorylates and activates L-type VDCCs, with *RIM1*α playing a role that remains to be deciphered,

2) PKA activates *RIM1*α that, in turn tunes up L-type VDCCs.

However, an additional set of data should be considered: at the *RIM1*$\alpha^{-/-}$ synapses, the L-type blockers are able to depress by 25% basal release of glutamate, indicating that the absence of *RIM1*α at the synapses does not effect on the synaptic expression of L-type VDCCs. However, we also found that the change in PPR extent produced by the L-type blockers does not occur at synapses lacking *RIM1*α. This clearly indicates that *RIM1*α functionally interacts with the L-type channels and, albeit indirectly, supports the idea that *RIM1*α may act as a relay for PKA to tune up L-types channels. This hypothesis need further work to be demonstrated but this is beyond my thesis program.

3) L-type VDCCs in pre- and postsynaptic long-term forms of synaptic plasticity in the CNS

My experimental data clearly support the proposal that, following release of glutamate by thalamic afferents and presynaptic activation of presynaptic NMDAR in the cortical afferents (cf Humeau et al., 2003), there is an activation of the AC-cAMP-PKA + possibly *RIM1*α pathway, which induces a long-term increased in L-type calcium current. The latter effect results in long-term increased release probability detected as LTP_{HA}. A large body of litterature reports postsynaptic implication of L-type VDCCs in postsynaptic forms of long-term plasticity. This is fully consistent with their localization at many dendrite spines. For

example, the induction of LTD in hippocampal CA1 pyramidal neurons in neonatal rats is shown to depend on postsynaptic calcium ion entry through L-type voltage-gated calcium channels paired with the activation of metabotropic glutamate receptors (Bolshakov and Siegelbaum, 1994). LTP induced by the K+ channel blocker tetraethylammonium chloride (TEA) at synapses of hippocampal CA1 pyramidal neurons implicates both NMDAR and L-type channels (Huber et al., 1995). Theta-burst stimulation (TBS) of Schaffer collaterals induced LTP in the CA1 region, which is reduced by L-type blockers (Evers et al., 2002).

To my knowledge, few examples of presynaptic form of synaptic plasticity involving L-type channels and PKA have been yet reported. In cultured hippocampal CA1–CA3 neurons from newborn rat pups, repetitive stimulations of presynaptically silent synapses allow their activation by converting silent release sites into active ones by a process that depends on both PKA and L-type VDCCs (Yao et al., 2006). Recently, by combining optical monitoring of exo-endocytosis (i.e. a presynaptic index) and postsynaptic recordings, the compound LTP that is induced postsynaptically at excitatory synapses between CA3 and CA1 pyramidal neurons has been reanalyzed. This led to its dissociation into a fast postsynaptic component during which NMDAR play crucial role, from a slow presynaptic phase, which involves PKA and L-type VDCCs (Bayazitov et al., 2007). The authors proposed that the postsynaptic sources of calcium are the NMDARs (together with L-type VDCC0073; see Zakharenko et al., 2001) and the presynaptic sources are the L-type VDCCs. Presynaptic L-type channels have been also implicated in presynaptic BDNF-induced-LTP (Zakharenko et al., 2003).

In the here above mentioned presynaptic LTPs implicating the L-type channels, L-type VDCCs are proposed to be the source of calcium ions that plays a role in the induction mechanisms of LTP. In the case of the LTP_{HA} that I have studied, the situation is different: L-type VDCCs are the final targets of the NMDAR-AC-cAMP-PKA-*RIM* pathway and they act in the final stage of the expression mechanisms. A same situation is illustrated during the adrenergic post-synaptic modulation of L-type current in the dendritic spines of CA1 pyramidal neurons: activation of G-coupled ß2 adrenergic receptors activates an AC-cAMP-PKA pathway leading to phosphorylation of L-type VDCCs (Hoogland and Saggau, 2004).

D) Conclusions

During this work, I have assembled a set of data supporting the proposal that the induction and expression mechanisms of LTP_{HA} are the following. Pairing of cortico-amygdala activity with that of the thalamo-amygdala afferents leads to an activation of

presynaptic NMDAR located onto the cortical afferents (Humeau et al., 2003). Indeed, the thalamic afferent release of glutamate can exert its conditioning function provided simultaneous depolarization of the cortical nerve endings occurs. The incoming action potentials allow removal of the Mg-block exerted onto the presynaptic cortical NMDAR. Activation of NMDAR is likely to allow a calcium influx sufficient to activate calcium-calmodulin forms of Adenylate Cyclase. These may comprise the AC1 or/and AC8 forms. As a result, an increase in cytosolic cAMP levels triggers activation of PKA. The next step is the phosphorylation of *RIM1*α. Phospho-*RIM1*α, by a mechanism that remains unclear, appears to tune up L-types VDCCs in a long-term manner. At this stage, I cannot exclude that PKA may phosphorylate directly the L-type channels. Thus, upon arrival of action potentials at the cortical afferents, the presynaptic calcium-influx is stronger than in control situation because, in addition to resident N- and P/Q-type VDCCs, a larger activable population of L-type channels is now available. More glutamate is released as manifested by enhanced release probability and expression of LTP. Thus LTP_{HA} is the first example of a LTP which ultimate expression mechanisms consists in tuning up L-type VDCCs.

.

X) MATERIALS AND METHODS

A) Mouse brain Slice Preparation

Brain coronal slices were prepared from four to six week old male mice. Mice were either from C57BL/6J background, or from heterozygotes mice for *RIM1α* gene coming from Thomas Südhof's lab.

Briefly, brains were dissected in ice-cold artificial cerebrospinal fluid (ACSF), mounted on an agar block and sliced with a vibratome at 4ºC. Slices were maintained for 45 min at 35ºC in an interface chamber containing ACSF equilibrated with 95% O2/5% CO2 and containing (in mM): 124 NaCl, 2.7 KCl, 2 CaCl2, 1.3 MgCl2, 26 NaHCO3, 0.4 NaH2PO4, 18 glucose, 2.25 ascorbate, and then for at least 45 min. at room temperature before being transferred to a superfusing recording chamber.

B) Electrophysiological recordings

In this study whole-cell patch-clamp recordings were obtained from projection neurons in the dorsolateral portion of the LA at 30°C–32°C in a superfusing chamber with a constant renewing of the ACSF. For some recordings, the composition of the ACSF was modified for $CaCl_2$ and $MgCl_2$ concentrations (in mM):

	$CaCl_2$	$MgCl_2$
ACSF modified 1	1	4
ACSF modified 2	2.5	2.5
ACSF modified 3	4	1

Neurons were visually identified with infrared video microscopy using an upright microscope equipped with a x40 objective (Olympus). Patch electrodes (3-5MΩ) were pulled from borosilicate glass tubing and were filled with an intracellular solution consisting of (in mM): 140 potassium-gluconate, 10 HEPES, 10 phosphocreatine, 4 Mg-ATP, 0.3 Na-GTP, 20 KCl (pH adjusted to 7.25 with KOH, 300mOsm). For voltage-clamp experiments requesting a depolarization of the postsynaptic cell, potassium-gluconate was replaced by equiosmolar cesium-gluconate, and the pH was adjusted with KOH. In current-clamp recordings, membrane potential was held manually at −70mV. Monosynaptic EPSPs were elicited by

stimulation of afferent fibers with a bipolar twisted platinum/10% iridium wire (25µm diameter). Bipolar stimulating electrodes were placed on afferent fibers from the internal capsule (containing thalamic afferents) or from the external capsule (containing cortical afferents). All recordings were performed in the presence of 100µM picrotoxin, a $GABA_A$ antagonist.

C) LTP induction protocol

To mimic the physiological activity of converging thalamic and cortical afferents during fear conditioning (Quirk et al., 1997; Rosenkranz and Grace, 2002), both afferents were stimulated simultaneously for 1.5s at an average frequency of 30 Hz using two different Poisson-distributed stimulation protocols stimuli.

D) Drugs

Stock solutions of Rp-cAMPs, forskolin, bisindolylmaleimide II, H89, PDBu, γDGG, MK801, NBQX, nimodipine and verapamil were prepared with DMSO, and diluted in ACSF to 1‰ final DMSO concentration. Stock solutions of picrotoxin, ω-agatoxin IVA and ω-conotoxin GVIA were prepared in double distilled water.
Rp-cAMPs were applied to brain slices 1h30 prior to recording.
Picrotoxin, PdBu, ω-agatoxin IVA and verapamil were from Sigma-Aldrich Chemie GmbH (Buchs, Switzerland); Forskolin, Rp-cAMPs, H89, γDGG, MK801, NBQX and nimodipine were from Tocris Bioscience (Bristol, United Kingdom); ω-conotoxin GVIA was from Alomone labs LTD (Jerusalem, Israel).

E) MK801 experiments

The cells were filled with cesium-based intracellular solution containing 1mM of MK801, the extracellular ACSF contained 20µM NBQX. The neurons were depolarized at +30mV to record NMDAR-mediated EPSC decay, then the cells were repolarized at -70mV for 5 minutes and LTP was induced. Neurons are then clamped again at +30mV for the rest of the

experiment. For the experiments with the complete NMDAR blockade, the MK801 concentration was 4mM.

F) Data analysis

Data were acquired and analyzed with pClamp9.0 (Axon Instruments, Union City, CA, USA). Poisson-trains stimuli were generated using custom software obtained from N. Buchs (University of Bern, Switzerland). Data were recorded with an Axopatch200B, filtered at 2 kHz and digitized at 10 kHz. Series resistance was monitored throughout the experiments by applying a hyperpolarizing pulse. Any modification of the series resistance exceeding 20% was a cause of the exclusion of the data from the analysis. LTP was quantified for statistical comparisons by normalizing and averaging EPSP amplitudes or slopes during the five last minutes of the experiments relative to the 5 minutes of stable baseline recorded. All values are expressed as means ± s.e.m. Statistical comparisons were done with paired or unpaired Student's t-test as appropriate (two-tailed $p < 0.05$ was considered significant).

G) Variance-mean analysis

The variance-mean analysis allows easy graphical distinctions in the changes in *N*, *P*, *Q* (Foster and Regehr, 2004; Humeau et al., 2001; Humeau et al., 2002; Silver, 2003; Silver et al., 1998). The rationale for variance-mean analysis is the following. Consider a hypothetical synapse consisting of a single exocytotic site at which release of one SV with a given probability produces a postsynaptic response of fixed amplitude *q*. According to the binomial statistics, at a release site, the average postsynaptic response amplitude μ is:

(1) $\mu = p*q$

with variance

(2) $\mathrm{Var} = p*(1-p)*q^2$

Now, if we consider the *N* contacts between a presynaptic neuron and its postsynaptic target and assume that the release process at each site is independent of that at the other sites, and quanta sum up linearly. The mean amplitudes and variances at the *N* sites add linearly, and the mean amplitude of the compound response is:

(3) $I_{mean} = \Sigma_{i=1 \rightarrow N} \mu_i$

This can be rearranged as:

(4) $I_{mean} = N*P*Q$

where P is the average release probability observed at the N sites and Q the average amplitude of the quantum of response at the N sites. The fluctuations of the responses around the mean have a variance of the form:

(5) $Var = N*P*(1-P)*Q^2$

Indeed, this relationship can be re-expressed as a function of I_{mean}:

(6) $Var = Q*I_{mean} - (1/N)*I_{mean}^2$

which can be fitted by a simple parabola of equation:

(7) $Var = A*I_{mean}-B*I_{mean}^2$

This allows determination of two parameters: A, the initial slope of the parabola, and B the extent factor of the parabola. Parameter A refers to Q. However quantal variability also contributes to Var. Therefore, A provides an overestimate of Q (Oleskevich et al., 2000; Reid and Clements, 1999; Scheuss and Neher, 2001; Silver et al., 1998).

(8) $A = Q*(1+CV^2)$

Parameter B refers to $1/N$. However, probability parameter P is heterogeneous between the releases sites at vertebrate synapses (Murthy et al., 1997; Rosenmund et al., 1993). Therefore, 1/B underestimates N according to the equation:

(9) $1/B = N / [(1 + CV_p^2)*(1+\beta CV_q^2)]$

in which, CV_p is the average variation of P and βCV_q the fraction of quantal variance due to intersite variability (Brown et al., 1976; Meyer et al., 2001; Scheuss and Neher, 2001; Silver et al., 1998). However, we want to understand what synaptic parameters are affected rather than measuring the absolute values for N, P or Q. Therefore, I did not take into account variability parameters.

From equations 4 and 5, it can be deduced that when only P is modified, $Var = f(I_{mean})$ has the form of a simple parabola of initial slope Q:

(10) $Var = Q*I_{mean}-I_{mean}^2/N$,

whose initial slope and parabola extent allows determining Q and N. When only N is changed, $Var = f(I_{mean})$ follows a linear function:

(11) $Var = Q*(1-P)*I_{mean}$

When only Q is modified, $Var = f(I_{mean})$ is a quadratic function of positive curvature:

(12) $Var = I_{mean}^2*(1-P)/N*P$

In order to construct the $Var = f(I_{mean})$ representation, I artificially varied the probability of release by changing the calcium and magnesium concentrations in the ACSF. When the

amplitude of the response was stabilised, the amplitude and the variability of the response for each cell were averaged on a period of 10 minutes.

By normalizing Var to I_{mean}, this representation simplifies the pooling of data obtained from different experiments. Individual Var = *f*(I_{mean}) plots were normalized to the maximum Var (Var_{max}) and corresponding I_{mean} (I_{mean}-to-Var_{max}) determined by fitting the Var = *f*(Imean) plot from each experiment by a quadratic function of the form $y = y0+a*x+b*x^2$, with all parameters left free, using the non-linear regression procedure running under SigmaPlot 9 (Systat Software Inc). Then, the normalized data from the *n* experiments were pooled and used to make the corresponding plots of normalized Var = *f*(normalized I_{mean}) and normalized Var/I_{mean} = *f*(normalized I_{mean}). When Var = *f*(I_{mean}) did not display a parabolic shape, datas were excluded from the analysis.

Normalisation of Var, I_{mean} and Var/I_{mean} data introduced loss of information on the actual amplitude of the release parameters, but preserved the determination of their relative changes. Indeed, when the normalized Var = *f*(I_{mean}) is a parabola, Var_{max} is reached for $P = 0.5$ as in non-normalized plots, allowing determining a corresponding P (e.g., $I_{mean} = 0 \rightarrow P = 0$; $I_{mean} = I_{max}/4 \rightarrow P = 0.25$; $I_{mean} = I_{max}/2 \rightarrow P = 0.5$; …) at each point of the parabola. Initial slope and parabola extent do not allow the estimation of Q and N, respectively. Q and N data were then collected directly from the individual non-normalized parabolas and then averaged.

APPENDIX A: STRUCTURE OF A GLUTAMATERGIC SYNAPSE

A) Presynapse, postsynapse and synaptic cleft

Chemical synapses in the CNS are all constituted by a presynaptic terminal in a close apposition to a postsynaptic element, with a synaptic cleft in between (Figure 22).
The presynaptic terminal, also called presynaptic bouton, is characterized by the presence of neurotransmitter vesicles. Some of the vesicles are adjacent to a specialized portion of the presynaptic membrane, the active zone, and are called docked vesicles. Vesicle exocytosis occurs at the active zone, in regard of which is the so called postsynaptic density (PSD) (Gundelfinger et al., 2003). The active zone is surrounded by the perisynaptic zone, in which some of the synaptic vesicles that have undergone fusion are retrieved by clathrin-mediated endocytosis (Wong and Wong, 2000; Ziv and Garner, 2001). The PSD can be directly present on the dendrite or it can be present on a highly specialized structure called dendritic spine.

Synapses are formed after the encounter of two motile structures, an axonal growth cone and a dendritic filopodia (Murthy and De Camilli, 2003; Ziv and Garner, 2001). Presynaptic and postsynaptic elements are held in close vicinity thanks to several kinds of transmembrane adhesion molecules present at the edges of the active zone. Some of those molecules have cytosolic sequence motifs that bind PDZ domains present in scaffolding proteins. This leads for example to the formation of a complex molecular structure which in turn allows the recruitment and the aggregation of glutamate receptors at the PSD (for review, Dresbach et al., 2001).

B) Cytoskeletal matrix at the presynapse

The active zone is tightly associated with a cytoskeletal matrix, which is referred to as cytomatrix at the active zone (CAZ) or presynaptic grid (Bloom and Aghajanian, 1968; Gray, 1975; Landis, 1988; Landis et al., 1988; Pfenninger et al., 1972; Phillips et al., 2001). The CAZ is a web-like pattern, formed by a regular array of electron-dense cone-shaped particles that extend approximately 50 nm into the cytoplasm (Akert et al., 1971). The 50-nm pyramid-

shaped particles are interconnected by a meshwork of cytoskeletal filaments, and long filamentous strands extend deeply into the presynaptic bouton.

Synaptic vesicles are nested at different levels within this network (Rizzoli and Betz, 2005). Physiologically, they are separated in two groups. Until recently, it was assumed that these pools were anatomically segregated in different areas in presynaptic terminals: the recycling pool, formed by vesicles close enough to the active zone to be quickly released or engaged in the process of endoycytosis (5 to 20% of the vesicles); and the reserve pool, further away from the release area (80 to 95% of the vesicles) (Figure 23). From this difference resulted the selective recrutement of recycling vesicles in normal conditions, the reserve pool being recruited only in case of severe vesicle depletion. A specific set of vesicles can be even subselected out of the recycling pool, they are the vesicle already in a very close vicinity with the membrane and engaged in the release process. They are called the readily-releasable pool (RRP, 0.1 to 2% of the total vesicles, about 5/10 vesicles per active zone). However, this anatomical segregation is brought into question since a few years, vesicles from recycling or reserve pools can be recruited in case of repetitive stimulation (for review, Borgdorff and Choquet, 2002; Choquet and Triller, 2003).

The microfilaments comprised in the CAZ are the support for the vesicular traffic to the membrane. Some of the CAZ proteins interact as well with molecules essential for the binding and fusion processes at the membrane. Indeed, the CAZ bring together all the elements necessary for the vesicular cycle.

C) Postsynaptic density, intrasynaptic and extrasynaptic receptors

Postsynaptic glutamate receptor are either intrasynaptic, meaning they are concentrated in the PSD directly facing of the active zone, or extrasynaptic. Intrasynaptic receptors are generally thought to be responsible for signal propagation, whereas extrasynaptic receptors are rather considerated as a reserve pool of receptors, which allow a quick regulation of the synaptic receptor number. AMPA receptors (AMPAR) have been shown to diffuse easily in neuronal membrane and thus moving in and out of the PSD. On cultured neurons, tracking single AMPAR showed that the high mobility of extrasynaptic receptors is extremely reduced when they enter the synapse, they look being trapped (Tovar and Westbrook, 2002). Synaptic and extrasynaptic NMDA receptors (NMDAR) are rapidly exchanged through lateral diffusion in the plasma membrane as well (Hardingham and Bading, 2003). Extrasynaptic NMDARs are thought to play an important role in excitotoxicity, while synaptic NMDAR

activation appears neuroprotective (Nakanishi et al., 1997; Vogt and Nicoll, 1999). However, the relationship between synaptic and extrasynaptic receptors remains still unclear.

On the other hand, receptors are also present at the presynaptic side and involved in presynaptic regulation. They include receptors for peptide neurohormone and nonpeptide neurotransmitters released by synaptic vesicles. They can be responsible for autocrine effects as well as heterosynaptic modulation (Conn and Pin, 1997; Kandel and Tauc, 1964).

D) Glutamate receptors

Glutamate receptors are splitted in 2 categories (Figure 24):

- inotropic receptors (iGluR), which are responsible for the fast component of synaptic transmission
- metabotropic receptors (mGluR), which are linked to intracellular second messenger cascade and are involved in the slow component of synaptic transmission..

1) Ionotropic receptors

Ionotropic receptors are separated in three categories: NMDA (N-Methyl-D-Aspartate), AMPA (α-Amino-3-hydroxy-5-Methyl-4-isoxazolepropionique acid) and kaïnate receptors. Kaïnate receptor family is constituted by 5 genes coding the following subunits: GluR5, GluR6, GluR7, KA1 and KA2. The ionic channel is selective to cations, principally to sodium ions. Those receptors are present at the presynaptic as well as at the postsynaptic side. They are thought to be important for the regulation of the synaptic transmission and neuronal activity.

NMDA receptors are present as well on both sides of the synapse. Seven genes are coding for the subunits NR1, NR2A, NR2B, NR2C, NR2D, NR3A, NR3B. NR1 subunit is necessary for the formation of a functional receptor. The ionic channel is selective for cations, including calcium ions. Those receptors are characterized as well by their voltage-dependent blockade of the channel by magnesium ions. The functional consequence is that NMDAR are not permeable at resting membrane potential, they request a depolarization in addition to glutamate binding in order to let ion flowing. NMDAR can be regulated by their interaction with numerous intracellular proteins. NMDAR are particularly studied for their involvement in long-term plasticity.

AMPA receptors are only present at the postsynaptic side of the synapse. They are responsible for the main part of the fast glutamatergic conductance. There are four AMPA

subunits: GluR1, GluR2, GluR3 and GluR4. AMPAR containing GluR2 subunit are selective to sodium ions, AMPAR lacking GluR2 subunit are permeable to sodium and calcium ions.

2) Metabotropic receptors

Metabotropic receptors (mGluR) belong to the super family of seven-transmembrane domain receptors coupled to heterotrimeric G protein. Three groups of mGluR can be distinguished by the sequence homology, the pharmacology and the transduction pathways they are coupled with. Group I include mGluR1 and mGluR5 receptors, their activation stimulate the phospholipase C via recruitment of the G protein subtype Gq. Group II involves mGluR2 and mGluR3 receptors, and group III include mGluR4, mGluR6, mGluR7 and mGluR8 receptors. They are all negatively coupled to adenylyl cyclase through G protein subtype Gi/Go activation. Thanks to their coupling to intracellular transduction pathways, mGluR activation regulates the activity of numerous ionic channels and ionotropic glutamate receptors function (Danbolt, 2001).

E) Glutamate uptake

Regulator mechanisms of synaptic glutamate concentration allow to keep a good signal-to-noise ratio for synaptic transmission and to avoid the excitotoxicity induced by high concentrations of glutamate. Glutamate uptake is mainly done by five specific transporters called excitatory amino acid transporters (EAAT). Glutamate is cotransported with two to three sodium ions and a proton against the exit of a potassium ion. In addition, glutamate fixation to the transporter can induce a chloride permeability of the transporter (for review, Chaudhry et al., 1995).

At the subcellular level, EAAT1 and EAAT2 are highly expressed at the plasma membrane from astrocytes associated to glutamatergic synaptic contacts (Dehnes et al., 1998; Rothstein et al., 1994). EAAT3 and EAAT4 are localized at the neuronal soma and dendrites (Arriza et al., 1997). EAAT5 seems to be specifically present in the retina (Michaelson et al., 1983).

APPENDIX B: SYNAPTIC VESICLE CYCLE

Neurotransmitter molecules are stored and concentrated in structures called synaptic vesicles in the presynapse, and the regulated release of neurotransmitter is mainly mediated by selective exocytosis of presynaptic vesicles at the active zone.

Synaptic vesicles are small spherical organelles (50 to 60nm radius) specifically dedicated to uptake and release of neurotransmitters. Synaptic vesicles also contain various membrane proteins which can be divided in two categories:

- transport proteins involved in neurotransmitter uptake
- trafficking proteins participating in synaptic vesicle exo- and endocytosis and recycling.

A) Vesicular release

The vesicular cycle is divided in 4 main step called tethering or docking, priming, fusion and recycling (Figure 25). The recycling will not be addressed in this issue.

1) Tethering/docking

The mechanisms allowing the addressing and the recognition of the vesicles by the plasma membrane are not yet clearly identified.

2) Priming

This crucial step confers fusion competences to docked vesicles, enabling them to undergo rapid exocytosis upon calcium influx (Rothman, 1994). Once bound to the plasma membrane, synaptic vesicles will come in a closer apposition to it thanks to another multiprotein complex called SNAREs. These proteins ares characterized by a common coil-coil domain called the SNARE motif. This complex was initially splitted in two groups, v-SNAREs (or vesicular SNAREs), and t-SNAREs (for target SNAREs, at the plasma membrane) (Fasshauer et al., 1998). They were later classified as R-SNAREs and Q-SNAREs according to the central amino-acid of the SNARE motif (Poirier et al., 1998; Sutton et al., 1998).

Synaptic vesicle exocytosis requires three SNAREs: one R-SNARE at the vesicle membrane, called vesicle-associated membrane protein (VAMP2) or synaptobrevin; and two Q-SNAREs at the plasma membrane, syntaxin 1 and the 25 kDa synaptosomal-associated protein (SNAP-25). SNARE proteins associate into core complexes, at the ratio 1-1-1, in order to form a parallel four-helix bundle on assembly (coiled-coil) (Hanson et al., 1997; Lin and Scheller, 1997). The soluble SM proteins (Sec1/Munc18-like proteins) are often associated with syntaxin-like SNAREs and participate to the priming.

The SNARE complex is first in a relaxed state, then it reassemble in a zipper-like fashion from the N-terminal end of the SNARE motifs towards the C-terminal membrane anchors. This is powerful enough to overcome the natural repulsion occurring between the two membranes and pulls them close together in a fusion-ready manner (Gerst, 1999). The complex thus formed is extremely stable and will be disassembled later in the vesicular cycle only with the help of the ATPase activity of NSF.

SNAREs interact with a large number of other proteins (for review, Augustin et al., 1999; Geppert et al., 1994; Richmond et al., 2001; Varoqueaux et al., 2002). Among them, Munc13/Unc13 seems to be essential for priming. Indeed, the deletion of Munc13-1 in mice leads to the complete abolition of glutamate exocytosis in the hippocampus, while the number of docked vesicles does not change. However, GABA release is not affected, which suggests that priming can be due to different molecules depending on the studied model (Basu et al., 2005; Madison et al., 2005; Stevens et al., 2005). Recent studies with deletion constructs have now shown that the priming function is mediated by the ”Munc homology domains” (MHDs) located in the C-terminal end of Munc13 proteins (Madison et al., 2005; Stevens et al., 2005). Point mutations in the MHDs and the C-terminal C2 domain identified in yeast two-hybrid screens indicated that the binding of these regions to syntaxin is required for efficient priming (Betz et al., 2001).

Munc13 interacts also with *RIM1*α, and this interaction is critical for priming (Galli and Haucke, 2004). The authors demonstrated that Munc13-1 and Rab3A interact with the same zinc finger region of *RIM1*α. Moreover, they showed that Munc13-1 and Rab3A binding to *RIM1*α is mutually exclusive, meaning that they compete for *RIM1*α binding site. Their hypothesis is that *RIM1*α may contribute to vesicle tethering by binding to Rab3A and creates a physical link between the tethering and the priming apparatus through interactions with Munc13-1. *RIM1*α would allow spatial and temporal coordination of the first vesicle trafficking steps.

3) Fusion and recycling of the vesicles

Two fusion processes were described: the first is a full collapse of the vesicle membrane with the plasma membrane. As a result, the recycling of vesicular constituents involve a clathrin-mediated endocytosis, a quite slow process occurring at the periphery of the active zone. The second hypothesis is a partial fusion with the opening and closing of a fusion pore. This mode, called kiss-and-run, should be much faster, the only limiting factor being the refilling of the vesicle (for review, Sudhof, 2004) (Figure 26). A last hypothesis is derived from the kiss and run hypothesis, the kiss-and-stay: the vesicle, once the fusion pore is closed, stay docked at the same site and would be eventually refilled on site. The consequence is that some steps of the vesicular cycle are bypassed, allowing even faster release (for review, Sun et al., 2002). The time constant of neuronal neurotransmitter release claim more in favor of the kiss-and-run or kiss-and-stay hypothesis, but clathrin-mediated endocytosis can be accelerated by specific proteins present in nerve terminals (for review, Jackson and Chapman, 2006; Kavalali, 2007). It is very probable that those three forms of release coexist.

The fusion pore is another mystery in the vesicular cycle: is this fusion pore constituted by lipids, proteins, or both? This question is still widely open, one of the main difficulties for the study of fusion pores is the study of very early steps of their formation (Marqueze et al., 2000; Mikoshiba et al., 1999).

B) Calcium flow and release

When an action potential reaches the presynaptic terminal, it induces the opening of voltage-dependent calcium channels (VDCCs) and the cytosolic calcium concentration increases. Several families of VDCCs exist (for more details see chapters VII and VIII). Calcium entry through a single channel forms a nanodomain, with a high calcium concentration (up to hundreds of micromolar) localized in a close vicinity around the calcium channel. However, considering that a synaptic vesicle is 50 to 60nm large, one vesicle is probably surrounded by several calcium channels. The calcium domain resulting from the simultaneous opening of several calcium channels is called microdomain.

C) Calcium sensors

Several steps of the release machinery are dependent on a calcium signal. One of them is the SNARE zippering leading to the fusion of the vesicle with the plasma membrane. As SNARE protein are insensitive to calcium, people searched for a protein able to bind SNARE and Ca^{2+} ions. One good candidate is synaptotagmin. It can bind SNARE molecules, calcium channels and other proteins important for the exocytosis (for review, Nishizuka, 1988). Moreover, it contains two C2 domains, which are homolog domains to the Ca^{2+} binding site of the protein kinase PKC, and could lead to the binding of a protein to the membrane in a Ca^{2+}-dependent manner (Fernandez-Chacon et al., 2002).

Inhibition studies showed that the absence of synaptotamin I drastically reduced the Ca^{2+}-dependent synchronous release (Chapman, 2002; for review Burgoyne and Morgan, 1998). Synaptotagmins are considered to be a key element for the Ca^{2+}-induced vesicular fusion, a kind of "calcium switch".

However, synaptotagmin is probably not the only protein allowing the coupling between Ca^{2+} entry and exocytosis machinery . Other protein with tandem C2 domains are present on the vesicle (for example, rabphilin) or at the active zone (for example, *RIM1*α and piccolo). In case of *RIM1*α, C2 domains are degenerated and lack the amino-acid requested for Ca^{2+} binding (Wang et al., 1997). On the other hand, *RIM1*α bind other protein containing functional C2 domains, as for example Munc13-1, thus it can be indirectly involved in calcium sensing.

To summarize, several proteins should be important for a very tight tunning of all the exocytosis steps by calcium ions.

APPENDIX C: PAPERS

Dendritic Spine Heterogeneity Determines

Afferent-Specific Hebbian Plasticity

in the Amygdala

Synaptic organization of the mouse cerebellar cortex

in organotypic slice cultures

Neuron, Vol. 45, 119–131, January 6, 2005, Copyright ©2005 by Elsevier Inc. DOI 10.1016/j.neuron.2004.12.019

Dendritic Spine Heterogeneity Determines Afferent-Specific Hebbian Plasticity in the Amygdala

Yann Humeau,[1,2] Cyril Herry,[1] Nicola Kemp,[3] Hamdy Shaban,[1] Elodie Fourcaudot,[1,2] Stephanie Bissière,[1] and Andreas Lüthi[1,3,*]
[1]Friedrich Miescher Institute
Maulbeerstrasse 66
CH-4058 Basel
Switzerland
[2]UPR2356
CNRS
F-67084 Strasbourg
France
[3]Biozentrum
University of Basel
Klingelbergstrasse 70
CH-4056 Basel
Switzerland

Summary

Functional compartmentalization of dendrites is thought to underlie afferent-specific integration of neural activity in laminar brain structures. Here we show that in the lateral nucleus of the amygdala (LA), an area lacking apparent laminar organization, thalamic and cortical afferents converge on the same dendrites, contacting neighboring but morphologically and functionally distinct spine types. Large spines contacted by thalamic afferents exhibited larger Ca^{2+} transients during action potential backpropagation than did small spines contacted by cortical afferents. Accordingly, induction of Hebbian plasticity, dependent on postsynaptic spikes, was restricted to thalamic afferents. This synapse-specific effect involved activation of R-type voltage-dependent Ca^{2+} channels preferentially located at thalamic inputs. These results indicate that afferent-specific mechanisms of postsynaptic, associative Hebbian plasticity in LA projection neurons depend on local, spine-specific morphological and molecular properties, rather than global differences between dendritic compartments.

Introduction

Neuronal network function relies on precise and input-specific changes in synaptic strength. Induction of associative, Hebbian synaptic plasticity at excitatory synapses onto principal (projection) neurons is classically mediated by postsynaptic Ca^{2+}-dependent mechanisms (Bliss and Collingridge, 1994; Bi and Poo, 2001). Input specificity of postsynaptic Ca^{2+} signaling, and hence Hebbian plasticity, is thought to require compartmentalization of local synaptic Ca^{2+} transients in dendritic spines (Harris and Kater, 1994; Yuste et al., 2000; Nimchinsky et al., 2002).

Projection neurons receive converging presynaptic afferents originating from different brain areas, providing feedforward or recurrent excitatory input. These inputs often differ not only in terms of afferent activity but also with respect to postsynaptic mechanisms of activity-dependent synaptic plasticity (Nicoll and Malenka, 1995; Hansel and Linden, 2000). Structural and functional features of the postsynaptic component, especially of dendritic spines, play an important role in determining the influence of specific afferents impinging on the same dendritic arbor. Presently, this form of organization is well established for brain areas with a laminar structure, like the hippocampus, the neocortex, and the cerebellum (Chicurel and Harris, 1992; Harris and Kater, 1994; Yuste and Bonhoeffer, 2004), but it is unclear whether the same basic principle operates in nuclear structures such as the amygdala. It is thus a crucial question of whether, and if so how, structural partitioning of afferents to postsynaptic sites on dendrites occurs or, if this is not the case, then what principles of afferent specificity apply in these cases.

Projection neurons in the lateral nucleus of the amygdala (LA) exhibit dendritic arbors largely lacking spatial polarization (Paré et al., 1995; Faber et al., 2001) and receive converging excitatory inputs from the thalamus and from the cortex (Carlsen and Heimer, 1988; Farb and LeDoux, 1997, 1999; Smith et al., 2000). Activity-dependent Hebbian plasticity at cortical and/or thalamic afferents to LA projection neurons is generally thought to underlie, at least in part, classical Pavlovian fear conditioning (LeDoux, 2000; Maren, 2001; Tsvetkov et al., 2002). In other brain areas, Hebbian long-term potentiation (LTP) or long-term depression (LTD) can be induced depending on the relative timing of presynaptic input and postsynaptic backpropagating action potentials (BPAPs) (Markram et al., 1997; Magee and Johnston, 1997; Debanne et al., 1998; Bi and Poo, 1998, 2001). This so-called spike timing-dependent plasticity (STDP) requires postsynaptic Ca^{2+} elevation (Mainen, 1999; Sjöström and Nelson, 2002). Several sources of Ca^{2+}, such as *N*-methyl-D-aspartate (NMDA) receptors and voltage-dependent Ca^{2+} channels (VDCCs), have been implicated in the induction of STDP (Magee, 1999; Mainen, 1999; Sabatini and Svoboda, 2000; Yasuda et al., 2003). BPAPs are particularly effective in activating VDCCs in the dendritic arbor of hippocampal and cortical pyramidal cells (Sabatini and Svoboda, 2000; Magee, 1999).

To investigate afferent specific plasticity at identified thalamic and cortical synapses on dendrites of LA projection neurons, we have used a combination of two-photon confocal imaging and whole-cell recording techniques. We find that the morphologies of spines located on the same dendritic branches are specifically matched to different presynaptic inputs. This morphological diversity is correlated with distinct spine Ca^{2+} dynamics and different mechanisms of Hebbian plasticity: BPAPs elicited greater Ca^{2+} transients in large, mushroom-shaped spines contacted by thalamic afferents than in small spines postsynaptic to cortical afferents. Consistent with spine type-specific Ca^{2+} dynamics, we found that induction of STDP was restricted to thalamic affer-

*Correspondence: andreas.luthi@fmi.ch

ents. Both action potential-evoked Ca^{2+} transients in large spines and the induction of STDP at thalamic afferent synapses required activation of postsynaptic R-type voltage-dependent Ca^{2+} channels (R-VDCCs). Pharmacological and immunohistochemical analysis of identified synapses revealed that α-1E containing R-VDCCs are preferentially located at and activated on thalamic spines. This indicates that in projection neurons in a nuclear brain structure, such as the LA, local and spine-specific morphological and molecular properties, rather than global differences between distinct parts of the dendritic arbor, underlie distinct, afferent specific mechanisms of functional synaptic plasticity.

Results

Dendritic Spines Contacted by Thalamic and Cortical Afferents Exhibit Different Morphologies

To investigate dendritic location, structure, and function of identified dendritic spines contacted by thalamic or cortical afferents, we imaged spines and dendrites of projection neurons located in the dorsal subdivision of the LA with a Ca^{2+}-sensitive fluorophore while stimulating afferent fibers from the internal capsule, containing thalamic afferents (Weisskopf et al., 1999), or from the external capsule, containing cortical afferents (Figure 1A; see Experimental Procedures; Huang and Kandel, 1998). Neurons in coronal slices prepared from 3- to 4-week-old male C57BL/6J mice were loaded with a Ca^{2+}-sensitive green dye (Fluo-5F) and a Ca^{2+}-insensitive red dye (Alexa-594) (Yasuda et al., 2003). Spines located on primary to quaternary dendrites exhibited a variety of morphologies including small stubby (type Ia; spine head radius < 0.55 μm), large stubby (type Ib; >0.55 μm), mushroom-shaped (type II; >0.55 μm), and thin spines with a small head (type III; <0.55 μm) (Figures 1B and 1C; Harris and Kater, 1994). Individual spines contacted by thalamic or cortical afferents were identified based on stimulation-induced NMDA (N-methyl-D-aspartate) receptor-mediated changes in the concentration of intracellular free Ca^{2+} (Δ [Ca^{2+}]) measured at +30 mV (Figures 1D and 1E). Spines postsynaptic to thalamic or cortical afferents were located at the same average distance from the soma (thalamic: 76 $\pm$ 8 μm; range, 27–122 μm; n = 17; cortical: 87 $\pm$ 8 μm; range, 42–153 μm; n = 19) and on dendrites of the same average branching order (thalamic: 3.37 $\pm$ 0.26, n = 17; cortical: 3.05 $\pm$ 0.30, n = 19). In some cases, they were on the same dendritic branch separated by less than 5 μm (Figure 1F). Notably, thalamic and cortical spines exhibited different morphologies. Whereas cortical spines generally belonged to the categories with small heads (0.51 $\pm$ 0.02 μm, n = 19; type Ia and type III; referred to as "small spines"), spines contacted by thalamic afferents had significantly larger spine heads (0.68 $\pm$ 0.04 μm, n = 17; $p < 0.001$; type Ib and type II; referred to as "large spines") (Figures 1G and 1H). There was no difference in the size of the parent dendrite for thalamic and cortical spines (cortical: 0.60 $\pm$ 0.03 μm, n = 19; thalamic: 0.59 $\pm$ 0.03 μm, n = 17; $p > 0.05$) (Figure 1H).

Spine Type-Specific Ca^{2+} Signaling during AP Backpropagation

To probe for functional differences between small and large spine types, we assessed Δ [Ca^{2+}] upon stimulation by brief trains of backpropagating postsynaptic action potentials (APs) (Sabatini and Svoboda, 2000). When compared to the amplitude of the [Ca^{2+}] transients in the parent dendrite, some spines showed larger and other spines smaller Ca^{2+} responses (Figure 2). After sorting the spines according to their morphological features as described above, we noticed a striking correlation between functional and morphological spine properties: stimulation with 5 APs at 30 Hz triggered significantly greater [Ca^{2+}] transients in large spines (types Ib, II) as compared to small spines (types Ia, III) (large spines: 43.8% $\pm$ 2.9% Δ G/R, n = 11; small spines: 29.5% $\pm$ 2.5% Δ G/R, n = 18; $p < 0.01$) (Figure 2). Δ [Ca^{2+}] was quantified as a ratio of green (Ca^{2+}-sensitive) over red (Ca^{2+}-insensitive) fluorescence to obtain Ca^{2+} measurements that are independent of spine volume (Oertner et al., 2002). These results suggest that dendritic spines on LA projection neurons, although located on the same dendrites, generally fall into two categories (small and large) associated with specific afferent input and differential [Ca^{2+}] dynamics.

Afferent-Specific Induction of STDP

Postsynaptic Ca^{2+} signaling properties are key determinants underlying the induction of Hebbian plasticity at many synapses in the brain (Mainen, 1999; Sjöström and Nelson, 2002). Coincidence between excitatory postsynaptic potentials (EPSPs) and backpropagating APs leads to the induction of LTP or LTD, depending on the relative timing of EPSPs and APs (Bi and Poo, 2001; Sjöström and Nelson, 2002). Since LA projection neurons can be driven to fire APs by somatosensory stimulation, such as foot-shocks used for fear conditioning (Romanski et al., 1993; Rosenkranz and Grace, 2002; Blair et al., 2003), we compared STDP at thalamic and cortical afferents.

Low-frequency baseline stimulation in the presence of the $GABA_A$ (γ-aminobutyric acid) receptor antagonist picrotoxin (100 μM) elicited monosynaptic EPSPs of similar amplitudes and slopes at both afferent inputs (thalamic: 4.4 $\pm$ 0.4 mV, 0.83 $\pm$ 0.06 mV ms^{-1}, n = 46; cortical: 4.1 $\pm$ 0.3 mV, 0.88 $\pm$ 0.06 mV ms^{-1}, n = 40). Pairing short bursts of 3 EPSPs and 3 APs (EPSP-AP delay +5 to +10 ms; intraburst frequency: 30 Hz; repeated 15 times at 0.2 Hz; Figure 3A) resulted in the induction of LTP at thalamic afferent synapses (132% $\pm$ 12% of baseline; n = 10; $p < 0.05$; Figures 3B and 3D; Bissière et al., 2003), similar to findings at excitatory inputs to cortical and hippocampal pyramidal cells (Bi and Poo, 2001). Presynaptic or postsynaptic stimulation alone did not result in LTP induction (EPSPs alone: 101% $\pm$ 11% of baseline, n = 5; APs alone: 102% $\pm$ 11% of baseline, n = 5; Figure 3C). In contrast to LTP at cortical afferents (Tsvetkov et al., 2002; Humeau et al., 2003), STDP at thalamic afferents was not associated with a change in paired-pulse facilitation, indicating distinct mechanisms of LTP expression (Figure 3E). Reversing the EPSP-AP sequence during pairing (−5 to −10 ms delay) led to the induction of LTD (74% $\pm$ 8% of baseline, n = 10; $p < 0.01$; Figures 3B and 3D). Induction of LTP and LTD was blocked by the competitive NMDA receptor antagonist CPP (20 μM; +10 ms: 106% $\pm$ 8% of baseline, n = 8; −10 ms: 108% $\pm$ 10% of baseline, n = 5; Figure 3C) and by postsynaptic perfu-

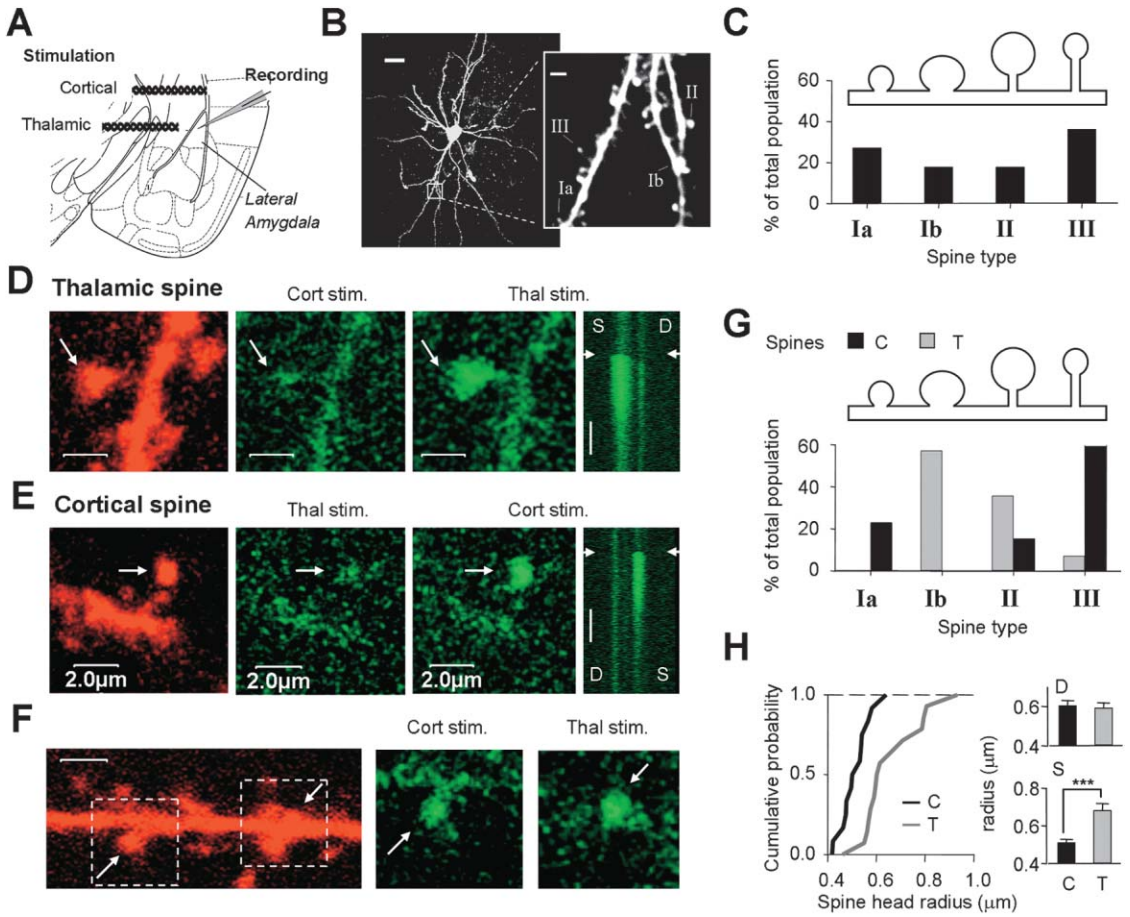

Figure 1. Identification and Morphological Characterization of Dendritic Spines Contacted by Thalamic or Cortical Afferents

(A) Placement of stimulating and recording electrodes.

(B) Left: dye-filled LA projection neuron, scale bar equals 20 μm. Right: higher magnification of a tertiary dendrite illustrating different spine types, scale bar equals 2 μm.

(C) Classification of spine types (n = 124 analyzed spines from 12 different neurons).

(D and E) Left: visualization of the spine (red fluorescence, Alexa-594). Middle: [Ca^{2+}] transient after cortical or thalamic stimulation (green fluorescence, Fluo-5F), scale bars equal 2 μm. Right: line scan across spine head and parent dendrite. White arrows indicate the time of afferent stimulation. Scale bars equal 0.5 s.

(F) Thalamic and cortical spines are located on the same dendritic branches.

(G) Classification of identified spines contacted by thalamic (n = 17) or cortical (n = 18) afferents.

(H) Left: cumulative plot of spine head radius for thalamic and cortical spines. Right: averaged radius of thalamic (T) and cortical (C) spines and the corresponding parent dendrites. Thalamic spines exhibit significantly larger spine heads ($p < 0.001$).

sion with the Ca^{2+} chelator BAPTA (30 mM; +10 ms: 85% ± 13% of baseline, n = 3; −10 ms: 94% ± 13% of baseline, n = 6; Figure 3C).

In contrast to thalamic afferents, application of the same pairing protocol to cortical afferent synapses did not result in the induction of spike timing-dependent LTP or LTD at any of the tested EPSP-AP delays (+10 ms: 102% ± 9% of baseline, n = 6; $p > 0.05$; −10 ms: 93% ± 11% of baseline, n = 5; $p > 0.05$; Figure 3F). Confirming earlier studies (Mahanty and Sah, 1999; Tsvetkov et al., 2004; but see Weisskopf and LeDoux, 1999), we found no significant difference between the two afferents in the voltage dependence of the NMDA or the AMPA (α-amino-3-hydroxy-5-methyl-4-isoxazole-propionate) receptor-mediated components of the EPSC, or in the ratio between the AMPA and the NMDA component (see Supplemental Figure S1 at http://www.neuron.org/cgi/content/full/45/1/119/DC1/). Furthermore, cortical and thalamic afferents exhibited similar temporal summation of EPSPs elicited by three stimulations at 30 Hz (not shown), and similar miniature EPSC waveforms (evoked in the presence of Sr^{2+}) (see Supplemental Figure S1), which is in agreement with our imaging data showing that thalamic and cortical afferent synapses are located on the same dendrites. Thus, the complete absence of STDP at cortical afferent synapses cannot be explained by differences in NMDA or AMPA receptor-mediated synaptic transmission or by a different synaptic location on the dendritic tree.

Postsynaptic Induction of Synaptic Plasticity at Cortical Afferents

In previous studies, tetanic stimulation (Huang and Kandel, 1998) or presynaptic stimulation paired with prolonged postsynaptic depolarization (Tsvetkov et al., 2002, 2004) was used to induce NMDA receptor-depen-

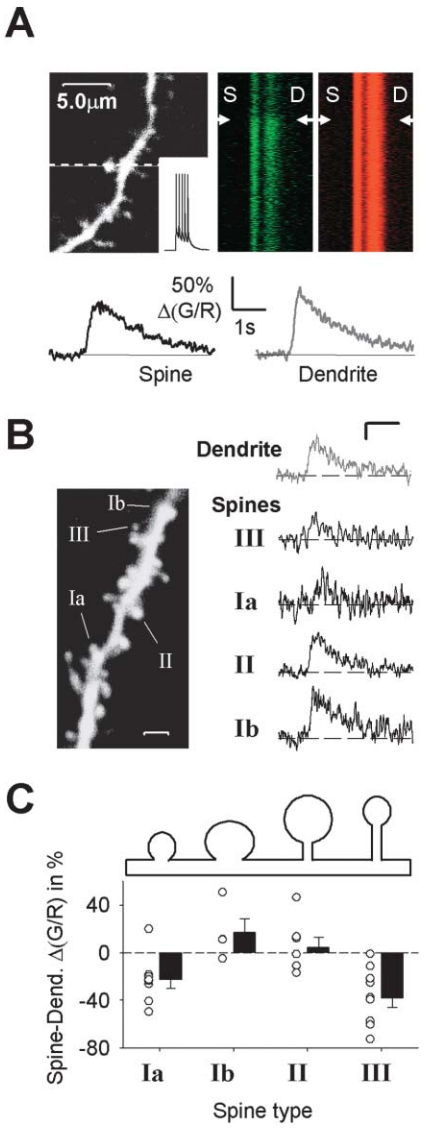

Figure 2. Spine Type-Specific Ca^{2+} Signaling during AP Backpropagation

(A) Left: dendritic branch with analyzed spine. Dashed line indicates the position of the line scan. Right: red and green fluorescence during the backpropagation of a short burst of action potentials (5 APs, see inset). Time of stimulation is indicated by the white arrows, scale bar equals 0.8 s. Bottom: time course of fluorescence intensity in the green channel normalized to the red channel (ΔG/R), in the spine and in the parent dendrite.

(B) Fluorescence intensity (ΔG/R) changes in different spine types apposed to the same parent dendrite during AP backpropagation. Scale bars equal 20% Δ(G/R), 0.8 s.

(C) Analysis of the $[Ca^{2+}]$ transient triggered by backpropagating APs in different spine types (n = 8, 4, 7, and 11 for types Ia, Ib, II, and III, respectively), compared to the $[Ca^{2+}]$ transient in the corresponding parent dendrite. Type Ia and type III spines exhibited significantly smaller $[Ca^{2+}]$ transients than their parent dendrites ($p < 0.01$).

dent LTP at cortical afferents. Here, depolarization provided by the short trains of APs during the induction of STDP is very brief, and postsynaptic Ca^{2+} levels may not reach threshold for induction of synaptic plasticity.

To assess whether there was a causal relationship between postsynaptic Ca^{2+} dynamics and induction of synaptic plasticity at cortical afferents, we applied the smooth endoplasmic reticulum calcium ATPase (SERCA) inhibitor cyclopiazonic acid (CPA; 15 μM). CPA slows down $[Ca^{2+}]$ decay kinetics in spines and dendrites, thereby increasing the integral of the $[Ca^{2+}]$ transients during repetitive AP backpropagation (Holthoff et al., 2002). Consistent with the hypothesis that the lack of STDP at cortical afferents is caused by lower $[Ca^{2+}]$ transients than at thalamic synapses, we found that in the presence of CPA pairing, brief bursts of presynaptic stimulation with postsynaptic APs induced LTD at cortical afferents (72% ± 19% of baseline, n = 4; $p < 0.05$; Figure 4A). Since we did not observe any difference in the mean decay time constant of $[Ca^{2+}]$ transients in spines exhibiting large or small BPAP-induced Δ $[Ca^{2+}]$ (corresponding to thalamic and cortical spine types, respectively; see Figure 2) (τ_{decay}: large Δ $[Ca^{2+}]$ spines: 340 ± 30 ms, n = 15; small Δ $[Ca^{2+}]$ spines: 297 ± 31 ms, n = 15; $p > 0.05$), it is unlikely that SERCA-mediated Ca^{2+} extrusion is simply more efficient at cortical synapses (Majewska et al., 2000). LTD induction occurred at EPSP/AP delays of +10 or −10 ms (but not at +20 or −20 ms), indicating that CPA did not increase the integral of the $[Ca^{2+}]$ transients sufficiently for induction of LTP. Therefore, we applied additional, sustained depolarization to −20 mV in between the APs during a burst. As expected, pairing the same presynaptic stimulation paradigm with sustained postsynaptic depolarization now resulted in LTP at cortical afferents (143% ± 17% of baseline, n = 12; $p < 0.05$; Figure 4B). Like LTD, LTP at cortical afferents was not affected by the relative timing between the first EPSP and the first AP, indicating that a general boosting of $[Ca^{2+}]$ transients can enable induction of LTD or LTP but that temporal precision of postsynaptic $[Ca^{2+}]$ transients might be insufficient for induction of STDP under these conditions.

We were concerned that cortical afferent synapses differed not only in terms of postsynaptic $[Ca^{2+}]$ transients but that LTP at these synapses was fundamentally different from LTP at thalamic synapses. We found, however, that LTP at cortical synapses, like LTP at thalamic inputs, was completely blocked by the NMDA receptor antagonist CPP (102% ± 12% of baseline, n = 5; $p > 0.05$; Figure 4B), by postsynaptic perfusion with BAPTA (101% ± 10% of baseline, n = 5; $p > 0.05$; Figure 4B), and by the CaMK-II antagonist KN62 (10 μM; cortical: 98% ± 12% of baseline, n = 5; $p > 0.05$; thalamic: 101% ± 18% of baseline, n = 5; $p > 0.05$; Figure 4C). Thus, synaptic plasticity can be induced at cortical afferents and relies on similar mechanisms as at thalamic synapses, provided that postsynaptic $[Ca^{2+}]$ transients are sufficient.

VDCCs and Synaptic Plasticity at Thalamic and Cortical Afferents

We addressed the question of whether the differences in spine $[Ca^{2+}]$ dynamics and the differences in synaptic plasticity could be related to a single underlying mechanism. Given the spine type-specific impact of backprop-

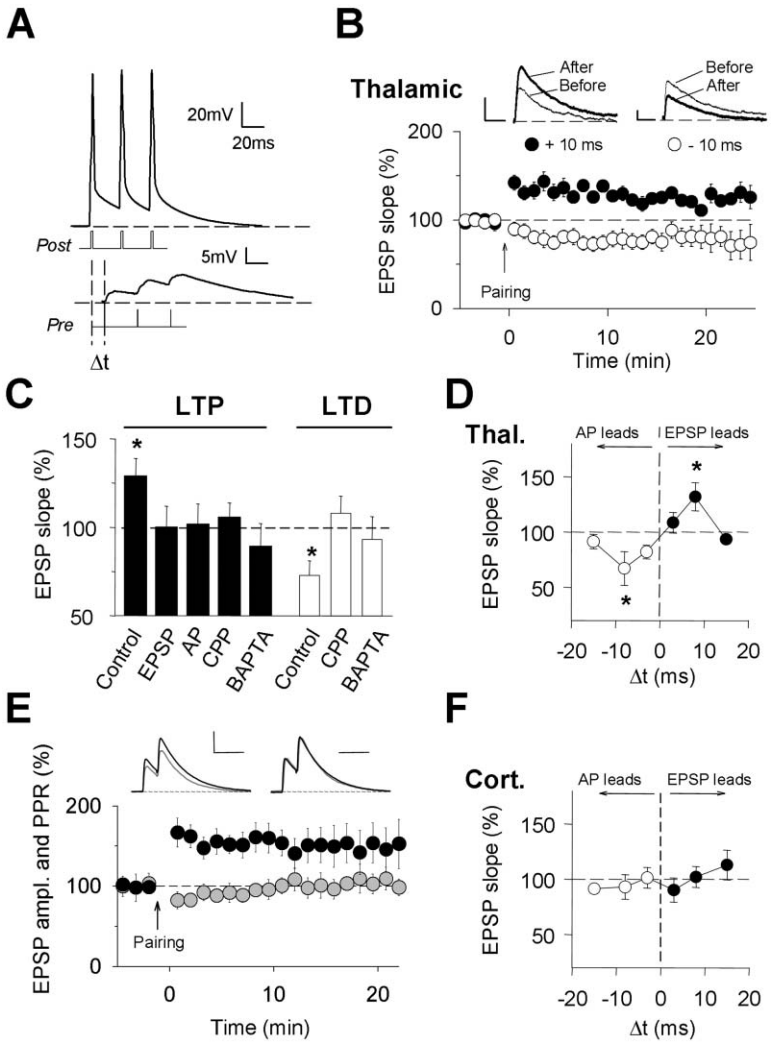

Figure 3. Input-Specific Induction of Spike Timing-Dependent Plasticity at Thalamic Afferents

(A) Schematic illustrating the induction protocol consisting of 15 bursts of 3 APs and 3 EPSPs at 30 Hz.

(B) Time course of bidirectional changes in EPSP slope at thalamic afferents induced by EPSP-AP pairing at +5 to +10 ms (n = 10) or −5 to −10 ms (n = 5). Scale bars equal 1.5 mV and 40 ms.

(C) Spike timing-dependent LTP is associative since it cannot be induced by EPSPs alone (n = 5, $p > 0.05$) or APs alone (n = 5, $p > 0.05$). It is blocked by the NMDA receptor antagonist CPP (n = 8, $p > 0.05$) and by postsynaptic perfusion with the Ca^{2+} chelator BAPTA (n = 3, $p > 0.05$). Spike timing-dependent LTD requires NMDA receptor activation (CPP; n = 5, $p > 0.05$) and postsynaptic Ca^{2+} elevation (BAPTA; n = 6, $p > 0.05$).

(D) Plot illustrating the time windows for the induction of LTP and LTD at thalamic afferents. EPSP-AP delays were binned into ranges from +20 to +10 ms (n = 6); +10 to +6 ms (n = 5; $p < 0.05$); +6 to 0 ms (n = 12); 0 to −6 ms (n = 4); −6 to −10 ms (n = 5; $p < 0.05$); and −10 to −25 ms (n = 9).

(E) Spike timing-dependent LTP at thalamic afferents (filled circles) does not affect the paired pulse ratio (gray circles; PPR; n = 5; $p > 0.05$). Scale bars equal 4 mV and 100 ms.

(F) Plot illustrating the complete lack of STDP at cortical afferents. EPSP-AP delays were binned into ranges from +20 to +10 ms (n = 10); +10 to +6 ms (n = 6); +6 to 0 ms (n = 6); 0 to −6 ms (n = 5); −6 to −10 ms (n = 5); and −10 to −20 ms (n = 8).

agating APs on spine $[Ca^{2+}]$ transients, presumably reflecting differential activation of VDCCs (Sabatini and Svoboda, 2000), we assessed the contribution of specific VDCCs to STDP induction. L-type Ca^{2+} channels (L-VDCCs) have previously been reported to contribute to LTP induction in the hippocampus (Morgan and Teyler, 2001) and in the LA (Huang and Kandel, 1998; Weisskopf et al., 1999; Bauer et al., 2002; Shinnick-Gallagher et al., 2003). Indeed, we found that the L-VDCC antagonist verapamil (50 μM) blocked spike timing-dependent LTP at thalamic afferents (95% ± 14% of baseline, n = 5; Figure 5A). Verapamil did not affect presynaptic release as assessed by three stimulations at 30 Hz (n = 4; $p > 0.05$; see Supplemental Figure S2). In contrast to LTP, induction of LTD at thalamic afferents did not require activation of L-VDCCs (58% ± 9% of baseline, n = 4; $p < 0.05$; Figure 5B), indicating that different Ca^{2+} sources contribute to the induction of spike timing-dependent LTP and LTD. To compare the role of L-VDCCs during LTP induction at thalamic and cortical afferents, we assessed the effect of verapamil on cortical LTP induced by presynaptic stimulation combined with strong, sustained postsynaptic depolarization. Consistent with an equal contribution of L-VDCCs to Ca^{2+} signaling at both inputs, we found that no significant LTP was induced at cortical synapses in the presence of verapamil (109% ± 19% of baseline, n = 5; $p > 0.05$; Figure 5C).

Based on previous studies demonstrating activation of dendritic R-VDCCs by BPAPs in cortical pyramidal cells (Sabatini and Svoboda, 2000; Yasuda et al., 2003), we assessed the effect of R-type channel blockers on STDP at thalamic afferents. A low concentration of Ni^{2+} (10 μM) specifically blocking R- and T-type Ca^{2+} channels (Yasuda et al., 2003) completely abolished LTP (86% ± 14% of baseline, n = 8; $p > 0.05$; Figure 5A) and LTD (100% ± 4% of baseline, n = 5; $p > 0.05$; Figure 5B). There was no effect of Ni^{2+} on presynaptic release at thalamic or cortical afferents as indicated by a lack of effect on EPSP amplitude and on paired-pulse ratio during repetitive stimulation (n = 5; $p > 0.05$; see Supplemental Figure S2). To identify the Ca^{2+} channel subtype affected by Ni^{2+} application, we repeated the experiments in the presence of the specific R-VDCC blocker SNX482 (100 nM) (Newcomb et al., 1998; Wilson et al., 2000). SNX482 completely blocked LTP (96% ±

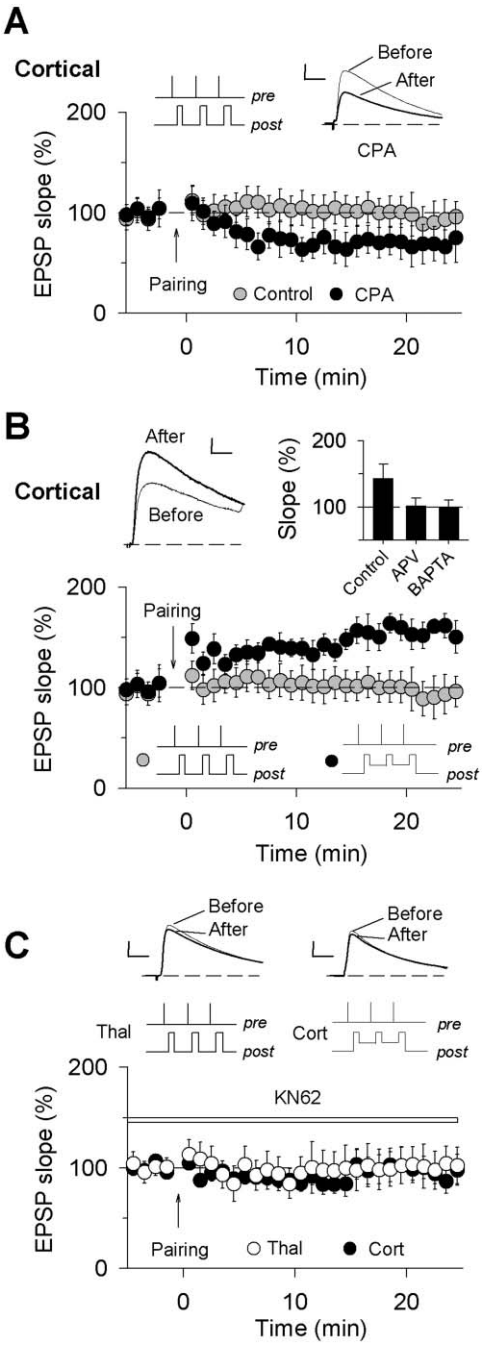

Figure 4. Postsynaptic Induction of Plasticity at Cortical Afferents Requires Elevated Postsynaptic Ca^{2+} Levels

(A) Induction of LTD at cortical afferents by pairing presynaptic stimulation with postsynaptic APs (see inset) in the presence of the CPA (black symbols; $n = 4$, $p < 0.05$) as compared to control conditions (gray symbols; $n = 6$, $p > 0.05$). Scale bars equal 2 mV and 20 ms.

(B) Top left and bottom: induction of LTP at cortical afferents by pairing presynaptic stimulation with sustained postsynaptic depolarization (black symbols; see inset; $n = 12$, $p < 0.05$) as compared to the same protocol in the absence of sustained depolarization (gray symbols; $n = 6$, $p > 0.05$). Top right: LTP at cortical afferents is blocked by application of the NMDA receptor antagonist CPP ($n = 5$, $p > 0.05$) and by postsynaptic perfusion with the Ca^{2+} chelator BAPTA ($n = 5$, $p > 0.05$). Scale bars equal 2 mV and 10 ms.

14% of baseline, $n = 5$; Figure 5A) and LTD (93% ± 8% of baseline, $n = 5$; Figure 5B) without any effect on baseline synaptic transmission ($n = 4$; $p > 0.05$; see Supplemental Figure S2). In contrast to the equal blockade of LTP at thalamic and cortical afferent synapses by the L-VDCC antagonist verapamil, we found that Ni^{2+} did not interfere with cortical LTP (141% ± 13% of baseline, $n = 7$; $p < 0.05$; Figure 5C), suggesting that a preferential activation of R-VDCCs at thalamic synapses might underlie input-specific induction of STDP.

To assess whether the brief depolarization induced by somatic APs during induction of STDP would be sufficient for the activation of somatic or dendritic R-VDCCs, we measured the effect of SNX482 on membrane depolarization during short bursts of APs at 30 Hz. SNX482 induced a significant decrease in the afterdepolarization following APs in a 30 Hz burst in 3 out of 4 cells (see Supplemental Figure S2). Together, these data indicate that R-VDCCs play an essential role during EPSP/AP pairing at thalamic afferent synapses, suggesting that R-VDCCs, in synergy with NMDA receptors, might boost $[Ca^{2+}]$ transients and/or depolarization during coincident pre- and postsynaptic spiking.

Spine Type-Specific Activation of R-VDCCs by Backpropagating APs

Since large and small spine types exhibited differential postsynaptic $[Ca^{2+}]$ dynamics upon stimulation with backpropagating APs and because R-VDCCs are strongly activated by backpropagating APs, we tested whether R-VDCC activation in large spines could account for the observed spine type specificity. Indeed, we found that $NiCl_2$ (10 μM) reduced Δ $[Ca^{2+}]$ in spines exhibiting large $[Ca^{2+}]$ transients (S^+ spines; $n = 8$; $p < 0.001$), but not in spines showing small $[Ca^{2+}]$ transients (S^- spines; $n = 8$; $p > 0.05$) (Figures 6A and 6B). R-VDCC blockade essentially transformed spines with large Δ $[Ca^{2+}]$ into spines with small Δ $[Ca^{2+}]$ (Figure 6A). Application of Ni^{2+} slightly reduced $[Ca^{2+}]$ transients in parent dendrites (Figure 6B). However, this effect was not significantly different between dendrites close to S^+ or S^- spines (Figure 6B). Nevertheless, this raises the question of whether blockade of STDP at thalamic afferents (contacting S^+ spines) by Ni^{2+} was due to an effect on dendritic rather than on spine $[Ca^{2+}]$ transients. Therefore, we tried to induce LTP at thalamic afferents 5 min after the start of Ni^{2+} application. At this time point, 10 μM Ni^{2+} significantly reduced Δ $[Ca^{2+}]$ in S^+ spines but did not have any effect on parent dendrites (spine: 83% ± 4% of baseline, $n = 8$; $p < 0.01$; dendrite: 96% ± 4% of baseline, $n = 8$; $p > 0.05$; see Supplemental Figure S3). However, even after 5 min of Ni^{2+} application, LTP at thalamic synapses was completely blocked (93% ± 13% of baseline, $n = 5$; $p > 0.05$; see Supplemental Figure S3), indicating that a reduction in spine $[Ca^{2+}]$ underlies the blockade of LTP induction.

Consistent with a role for L-VDCCs in dendritic $[Ca^{2+}]$ dynamics, we found that the L-VDCC antagonist nimo-

(C) LTP at cortical and thalamic afferents is blocked by the CaMKII antagonist KN62 (cortical: black symbols, $n = 5$, $p > 0.05$; thalamic: white symbols; $n = 5$, $p > 0.05$). Scale bars equal 2 mV and 20 ms.

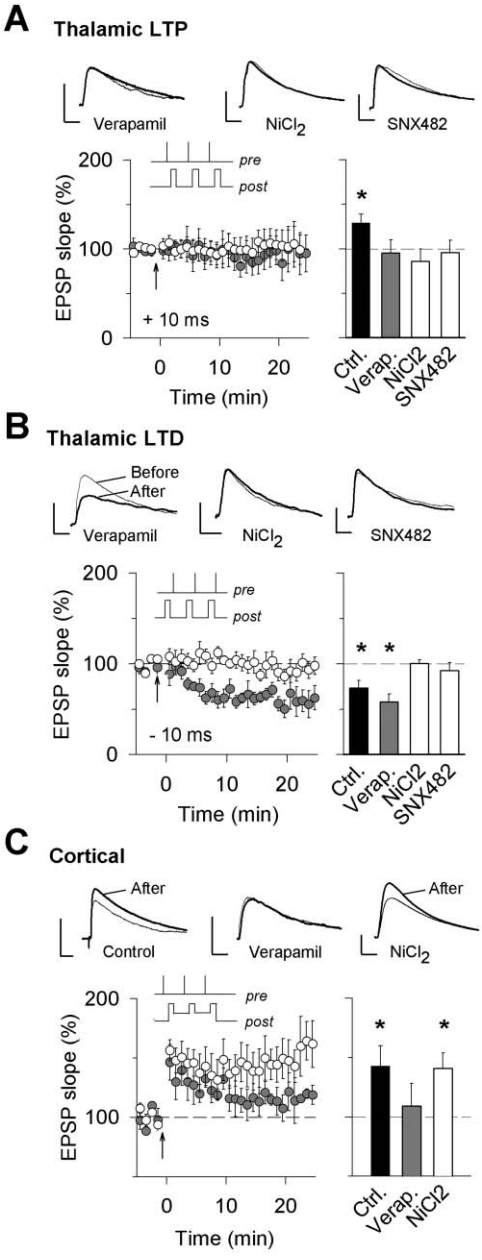

Figure 5. Voltage-Dependent Ca^{2+} Channels and Hebbian Plasticity at Thalamic and Cortical Afferents

(A) Thalamic spike timing-dependent LTP is completely blocked by verapamil ($n = 5$), Ni^{2+} ($n = 8$), and the specific R-VDCC antagonist SNX482 ($n = 5$). Scale bars equal 4 mV and 20 ms.

(B) Thalamic spike timing-dependent LTD is verapamil insensitive ($n = 4$) but is blocked by Ni^{2+} ($n = 5$) and SNX-482 ($n = 5$). Scale bars equal 4 mV and 20 ms.

(C) Cortical LTP induced by sustained postsynaptic depolarization is abolished by the L-type Ca^{2+} channel antagonist verapamil ($n = 5$, $p > 0.05$) and is Ni^{2+} resistant ($n = 7$, $p < 0.01$). Scale bars equal 4 mV and 20 ms.

dipine (2 μM) affected Δ [Ca^{2+}] more strongly in dendrites than in spines and did not differentially affect distinct spine types (Figures 6C and 6D). Together, these findings indicate that a preferential activation of R-VDCCs on large spines contributes to the differential [Ca^{2+}] dynamics in different spine types and possibly to afferent specificity of STDP.

R-VDCC Activation at Thalamic Spines

To directly show the specific activation of R-VDCCs at thalamic afferent synapses, we assessed the effect of R-VDCC blockade on BPAP-induced [Ca^{2+}] transients at identified cortical and thalamic synapses. We identified single spines contacted by cortical or thalamic axons using afferent stimulation-induced [Ca^{2+}] transients and subsequently imaged Δ [Ca^{2+}] in response to brief bursts of BPAPs (Figures 7A–7C). Consistent with the previous results, we found that Δ [Ca^{2+}] in thalamic spines was significantly reduced by application of Ni^{2+}, whereas cortical spines and parent dendrites were not significantly affected (thalamic: 67% $\pm$ 8% of baseline, $n = 7$; $p < 0.01$; cortical: 89% $\pm$ 15% of baseline, $n = 6$; $p > 0.05$; parent dendrite: 88% $\pm$ 9% of baseline, $n = 13$; $p > 0.05$) (Figure 7D). This indicates either that R-VDCCs are located preferentially on dendritic spines contacted by thalamic afferents or that there exist input-specific mechanisms selectively coupling or uncoupling homogeneously distributed R-VDCCs to/from Ca^{2+}-dependent signaling at thalamic or cortical inputs.

α-1E Containing R-VDCCs Are Preferentially Located at Thalamic Afferent Synapses

To distinguish between these two scenarios, we performed an immunohistochemical analysis using antibodies against the R-VDCC-specific Ca^{2+} channel subunit α-1E (Newcomb et al., 1998; Wilson et al., 2000). We found that α-1E immunoreactive puncta colocalized with the postsynaptic density marker protein PSD-95 (Figure 8A). PSD-95/α-1E colocalization correlated with the apparent size of the PSD-95 clusters. Whereas small PSD-95 clusters did show low levels of colocalization, larger PSD-95 clusters were mostly colocalized with α-1E immunoreactivity (Figure 8A), suggesting that α-1E containing R-VDCCs are postsynaptic to thalamic afferents. Moreover, α-1E immunoreactivity was found juxtaposed to punctate staining for the presynaptic marker protein synaptophysin, indicating that postsynaptic spines expressing α-1E-containing R-VDCCs are contacted by presynaptic afferents (Figure 8B). To directly compare postsynaptic α-1E expression at thalamic and cortical afferents, we used in vivo injections of the anterograde tracer *Phaseolus vulgaris*-leucoagglutinin (PHA-L) into the auditory thalamic nuclei (MGm/PIN) and into the auditory cortex (area Te3) projecting to the basolateral amygdala (LeDoux, 2000). α-1E immunohistochemistry on slices obtained from PHA-L-injected animals revealed that thalamic PHA-L-labeled fibers formed putative presynaptic boutons that were significantly more likely to be apposed to α-1E-immunoreactive puncta as compared to cortical boutons (cortical: $n = 101$ boutons from 8 slices; thalamic: $n = 114$ boutons from 8 slices; $p < 0.05$; Figures 8C and 8D). Even though the population of cortical and thalamic afferents labeled by in vivo PHA-L injections might not be completely identical to those afferents stimulated in the slice preparation, this indicates that R-VDCCs are not only preferentially activated, but also asymmetrically located at thalamic and cortical afferents to the LA.

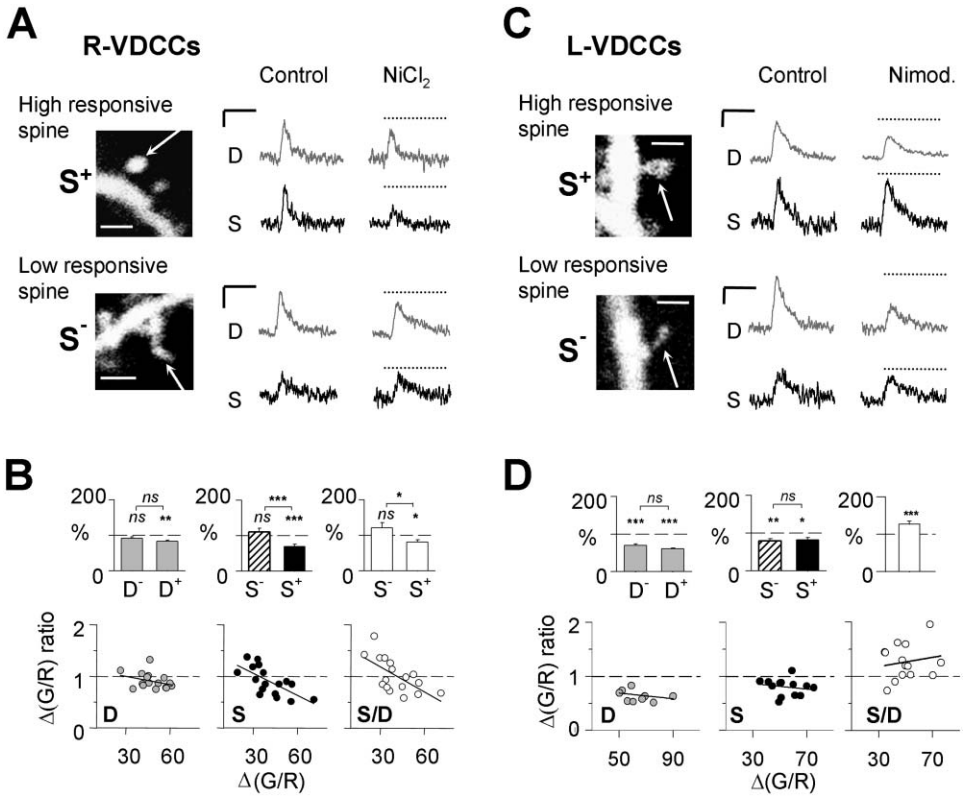

Figure 6. Asymmetric Contribution of R-Type Ca^{2+} Channels to $[Ca^{2+}]$ Transients Induced by Backpropagating Action Potentials in Small and Large Spines

(A) Effect of inactivation of R-VDCCs on spine and dendrite $[Ca^{2+}]$ transients triggered by backpropagating APs. Left: analyzed spines (arrow) and parent dendrites. Scale bars equal 2 μm. Right: $[Ca^{2+}]$ transients (ΔG/R) before (control) and after 10 min of Ni^{2+} application in high responsive (S^+, top) and low responsive (S^-, bottom) spines. Scale bars equal 20% ΔG/R, 1 s.

(B) Summary graphs of Ni^{2+} effects on $[Ca^{2+}]$ transients in low- and high-responsive dendrites (D^-, D^+, left) showing no significant difference in Ni^{2+} sensitivity between D^+ and D^- dendrites. Middle and right: summary graphs of Ni^{2+} effects on $[Ca^{2+}]$ transients in low (S^-, $n = 7$) and high (S^+, $n = 7$; $p < 0.001$) responsive spines illustrating that Ni^{2+} specifically reduces $[Ca^{2+}]$ transients in S^+ spines and that this effect cannot be explained by a selective action on the parent dendrite.

(C and D) L-VDCC blockade preferentially reduces dendritic $[Ca^{2+}]$ transients and does not differentially affect S^+ and S^- spines. Time course of dendritic and spine $[Ca^{2+}]$ transients (ΔG/R) upon blockade of L-VDCCs. Data presented as in (A) and (B). Scale bars equal 25% ΔG/R, 1 s.

Discussion

Our present results show that LA projection neurons are equipped with two morphologically and functionally distinct types of dendritic spines that are contacted by different presynaptic afferents. In particular, we found that spines postsynaptic to thalamic afferents exhibit larger spine heads than cortical spines and that they harbor different complements of VDCCs. Most importantly, the presence of R-type VDCCs endows thalamic synapses with the capacity to express associative long-term modifications of synaptic strength depending on the precise timing of pre- and postsynaptic activity. Our finding that R-VDCCs are preferentially contributing to spine Ca^{2+} transients in response to AP backpropagation is consistent with previous experiments in hippocampal CA1 pyramidal cells (Sabatini and Svoboda, 2000).

Asymmetric Activation of R-VDCCs at Thalamic and Cortical Afferents

In LA projection neurons, R-VDCCs appear to be preferentially located on and activated at spines contacted by thalamic afferents. This is indicated by several lines of evidence: first, we observed that $[Ca^{2+}]$ transients induced by trains of BPAPs were larger in big spines as compared to small spines and could be essentially transformed into small $[Ca^{2+}]$ transients by R-VDCC blockade. In contrast, $[Ca^{2+}]$ transients in small spines did not involve R-VDCCs. Since spines contacted by thalamic afferents exhibit significantly larger spine heads as compared to cortical spines, these experiments indicate that R-VDCCs specifically contribute to BPAP-induced $[Ca^{2+}]$ transients at thalamic spines. Second, experiments in which we first identified the presynaptic input by recording afferent stimulation-induced synaptic, NMDA receptor-mediated $[Ca^{2+}]$ transients clearly demonstrated that subsequent BPAP-induced $[Ca^{2+}]$ transients were R-VDCC antagonist sensitive at thalamic synapses, but not at cortical synapses. Third, by using an immunohistochemical approach, we could show that R-VDCCs colocalize with the postsynaptic density marker protein PSD-95. Consistent with our previous experiments, we found a correlation between the apparent size of the PSD-95 clusters, presumably reflecting spine head diameter and R-VDCC colocaliza-

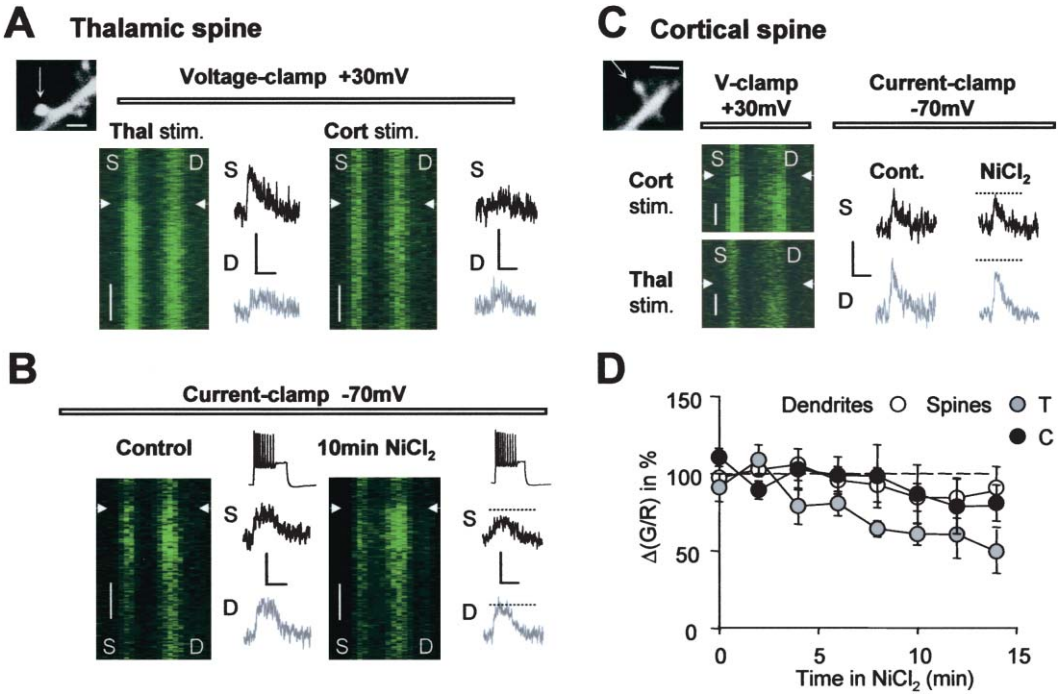

Figure 7. Asymmetric Activation of R-VDCCs on Thalamic and Cortical Spines

(A) Top left: identified thalamic spine, scale bar equals 2 μm. Identification was performed at +30 mV. The increase of intracellular [Ca^{2+}] at this potential is due to synaptic NMDA receptor activation induced by thalamic afferent stimulation (left) but not upon cortical afferent stimulation (right).

(B) The same cell is subsequently repolarized to −70 mV, and brief bursts of backpropagating APs were induced (see inset). The resulting [Ca^{2+}] transients were assessed at identified thalamic spines (S) and their parent dendrites (D) under control conditions (Control) and after 10 min of Ni^{2+} application. Scale bars equal 0.7 s (line scan); 50% ΔG/R and 1 s.

(C) Same experiment for an identified cortical spine. Scale bars equal 0.5 s (line scan); 30% ΔG/R and 1 s.

(D) Averaged data illustrating the time course of Δ [Ca^{2+}] during Ni^{2+} application in dendrites ($n = 13$, $p > 0.05$), thalamic spines ($n = 7$, $p < 0.05$), and cortical spines ($n = 6$, $p > 0.05$).

tion. Fourth, by using in vivo injection of an anterograde tracer into the auditory thalamic nuclei (MGm/PIN) and into the auditory cortex (area Te3) projecting to the LA, we found that α-1E-containing R-VDCCs are significantly more likely to be postsynaptic to putative thalamic boutons. Taken together, these experiments indicate that the asymmetric activation and location of R-VDDCs at thalamic and cortical spines promote the afferent-specific induction of STDP. Our results do not exclude the possibility, however, that additional spine type-specific signaling pathways might also contribute.

Afferent-Specific Spine Morphology

While our data clearly demonstrate an association between morphological and functional spine properties, there remains the question of whether the morphological differences are causally linked to spine type-specific Ca^{2+} signaling. Recent studies are consistent with our observations suggesting that morphology is a crucial determinant of Ca^{2+} signaling in dendritic spines (Yuste et al., 2000). In the LA projection neurons studied here, spine morphology and spine type-specific location of R-VDCCs may depend on extrinsic factors, such as thalamic afferent innervation or previous activity (Yasuda et al., 2003; Matsuzaki et al., 2004). Alternatively, cell-autonomous mechanisms may underlie the precise matching of pre- and postsynaptic functional and morphological features.

Our results raise the question of whether differences in spine morphology at thalamic and cortical synapses might be reflected by functional differences in basal synaptic transmission. Based on our recordings of evoked EPSCs, we could not detect any differential contribution of either AMPA or NMDA receptors to excitatory transmission at either input. Moreover, recordings of spontaneous mEPSCs revealed similar amplitudes and kinetics for quantal events at thalamic and cortical synapses. Considering their equidistance from the soma, this indicates that similar subunit combinations contribute to AMPA receptor-mediated EPSCs at both inputs. However, considering the most likely imperfect voltage-clamp of dendritic spines, we cannot rule out that additional voltage-dependent conductances specifically located at thalamic or cortical spines might have compensated for possible differences in mEPSC kinetics (Tsay and Yuste, 2004). Future electron microscopical and imaging experiments will have to show whether specific spine morphologies are associated with structural and/or functional pre- and postsynaptic differences.

Synaptic Plasticity at Cortical Afferents

The present results indicate that cortical afferent synapses, in contrast to thalamic afferents, are insensitive to brief periods of coincident pre- and postsynaptic spiking. Previous experiments from our laboratory have

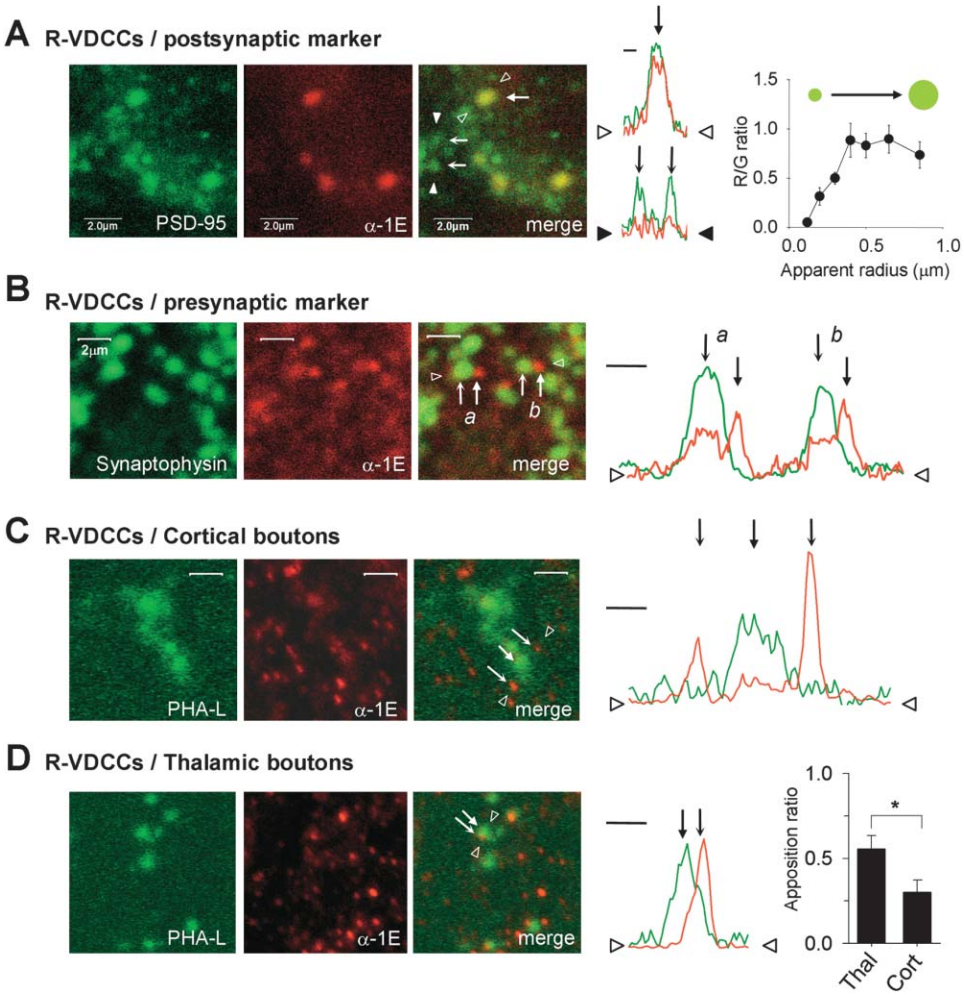

Figure 8. Preferential Location of R-VDCCs at Thalamic Spines

(A) Immunohistochemical distribution of α-1E-containing R-VDCCs in the dorsolateral LA. Left: double-labeled sections for the R-VDCC subunit α-1E (red) and the postsynaptic density marker PSD-95 (green). Middle: fluorescence intensity profiles along defined lines (between triangles) obtained from single optical sections illustrate α-1E/PSD-95 colocalization in large PSD-95 clusters (thick arrow), but not in adjacent small clusters (thin arrows). Scale bar equals 1 μm. Right: colocalization of PSD-95 and α-1E depends on the apparent size of the PSD-95 clusters.
(B) Left: double-labeled sections for the R-VDCC subunit α-1E (red) and the presynaptic marker synaptophysin (green) showing close apposition of presynaptic structures with α-1E-immunoreactive puncta. Right: fluorescence intensity profiles along a defined line (between triangles) obtained from single optical sections illustrate α-1E/synaptophysin apposition. Scale bar equals 1 μm.
(C) Left: double-labeled sections showing cortical afferents stained with the anterograde tracer PHA-L (green), and α-1E immunoreactive clusters (red, thin arrow) not apposed to putative presynaptic cortical boutons (thick arrow). Right: intensity profiles along a defined line (between triangles) were obtained from five projected optical sections separated by 1 μm in z. Scale bar equals 0.5 μm.
(D) Left: double-labeled sections showing thalamic afferents stained with the anterograde tracer PHA-L (green), and α-1E-immunoreactive clusters (red, thin arrow) apposed to putative presynaptic thalamic boutons (thick arrow). Middle: intensity profiles along a defined line (between triangles) were obtained from five projected optical sections separated by 1 μm in z. Scale bar equals 0.5 μm. Right: bar graph illustrating that a larger proportion of thalamic than cortical boutons are apposed to α-1E-immunoreactive clusters (thalamic: n = 114 boutons from 8 slices; cortical: n = 101 boutons from 8 slices, see Experimental Procedures for quantification).

shown that LTP at cortical afferents can even occur completely independent of postsynaptic activity (Humeau et al., 2003). Nevertheless, experiments presented here and work by others suggests that LTD and LTP can also be induced postsynaptically at cortical synapses (Huang and Kandel, 1998; Tsvetkov et al., 2002, 2004; Humeau et al., 2003). Postsynaptic induction of plasticity at cortical synapses appears to depend on the amplitude and duration of postsynaptic depolarization and Ca^{2+} dynamics. Interestingly, postsynaptically induced LTP at cortical afferents is R-VDCC independent (this study) and occludes with LTP induced via a presynaptic mechanism, indicating, at least in part, a shared presynaptic mechanism of expression (Humeau et al., 2003). In contrast to cortical LTP (Tsvetkov et al., 2002; Humeau et al., 2003), induction of STDP at thalamic afferents was not associated with a change in PPR, which is generally taken as an index for alterations in the presynaptic probability of neurotransmitter release. This indicates that, at least under our experimental conditions, cortical and thalamic afferent synapses onto LA projection neurons differ not only with respect to the locus of

LTP induction, but also with respect to the expression mechanism.

Consistent with an important role for L-VDCCs during fear conditioning (Bauer et al., 2002; Shinnick-Gallagher et al., 2003; but see Cain et al., 2002), L-VDCC activation appeared to be required for the postsynaptic induction LTP at thalamic and cortical afferents, irrespective of whether it was induced by BPAPs or sustained postsynaptic depolarization. At thalamic synapses, induction of spike timing-dependent LTD differed from its counterpart LTP in that it was L-VDCC independent. Apart from L-VDCC activation, spike timing-dependent LTD and LTP exhibited the same pharmacology, suggesting additional LTD-specific routes of Ca^{2+} entry, such as metabotropic glutamate receptor-induced release from intracellular Ca^{2+} stores (Heinbockel and Pape, 2000; Normann et al., 2000).

Structural Basis and Functional Implications of Afferent-Specific Plasticity in the Amygdala

What might be the physiological relevance for afferent-specific changes in synaptic efficacy in the LA? Recent evidence indicates that postsynaptic spiking of LA projection neurons is not necessary for fear learning to occur but that postsynaptic spiking is associated with a more efficient acquisition of fear conditioning (Rosenkranz et al., 2003). In keeping with the notion that R-VDCCs are most efficiently activated by backpropagating APs (Sabatini and Svoboda, 2000), it has been shown that mice deficient for the R-type-specific α-1E subunit exhibit a delayed acquisition of cued auditory fear conditioning (Kubota et al., 2001). This might indicate that whereas cortical afferent synapses are able to sample surrounding patterns of activity of thalamic afferents by means of presynaptic NMDA receptors (Humeau et al., 2003), a process that could possibly be involved in stimulus discrimination (Jarrell et al., 1987; but see Armony et al., 1997), thalamic afferent synapses appear to be particularly suited to mediate rapid acquisition of conditioned fear during periods of strong sensory experience associated with postsynaptic AP firing in LA projection neurons.

Unlike other projection neurons, such as hippocampal or cortical pyramidal cells or cerebellar Purkinje cells, where functionally distinct afferent inputs impinge on different dendritic compartments (Magee, 1999; Holthoff et al., 2002; Nimchinsky et al., 2002; Isomura et al., 2002; Yuste and Bonhoeffer, 2004), cortical and thalamic spines on LA projection neurons are intermingled on the same dendritic branches. Moreover, in keeping with the nuclear organization, LA projection neuron dendrites do not exhibit any apparent polarization into basal and apical dendrites, nor do they show tuft-like distal arborizations that can form a functionally separate compartment allowing sub- and suprathreshold integration of distal synaptic input (Larkum et al., 1999; Magee, 2000; Häusser et al., 2000; Wei et al., 2001; Williams and Stuart, 2003). Thus, consistent with recent physiological findings (Humeau et al., 2003; Doyère et al., 2003; Tsvetkov et al., 2004), our morphological data indicate that there may be close functional interactions between cortical and thalamic sensory input, possibly at the level of individual synapses. At the same time, the precise matching of presynaptic input and dendritic spines enables LA projection neurons to independently integrate thalamic and cortical sensory input and to adjust synaptic efficacy in an afferent-specific manner.

Experimental Procedures

Slice Preparation

Standard procedures were used to prepare 350 μm thick coronal slices from 3- to 4-week-old male C57BL/6J mice following a protocol approved by the Veterinary Department of the Canton of Basel-Stadt (Humeau et al., 2003). Briefly, the brain was dissected in ice-cold artificial cerebrospinal fluid (ACSF), mounted on an agar block, and sliced with a Dosaka vibratome (Kyoto, Japan) at 4°C. Slices were maintained for 45 min at 35°C in an interface chamber containing ACSF equilibrated with 95% O_2/5% CO_2 and containing (in mM) 124 NaCl, 2.7 KCl, 2 $CaCl_2$, 1.3 $MgCl_2$, 26 $NaHCO_3$, 0.4 NaH_2PO_4, 18 glucose, 4 ascorbate, and then for at least 45 min at room temperature before being transferred to a superfusing recording chamber.

Electrophysiology

Whole-cell recordings from LA projection neurons were performed at 30°C–32°C in a superfusing chamber. Neurons were visually identified with infrared videomicroscopy using an upright microscope equipped with a 40× objective (Olympus). Patch electrodes (3–5 MΩ) were pulled from borosilicate glass tubing and normally filled with a solution containing (in mM) 120 K-gluconate, 20 KCl, 10 HEPES, 10 phosphocreatine, 4 Mg-ATP, and 0.3 Na-GTP (pH adjusted to 7.25 with KOH or CsOH, respectively, 295 mOsm). For voltage-clamp experiments, K-gluconate was replaced by equimolar Cs-gluconate. All experiments were performed in the presence of picrotoxin (100 μM). In current-clamp recordings, membrane potential was kept manually at −70 mV. Data were recorded with an Axopatch200B, filtered at 2 kHz, and digitized at 10 kHz. In all experiments, series resistance was monitored throughout the experiment by applying a hyperpolarizing current or voltage pulse, and if it changed by more than 15%, the data were not included in the analysis. Data were acquired and analyzed with ClampEx8.0, ClampFit8.0 (Axon Instruments, CA), Mini Analysis Program (Synaptosoft, CA), and the LTP Program (W. Anderson, University of Bristol, UK). Monosynaptic EPSPs exhibiting constant 10%–90% rise times and latencies were elicited by stimulation of afferent fibers with a bipolar twisted platinum/10% iridium wire (25 μm diameter). Although we never observed any antidromic spikes, we cannot exclude that some efferent fibers originating from LA projection neurons were stimulated. LTP was induced by pairing 3 monosynaptic EPSPs with 3 APs elicited by 0.5 nA, 5 ms current steps at 30 Hz (*18*). Pairing patterns were repeated 15× at 0.2 Hz. EPSP-AP delays were determined from the onset of the EPSP to the peak of the AP. LTP or LTD were quantified for statistical comparisons by normalizing and averaging EPSP slopes during the last 5 min of experiments relative to 5 min of baseline. Depicted traces show averaged EPSPs for 2 min of baseline and 2 min of LTP/LTD (20–25 min after pairing). All values are expressed as means ± SEM. Statistical comparisons were done with paired or unpaired Student's t test as appropriate (two-tailed $p < 0.05$ was considered significant).

Imaging

Cells were filled via a patch pipette with normal K^+ or Cs^+ based intracellular solution containing 40 μM Alexa-594 (Ca^{2+}-insensitive dye, red fluorescence) and 200 μM Fluo-5F (medium-affinity Ca^{2+}-indicator, green fluorescence). After gaining access to the cell, dyes were allowed to equilibrate by diffusion for at least 15 min. For the optical measurements, we used a custom-made two-photon laser scanning microscope based on a modified Fluoview (Olympus, Switzerland) confocal microscope using a 60 × 0.9NA objective (LUMPlanFI, Olympus) coupled to an ultrafast Ti:sapphire laser (Mai-Tai, Spectra-Physics, Germany) tuned to a λ of 800 nm. Fluorescence was detected as epifluorescence by 2 internal PMTs (Olympus). SDM570 and BA510IF and BA565IF barrier filters were placed in the "green" and the "red" pathways, respectively, to eliminate transmitted or reflected excitation light. Fluorescence intensities were acquired and analyzed with Fluoview software (FV300, Olympus). The

ratio G/R (Fluo5F/Alexa594) was used to avoid large errors due to the very low resting fluorescence of Fluo5F and to eliminate movement artifacts (Yasuda et al., 2003). [Ca^{2+}] changes were measured as the difference between the ratios G/R before and after stimulation and expressed as Δ(G/R) in % of baseline value.

Active spines were detected by scanning along dendritic branches (from proximal to distal) at various focal planes while stimulating both afferent pathways simultaneously (5 EPSCs, 20 Hz, at +30 mV). After detection of [Ca^{2+}] changes in a particular spine, cortical or thalamic afferents were stimulated separately to assess afferent input. To increase the rate of detection of "randomly" distributed active spines on the dendritic arbor, the point-spread function (PSF) of the focal volume was increased to 0.8 μm (full-width at half-maximum) laterally and to 4.2 μm axially by underfilling the objective back aperture. To estimate the volume of compartments smaller than the point-spread function, spine fluorescence (Alexa-594) was compared to peak fluorescence at the cell body, where the cell volume was larger than the PSF (Nimchinsky et al., 2004).

PHA-L Injections and Immunohistochemistry

Mice were anesthetized with 1.5%–4% isoflurane in O_2 and secured in a stereotaxic frame (Kopf, Tujunga, CA). *Phaseolus vulgaris*-Leucoagglutinin (PHA-L) Alexa-488 conjugated anterograde tracer (2.5% in 0.1 M sodium phosphate buffer [pH 8.0]) was injected bilaterally by pressure (0.2 μl per side) into the auditory thalamus (medial division of the medial geniculate body [MGm], 3.3 mm posterior, 1.75 mm lateral to the bregma, 3.2 mm deep from the cortical surface [Franklin and Paxinos, 1997]) or the auditory cortex (Te3, 3.0 mm posterior, 4.0 mm lateral to the bregma, 2.6 mm deep from the cortical surface [Franklin and Paxinos, 1997]). 7 days later, mice were transcardially perfused with 4% paraformaldehyde in PBS. After 4 hr postfixation in the same fixative at 4°C, coronal sections (50 μm) were cut on a vibratome (Leica, Glattbrugg, Switzerland) and collected in PBS. Sections were incubated overnight at 4°C in a blocking solution (10% bovine serum albumin [BSA]) containing primary polyclonal rabbit anti-α1E (1:200). For labeling of pre- and postsynaptic markers, slices were incubated with primary monoclonal mouse anti-postsynaptic density protein (PSD-95, 1:200), or primary monoclonal mouse anti-synaptophysin (1:200). After four rinses in PBS, sections were incubated for 1 hr at room temperature with either Alexa Fluor 594 conjugated goat anti-rabbit IgG (1:1000) or FITC conjugated goat anti-mouse IgG (1:100). Finally, immunolabeled sections were washed in PBS, mounted on gelatin-coated slides, and coverslipped with Fluorostab (Bio-Science, Emmenbrücke, Switzerland). For quantification of the proportion of putative thalamic and cortical boutons apposed to α1E-immunoreactive clusters, all putative boutons on several consecutive confocal sections were scored for the presence of an α1E-immunoreactive cluster within 1 μm. The analysis was performed blind to the location of the injection site.

Reagents

BAPTA, CPA, NBQX, CPP, KN62, nimodipine, and verapamil were from Tocris-Cookson (Bristol, UK), QX-314 Cl^- was from Alomone Labs (Jerusalem, Israel), and SNX-482 was from Peptides International (Louisville, KY). Fluo-5F, Alexa-594, *Phaseolus vulgaris*-Leucoagglutinin (PHA-L) Alexa Fluor 488 conjugated anterograde tracer (L-11270), and Alexa Fluor 594 goat anti-rabbit IgG (A11012) were from Molecular Probes (Eugene, OR). Monoclonal anti-PSD95 and anti-synaptophysin Abs were from Sigma Aldrich (St. Louis, MO). FITC-conjugated goat anti-mouse (115-095-146) was from Jackson ImmunoResearch Labs (West Grove, PA) and anti-α1E (AB5248) from Chemicon International (Temecula, CA). All other drugs were from Fluka/Sigma (Buchs, Switzerland).

Acknowledgments

We thank T. Oertner, B. Gähwiler, A. Matus, B. Poulain, M. Scanziani, and all members of the Lüthi lab for helpful discussions and comments on the manuscript. Supported by the Swiss National Science Foundation, the Borderline Personality Disorder Research Foundation, ELTEM, and the Novartis Research Foundation.

Received: August 16, 2004
Revised: October 12, 2004
Accepted: November 22, 2004
Published: January 5, 2005

References

Armony, J.L., Servan-Schreiber, D., Romanski, L.M., Cohen, J.D., and LeDoux, J.E. (1997). Stimulus generalization of fear responses: effects of auditory cortex lesions in a computational model and in rats. Cereb. Cortex *7*, 157–165.

Bauer, E.P., Schafe, G.E., and LeDoux, J.E. (2002). NMDA receptors and L-type voltage-gated calcium channels contribute to long-term potentiation and different components of fear memory formation in the lateral amygdala. J. Neurosci. *22*, 5239–5249.

Bi, G.Q., and Poo, M.M. (1998). Synaptic modifications in cultured hippocampal neurons: dependence on spike timing, synaptic strength, and postsynaptic cell type. J. Neurosci. *18*, 10464–10472.

Bi, G.Q., and Poo, M.M. (2001). Synaptic modification by correlated activity: Hebb's postulate revisited. Annu. Rev. Neurosci. *24*, 139–166.

Bissière, S., Humeau, Y., and Lüthi, A. (2003). Dopamine gates LTP induction in lateral amygdala by suppressing feedforward inhibition. Nat. Neurosci. *6*, 587–592.

Blair, H.T., Tinkelman, A., Moita, M.A., and LeDoux, J.E. (2003). Associative plasticity in neurons of the lateral amygdala during auditory fear conditioning. Ann. N Y Acad. Sci. *985*, 485–487.

Bliss, T.V., and Collingridge, G.L. (1994). A synaptic model of memory: long-term potentiation in the hippocampus. Nature *361*, 31–39.

Cain, C.K., Blouin, A.M., and Barad, M. (2002). L-type voltage-gated calcium channels are required for extinction, but not for acquisition or expression, of conditional fear in mouse. J. Neurosci. *22*, 9113–9121.

Carlsen, J., and Heimer, L. (1988). The basolateral amygdaloid complex as a cortical-like structure. Brain Res. *441*, 377–380.

Chicurel, M.E., and Harris, K.M. (1992). Three-dimensional analysis of the structure and composition of CA3 branched dendritic spines and their synaptic relationship with mossy fiber boutons in the rat hippocampus. J. Comp. Neurol. *325*, 169–182.

Debanne, D., Gähwiler, B.H., and Thompson, S.M. (1998). Long-term synaptic plasticity between pairs of individual CA3 pyramidal cells in rat hippocampal slice cultures. J. Physiol. (Lond.) *507*, 237–247.

Doyère, V., Schafe, G.E., Sigurdsson, T., and LeDoux, J.E. (2003). Long-term potentiation in freely moving rats reveals asymmetries in thalamic and cortical inputs to the lateral amygdala. Eur. J. Neurosci. *17*, 2703–2715.

Faber, E.S.L., Callister, R.J., and Sah, P. (2001). Morphological and electrophysiological properties of principal neurons in the rat lateral amygdala in vitro. J. Neurophysiol. *85*, 714–723.

Farb, C.R., and LeDoux, J.E. (1997). NMDA and AMPA receptors in the lateral nucleus of the amygdala are postsynaptic to auditory thalamic afferents. Synapse *27*, 106–121.

Farb, C.R., and LeDoux, J.E. (1999). Afferents from rat temporal cortex synapse on lateral amygdala neurons that express NMDA and AMPA receptors. Synapse *33*, 218–229.

Franklin, K.B.J., and Paxinos, G. (1997). The Mouse Brain in Stereotaxic Coordinates (San Diego: Academic Press).

Hansel, C., and Linden, D.J. (2000). Long-term depression of the cerebellar climbing fiber-Purkinje neuron synapse. Neuron *26*, 473–482.

Häusser, M., Spruston, N., and Stuart, G.J. (2000). Diversity and dynamics of dendritic signaling. Science *290*, 739–744.

Harris, K.M., and Kater, S.B. (1994). Dendritic spines: cellular specializations imparting both stability and flexibility to synaptic function. Annu. Rev. Neurosci. *17*, 341–371.

Heinbockel, T., and Pape, H.C. (2000). Input-specific long-term depression in the lateral amygdala evoked by theta frequency stimulation. J. Neurosci. *20*, RC68.

Holthoff, K., Tsay, D., and Yuste, R. (2002). Calcium dynamics of spines depend on their dendritic location. Neuron *33*, 425–437.

Huang, Y.Y., and Kandel, E.R. (1998). Postsynaptic induction and PKA-dependent expression of LTP in the lateral amygdala. Neuron *21*, 169–178.

Humeau, Y., Shaban, H., Bissière, S., and Lüthi, A. (2003). Presynaptic induction of heterosynaptic associative plasticity in the mammalian brain. Nature *426*, 841–845.

Isomura, Y., Fujiwara-Tsukamoto, Y., Imanishi, M., Nambu, M., and Takada, M. (2002). Distance-dependent Ni^{2+}-sensitivity of synaptic plasticity in apical dendrites of hippocampal CA1 pyramidal cells. J. Neurophysiol. *87*, 1169–1174.

Jarrell, T.W., Gentile, C.G., Romanski, L.M., McCabe, P.M., and Schneiderman, N. (1987). Involvement of cortical and thalamic auditory regions in retention of differential bradycardia conditioning to acoustic conditioned stimuli in rabbits. Brain Res. *412*, 285–294.

Kubota, M., Murakoshi, T., Saegusa, H., Kazuno, A., Zong, S., Hu, Q., Noda, T., and Tanabe, T. (2001). Intact LTP and fear memory but impaired spatial memory in mice lacking Ca(v)2.3 (alpha(1E)) channel. Biochem. Biophys. Res. Commun. *282*, 242–248.

Larkum, M.E., Zhu, J.J., and Sakmann, B. (1999). A new cellular mechanism for coupling inputs arriving at different cortical layers. Nature *398*, 338–341.

LeDoux, J.E. (2000). Emotion circuits in the brain. Annu. Rev. Neurosci. *23*, 155–184.

Majewska, A., Brown, E., Ross, J., and Yuste, R. (2000). Mechanisms of calcium decay kinetics in hippocampal spines: role of spine calcium pumps and calcium diffusion through the spine neck in biochemical compartmentalization. J. Neurosci. *20*, 1722–1734.

Markram, H., Lübke, J., Frotscher, M., and Sakman, B. (1997). Regulation of synaptic efficacy by coincidence of postsynaptic APs and EPSPs. Science *275*, 213–215.

Magee, J.C. (1999). Voltage-gated ion channels in dendrites. In Dendrites, G. Stuart, N. Spruston, and M. Häusser, eds. (Oxford: Oxford University Press), pp. 139–160.

Magee, J.C. (2000). Dendritic integration of excitatory synaptic input. Nat. Rev. Neurosci. *1*, 181–190.

Magee, J.C., and Johnston, D. (1997). A synaptically controlled, associative signal for Hebbian plasticity in hippocampal neurons. Science *275*, 209–213.

Mahanty, N.K., and Sah, P. (1999). Excitatory synaptic inputs to pyramidal neurons of the lateral amygdala. Eur. J. Neurosci. *11*, 1217–1222.

Mainen, Z. (1999). Functional plasticity at dendritic synapses. In Dendrites, G. Stuart, N. Spruston, and M. Häusser, eds. (Oxford: Oxford University Press), pp. 310–338.

Maren, S. (2001). Neurobiology of Pavlovian fear conditioning. Annu. Rev. Neurosci. *24*, 897–931.

Matsuzaki, M., Honkura, N., Ellis-Davies, G.C.R., and Kasai, H. (2004). Structural basis of long-term potentiation in single dendritic spines. Nature *429*, 761–766.

Morgan, S.L., and Teyler, T.J. (2001). Electrical stimuli patterned after the theta-rhythm induce multiple forms of LTP. J. Neurophysiol. *86*, 1289–1296.

Newcomb, R., Szoke, B., Palma, A., Wang, G., Chen, X., Hopkins, W., Cong, R., Miller, J., Urge, L., Tarczy-Hornoch, K., et al. (1998). Selective peptide antagonist of the class E calcium channel from the venom of the tarantula *Hysterocrates gigas*. Biochemistry *37*, 15353–15362.

Nicoll, R.A., and Malenka, R.C. (1995). Contrasting properties of two forms of long-term potentiation in the hippocampus. Nature *377*, 115–118.

Nimchinsky, E.A., Sabatini, B.L., and Svoboda, K. (2002). Structure and function of dendritic spines. Annu. Rev. Physiol. *64*, 313–353.

Nimchinsky, E.A., Yasuda, R., Oertner, T.G., and Svoboda, K. (2004). The number of glutamate receptors opened by synaptic stimulation in single hippocampal spines. J. Neurosci. *24*, 2054–2064.

Normann, C., Peckys, D., Schulze, C.H., Walden, J., Jonas, P., and Bischofberger, K. (2000). Associative long-term depression in the hippocampus is dependent on postsynaptic N-type Ca^{2+} channels. J. Neurosci. *20*, 8290–8297.

Oertner, T.G., Sabatini, B.L., Nimchinsky, E., and Svoboda, K. (2002). Facilitation at single synapses probed with optical quantal analysis. Nat. Neurosci. *5*, 657–664.

Paré, D., Pape, H.-C., and Dong, J. (1995). Bursting and oscillating neurons of the cat basolateral amygdaloid complex in vivo: electrophysiological properties and morphological features. J. Neurophysiol. *74*, 1179–1191.

Romanski, L.M., Clugnet, M.C., Bordi, F., and LeDoux, J.E. (1993). Somatosensory and auditory convergence in the lateral nucleus of the amygdala. Behav. Neurosci. *107*, 444–450.

Rosenkranz, J.A., and Grace, A.A. (2002). Dopamine-mediated modulation of odour-evoked amygdala potentials during pavlovian conditioning. Nature *417*, 282–287.

Rosenkranz, J.A., Moore, H., and Grace, A.A. (2003). The prefrontal cortex regulates lateral amygdala neuronal plasticity and responses to previously conditioned stimuli. J. Neurosci. *23*, 11054–11064.

Sabatini, B.L., and Svoboda, K. (2000). Analysis of calcium channels in single spines using optical fluctuation analysis. Nature *408*, 589–593.

Shinnick-Gallagher, P., McKernan, M.G., Xie, J., and Zinebi, F. (2003). L-type voltage-gated calcium channels are involved in the in vivo and in vitro expression of fear conditioning. Ann. N Y Acad. Sci. *985*, 135–149.

Sjöström, P.J., and Nelson, S.B. (2002). Spike timing, calcium signals and synaptic plasticity. Curr. Opin. Neurobiol. *12*, 305–314.

Smith, Y., Paré, J.-F., and Paré, D. (2000). Differential innervation of parvalbumin-immunoreactive interneurons of the basolateral amygdaloid complex by cortical and intrinsic inputs. J. Comp. Neurol. *416*, 496–508.

Tsay, D., and Yuste, R. (2004). On the electrical function of dendritic spines. Trends Neurosci. *27*, 77–83.

Tsvetkov, E., Carlezon, W.A., Benes, F.M., Kandel, E.R., and Bolshakov, V.Y. (2002). Fear conditioning occludes LTP-induced presynaptic enhancement of synaptic transmission in the cortical pathway to the lateral amygdala. Neuron *34*, 289–300.

Tsvetkov, E., Shin, R.M., and Bolshakov, V.Y. (2004). Glutamate uptake determines pathway specificity of long-term potentiation in the neural circuitry of fear conditioning. Neuron *41*, 139–151.

Wei, D.S., Mei, Y.A., Bagal, A., Kao, J.P., Thompson, S.M., and Tang, C.M. (2001). Compartmentalized and binary behavior of terminal dendrites in hippcampal pyramidal neurons. Science *293*, 2272–2275.

Weisskopf, M.G., and LeDoux, J.E. (1999). Distinct populations of NMDA receptors at subcortical and cortical inputs to principal cells of the lateral amygdala. J. Neurophysiol. *81*, 930–934.

Weisskopf, M.G., Bauer, E.P., and LeDoux, J.E. (1999). L-type voltage-gated calcium channels mediate NMDA-independent associative long-term potentiation at thalamic input synapses to the amygdala. J. Neurosci. *19*, 10512–10519.

Williams, S.R., and Stuart, G.J. (2003). Role of dendritic synapse location in the control of action potential output. Trends Neurosci. *26*, 147–154.

Wilson, S.M., Toth, P.T., Oh, S.B., Gillard, S.E., Volsen, S., Ren, D., Philipson, L.H., Lee, E.C., Fletcher, C.F., Tessarollo, L., et al. (2000). The status of voltage-dependent calcium channels in alpha-1E knock-out mice. J. Neurosci. *20*, 8566–8571.

Yasuda, R., Sabatini, B.L., and Svoboda, K. (2003). Plasticity of calcium channels in dendritic spines. Nat. Neurosci. *6*, 948–955.

Yuste, R., and Bonhoeffer, T. (2004). Genesis of dendritic spines: insights from ultrastructural and imaging studies. Nat. Neurosci. Rev. *5*, 24–34.

Yuste, R., Majewska, A., and Holthoff, K. (2000). From form to function: calcium compartmentalization in dendritic spines. Nat. Neurosci. *3*, 653–659.

The Cerebellum. 2006; 5: 243–256

Taylor & Francis
Taylor & Francis Group

ORIGINAL ARTICLE

Synaptic organization of the mouse cerebellar cortex in organotypic slice cultures

JEAN-LUC DUPONT, ELODIE FOURCAUDOT, HUGUETTE BEEKENKAMP, BERNARD POULAIN & JEAN-LOUIS BOSSU

Institut des Neurosciences Cellulaires et Intégratives, UMR 7168 LC2 CNRS/ULP, Department of Neurotransmission et Sécrétion Neuroendocrine, Centre de Neurochimie, Strasbourg Cedex, France

Abstract
The cellular and synaptic organization of new born mouse cerebellum maintained in organotypic slice cultures was investigated using immunohistochemical and patch-clamp recording approaches. The histological organization of the cultures shared many features with that observed *in situ*. Purkinje cells were generally arranged in a monolayer surrounded by a molecular-like neuropil made of Purkinje cell dendritic arborizations. Purkinje cell axons ran between clusters of small round cells identified as granule cells by Kv3.1b potassium channel immunolabelling. The terminal varicosities of the Purkinje cells axons enwrapped presumptive neurons of the cerebellar nuclei whereas their recurrent collaterals were in contact with Purkinje cells and other neurons. Granule cell axons established contacts with Purkinje cell somata and dendrites. Parvalbumin and glutamine acid decarboxylase (GAD) immunohistochemistry revealed the presence of presumptive interneurons throughout the culture. The endings of granule cell axons were observed to be in contact with these interneurons. Similarly, interneurons endings were seen close to Purkinje cells and granule cells. Whole cell recordings from Purkinje cell somata showed AMPA receptor-mediated spontaneous excitatory post-synaptic currents (sEPSCs) and $GABA_A$ receptor-mediated spontaneous inhibitory post-synaptic currents (sIPSCs). Similar events were recorded from granule cell somata except that in this neuronal type EPSPs have both a NMDA component and an AMPA component. In addition, pharmacological experiments demonstrated a GABAergic control of granule cell activity and a glutamatergic control of GABAergic neurons by granule cells. This study shows that a functional neuronal network is established in such organotypic cultures even in the absence of the two normal excitatory afferents, the mossy fibers and the climbing fibers.

Key words: *Cerebellum, neuronal network, organotypic cultures, excitatory synapses, inhibitory synapses*

Introduction

Since Ramón y Cajal's description of the cerebellum more than a century ago (1), extensive immunohistological and electrophysiological studies of this structure have precisely determined the synaptic relationships between cerebellar neurons, as well as their neurotransmitters (2). *In situ*, Purkinje cells receive excitatory inputs from glutamatergic granule cells and olivary neurons via parallel and climbing fibers respectively, and inhibitory inputs from several types of GABAergic and glycinergic interneurons (basket and stellate cells). Purkinje cells via their axons exert GABAergic inhibition on neurons of the deep nuclei. Granule cells receive excitatory inputs via mossy fibers and inhibitory inputs mainly from Golgi cell interneurons.

Studies of *in vitro* preparations such as acute slices from guinea pig (3,4), rat (5) and mouse (6), organotypic cultures from rat (7–11), mouse (12–14) and kitten (15) and dissociated cell cultures from rat (16–18) and mouse (19,20) have increased our knowledge of cerebellar development, and neuron-specific electrophysiology.

In addition, important insights into critical cellular and molecular mechanisms governing neurogenesis and cell survival have emerged from studies on mice displaying natural mutations which affect the cerebellum (see 21 and 22 for reviews). Investigating the role of critical proteins in cerebellar physiology and pathology is now possible by using transgenic mice. However, because of the ubiquitous functions of the targeted proteins, normal development and survival of transgenic animals could be impaired and consequently specific studies of such proteins require appropriate *in vitro* models. Here using electrophysiological and immunohistochemical approaches we show that after several weeks *in vitro*, cerebellar slices

Correspondence: J. L. Bossu, Institut des Neurosciences Cellulaires et Intégratives, UMR 7168 LC2 CNRS/ULP, Department of Neurotransmission et Sécrétion Neuroendocrine, Centre de Neurochimie, 5 rue Blaise Pascal, F-67084 Strasbourg Cedex, France. E-mail: jlbossu@neurochem.u-strasbg.fr

ISSN 1473-4222 print/ISSN 1473-4230 online
DOI: 10.1080/14734220600905317

originating from new born mice display the main characteristics of mature cerebellum. We propose that organotypic slice cultures of mouse cerebellar cortex can be used to analyze the consequences of mutations and pathologies on neuronal function and survival.

Materials and methods

Cerebellar slice cultures

Organotypic cerebellar slice cultures were prepared from mice using the roller tube technique as described by Gähwiler (9). Briefly, the cerebellum was removed under aseptic conditions from 0–1 day-old-mice after decapitation. Parasagittal slices of $\sim$400μm-thick were cut using a McIlwain tissue chopper. Individual slices were attached to glass coverslips in a film of clotted chicken plasma (Cocalico, Reamstown, PA, USA) and placed in culture tubes containing 750 μl of culture medium made of 25% heat-inactivated horse serum, 50% Eagle's basal medium, 25% HBSS supplied with 33.3 mM D-glucose and 0.1 mM glutamine. The tubes were put in a roller drum placed inside an incubator at 36°C. Uridine (Sigma), cytosine-β-D-arabino-furanoside (Sigma) and 5-fluorodeoxyuridine (Sigma) were used in combination (10^{-7}M working solution) and added to the culture medium for 24 h, 2–4 days after the culture was started in order to retard the overgrowth of macrophages, glial cells and fibroblasts. The cultures were fed once a week by renewing the culture medium. Electrophysiological recordings and immunohistochemistry were performed after a period of at least 2–3 weeks.

Immunocytochemistry

Granule cells and neurons from cerebellar nuclei were identified using an anti- Kv3.1b potassium channel subunit antibody (rabbit polyclonal; Sigma; 1/300). A mouse monoclonal anti-calbindin D-28K antibody (Sigma; 1/1500) was used as a specific marker of Purkinje cells. A mouse monoclonal anti-parvalbumin antibody (Sigma; 1/1500) and rabbit polyclonal anti-Glutamic Acid Decarboxylase antibody (anti-GAD Chemicon; 1/1000) were used to label both Purkinje cells and GABAergic interneurons. In some instances, a mouse monoclonal anti-synaptophysin antibody (Sigma; 1/500) was used to detect presynaptic axonal sites.

The cultures were fixed in 4% paraformaldehyde in phosphate-buffered saline (PBS) overnight at 4°C after a brief wash (PBS; pH 7.4). Then the cultures were washed three times in PBS and immersed for 6 h in a PBS solution containing 0.1% Triton X-100 (PBST) to permeabilize cell membranes. They were further incubated for 2 h in PBST containing 10% normal goat serum (NGS) and 0.3% Bovine Serum Albumin (BSA) to block non specific binding of the antibodies. The cultures were then incubated for 24 h at 4°C with the primary antibodies diluted in the PBST containing 5% NGS and 0.3% BSA. After three washes in this antibody dilution medium, the cultures were incubated overnight at 4°C with Alexa 488-conjugated anti-rabbit or anti-mouse antibodies (1/4000; Molecular Probes) and /or with Cyanine3-conjugated anti-mouse or anti-rabbit antibodies (1/4000; Jackson ImmunoResearch). Finally the cultures were washed 3 times in PBS and mounted in Mowiol. Double labelling assays were performed by incubating the cultures with mixed monoclonal and polyclonal primary antibodies diluted as in single labelling experiments. The co-localization for Kv3.1b with GAD was analyzed by double immunofluorescence. In this case, Kv3.1b immunofluorescence detection was performed first and the culture was postfixed in 4% paraformaldehyde in PBS for 20 min. After an additional fixation in 70% ethanol for 20 min, the culture was submitted to the GAD immunodetection protocol. Negative controls were made by omitting the primary antibody. The cultures were analyzed with an inverted microscope equipped for epi-fluorescence (Nikon DIAPHOT-TMD) and a confocal microscope (Zeiss LSM 510, software release 3.2). All confocal pictures illustrated in the figures are single sections (pinhole: red channel 106 μm; green channel 98 μm). Evaluation of the ratio of granule cells to Purkinje cells was carried out by counting Kv31.b positive granule cell and calbindin positive Purkinje cell number in seven fields chosen on seven slice cultures that had apparently well developed cortical lamination.

Electrophysiology

Cerebellar slice cultures were transferred to a recording chamber fixed on the stage of a Nikon Optiphot2 microscope. Patch-clamp recordings were carried out under voltage or current clamp in the whole-cell recording mode (WCR) using an Axopatch 200 A amplifier (Axon Instruments, Foster City, CA). Cells were visualized on a monitor screen using an infra-red camera (T.I.L.L. Photonics, Planegg, Germany). Purkinje cells and granule cells were identified by their typical morphology. Purkinje cells are large (15–20 μM) neurons localized at the periphery of the cultures displaying a well developed dendritic arborization and a highly refringent nucleoli. Granule cells are small (5–8 μm) spherical cells. Electrodes of 5 MΩ (for Purkinje cell recordings) and of 10 MΩ (for granule cell recordings) were pulled from borosilicate glass capillaries (Clark Electromedical Instruments, Pangbourne, England) with a horizontal micropipette puller (BB-CH-PC, Mecanex, Geneva, Switzerland), and filled with a solution

containing in mM: K^+-gluconate 132, EGTA/KOH 1, $MgCl_2$ 2, NaCl 2, Hepes/KOH 10, MgATP 2, and GTP 0.5. pH was adjusted to 7.2 with TrisOH. The cultures were perfused at 20°C with a bath solution containing in mM: NaCl 130, KCl 2.7, $CaCl_2$ 5, $MgCl_2$ 0.5, Hepes/Tris 10, glucose 5.6. pH was adjusted to 7.4 with TrisOH. The current and voltage traces were digitized using a digital data recorder (VR-10B, Instrutech, Great Neck, NY, USA) before storage on a Panasonic video recorder (Matsushita Electric Industrial, Osaka, Japan), for off-line analysis by using MiniAnalysis (Synaptosoft) and Pclamp 8 (Axon Instruments) softwares.

Bicuculline methiodide, (Sigma, St Louis, USA), SR 95531 hydrobromide (Tocris, Ellisville, USA) were prepared as 10^{-2} M stock solution in distilled water, and CNQX (Tocris Cookson, Bristol, England) as 10^{-2} M stock solution in DMSO. D(-)-APV (Sigma, St Louis, USA) was extemporaneously prepared in the perfusion medium (free Mg^{2+}) at a working dilution of 10^{-5}M.

Results

Immunohistology of the cerebellar slices

Mouse cerebellar slices cultured with the roller tube method display a cytoarchitectural organization very similar to that of the adult mouse cerebellum *in situ*. Indeed, the cortical lamination is conserved despite the fact that the culture procedure generally alters cerebellar foliation. Anti-calbindin immunofluorescence disclosed Purkinje cell bodies often organized in a single row (Figure 1A, 1B1, 1B3). Purkinje cells generally displayed a well polarized morphology with a single apical dendritic arborisation extending in a molecular like-layer and both proximal and distal branches forming the dendritic arborization were decorated with spiny processes (Figure 1 A2). Purkinje cells emitting two or three dendritic trees were also seen (Figure 1F), but this feature was mainly restricted to ectopic neurons that were most often encountered in cultures that did not reach an advanced state of cortical lamination. The Purkinje cell bodies extend a thin varicose axon with a beaded appearance through an internal granule cell like-layer containing numerous small Kv3.1b-positive granule cells (6 to 8 μm in diameter, Figure 1, B2, B3) and through the core of the culture (Figure 1D). Since granule cell precursors are located in the external germinative layer at the time where the cultures were made (postnatal days 0 and 1), this indicates that granule cells in culture, are able to migrate as *in vivo*, to form the internal granular layer three to four weeks later. The axons of granule cells extended into the Purkinje cell-containing area (Figure 1, B2, B3). In some cultures when isolated granule cells could be observed (Figure 1 A3), the ascending axon emerging from the cell body often split into a typical T-shape between two parallel fibers. In slices where the cortical lamination was resected counts of granule cells as a function of Purkinje cell number gave ratios ranging between 42 and 98 (mean=63.71 $\pm$ 6.6, n=7, SEM). These values are much lower than estimates about 235 granule cells per Purkinje cell reported for normal and mutant adult mouse cerebella (23,24).

In the core of the culture, the Purkinje cell axons reached large neurons (more than 15 μm in diameter) confined in a nucleus-like formation (Figure 1, C1–C3). These neurons were closely surrounded by calbindin-positive Purkinje cell axon varicosities and displayed an intense Kv3.1b immunofluorescence. These neurons probably belong to cerebellar nuclei. In many slices where these neurons were lacking, the Purkinje cell axons ran back throughout the Purkinje cell layer (not shown).

Medium-sized (10–15 μm) neurons exhibited GAD, but not calbindin immunostaining throughout the culture (Figure 1D). These neurons were immunolabelled by antibodies raised against parvalbumin (Figure 1E), a calcium-binding protein only present in GABAergic neurons in the cerebellum. These calbindin-negative neurons displayed morphological features different from those of Purkinje cells and were likely GABAergic interneurons.

Detailed examination of these neurons indicates that in many cases they have established connections similar to that described *in situ*. Purkinje cell bodies and dendrites (Figure 2A) as well as parvalbumin-labelled interneurons (Figure 1E) were closely underlined by Kv3.1b-positive presynaptic endings of presumptive granule cell axons. Calbindin-positive Purkinje cell axons were often observed running back close to Purkinje cell soma (Figure 1A). Such axons correspond to recurrent axon collaterals of Purkinje cells. Whether some of these collaterals made autapses on the originating neuron could not be ascertained. In addition, Purkinje cell bodies were surrounded by a dense network of GAD-positive, calbindin-negative nerve endings (Figure 2B) indicating that inhibitory interneurons innervated Purkinje cells in the cultures. GAD positive varicosities were also found close to small Kv3.1b immunolabelled neurons resembling granule cells (Figure 2C). The assumption that the immunolabelled nerve endings described in this study correspond to real presynaptic sites was supported by their immunoreactivity for synaptophysin suggesting that synaptic vesicles are present in these structures (Figure 2 D1–D3).

Electrophysiological recordings of Purkinje cells

This first series of experiments was performed to determine which type of spontaneous activity Purkinje cells display in the cultures. Typically,

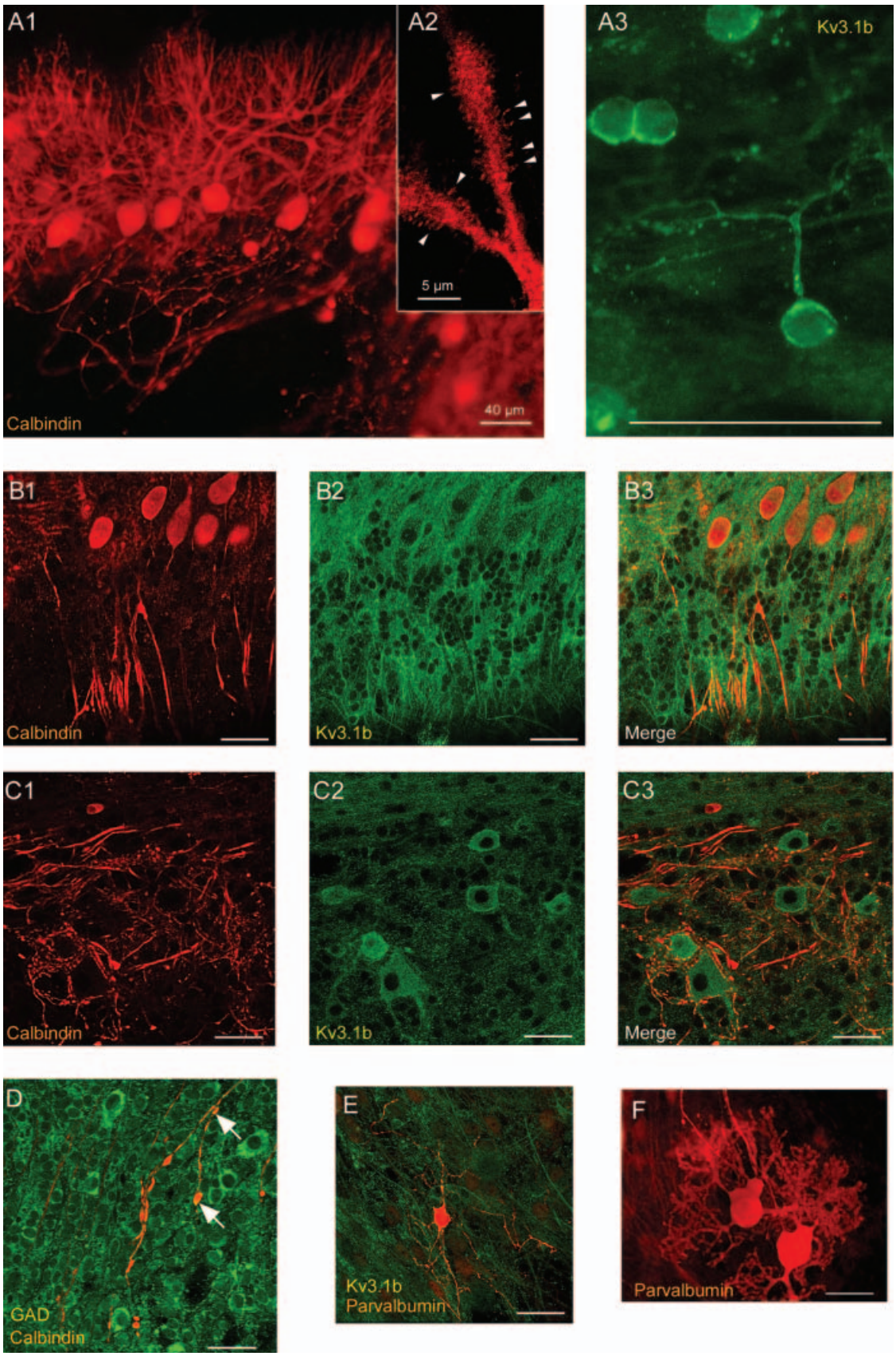

Figure 1. General organization of the cerebellar slice cultures after 3 weeks *in vitro*. (A1) Purkinje cells labelled with the anti-calbindin antibody. Note that Purkinje cells generally display a well polarized morphology and are organized in a single row to form a typical layer. (A2) Confocal picture of calbindin immunopositive Purkinje cell main dendritic branches covered with numerous spine like processes (arrows). (A3) Isolated granule cells labelled with an antibody raised against the Kv3.1b potassium channel subunit. Note that the axon emerging from the cell body split in a T shape manner into two parallel fibers. (B1, B2 and B3) Same fields showing confocal pictures of Purkinje cells labelled with the anti-calbindin antibody (B1), small round granule cells labelled with the anti-Kv3.1b potassium channel

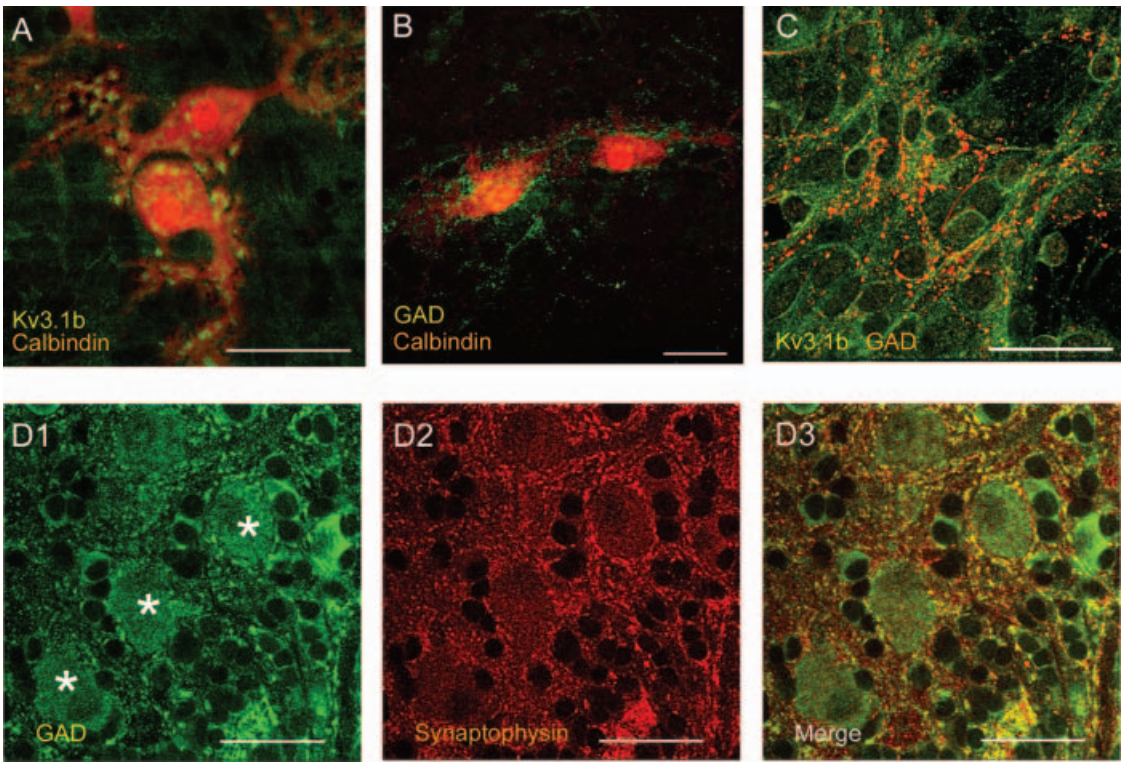

Figure 2. Putative synaptic contacts between distinct cell populations: evidence in the slice culture after 3 weeks *in vitro*. (A) Confocal image of a field showing Purkinje cells labelled with the anti-calbindin antibody (in red) exhibiting spots positive to the Kv3.1b potassium channel antibody on their somata and dendrites (in green) corresponding to nerve endings, presumably granule cell axon endings, in contact with the Purkinje cells. (B) Confocal image showing nerve endings immunopositive for GAD (in green) but negative for calbindin in contact with the soma and dendrites of Purkinje cells immunostained with the anti-calbindin antibody (in red). (C) Confocal picture showing GAD positive nerve endings (in red) in contact with Kv3.1b potassium channel positive granule cells (in green). (D1, D2 and D3) Same fields showing in D1 neurons labelled with the antibody raised against GAD (in green, asterisks indicate soma of Purkinje cells) and in D2 the presence of presynaptic sites as revealed by the use of an antibody raised against the vesicular protein synaptophysin (in red). In D3 the two immunostainings are merged showing that GAD positive synaptic contacts take place on neurons including Purkinje cells. Calibration bar: 40 μm.

when Purkinje cell somata were voltage clamped in a classical saline solution at a holding potential of -60 mV with a K-gluconate-filled patch pipette (i.e., E_K and $E_{Cl} \sim -80$ mV), spontaneous postsynaptic transient inward currents will be referred to as spontaneous postsynaptic excitatory currents (sEPSCs) were recorded in all cases (Figure 3A, n=43). Such events appeared with a mean frequency of 7.3 ± 1.5 Hz and a mean amplitude of 31 ± 4 pA. The amplitude distribution of sEPSCs (Figure 3A, lower panel) was skewed, with a main peak fitted with a gaussian function at 14.5 ± 0.7 pA (n=37). In 10 Purkinje cells (23%), spontaneous postsynaptic outward currents (spontaneous inhibitory postsynaptic currents, sIPSCs) also occurred (Figure 3B) with a mean frequency and amplitude of 2.5 ± 0.6 Hz and 28 ± 5 pA, respectively. The amplitude distribution of sIPSCs revealed a main peak at 14 ± 2 pA (n=10, Figure 3B, lower panel). The sIPSCs were blocked by a bath application of 10^{-5} M bicuculline (Figure 4, middle trace, n=4). Applications of 10^{-5} M CNQX blocked the sEPSCs whereas sIPSCs currents were still recorded (Figure 4, right trace, n=6). These pharmacological data demonstrate that in our culture system, Purkinje cell spontaneous synaptic activity mainly

←

antibody (B2) and the fusion of these two fields (B3) emphasizing the lamination of the structure. Purkinje cells stand in a layer localized at the periphery of the slice with their axons that run downwards in the putative internal granular layer. (C1, C2 and C3) Confocal pictures of the same field taken in the center of the same culture as in B. C1 shows the endings of Purkinje cell axons immunopositive to the calbindin antibody; in C2, immunostaining with the anti-Kv3.1b potassium channel antibody revealed that positive macroneurons are confined in a nucleus like structure; C3: the two immunostainings are merged and show Purkinje cell axon endings surrounding these macroneurons. (D) Confocal picture showing Purkinje cell axons beaded of varicosities labelled with the anti-calbindin antibody (in red) and GABAergic interneurons labelled with an antibody raised against GAD (in green). Note that Purkinje cell axons varicosities also contain GAD (arrows). (E) Confocal picture of a cell showing a clear immunopositivity to parvalbumin (in red) and morphologically different from Purkinje cells and so assumed to be an inhibitory interneuron. That neuron displayed many contacts with Kv3.1b positive endings (in green). (F) Like all GABAergic neurons in the cerebellum, Purkinje cells are labelled with antibodies raised against Parvalbumin. Note that these neurons exhibit several dendritic arborizations arising from a same cell body. Calibration bar: 40 μm except for A2: 5 μm.

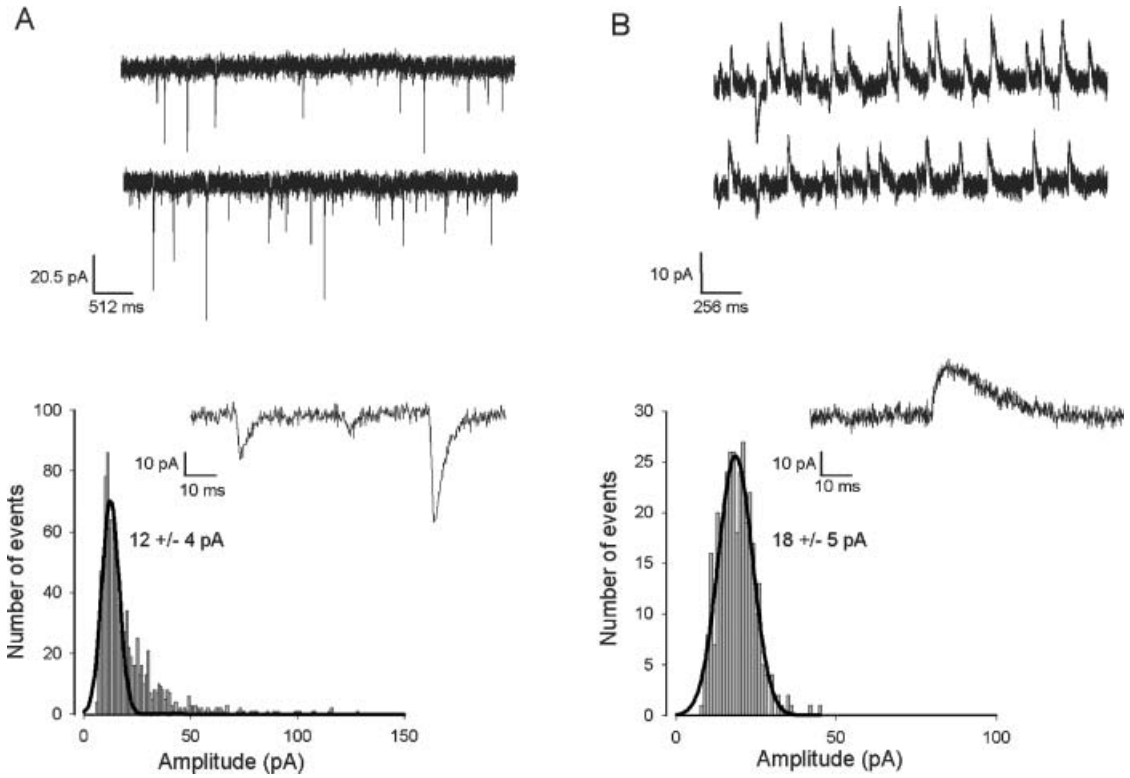

Figure 3. Spontaneous synaptic activity in Purkinje cells. (A and B) *Upper part*: representative current traces of the spontaneous synaptic activity recorded in control conditions at −60 mV: excitatory post synaptic currents in A (as shown with an expended time scale in the middle part) and mainly inhibitory post synaptic currents in B (as shown with an expended time scale in the middle part) are depicted. *Lower panel*: the amplitude histogram of sEPSCs in A and of sIPSCs in B. In both cases histograms display a main peak fitted by a gaussien function (represented by lines).

consists of AMPA receptor-mediated sEPSCs, and occasionally, $GABA_A$ receptor-mediated sIPSCs. This indicates that Purkinje cells receive functional excitatory inputs from presumptive granule cells and inhibitory inputs from presumptive interneurons and/or possibly Purkinje cell axon collaterals. Furthermore, sEPSC/sIPSCs sequences were detected (data not shown) indicating that granule cells could activate simultaneously a Purkinje cell and an inhibitory interneuron connected to the same Purkinje cell. A tetrodotoxin (TTX) application drastically reduced the frequency of both sIPSCs and sEPSCs (data not shown) indicating that a large proportion of synaptic events were action potential-dependent.

Electrophysiological recordings of granule cells

In the slice culture system, the excitatory circuitry mainly emanates from the numerous granule cells present in the slice. Synaptic activities afferent to these neurons have been recorded at −40 mV. Spontaneous transient inward and outward synaptic currents were recorded (Figure 5A) similarly as in Purkinje cells. Inward current (sEPSCs) were recorded in 100% of granule cells with a mean frequency of 0.84 ± 0.29 Hz ($n=12$) and a mean amplitude of 27 ± 4 pA. The distribution of sEPSCs amplitude (Figure 5B) was skewed, with a main peak at 13 ± 1 pA ($n=12$). The outward currents (sIPSCs) were recorded in 9 out of 12 granule cells with a mean frequency of 0.39 ± 0.13 Hz and mean amplitude of 16 ± 2 pA. The distribution of sIPSCs amplitude (Figure 5C) showed a main peak at 12 ± 1 pA ($n=5$).

Recording spontaneous activities in granule cells in the cultures model reveals functional granule cell-granule cell excitatory interactions (that appear specific to cerebellar cultures) as well as granule cell-interneuron and/or granule cell-Purkinje cell inhibitory interactions.

Contribution of NMDA receptors in EPSCs recorded in granule cells and Purkinje cells

To determine the possible implication of NMDA receptors in EPSCs in granule cells and Purkinje cells the synaptic activity was recorded in both cell types at −40 mV using a free Mg^{2+} external solution supplemented with Ca^{2+}. The characteristics of EPSCs (decay kinetic and amplitude) were analysed and compared before and after bath application of APV (10^{-5} M), a specific antagonist of NMDA receptors (Figure 6).

After a fast activation, the EPSCs in granule cells decayed with a fast component followed by a slow tail exhibiting channel-like activities with an amplitude of about 2 pA (Figure 6A upper part, control

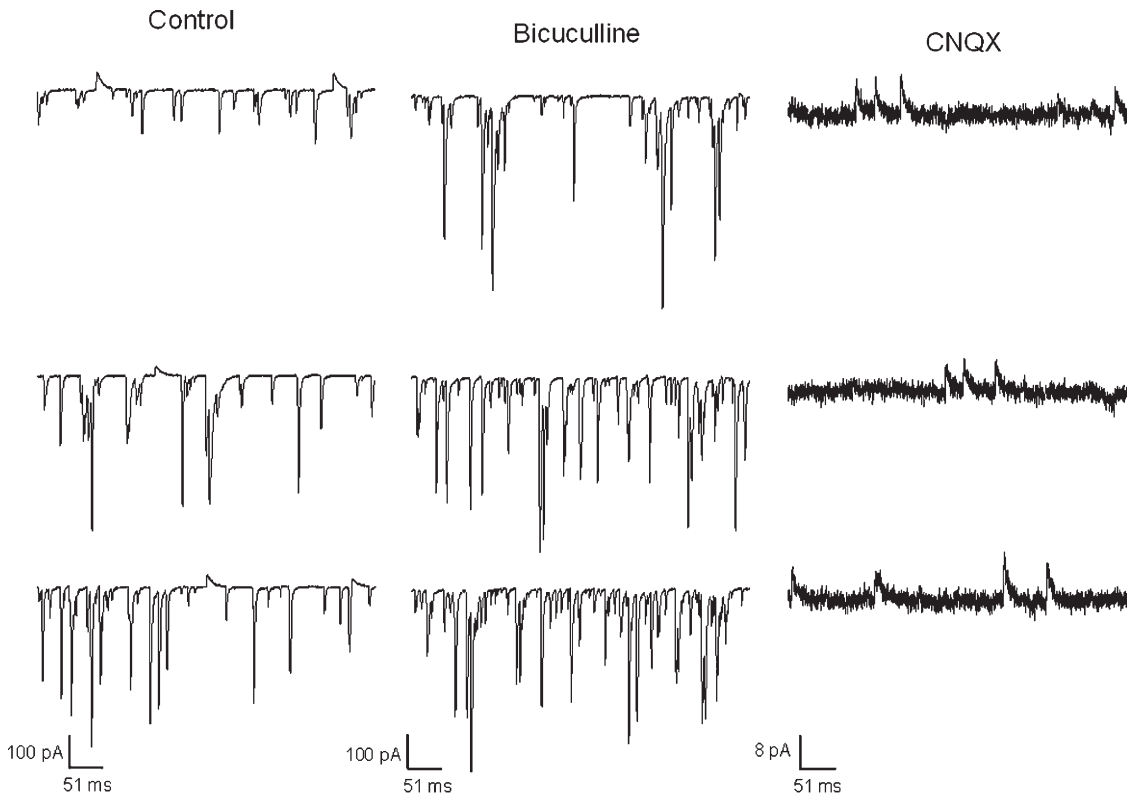

Figure 4. Pharmacological characterization of synaptic events depicted in Purkinje cells.Left traces are currents traces recorded in control conditions at −60 mV where both sEPSCs and sIPSCs are present. Middle and right traces are current traces recorded in the same cell after a bath application of bicuculline and CNQX respectively. Note that in the presence of bicuculline sIPSCs are blocked specifically whereas in the presence of CNQX only sIPSCs are recorded.

trace). Averaging a hundred isolated EPSCs (Figure 6A, lower part, control trace) allowed us to determine the mean amplitude (16 ± 4 pA, $n=6$), the time constant of the fast (2.2 ms $\pm$ 0. 28, $n=6$), and slow (37 ± 13 ms, $n=6$) components of these granule cells EPSCs. After bath application of APV, the slow tail of channel activities was almost abolished (Figure 6A upper part, APV trace). Averaging granule cell EPSCs in the presence of APV (Figure 6A, lower part, APV trace in red) revealed that the slow component was selectively abolished in 3 cells and reduced by about 60% in the 3 remaining cells. In the presence of CNQX ($n=3$) only the channel like activity was recorded (Figure 6A upper part, CNQX trace).

Single EPSCs recorded in Purkinje cells did not display the slow tail (Figure 6B, upper part, control trace, note the different time scale in A and B). Averaging isolated events (Figure 6B, lower part, control trace suppressed in black) gave rise to a current of 38 ± 8 pA which decayed, following a single exponential with a fast time constant of 3.7 ± 1.4 ms ($n=9$). Single EPSCs were not affected by bath application of the NMDA receptor antagonist (Figure 6B, upper part, APV trace) but were abolished by CNQX (not shown). Averaging isolated EPSCs recorded in the presence of APV (Figure 6B, lower part, APV trace suppressed in red) revealed that the fast component was not affected by APV (time constant of 3.8 ± 1.6, $n=9$).

Inhibitory inputs control excitatory transmission in Purkinje cells and granule cells

Blocking GABAergic inhibitory circuitry with bicuculline produced a large increase of sEPSCs frequency in all Purkinje cells ($n=17$, Figure 7A). Quantification of this bicuculline effect on the frequency and mean amplitude of sEPSCs was performed on 12 Purkinje cells (Figure 7A, lower panel) and showed a mean frequency increase from 6.4 ± 1.7 Hz to 26.0 ± 5.0 Hz (Figure 7A, lower panel, left histograms). In addition, the mean amplitude of sEPSCs also increased from 21 ± 5 pA to 35 ± 7 pA after bicuculline application (lower panel, right histograms). Furthermore, SR 95531 (10^{-6} M), a very specific inhibitor of $GABA_A$ receptors, reproduced the same effect on the excitatory synaptic transmission as bicuculline (Figure 7B, $n=6$). The mean frequency of sEPSCs increased from a mean of 4.7 ± 2.3 Hz to a mean of 27.4 ± 7.5 Hz (lower panel, left histograms) while the mean amplitude shifted from 15.3 ± 1.4 pA to 20.5 ± 1.9 pA (lower panel, right histograms). These observations suggest that the excitatory activities afferent to Purkinje cells are, presumably via the

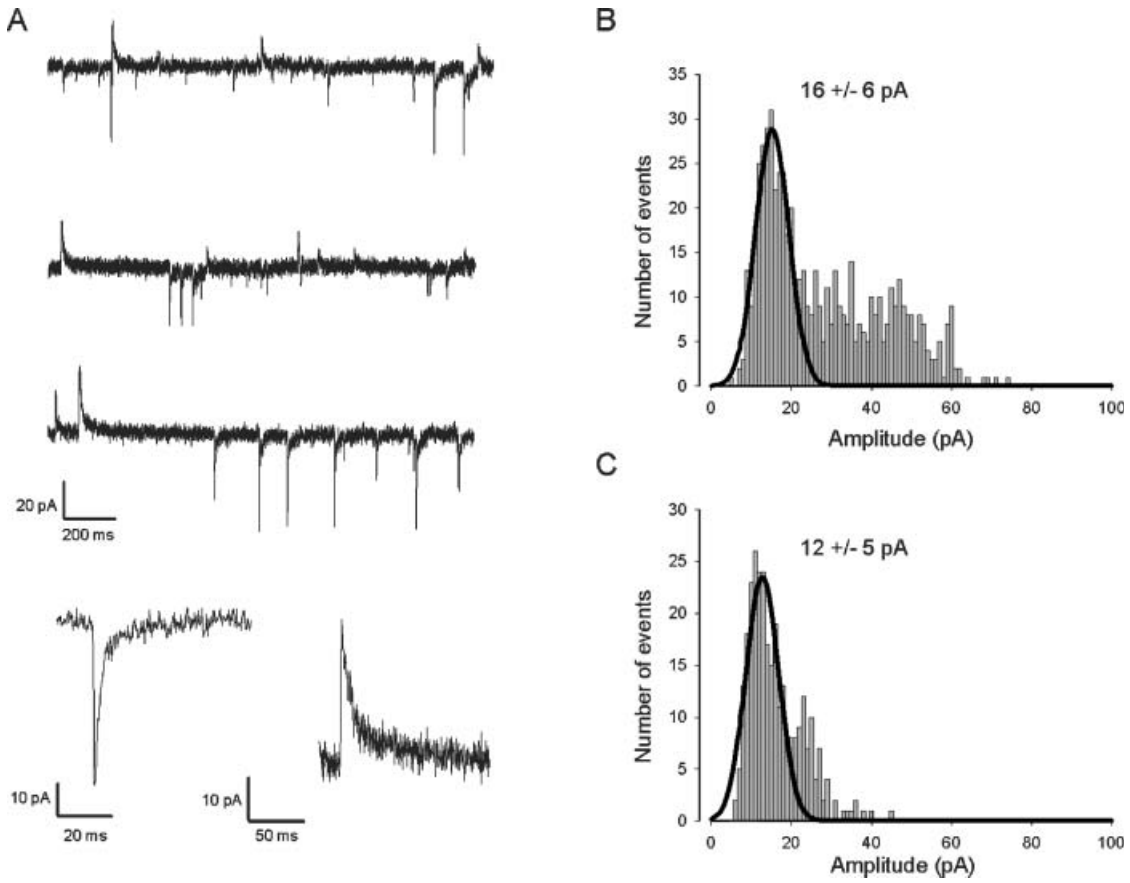

Figure 5. Spontaneous synaptic activity in granule cells. (A) Representative current traces of the spontaneous synaptic activity recorded in control conditions at −40 mV: excitatory post synaptic currents (as shown with an expended time scale lower part) and inhibitory post synaptic currents (as shown with an expended time scale in the lower) are depicted. (B) The amplitude histogram of sEPSCs and (C) the amplitude histogram of sIPSCs. In both cases histograms display a main peak fitted by a gaussien function (represented by lines).

granule cells, under the control of inhibitory GABAergic neurons.

In granule cells, applications of bicuculline blocked sIPSCs ($n=4$, not shown) and led to an increase of the frequency of sEPSCs in 3 out of 7 granule cells.

Excitatory inputs control inhibitory synaptic transmission in Purkinje cells

The next set of experiments was carried out to determine if sIPSCs detected in Purkinje cell are affected by blockade of AMPA receptors by CNQX. Typically, as illustrated in Figure 8 ($n=6$), whereas the frequency of sIPSCs was not affected by CNQX (2.6 ± 0.5 Hz in control and 3.1 ± 1.5 Hz after CNQX) the mean amplitude of sIPSCs decreased from 29.0 ± 7.7 pA in controls to 13.3 ± 4.7 after CNQX applications. Comparison between sIPSCs amplitude histograms in control and CNQX conditions (Figure 8, lower panel) revealed that although the main peak of sIPSCs amplitude was not affected (12.7 ± 1.9 in control against 11.4 pA $\pm$ 1.3 pA after CNQX), large amplitude events were abolished. These results indicate that activation of AMPA receptors by excitatory inputs controls the activity of GABAergic neurons innervating Purkinje cells.

Inhibitory inputs control the firing rate of Purkinje and granule cells

Finally, modifications of the firing rate in Purkinje cells and in granule cells were investigated following a blockade of GABAergic transmission. Current clamp recordings of Purkinje and granule cells at the resting membrane potential were performed. In Purkinje cells, bath applications of bicuculline induced a 5–10 mV depolarization which was associated with an increase of the synaptic noise ($n=5$). Together these effects contributed to increase the firing rate of action potentials (Figure 9A). In granule cells (Figure 9B), a similar effect was observed but the depolarization was not large enough to trigger a discharge of action potentials in 2 out of the 4 neurons recorded.

Discussion

Investigation of central neurophysiology has been greatly facilitated by *in vitro* methods. Mutant mice now make it possible to study the neurophysiological functions of an increasing number of critical proteins linking phenotypes to specific cellular and molecular defects. In this respect, the use of *in vitro* preparations from mutant mice is an important

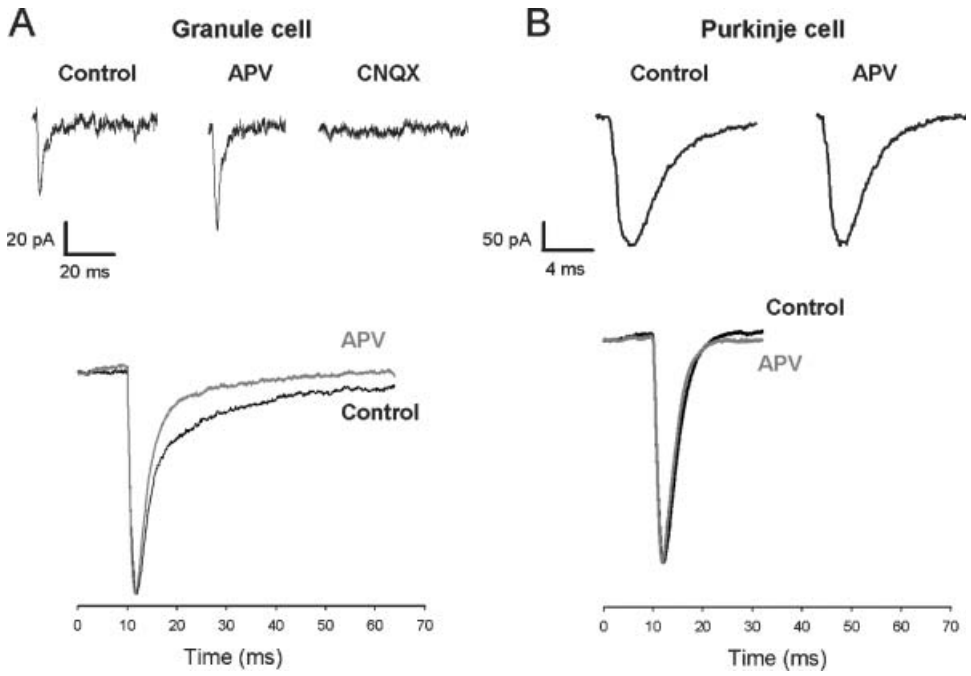

Figure 6. NMDA receptors and EPSCs recorded in granule cells and Purkinje cells. (A) *Upper part*: single EPSCs recorded at −40mV in a granule neuron in control conditions in a Mg-free saline (left trace) and after a bath application of APV at a concentration of 10^{-5}M (middle trace), note that the channel like activity underlying a slow tail current is nearly abolished by APV. In the presence of CNQX (10^{-5}M) only the channel like activity is recorded (right trace). *Lower part*: corresponds to an average of a hundred of EPSCs normalized to the peak amplitude recorded in control conditions (lower trace) and in the presence of APV (upper trace). Note that the slow decaying component of the averaged EPSC is affected by APV. (B) *Upper part*: illustrates single EPCS recorded in a Purkinje cell in control conditions at −40mV in a Mg-free saline (left trace) and after a bath application of APV at a concentration of 10^{-5}M (right trace), note that single EPSCs are fast decaying when compared to EPSCs recorded in granule cells (note the different time scale in A and B). (B) *Lower part*: represents the average of a hundred of EPSCs normalized to the peak amplitude recorded in a Purkinje cell in control conditions (upper trace) and in the presence of APV (lower trace). Note that the EPSC decay is not affected by APV.

methodological advance. Studies on dissociated cell cultures are unfortunately limited to single cell level or to simple neuronal networks. Acute slices mainly offer the interest of an intact cellular organization and synaptic connectivity within the cerebral structure, but do not allow long lasting pharmacological treatments. Furthermore, investigations cannot be performed during the late postnatal period and adulthood in acute slices when the mutation of interest causes early postnatal death. As an alternative, organotypic cultures have been developed using roller tubes (25,26), collagen coverslips in Maximow chambers (27), or polycarbonate membranes (28) and permit long term studies on organized structures. However, development as well as cellular organization of the neuronal circuits may be modified in organotypic cultures. This is particularly true for the cultures that are obtained from immature cerebellum of newborn animals. Before analyzing the effects of a given mutation, characterization of the cellular and synaptic organization of these organotypic cultures after several weeks in culture is necessary. The organotypic cultures of mouse cerebellum that we have developed in roller tubes offer certain advantages as they permit an easy electrophysiological approach to different cell types. The aim of the present study was to provide an overview on the general cellular and functional organization of the mouse cerebellar organotypic slice cultures (see Figure 10). The discussion will firstly consider the general cellular organization and morphology of the cerebellar organotypic culture and secondly the synaptic relationships established by the cerebellar neurons after 3–4 weeks *in vitro*.

Structural organization of the organotypic cerebellar cultures

This study demonstrates that even in the absence of external inputs (mossy and climbing fibers), the general cytoarchitecture of the mouse cerebellum is relatively preserved in the organotypic cultures as shown by using antibodies directed against specific markers of different types of cerebellar neurons.

Layers of Purkinje cells occupy the periphery of the slice extending axons to presumptive central nuclear neurons. Granule cells form a layer resembling the internal granular layer. Numerous putative GABAergic interneurons are differentiated within the organotypic cultures, but no attempt was made in this study to identify these interneurons. Organotypic cultures from rat cerebellum displayed similar structural organization independently of the method used, i.e., roller tubes (10,26) or polycarbonate membrane (29,30). The organization of mouse cerebellar cortex is also relatively preserved after

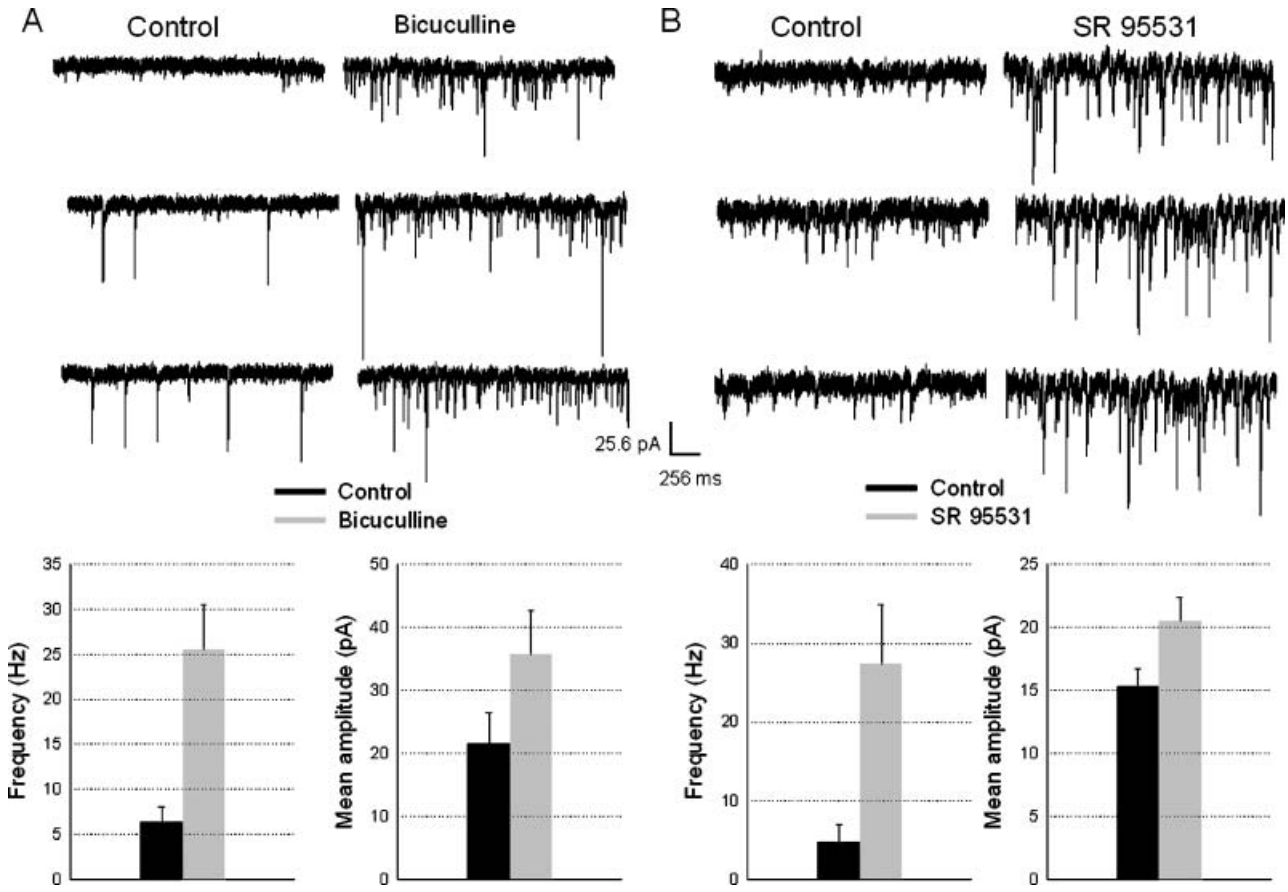

Figure 7. GABAergic neurons control the excitatory synaptic transmission on Purkinje cells. (A) Effects of bicuculline on sEPSCs mean frequency and mean amplitude. The upper traces are currents traces of sEPSCs recorded in control conditions (left) and after bicuculline bath application at 10^{-5} M (right). In the lower panel we compare the mean frequency (left) and the mean amplitude (right) of sEPSCs recorded in control conditions (black bars) with the mean frequency of sEPSCs and the mean amplitude recorded in the same cells ($n=12$) after bath applications of bicuculline (gray bars). (B) Effects of SR 95531 on sEPSCs mean frequency and mean amplitude. The upper traces are currents traces of sEPSCs recorded in control conditions (left) and after SR 95531 bath applications at 10^{-5} M (right). In the lower panel we compare the mean frequency (left) and the mean amplitude (right) of sEPSCs recorded in control conditions (black bars) with the mean frequency of sEPSCs and the mean amplitude recorded in the same cells ($n=6$) after bath applications of SR 95531 (gray bars). Recordings were performed at -60 mV.

several weeks in *vitro* using Maximow chambers (see 31 and 32 for reviews). Furthermore, we showed that Purkinje cells and interneurons were closely surrounded by granule cell presynaptic-like terminals and that interneuron presynaptic-like terminals surrounded Purkinje cell profiles and granule cell as well. The large number of main Purkinje cell axons running back within the Purkinje cell layer in cultures devoid of nuclear neurons suggests that Purkinje cells are extensively self-innervated in our slice cultures. Whether such axons form functional synapses between Purkinje cells will be interesting to investigate using a paired recording approach.

In the organotypic cultures, the morphology of the Purkinje cells looks similar to that observed in the cerebellar cortex of adult mice with a 20–30 μm large cell body, a well developed isoplanar dendritic tree oriented towards the periphery of the culture. However, Purkinje cells display abnormal morphological features such as multiple primary dendrites some of which are oriented towards the core of the culture. These dendritic patterns typically affected isolated or ectopic Purkinje cells, i.e., cells that had grown in an abnormal environment. The dendritic arborizations of Purkinje cells exhibit a great variety of shapes when these neurons develop in an almost complete absence of granule cells in agreement with previous reports (22 for a review).

In our study, Kv3.1b positive endings, presumably granule cell axon endings, were shown to terminate on proximal and distal branches on Purkinje cell dendrites. According to this observation, numerous spines-like processes are present on the main dendritic branches of the Purkinje cells. Such ectopic spines have already been described *in vivo* as *in vitro* when Purkinje cells were devoid of their climbing fiber innervation and were shown to be mainly connected by parallel fibers (22 for a review). The role of the cellular environment, in particular the formation of granule cells and parallel fibers on the modelling of the Purkinje cell dendritic arborization has already been well documented (22 for a review). In this study, the granule cell to Purkinje cell ratio is about four times lower than *in situ*

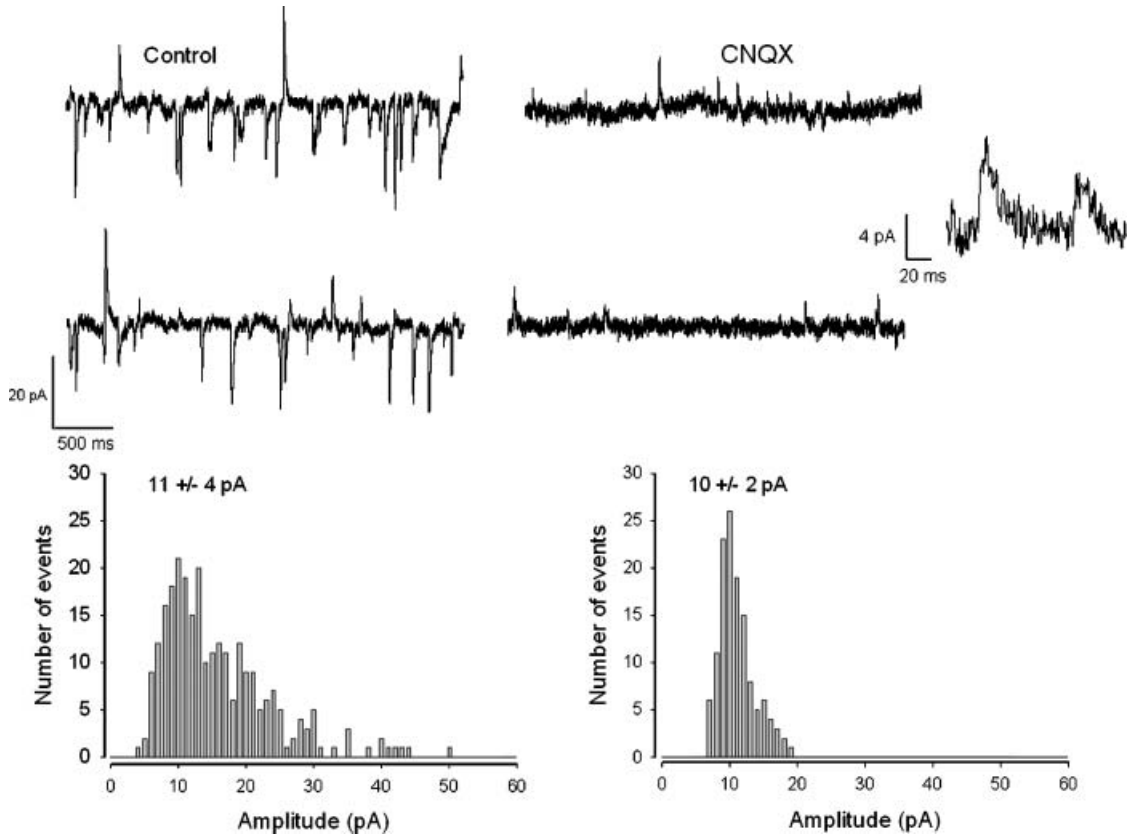

Figure 8. Glutamatergic synaptic transmission control sIPSCs recorded in Purkinje cells. Upper part are current traces recorded at −60 mV in control conditions (left) where both sEPSCs and sIPSCs are depicted and current traces recorded after a bath application of CNQX at 10^{-5} M. Note that in the presence of CNQX, sEPSCs are abolished whereas sIPSCs of small amplitude are still present (shown in the inset using an expanded time scale). The lower part represents the amplitude histogram for sIPSCs recorded in control conditions (left) and the amplitude histogram for sIPSCs recorded in the presence of CNQX. Both histograms present a mean peak (values are given on top of the histograms). Note that in the presence of CNQX, events with amplitude larger than 20 pA are abolished by CNQX.

estimates in the mouse (23,24). Such a difference originates, at least in part, from the fact that DNA synthesis inhibitors were added for 24 h to the culture medium in order to prevent glial cell proliferation 2–4 days after the start of the culture. As most of the granule cell precursors during that period are dividing neuroblasts in the external germinal layer, the exposure to the antimitotic agents could result in the elimination of many granule cells. Thereafter, the surviving granule cell precursors were able to migrate to form the internal granular layer while Purkinje cells apparently differentiated a developed dendritic arborization despite the loss of numerous granule cells. Whether these Purkinje cells give rise to a fully developed dendritic tree in terms of extent and branching complexity like *in situ* is probably not the case as these dendritic trees appear short and immature. This point will be interesting to investigate but a morphometric analysis of the dendrites of these neurons will be a difficult task using calbindin immunolabelled material because of the overlaps of the dendritic arborisations between neighbouring Purkinje cells. Numerous recurrent collaterals of Purkinje cell axons were observed running back into the Purkinje cell layer. This has been previously described in organotypic cultures of mouse (27) and rat (10), but also represents a normal feature of Purkinje cell axons *in vivo* (33). These Purkinje cell axon collaterals are often seen to terminate close to dendrites of either neighboring or distant Purkinje cells (see also 27) although the establishment of autaptic contacts could not be ruled out.

Electrophysiological recordings reveal the presence of two types of synaptic events in Purkinje cells. Excitatory AMPA-dependent and inhibitory $GABA_A$-dependent currents indicated that excitatory neurons (mainly granule cells), and GABAergic neurons have established functional synapses on Purkinje cells. The presence of similar inputs on Purkinje cells has been previously identified in rat organotypic cultures (10,11) and in both mouse (34) and rat (35) primary cultures. No NMDA dependent component was detected in the synaptic excitatory response recorded in Purkinje cells thus confirming that the parallel fibers in this culture system preferentially act on Purkinje cells via non-NMDA receptors (36).

The Purkinje cell synaptic activity characterized in these organotypic cultures displayed several differences when compared to Purkinje cells in acute slices of adult rat (37,38) and mice (39) cerebellum.

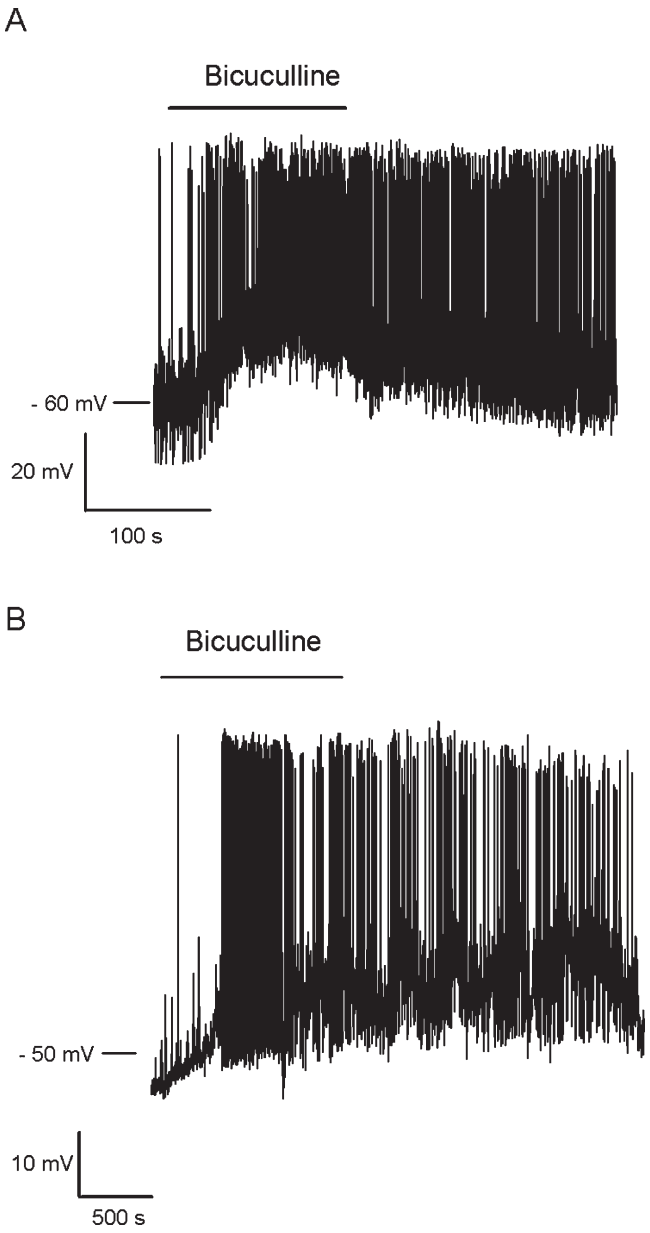

Figure 9. Blockade of GABAergic inhibition induces a depolarization and a discharge of action potentials in Purkinje cells and in granule cells. (A) Current clamp recording of a Purkinje cell. (B) Current clamp recording of granule cell applications of bicuculline 10^{-5} M are indicated by the black bars.

Firstly, almost all the spontaneous postsynaptic currents recorded in Purkinje cells were mediated by $GABA_A$ receptors in acute slices, whereas such sIPSCs were recorded in only 23% of Purkinje cells in organotypic cultures. Secondly, the frequency of Purkinje cells sIPSCs was very low (2.5 Hz, in 5 mM Ca^{2+}, 0,5 mM Mg^{2+}) in organotypic cultures as compared with the Purkinje cells sIPSCs frequency (18 Hz, in 2 mM Ca^{2+}, 1 mM Mg^{2+}) in adult rat acute slices (40). This discrepancy suggests that inhibitory interneurons have a lower spontaneous activity and/or that the inhibitory network is not as developed as in acute slices from adult rat. Indeed, the latter explanation is supported by the very low frequency of Purkinje cells sIPSCs (1Hz) recorded in acute slices from newborn rats (40).

As *in vivo*, we have demonstrated that the activity of GABAergic interneurons innervating Purkinje cells (probably stellate and basket cells) is controlled by excitatory inputs arising from granule cells. Indeed, whereas Kv3.1b-positive terminals were observed close to interneurons immunolabeled for parvalbumin, the large amplitude Purkinje cells IPSCs could be abolished by CNQX and sEPSC/sIPSC sequences could be observed.

In organotypic cultures, the spontaneous synaptic activity recorded in granule cells was also composed of two types of events: a composite AMPA/NMDA receptor-mediated sEPSPs and $GABA_A$ receptor-mediated sIPSCs. In mouse acute slices, composite evoked responses were described at the mossy fiber–granule cells synapse (41). In acute slices of rat

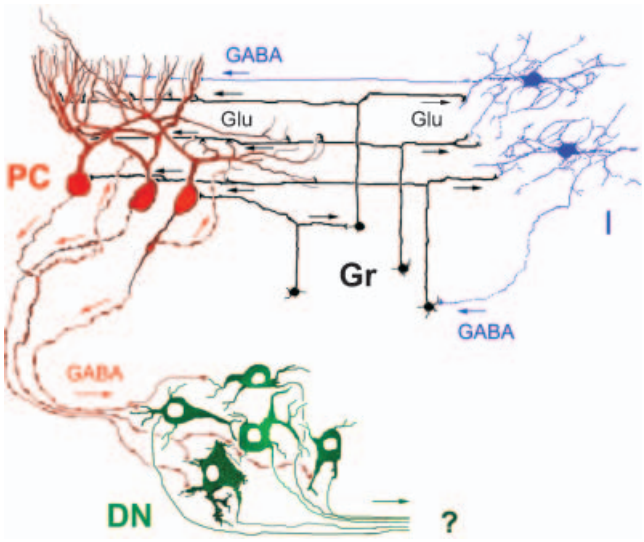

Figure 10. Schematic representation of the cellular and functional organization of the mouse cerebellar organotypic slice cultures. PC, Purkinje cell; I, Interneuron; Gr, Granule cell; DN, nuclei neuron.

cerebellum, granule cell sIPSPs were shown to be mediated by GABA released by Golgi interneurons (42). The frequency (7 Hz) and mean amplitude (116 pA) of sIPSPs recorded in granule cells in acute slices (43) were significantly larger than in our organotypic cultures (0.39 Hz and 16 pA) indicating that the Golgi interneurons-granule cell synapses are poorly active in the latter conditions.

Interestingly, GABAergic neurons, in spite of a low frequency for granule cell sIPSPs, exerted a powerful control on the excitatory input to Purkinje cells. Indeed, the application of $GABA_A$ receptor antagonists dramatically increased the frequency of Purkinje cell sEPSPs. This increase was mediated by granule cell depolarization that produced firing of action potential. Different modes of granule cell inhibition by Golgi cells have been previously shown. The initial phasic mode is mediated by synaptic release of GABA, and the tonic mode is mediated by an action potential-independent non vesicular release of GABA (44,45). This latter mode of inhibition may contribute, to the spectacular effect of bicuculline we observed on sEPSPs frequency in our organotypic cultures, as it does in acute slices.

The role of inhibitory interneurons in cerebellar control of motor coordination is crucial. Indeed, over-excitation of granule cells observed after the specific destruction of their GABAergic inhibitory inputs results in severe ataxia (46). Finally, we show that desinhibition of granule cells increased the firing rate of Purkinje cells by producing a depolarization of the neuron and increasing the frequency of excitatory events. This is the most likely explanation for the increase in Purkinje cell firing rate observed in the presence of bicuculline in agreement with results obtained in rat organotypic cultures (47).

Conclusion

We have shown that after 3–4 weeks *in vitro* organotypic cultures of mouse cerebellum display a cellular organization exhibiting the main features of the adult cerebellar cortex *in situ*. The main cell types are present and form homologous functional synaptic contacts (see Figure 10). We provide evidence that inhibitory interneurons control excitatory inputs to Purkinje cells in organotypic cultures. The modality of such a control (phasic versus tonic release of GABA) remains to be investigated pharmacologically. We propose that mouse cerebellar organotypic cultures using roller tubes could be used as a model to study alterations of synaptic transmission in cerebellar mutant mice.

Acknowledgements

This work was supported by a Délégation Générale à l'Armement (contract N° DGA 03-34-046) grant to Bernard Poulain.

We thank Dr Yannick Bailly and Dr Yann Humeau for comments on this manuscript.

References

1. Ramón y Cajal S. (1911) Histologie du Système Nerveux de l'Homme & des Vertébres, 2 vols. Ed. francaise rev. & mise à jour par l'auteur. Traduite de l'espagnol par L. Azoulay. Reprinted by Instituto Ramón y Cajal del Consejo Superior de Investigaciones Cientificas, Madrid, 1955.
2. Ito M. The cerebellum and neural control. New York: Raven Press, 1984.
3. Llinás R, Sugimori M. Electrophysiological properties of in vitro Purkinje cell somata in mammalian cerebellar slices. J Physiol. 1980;305:171–95.
4. Llinás R, Sugimori M. Electrophysiological properties of in vitro Purkinje cell dendrites in mammalian cerebellar slices. J Physiol. 1980;305:197–213.

5. Crepel F, Dhanjal SS, Garthwaite J. Morphological and electrophysiological characteristics of rat cerebellar slices maintained in vitro. J Physiol. 1981;316:127–38.
6. Crepel F, Dupont JL, Gardette R. Selective absence of calcium spikes in Purkinje cells of staggerer mutant mice in cerebellar slices maintained in vitro. J Physiol. 1984;346: 111–25.
7. Gähwiler BH. Inhibitory action of noradrenaline and cyclic AMP in explant cerebellum. Nature. 1976;259:483–84.
8. Gähwiler BH. Spontaneous bioelectric activity of cultured Purkinje cells during exposure to glutamate, glycine, and strychnine. J Neurobiol. 1976;7:97–107.
9. Gähwiler BH. Morphological differentiation of nerve cells in thin organotypic cultures derived from hippocampus and cerebellum. Proc R Soc Lond B Sci. 1981;211:287–90.
10. Jaeger CB, Kappor R, Llinas R. Cytology and organization of rat cerebellar organ cultures. Neuroscience. 1988;26:509–38.
11. Kappor R, Jaeger CB, Llinás R. Electrophysiology of the mammalian cerebellar cortex in organ culture. Neuroscience. 1988;26:493–507.
12. Leiman AL, Seil FJ. Spontaneous and evoked bioelectric activity in organized cerebellar tissue cultures. Exp Neurol. 1973;40:748–58.
13. Seil FJ, Kelly JM, Leiman AL. Anatomical organization of cerebral neocortex in tissue cultures. Exp Neurol. 1974;45:435–50.
14. Seil AJ, Leiman AL. Development of spontaneous and evoked electrical activity of cerebellum in tissue culture. Exp Neurol. 1979;64:61–75.
15. Calvet MC, Calvet J, Camacho-Garcia R. The Purkinje cell dendritic tree: a computer-aided study of its development in the cat and in culture. Brain Res. 1985;331:235–50.
16. Hirano T, Kubo Y, Wu MM. Cerebellar granule cells in culture: monosynaptic connections with Purkinje cells and ionic currents. Proc Natl Acad Sci USA. 1986;83:4957–61.
17. Hirano T, Hagiwara S. Kinetics and distribution of voltage-gated Ca, Na and K channels on the somata of rat cerebellar Purkinje cells. Pflugers Arch. 1989;413:463–69.
18. Gruol D L, Franklin C L. Morphological and physiological differentiation of Purkinje neurons in cultures of rat cerebellum. J Neurosci. 1987;7:1271–93.
19. Nelson PG, Peacock JH. Electrical activity in dissociated cell cultures from fetal mouse cerebellum. Brain Res. 1973;61: 163–74.
20. Orkand PM, Lindner J, Schachner M. Specificity of histiotypic organization and synaptogenesis in the reaggreting cell cultures of mouse cerebellum. Brain Res. 1984;318:119–34.
21. Grusser-Cornehls U, Baurle J. Mutant mice as a model for cerebellar ataxia. Prog Neurobiol. 2001;63:489–540.
22. Sotelo C. Cellular and genetic regulation of the development of the cerebellar system. Prog Neurobiol. 2004;72:295–339.
23. Herrup K, Sunter K. Numerical matching during cerebellar development: quantitative analysis of granule cell death in Staggerer mouse chimeras. J Neurosci. 1987;7:829–36.
24. Zanjani HS, Vogel MW, Delhaye-Bouchaud N, Martinou JC, Mariani J. Increases inferior olivary neuron and cerebellar granule cells numbers in transgenic mice overexpressing the human Bcl-2 gene. J Neurobiol. 1997;32:502–16.
25. Costero I, Pomerat CM. Cultivation of neurons from the adult human cerebral and cerebellar cortes. Am J Anat. 1951;89:405–67.
26. Gähwiler BH. Slice cultures of cerebellar, hippocampal and hypothalamic tissue. Experientia. 1984;40:235–43.
27. Seil FJ. Neuronal groups and fiber patterns in cerebellar tissue cultures. Brain Res. 1972;42:33–51.
28. Stoppini L, Buchs PA, Muller D. A simple method for organotypic cultures of nervous tissue. J Neurosci Methods. 1991;37:173–82.
29. Tanaka M, Tomita A, Yoshida S, Yano M, Shimizu H. Observation of the highly organized development of granule cells in rat cerebellar organotypic cultures. Brain Res. 1994;641:319–27.
30. Tauer U, Volk B, Heimrich B. Differentiation of Purkinje cells in cerebellar slice cultures: an immunocytochemical and Golgi EM study. Neuropathol Appl Neurobiol. 1996;4: 361–69.
31. Hendelmann WJ, Aggerwal AS. The Purkinje neuron: I. A golgi study of its development in the mouse and in culture. J Comp Neurol. 1980;193:1063–79.
32. Seil FJ. Neural plasticity in cerebellar cultures. Prog Neurol. 1996;50:533–56.
33. Crepel F, Delhaye-Bouchaud N, Dupont JL, Sotelo C. Dendritic and axonic fields of Purkinje cells in developing and X-irradiated rat cerebellum. A comparative study using intracellular staining with horseradish peroxidase. Neuroscience. 1980;5:333–47.
34. Weber A, Schachner M. Maintenance of immunocytologically identified Purkinje cells from mouse cerebellum in monolayer culture. Brain Res. 1984;311:119–30.
35. Gruol DL. Cultured cerebellar neurons: endogenous and exogenous components of Purkinje cell activity and membrane response to putative transmitters. Brain Res. 1983;263: 223–41.
36. Crepel F, Dupont JL, Gardette R. Voltage clamp analysis of the effect of excitatory amino acids and derivatives on Purkinje cell dendrites in rat cerebellar slices maintained in vitro. Brain Res. 1983;279:311–15.
37. Konnerth A, Llano I, Armstrong CM. Synaptic currents in cerebellar Purkinje cells. Proc Natl Acad Sci USA. 1990;87: 2662–5.
38. Puia G, Costa E, Vicini S. Functional diversity of GABA-activated Cl^- currents in Purkinje versus granule neurons in rat cerebellar slices. Neuron. 1994;12:117–26.
39. Zhang CL, Messing A, Chiu SY. Specific alteration of spontaneous GABAergic inhibition in cerebellar Purkinje cells in mice lacking the potassium channel Kv1.1. J Neurosci. 1999;19:2852–64.
40. Kawa K. Acute synaptic modulation by nicotinic agonists in developing cerebellar Purkinje cells of the rat. J Physiol. 2002;538:87–102.
41. Cathala l, Brickley S, Cull-Candy S, Farrant M. Maturation of EPSCs and intrinsic membrane properties enhances precision at a cerebellar synapse. J Neurosci. 2003;23: 6074–85.
42. Kaneda M, Farrant M, Cull-Candy SG. Whole-cell and single-channel currents activated by GABA and glycine in granule cells of the rat cerebellum. J Physiol. 1995;485: 419–35.
43. Yuan Y, Atchison WD. Methylmercury differentially affects GABA(A) receptor-mediated spontaneous IPSCs in Purkinje and granule cells of rat cerebellar slices. J Physiol. 2003;550: 191–204.
44. Hamann M, Rossi DJ, Attwell D. Tonic and spillover inhibition of granule cells control information flow through cerebellar cortex. Neuron. 2002;33:625–33.
45. Rossi DJ, Hamann M, Attwell D. Multiple modes of GABAergic inhibition of rat cerebellar granule cells. J Physiol. 2003;548:97–110.
46. Hirano T, Watanabe D, Kawaguchi SY, Pastan I, Nakanishi S. Roles of inhibitory interneurons in the cerebellar cortex. Ann N Y Acad Sci. 2002;978:405–12.
47. Gähwiler BH. The effects of GABA, picrotoxin and bicuculline on the spontaneous bioelectric activity of cultured cerebellar Purkinje cells. Brain Res. 1975;99:85–95.

XI) BIBLIOGRAPHY

Abel, T. and Kandel, E. (1998). Positive and negative regulatory mechanisms that mediate long-term memory storage. *Brain Res Brain Res Rev* **26**, 360-78.

Abraham, W. C. and Otani, S. (1991). Macromolecules and the maintenance of long-term potentiation In Kindling and Synaptic Plasticity.

Aggleton, J. P. (2000). The amygdala: Oxford University Press.

Aicardi, G. and Schwartzkroin, P. A. (1990). Suppression of epileptiform burst discharges in CA3 neurons of rat hippocampal slices by the organic calcium channel blocker, verapamil. *Exp Brain Res* **81**, 288-96.

Akert, K., Moor, H. and Pfenninger, K. (1971). Synaptic fine structure. *Adv Cytopharmacol* **1**, 273-90.

Andrews-Zwilling, Y. S., Kawabe, H., Reim, K., Varoqueaux, F. and Brose, N. (2006). Binding to Rab3A-interacting molecule RIM regulates the presynaptic recruitment of Munc13-1 and ubMunc13-2. *J Biol Chem* **281**, 19720-31.

Anwyl, R. (1999). Metabotropic glutamate receptors: electrophysiological properties and role in plasticity. *Brain Res Brain Res Rev* **29**, 83-120.

Anwyl, R. (2006). Induction and expression mechanisms of postsynaptic NMDA receptor-independent homosynaptic long-term depression. *Prog Neurobiol* **78**, 17-37.

Arnsten, A. F., Ramos, B. P., Birnbaum, S. G. and Taylor, J. R. (2005). Protein kinase A as a therapeutic target for memory disorders: rationale and challenges. *Trends Mol Med* **11**, 121-8.

Arriza, J. L., Eliasof, S., Kavanaugh, M. P. and Amara, S. G. (1997). Excitatory amino acid transporter 5, a retinal glutamate transporter coupled to a chloride conductance. *Proc Natl Acad Sci U S A* **94**, 4155-60.

Augustin, I., Korte, S., Rickmann, M., Kretzschmar, H. A., Sudhof, T. C., Herms, J. W. and Brose, N. (2001). The cerebellum-specific Munc13 isoform Munc13-3 regulates cerebellar synaptic transmission and motor learning in mice. *J Neurosci* **21**, 10-7.

Augustin, I., Rosenmund, C., Sudhof, T. C. and Brose, N. (1999). Munc13-1 is essential for fusion competence of glutamatergic synaptic vesicles. *Nature* **400**, 457-61.

Avery, R. B. and Johnston, D. (1996). Multiple channel types contribute to the low-voltage-activated calcium current in hippocampal CA3 pyramidal neurons. *J Neurosci* **16**, 5567-82.

Azad, S. C., Monory, K., Marsicano, G., Cravatt, B. F., Lutz, B., Zieglgansberger, W. and Rammes, G. (2004). Circuitry for associative plasticity in the amygdala involves endocannabinoid signaling. *J Neurosci* **24**, 9953-61.

Bailey, C. H., Bartsch, D. and Kandel, E. R. (1996). Toward a molecular definition of long-term memory storage. *Proc Natl Acad Sci U S A* **93**, 13445-52.

Balendran, A., Biondi, R. M., Cheung, P. C., Casamayor, A., Deak, M. and Alessi, D. R. (2000). A 3-phosphoinositide-dependent protein kinase-1 (PDK1) docking site is required for the phosphorylation of protein kinase Czeta (PKCzeta) and PKC-related kinase 2 by PDK1. *J Biol Chem* **275**, 20806-13.

Barclay, J. W., Morgan, A. and Burgoyne, R. D. (2005). Calcium-dependent regulation of exocytosis. *Cell Calcium* **38**, 343-53.

Basu, J., Shen, N., Dulubova, I., Lu, J., Guan, R., Guryev, O., Grishin, N. V., Rosenmund, C. and Rizo, J. (2005). A minimal domain responsible for Munc13 activity. *Nat Struct Mol Biol* **12**, 1017-8.

Bauer, E. P., Schafe, G. E. and LeDoux, J. E. (2002). NMDA receptors and L-type voltage-gated calcium channels contribute to long-term potentiation and different components of fear memory formation in the lateral amygdala. *J Neurosci* **22**, 5239-49.

Bayazitov, I. T., Richardson, R. J., Fricke, R. G. and Zakharenko, S. S. (2007). Slow presynaptic and fast postsynaptic components of compound long-term potentiation. *J Neurosci* **27**, 11510-21.

Bean, B. P., Nowycky, M. C. and Tsien, R. W. (1984). Beta-adrenergic modulation of calcium channels in frog ventricular heart cells. *Nature* **307**, 371-5.

Beaumont, V. and Zucker, R. S. (2000). Enhancement of synaptic transmission by cyclic AMP modulation of presynaptic Ih channels. *Nat Neurosci* **3**, 133-41.

Bellingham, M. C. and Walmsley, B. (1999). A novel presynaptic inhibitory mechanism underlies paired pulse depression at a fast central synapse. *Neuron* **23**, 159-70.

Benke, T. A., Luthi, A., Isaac, J. T. and Collingridge, G. L. (1998). Modulation of AMPA receptor unitary conductance by synaptic activity. *Nature* **393**, 793-7.

Betz, A., Thakur, P., Junge, H. J., Ashery, U., Rhee, J. S., Scheuss, V., Rosenmund, C., Rettig, J. and Brose, N. (2001). Functional interaction of the active zone proteins Munc13-1 and RIM1 in synaptic vesicle priming. *Neuron* **30**, 183-96.

Bi, G. Q. and Poo, M. M. (1998). Synaptic modifications in cultured hippocampal neurons: dependence on spike timing, synaptic strength, and postsynaptic cell type. *J Neurosci* **18**, 10464-72.

Bischoff, S., Leonhard, S., Reymann, N., Schuler, V., Shigemoto, R., Kaupmann, K. and Bettler, B. (1999). Spatial distribution of GABA(B)R1 receptor mRNA and binding sites in the rat brain. *J Comp Neurol* **412**, 1-16.

Bissiere, S., Humeau, Y. and Luthi, A. (2003). Dopamine gates LTP induction in lateral amygdala by suppressing feedforward inhibition. *Nat Neurosci* **6**, 587-92.

Bliss, T. V. and Collingridge, G. L. (1993). A synaptic model of memory: long-term potentiation in the hippocampus. *Nature* **361**, 31-9.

Bliss, T. V., Collingridge, G. L. and Morris, R. G. (2003). Introduction. Long-term potentiation and structure of the issue. *Philos Trans R Soc Lond B Biol Sci* **358**, 607-11.

Bliss, T. V. and Gardner-Medwin, A. R. (1973). Long-lasting potentiation of synaptic transmission in the dentate area of the unanaestetized rabbit following stimulation of the perforant path. *J Physiol* **232**, 357-74.

Bliss, T. V. and Lomo, T. (1970). Plasticity in a monosynaptic cortical pathway. *J Physiol* **207**, 61P.

Bliss, T. V. and Lomo, T. (1973). Long-lasting potentiation of synaptic transmission in the dentate area of the anaesthetized rabbit following stimulation of the perforant path. *J Physiol* **232**, 331-56.

Bloom, F. E. and Aghajanian, G. K. (1968). Fine structural and cytochemical analysis of the staining of synaptic junctions with phosphotungstic acid. *J Ultrastruct Res* **22**, 361-75.

Bolshakov, V. Y. and Siegelbaum, S. A. (1994). Postsynaptic induction and presynaptic expression of hippocampal long-term depression. *Science* **264**, 1148-52.

Borgdorff, A. J. and Choquet, D. (2002). Regulation of AMPA receptor lateral movements. *Nature* **417**, 649-53.

Bortolotto, Z. A., Lauri, S., Isaac, J. T. and Collingridge, G. L. (2003). Kainate receptors and the induction of mossy fibre long-term potentiation. *Philos Trans R Soc Lond B Biol Sci* **358**, 657-66.

Brown, T. H., Perkel, D. H. and Feldman, M. W. (1976). Evoked neurotransmitter release: statistical effects of nonuniformity and nonstationarity. *Proc Natl Acad Sci U S A* **73**, 2913-7.

Budde, T., Meuth, S. and Pape, H. C. (2002). Calcium-dependent inactivation of neuronal calcium channels. *Nat Rev Neurosci* **3**, 873-83.

Burgoyne, R. D. and Morgan, A. (1998). Calcium sensors in regulated exocytosis. *Cell Calcium* **24**, 367-76.

Buzsaki, G., Penttonen, M., Nadasdy, Z. and Bragin, A. (1996). Pattern and inhibition-dependent invasion of pyramidal cell dendrites by fast spikes in the hippocampus in vivo. *Proc Natl Acad Sci U S A* **93**, 9921-5.

Calakos, N., Schoch, S., Sudhof, T. C. and Malenka, R. C. (2004). Multiple roles for the active zone protein RIM1alpha in late stages of neurotransmitter release. *Neuron* **42**, 889-96.

Caldji, C., Diorio, J., Anisman, H. and Meaney, M. J. (2004). Maternal behavior regulates benzodiazepine/GABAA receptor subunit expression in brain regions associated with fear in BALB/c and C57BL/6 mice. *Neuropsychopharmacology* **29**, 1344-52.

Capron, B., Wattiez, R., Sindic, C., Godaux, E. and Ris, L. (2007). Tyrosine phosphorylation of rabphilin during long-lasting long-term potentiation. *Neurosci Lett* **414**, 257-62.

Carbone, E. and Lux, H. D. (1984). A low voltage-activated, fully inactivating Ca channel in vertebrate sensory neurones. *Nature* **310**, 501-2.

Castillo, P. E., Janz, R., Sudhof, T. C., Tzounopoulos, T., Malenka, R. C. and Nicoll, R. A. (1997). Rab3A is essential for mossy fibre long-term potentiation in the hippocampus. *Nature* **388**, 590-3.

Castillo, P. E., Schoch, S., Schmitz, F., Sudhof, T. C. and Malenka, R. C. (2002). RIM1alpha is required for presynaptic long-term potentiation. *Nature* **415**, 327-30.

Castillo, P. E., Weisskopf, M. G. and Nicoll, R. A. (1994). The role of Ca2+ channels in hippocampal mossy fiber synaptic transmission and long-term potentiation. *Neuron* **12**, 261-9.

Castro-Alamancos, M. A. and Calcagnotto, M. E. (1999). Presynaptic long-term potentiation in corticothalamic synapses. *J Neurosci* **19**, 9090-7.

Catterall, W. A. (2000). Structure and regulation of voltage-gated Ca2+ channels. *Annu Rev Cell Dev Biol* **16**, 521-55.

Chapman, E. R. (2002). Synaptotagmin: a Ca(2+) sensor that triggers exocytosis? *Nat Rev Mol Cell Biol* **3**, 498-508.

Chaudhry, F. A., Lehre, K. P., van Lookeren Campagne, M., Ottersen, O. P., Danbolt, N. C. and Storm-Mathisen, J. (1995). Glutamate transporters in glial plasma membranes: highly differentiated localizations revealed by quantitative ultrastructural immunocytochemistry. *Neuron* **15**, 711-20.

Chavez-Noriega, L. E. and Stevens, C. F. (1994). Increased transmitter release at excitatory synapses produced by direct activation of adenylate cyclase in rat hippocampal slices. *J Neurosci* **14**, 310-7.

Chen, G., Harata, N. C. and Tsien, R. W. (2004). Paired-pulse depression of unitary quantal amplitude at single hippocampal synapses. *Proc Natl Acad Sci U S A* **101**, 1063-8.

Chhatwal, J. P., Myers, K. M., Ressler, K. J. and Davis, M. (2005). Regulation of gephyrin and GABAA receptor binding within the amygdala after fear acquisition and extinction. *J Neurosci* **25**, 502-6.

Choquet, D. and Triller, A. (2003). The role of receptor diffusion in the organization of the postsynaptic membrane. *Nat Rev Neurosci* **4**, 251-65.

Christie, J. M. and Jahr, C. E. (2006). Multivesicular release at Schaffer collateral-CA1 hippocampal synapses. *J Neurosci* **26**, 210-6.

Chung, H. J., Steinberg, J. P., Huganir, R. L. and Linden, D. J. (2003). Requirement of AMPA receptor GluR2 phosphorylation for cerebellar long-term depression. *Science* **300**, 1751-5.

Clements, J. D. (2003). Variance-mean analysis: a simple and reliable approach for investigating synaptic transmission and modulation. *J Neurosci Methods* **130**, 115-25.

Colwell, C. S. and Levine, M. S. (1995). Excitatory synaptic transmission in neostriatal neurons: regulation by cyclic AMP-dependent mechanisms. *J Neurosci* **15**, 1704-13.

Conn, P. J. and Pin, J. P. (1997). Pharmacology and functions of metabotropic glutamate receptors. *Annu Rev Pharmacol Toxicol* **37**, 205-37.

Contractor, A., Rogers, C., Maron, C., Henkemeyer, M., Swanson, G. T. and Heinemann, S. F. (2002). Trans-synaptic Eph receptor-ephrin signaling in hippocampal mossy fiber LTP. *Science* **296**, 1864-9.

Cooper, D. M. (2003). Regulation and organization of adenylyl cyclases and cAMP. *Biochem J* **375**, 517-29.

Coppola, T., Magnin-Luthi, S., Perret-Menoud, V., Gattesco, S., Schiavo, G. and Regazzi, R. (2001). Direct interaction of the Rab3 effector RIM with Ca2+ channels, SNAP-25, and synaptotagmin. *J Biol Chem* **276**, 32756-62.

Crossthwaite, A. J., Seebacher, T., Masada, N., Ciruela, A., Dufraux, K., Schultz, J. E. and Cooper, D. M. (2005). The cytosolic domains of Ca2+-sensitive adenylyl cyclases dictate their targeting to plasma membrane lipid rafts. *J Biol Chem* **280**, 6380-91.

Danbolt, N. C. (2001). Glutamate uptake. *Prog Neurobiol* **65**, 1-105.

Danglot, L. and Galli, T. (2007). What is the function of neuronal AP-3? *Biol Cell* **99**, 349-61.

Dehnes, Y., Chaudhry, F. A., Ullensvang, K., Lehre, K. P., Storm-Mathisen, J. and Danbolt, N. C. (1998). The glutamate transporter EAAT4 in rat cerebellar Purkinje cells:

a glutamate-gated chloride channel concentrated near the synapse in parts of the dendritic membrane facing astroglia. *J Neurosci* **18**, 3606-19.

Delgado, J. M., Rosvold, H. E. and Looney, E. (1956). Evoking conditioned fear by electrical stimulation of subcortical structures in the monkey brain. *J Comp Physiol Psychol* **49**, 373-80.

Diana, M. A. and Marty, A. (2004). Endocannabinoid-mediated short-term synaptic plasticity: depolarization-induced suppression of inhibition (DSI) and depolarization-induced suppression of excitation (DSE). *Br J Pharmacol* **142**, 9-19.

Dietrich, D., Kirschstein, T., Kukley, M., Pereverzev, A., von der Brelie, C., Schneider, T. and Beck, H. (2003). Functional specialization of presynaptic Cav2.3 Ca2+ channels. *Neuron* **39**, 483-96.

Dresbach, T., Qualmann, B., Kessels, M. M., Garner, C. C. and Gundelfinger, E. D. (2001). The presynaptic cytomatrix of brain synapses. *Cell Mol Life Sci* **58**, 94-116.

Dudek, S. M. and Bear, M. F. (1993). Bidirectional long-term modification of synaptic effectiveness in the adult and immature hippocampus. *J Neurosci* **13**, 2910-8.

Dulubova, I., Lou, X., Lu, J., Huryeva, I., Alam, A., Schneggenburger, R., Sudhof, T. C. and Rizo, J. (2005). A Munc13/RIM/Rab3 tripartite complex: from priming to plasticity? *Embo J* **24**, 2839-50.

Eckert, R. and Chad, J. E. (1984). Inactivation of Ca channels. *Prog Biophys Mol Biol* **44**, 215-67.

Elmslie, K. S. (2003). Neurotransmitter modulation of neuronal calcium channels. *J Bioenerg Biomembr* **35**, 477-89.

Ertel, E. A., Campbell, K. P., Harpold, M. M., Hofmann, F., Mori, Y., Perez-Reyes, E., Schwartz, A., Snutch, T. P., Tanabe, T., Birnbaumer, L. et al. (2000). Nomenclature of voltage-gated calcium channels. *Neuron* **25**, 533-5.

Evans, G. J. and Morgan, A. (2003). Regulation of the exocytotic machinery by cAMP-dependent protein kinase: implications for presynaptic plasticity. *Biochem Soc Trans* **31**, 824-7.

Evers, M. R., Salmen, B., Bukalo, O., Rollenhagen, A., Bosl, M. R., Morellini, F., Bartsch, U., Dityatev, A. and Schachner, M. (2002). Impairment of L-type Ca2+ channel-dependent forms of hippocampal synaptic plasticity in mice deficient in the extracellular matrix glycoprotein tenascin-C. *J Neurosci* **22**, 7177-94.

Faber, E. S., Callister, R. J. and Sah, P. (2001). Morphological and electrophysiological properties of principal neurons in the rat lateral amygdala in vitro. *J Neurophysiol* **85**, 714-23.

Fasshauer, D., Sutton, R. B., Brunger, A. T. and Jahn, R. (1998). Conserved structural features of the synaptic fusion complex: SNARE proteins reclassified as Q- and R-SNAREs. *Proc Natl Acad Sci U S A* **95**, 15781-6.

Ferguson, G. D. and Storm, D. R. (2004). Why calcium-stimulated adenylyl cyclases? *Physiology (Bethesda)* **19**, 271-6.

Fernandez-Chacon, R., Shin, O. H., Konigstorfer, A., Matos, M. F., Meyer, A. C., Garcia, J., Gerber, S. H., Rizo, J., Sudhof, T. C. and Rosenmund, C. (2002). Structure/function analysis of Ca2+ binding to the C2A domain of synaptotagmin 1. *J Neurosci* **22**, 8438-46.

Foster, K. A. and Regehr, W. G. (2004). Variance-mean analysis in the presence of a rapid antagonist indicates vesicle depletion underlies depression at the climbing fiber synapse. *Neuron* **43**, 119-31.

Fu, Z., Lee, S. H., Simonetta, A., Hansen, J., Sheng, M. and Pak, D. T. (2007). Differential roles of Rap1 and Rap2 small GTPases in neurite retraction and synapse elimination in hippocampal spiny neurons. *J Neurochem* **100**, 118-31.

Fuchs, P. A., Evans, M. G. and Murrow, B. W. (1990). Calcium currents in hair cells isolated from the cochlea of the chick. *J Physiol* **429**, 553-68.

Fujii, S., Saito, K., Miyakawa, H., Ito, K. and Kato, H. (1991). Reversal of long-term potentiation (depotentiation) induced by tetanus stimulation of the input to CA1 neurons of guinea pig hippocampal slices. *Brain Res* **555**, 112-22.

Galli, T. and Haucke, V. (2004). Cycling of synaptic vesicles: how far? How fast! *Sci STKE* **2004**, re19.

Gao, T., Yatani, A., Dell'Acqua, M. L., Sako, H., Green, S. A., Dascal, N., Scott, J. D. and Hosey, M. M. (1997). cAMP-dependent regulation of cardiac L-type Ca2+ channels requires membrane targeting of PKA and phosphorylation of channel subunits. *Neuron* **19**, 185-96.

Garner, C. C., Kindler, S. and Gundelfinger, E. D. (2000). Molecular determinants of presynaptic active zones. *Curr Opin Neurobiol* **10**, 321-7.

Gasparini, S., Kasyanov, A. M., Pietrobon, D., Voronin, L. L. and Cherubini, E. (2001). Presynaptic R-type calcium channels contribute to fast excitatory synaptic transmission in the rat hippocampus. *J Neurosci* **21**, 8715-21.

Geppert, M., Bolshakov, V. Y., Siegelbaum, S. A., Takei, K., De Camilli, P., Hammer, R. E. and Sudhof, T. C. (1994). The role of Rab3A in neurotransmitter release. *Nature* **369**, 493-7.

Gerber, S. H., Garcia, J., Rizo, J. and Sudhof, T. C. (2001). An unusual C(2)-domain in the active-zone protein piccolo: implications for Ca(2+) regulation of neurotransmitter release. *Embo J* **20**, 1605-19.

Gerdeman, G. L. and Lovinger, D. M. (2003). Emerging roles for endocannabinoids in long-term synaptic plasticity. *Br J Pharmacol* **140**, 781-9.

Gerst, J. E. (1999). SNAREs and SNARE regulators in membrane fusion and exocytosis. *Cell Mol Life Sci* **55**, 707-34.

Goda, Y. and Stevens, C. F. (1994). Two components of transmitter release at a central synapse. *Proc Natl Acad Sci U S A* **91**, 12942-6.

Good, A. J. and Westbrook, R. F. (1995). Effects of a microinjection of morphine into the amygdala on the acquisition and expression of conditioned fear and hypoalgesia in rats. *Behav Neurosci* **109**, 631-41.

Gray, E. G. (1975). Synaptic fine structure and nuclear, cytoplasmic and extracellular networks: The stereoframework concept. *J Neurocytol* **4**, 315-39.

Gray, R. and Johnston, D. (1987). Noradrenaline and beta-adrenoceptor agonists increase activity of voltage-dependent calcium channels in hippocampal neurons. *Nature* **327**, 620-2.

Guarraci, F. A., Frohardt, R. J., Falls, W. A. and Kapp, B. S. (2000). The effects of intra-amygdaloid infusions of a D2 dopamine receptor antagonist on Pavlovian fear conditioning. *Behav Neurosci* **114**, 647-51.

Guarraci, F. A., Frohardt, R. J. and Kapp, B. S. (1999). Amygdaloid D1 dopamine receptor involvement in Pavlovian fear conditioning. *Brain Res* **827**, 28-40.

Gundelfinger, E. D., Kessels, M. M. and Qualmann, B. (2003). Temporal and spatial coordination of exocytosis and endocytosis. *Nat Rev Mol Cell Biol* **4**, 127-39.

Gustafsson, B. and Wigstrom, H. (1986). Hippocampal long-lasting potentiation produced by pairing single volleys and brief conditioning tetani evoked in separate afferents. *J Neurosci* **6**, 1575-82.

Hanson, P. I., Roth, R., Morisaki, H., Jahn, R. and Heuser, J. E. (1997). Structure and conformational changes in NSF and its membrane receptor complexes visualized by quick-freeze/deep-etch electron microscopy. *Cell* **90**, 523-35.

Hardingham, G. E. and Bading, H. (2003). The Yin and Yang of NMDA receptor signalling. *Trends Neurosci* **26**, 81-9.

Harris, E. W. and Cotman, C. W. (1986). Long-term potentiation of guinea pig mossy fiber responses is not blocked by N-methyl D-aspartate antagonists. *Neurosci Lett* **70**, 132-7.

Hebb, D. (1949). The Organization of Behavior: New York Wiley.

Heidelberger, R. and Matthews, G. (1992). Calcium influx and calcium current in single synaptic terminals of goldfish retinal bipolar neurons. *J Physiol* **447**, 235-56.

Heinemann, S. H., Terlau, H., Stuhmer, W., Imoto, K. and Numa, S. (1992). Calcium channel characteristics conferred on the sodium channel by single mutations. *Nature* **356**, 441-3.

Hering, S., Berjukow, S., Sokolov, S., Marksteiner, R., Weiss, R. G., Kraus, R. and Timin, E. N. (2000). Molecular determinants of inactivation in voltage-gated Ca2+ channels. *J Physiol* **528 Pt 2**, 237-49.

Hibino, H., Pironkova, R., Onwumere, O., Vologodskaia, M., Hudspeth, A. J. and Lesage, F. (2002). RIM binding proteins (RBPs) couple Rab3-interacting molecules (RIMs) to voltage-gated Ca(2+) channels. *Neuron* **34**, 411-23.

Higashima, M. and Yamamoto, C. (1985). Two components of long-term potentiation in mossy fiber-induced excitation in hippocampus. *Exp Neurol* **90**, 529-39.

Hoffman, D. A., Magee, J. C., Colbert, C. M. and Johnston, D. (1997). K+ channel regulation of signal propagation in dendrites of hippocampal pyramidal neurons. *Nature* **387**, 869-75.

Hoogland, T. M. and Saggau, P. (2004). Facilitation of L-type Ca2+ channels in dendritic spines by activation of beta2 adrenergic receptors. *J Neurosci* **24**, 8416-27.

Hrabetova, S. and Sacktor, T. C. (1996). Bidirectional regulation of protein kinase M zeta in the maintenance of long-term potentiation and long-term depression. *J Neurosci* **16**, 5324-33.

Hsu, S. F., Augustine, G. J. and Jackson, M. B. (1996). Adaptation of Ca(2+)-triggered exocytosis in presynaptic terminals. *Neuron* **17**, 501-12.

Huang, C. C. and Hsu, K. S. (2006). Presynaptic mechanism underlying cAMP-induced synaptic potentiation in medial prefrontal cortex pyramidal neurons. *Mol Pharmacol* **69**, 846-56.

Huang, Y. Y. and Kandel, E. R. (1998). Postsynaptic induction and PKA-dependent expression of LTP in the lateral amygdala. *Neuron* **21**, 169-78.

Huang, Y. Y., Kandel, E. R., Varshavsky, L., Brandon, E. P., Qi, M., Idzerda, R. L., McKnight, G. S. and Bourtchouladze, R. (1995). A genetic test of the effects of mutations in PKA on mossy fiber LTP and its relation to spatial and contextual learning. *Cell* **83**, 1211-22.

Huang, Y. Y., Zakharenko, S. S., Schoch, S., Kaeser, P. S., Janz, R., Sudhof, T. C., Siegelbaum, S. A. and Kandel, E. R. (2005). Genetic evidence for a protein-kinase-A-mediated presynaptic component in NMDA-receptor-dependent forms of long-term synaptic potentiation. *Proc Natl Acad Sci U S A* **102**, 9365-70.

Huber, K. M., Mauk, M. D. and Kelly, P. T. (1995). Distinct LTP induction mechanisms: contribution of NMDA receptors and voltage-dependent calcium channels. *J Neurophysiol* **73**, 270-9.

Humeau, Y., Doussau, F., Vitiello, F., Greengard, P., Benfenati, F. and Poulain, B. (2001). Synapsin controls both reserve and releasable synaptic vesicle pools during neuronal activity and short-term plasticity in Aplysia. *J Neurosci* **21**, 4195-206.

Humeau, Y., Herry, C., Kemp, N., Shaban, H., Fourcaudot, E., Bissiere, S. and Luthi, A. (2005). Dendritic spine heterogeneity determines afferent-specific Hebbian plasticity in the amygdala. *Neuron* **45**, 119-31.

Humeau, Y., Popoff, M. R., Kojima, H., Doussau, F. and Poulain, B. (2002). Rac GTPase plays an essential role in exocytosis by controlling the fusion competence of release sites. *J Neurosci* **22**, 7968-81.

Humeau, Y., Shaban, H., Bissiere, S. and Luthi, A. (2003). Presynaptic induction of heterosynaptic associative plasticity in the mammalian brain. *Nature* **426**, 841-5.

Inglis, F. M. and Moghaddam, B. (1999). Dopaminergic innervation of the amygdala is highly responsive to stress. *J Neurochem* **72**, 1088-94.

Iwasaki, S. and Takahashi, T. (1998). Developmental changes in calcium channel types mediating synaptic transmission in rat auditory brainstem. *J Physiol* **509 (Pt 2)**, 419-23.

Jackson, M. B. and Chapman, E. R. (2006). Fusion pores and fusion machines in Ca2+-triggered exocytosis. *Annu Rev Biophys Biomol Struct* **35**, 135-60.

Jaffe, D. and Johnston, D. (1990). Induction of long-term potentiation at hippocampal mossy-fiber synapses follows a Hebbian rule. *J Neurophysiol* **64**, 948-60.

Jensen, K. and Mody, I. (2001). L-type Ca2+ channel-mediated short-term plasticity of GABAergic synapses. *Nat Neurosci* **4**, 975-6.

Johnston, D., Williams, S., Jaffe, D. and Gray, R. (1992). NMDA-receptor-independent long-term potentiation. *Annu Rev Physiol* **54**, 489-505.

Jones, M. V. and Westbrook, G. L. (1996). The impact of receptor desensitization on fast synaptic transmission. *Trends Neurosci* **19**, 96-101.

Jones, S. W. (2003). Calcium channels: unanswered questions. *J Bioenerg Biomembr* **35**, 461-75.

Junge, H. J., Rhee, J. S., Jahn, O., Varoqueaux, F., Spiess, J., Waxham, M. N., Rosenmund, C. and Brose, N. (2004). Calmodulin and Munc13 form a Ca2+ sensor/effector complex that controls short-term synaptic plasticity. *Cell* **118**, 389-401.

Kahn, L., Alonso, G., Robbe, D., Bockaert, J. and Manzoni, O. J. (2001). Group 2 metabotropic glutamate receptors induced long term depression in mouse striatal slices. *Neurosci Lett* **316**, 178-82.

Kameyama, K., Lee, H. K., Bear, M. F. and Huganir, R. L. (1998). Involvement of a postsynaptic protein kinase A substrate in the expression of homosynaptic long-term depression. *Neuron* **21**, 1163-75.

Kandel, E. R. and Tauc, L. (1964). Mechanism Of Prolonged Heterosynaptic Facilitation. *Nature* **202**, 145-7.

Kaneko, M. and Takahashi, T. (2004). Presynaptic mechanism underlying cAMP-dependent synaptic potentiation. *J Neurosci* **24**, 5202-8.

Katona, I., Rancz, E. A., Acsady, L., Ledent, C., Mackie, K., Hajos, N. and Freund, T. F. (2001). Distribution of CB1 cannabinoid receptors in the amygdala and their role in the control of GABAergic transmission. *J Neurosci* **21**, 9506-18.

Katsuki, H., Kaneko, S., Tajima, A. and Satoh, M. (1991). Separate mechanisms of long-term potentiation in two input systems to CA3 pyramidal neurons of rat hippocampal slices as revealed by the whole-cell patch-clamp technique. *Neurosci Res* **12**, 393-402.

Katz, B. and Miledi, R. (1968). The role of calcium in neuromuscular facilitation. *J Physiol* **195**, 481-92.

Kavalali, E. T. (2007). Multiple vesicle recycling pathways in central synapses and their impact on neurotransmission. *J Physiol*.

Keef, K. D., Hume, J. R. and Zhong, J. (2001). Regulation of cardiac and smooth muscle Ca(2+) channels (Ca(V)1.2a,b) by protein kinases. *Am J Physiol Cell Physiol* **281**, C1743-56.

Kelso, S. R. and Brown, T. H. (1986). Differential conditioning of associative synaptic enhancement in hippocampal brain slices. *Science* **232**, 85-7.

Kelso, S. R., Ganong, A. H. and Brown, T. H. (1986). Hebbian synapses in hippocampus. *Proc Natl Acad Sci U S A* **83**, 5326-30.

Kemp, N. and Bashir, Z. I. (2001). Long-term depression: a cascade of induction and expression mechanisms. *Prog Neurobiol* **65**, 339-65.

Kennedy, M. B. (2000). Signal-processing machines at the postsynaptic density. *Science* **290**, 750-4.

Kim, J. J. and Jung, M. W. (2006). Neural circuits and mechanisms involved in Pavlovian fear conditioning: a critical review. *Neurosci Biobehav Rev* **30**, 188-202.

Klann, E., Chen, S. J. and Sweatt, J. D. (1993). Mechanism of protein kinase C activation during the induction and maintenance of long-term potentiation probed using a selective peptide substrate. *Proc Natl Acad Sci U S A* **90**, 8337-41.

Klüver, H. and Bucy, P., C. (1937). "Psychic blindness" and other symptoms following bilateral temporal lobectomy in rhesus monkeys. *Am. J. Physiol Rev* **119**, 352-53.

Kobayashi, K., Manabe, T. and Takahashi, T. (1999). Calcium-dependent mechanisms involved in presynaptic long-term depression at the hippocampal mossy fibre-CA3 synapse. *Eur J Neurosci* **11**, 1633-8.

Koushika, S. P., Richmond, J. E., Hadwiger, G., Weimer, R. M., Jorgensen, E. M. and Nonet, M. L. (2001). A post-docking role for active zone protein Rim. *Nat Neurosci* **4**, 997-1005.

Krettek, J. E. and Price, J. L. (1978). A description of the amygdaloid complex in the rat and cat with observations on intra-amygdaloid axonal connections. *J Comp Neurol* **178**, 255-80.

Kwan, E. P., Xie, L., Sheu, L., Ohtsuka, T. and Gaisano, H. Y. (2007). Interaction between Munc13-1 and RIM is critical for glucagon-like peptide-1 mediated rescue of exocytotic defects in Munc13-1 deficient pancreatic beta-cells. *Diabetes* **56**, 2579-88.

Landis, D. M. (1988). Membrane and cytoplasmic structure at synaptic junctions in the mammalian central nervous system. *J Electron Microsc Tech* **10**, 129-51.

Landis, D. M., Hall, A. K., Weinstein, L. A. and Reese, T. S. (1988). The organization of cytoplasm at the presynaptic active zone of a central nervous system synapse. *Neuron* **1**, 201-9.

Lang, E. J. and Pare, D. (1997). Similar inhibitory processes dominate the responses of cat lateral amygdaloid projection neurons to their various afferents. *J Neurophysiol* **77**, 341-52.

Langdon, R. B., Johnson, J. W. and Barrionuevo, G. (1995). Posttetanic potentiation and presynaptically induced long-term potentiation at the mossy fiber synapse in rat hippocampus. *J Neurobiol* **26**, 370-85.

LeDoux, J. (1996). Emotional networks and motor control: a fearful view. *Prog Brain Res* **107**, 437-46.

LeDoux, J. E. (2000). Emotion circuits in the brain. *Annu Rev Neurosci* **23**, 155-84.

Lee, H. K., Kameyama, K., Huganir, R. L. and Bear, M. F. (1998). NMDA induces long-term synaptic depression and dephosphorylation of the GluR1 subunit of AMPA receptors in hippocampus. *Neuron* **21**, 1151-62.

Levy, W. B. and Steward, O. (1983). Temporal contiguity requirements for long-term associative potentiation/depression in the hippocampus. *Neuroscience* **8**, 791-7.

Li, L. and Chin, L. S. (2003). The molecular machinery of synaptic vesicle exocytosis. *Cell Mol Life Sci* **60**, 942-60.

Lin, R. C. and Scheller, R. H. (1997). Structural organization of the synaptic exocytosis core complex. *Neuron* **19**, 1087-94.

Linden, D. J. and Ahn, S. (1999). Activation of presynaptic cAMP-dependent protein kinase is required for induction of cerebellar long-term potentiation. *J Neurosci* **19**, 10221-7.

Ling, D. S., Benardo, L. S., Serrano, P. A., Blace, N., Kelly, M. T., Crary, J. F. and Sacktor, T. C. (2002). Protein kinase Mzeta is necessary and sufficient for LTP maintenance. *Nat Neurosci* **5**, 295-6.

Lipscombe, D., Helton, T. D. and Xu, W. (2004). L-type calcium channels: the low down. *J Neurophysiol* **92**, 2633-41.

Lledo, P. M., Zhang, X., Sudhof, T. C., Malenka, R. C. and Nicoll, R. A. (1998). Postsynaptic membrane fusion and long-term potentiation. *Science* **279**, 399-403.

Lomo, T. (1966). Frequency potentiation of excitatory synaptic activity in the dentate area of the hippocampal formation.

Lonart, G., Schoch, S., Kaeser, P. S., Larkin, C. J., Sudhof, T. C. and Linden, D. J. (2003). Phosphorylation of RIM1alpha by PKA triggers presynaptic long-term potentiation at cerebellar parallel fiber synapses. *Cell* **115**, 49-60.

Lonart, G. and Sudhof, T. C. (1998). Region-specific phosphorylation of rabphilin in mossy fiber nerve terminals of the hippocampus. *J Neurosci* **18**, 634-40.

Lopez de Armentia, M. and Sah, P. (2004). Firing properties and connectivity of neurons in the rat lateral central nucleus of the amygdala. *J Neurophysiol* **92**, 1285-94.

Loretan, K., Bissiere, S. and Luthi, A. (2004). Dopaminergic modulation of spontaneous inhibitory network activity in the lateral amygdala. *Neuropharmacology* **47**, 631-9.

Lovinger, D. M. (2007). Endocannabinoid liberation from neurons in transsynaptic signaling. *J Mol Neurosci* **33**, 87-93.

Lu, W. Y., Xiong, Z. G., Lei, S., Orser, B. A., Dudek, E., Browning, M. D. and MacDonald, J. F. (1999). G-protein-coupled receptors act via protein kinase C and Src to regulate NMDA receptors. *Nat Neurosci* **2**, 331-8.

Lynch, M. A. (2004). Long-term potentiation and memory. *Physiol Rev* **84**, 87-136.

Madison, J. M., Nurrish, S. and Kaplan, J. M. (2005). UNC-13 interaction with syntaxin is required for synaptic transmission. *Curr Biol* **15**, 2236-42.

Mahanty, N. K. and Sah, P. (1998). Calcium-permeable AMPA receptors mediate long-term potentiation in interneurons in the amygdala. *Nature* **394**, 683-7.

Malenka, R. C. and Bear, M. F. (2004). LTP and LTD: an embarrassment of riches. *Neuron* **44**, 5-21.

Malenka, R. C. and Nicoll, R. A. (1999). Long-term potentiation--a decade of progress? *Science* **285**, 1870-4.

Mameli, M., Balland, B., Lujan, R. and Luscher, C. (2007). Rapid synthesis and synaptic insertion of GluR2 for mGluR-LTD in the ventral tegmental area. *Science* **317**, 530-3.

Man, H. Y., Lin, J. W., Ju, W. H., Ahmadian, G., Liu, L., Becker, L. E., Sheng, M. and Wang, Y. T. (2000). Regulation of AMPA receptor-mediated synaptic transmission by clathrin-dependent receptor internalization. *Neuron* **25**, 649-62.

Maren, S. (1999). Long-term potentiation in the amygdala: a mechanism for emotional learning and memory. *Trends Neurosci* **22**, 561-7.

Maren, S. and Quirk, G. J. (2004). Neuronal signalling of fear memory. *Nat Rev Neurosci* **5**, 844-52.

Markram, H., Lubke, J., Frotscher, M. and Sakmann, B. (1997). Regulation of synaptic efficacy by coincidence of postsynaptic APs and EPSPs. *Science* **275**, 213-5.

Marqueze, B., Berton, F. and Seagar, M. (2000). Synaptotagmins in membrane traffic: which vesicles do the tagmins tag? *Biochimie* **82**, 409-20.

Marsicano, G., Wotjak, C. T., Azad, S. C., Bisogno, T., Rammes, G., Cascio, M. G., Hermann, H., Tang, J., Hofmann, C., Zieglgansberger, W. et al. (2002). The endogenous cannabinoid system controls extinction of aversive memories. *Nature* **418**, 530-4.

Martin, S. J., Grimwood, P. D. and Morris, R. G. (2000). Synaptic plasticity and memory: an evaluation of the hypothesis. *Annu Rev Neurosci* **23**, 649-711.

Martina, M., Royer, S. and Pare, D. (1999). Physiological properties of central medial and central lateral amygdala neurons. *J Neurophysiol* **82**, 1843-54.

Mascagni, F. and McDonald, A. J. (2003). Immunohistochemical characterization of cholecystokinin containing neurons in the rat basolateral amygdala. *Brain Res* **976**, 171-84.

Matsuda, S., Launey, T., Mikawa, S. and Hirai, H. (2000). Disruption of AMPA receptor GluR2 clusters following long-term depression induction in cerebellar Purkinje neurons. *Embo J* **19**, 2765-74.

Maximov, A. and Bezprozvanny, I. (2002). Synaptic targeting of N-type calcium channels in hippocampal neurons. *J Neurosci* **22**, 6939-52.

McDonald, A. J. (1982). Neurons of the lateral and basolateral amygdaloid nuclei: a Golgi study in the rat. *J Comp Neurol* **212**, 293-312.

McDonald, A. J. and Augustine, J. R. (1993). Localization of GABA-like immunoreactivity in the monkey amygdala. *Neuroscience* **52**, 281-94.

McDonald, A. J. and Mascagni, F. (2001). Colocalization of calcium-binding proteins and GABA in neurons of the rat basolateral amygdala. *Neuroscience* **105**, 681-93.

McDonald, A. J., Mascagni, F. and Muller, J. F. (2004). Immunocytochemical localization of GABABR1 receptor subunits in the basolateral amygdala. *Brain Res* **1018**, 147-58.

McDonald, A. J. and Pearson, J. C. (1989). Coexistence of GABA and peptide immunoreactivity in non-pyramidal neurons of the basolateral amygdala. *Neurosci Lett* **100**, 53-8.

McGaugh, J. L. (1989). Involvement of hormonal and neuromodulatory systems in the regulation of memory storage. *Annu Rev Neurosci* **12**, 255-87.

McKernan, M. G. and Shinnick-Gallagher, P. (1997). Fear conditioning induces a lasting potentiation of synaptic currents in vitro. *Nature* **390**, 607-11.

Medina, J. F., Christopher Repa, J., Mauk, M. D. and LeDoux, J. E. (2002). Parallels between cerebellum- and amygdala-dependent conditioning. *Nat Rev Neurosci* **3**, 122-31.

Mellor, J. and Nicoll, R. A. (2001). Hippocampal mossy fiber LTP is independent of postsynaptic calcium. *Nat Neurosci* **4**, 125-6.

Meyer, A. C., Neher, E. and Schneggenburger, R. (2001). Estimation of quantal size and number of functional active zones at the calyx of held synapse by nonstationary EPSC variance analysis. *J Neurosci* **21**, 7889-900.

Michaelson, D. M., Barkai, G. and Barenholz, Y. (1983). Asymmetry of lipid organization in cholinergic synaptic vesicle membranes. *Biochem J* **211**, 155-62.

Mikoshiba, K., Fukuda, M., Ibata, K., Kabayama, H. and Mizutani, A. (1999). Role of synaptotagmin, a Ca2+ and inositol polyphosphate binding protein, in neurotransmitter release and neurite outgrowth. *Chem Phys Lipids* **98**, 59-67.

Miserendino, M. J., Sananes, C. B., Melia, K. R. and Davis, M. (1990). Blocking of acquisition but not expression of conditioned fear-potentiated startle by NMDA antagonists in the amygdala. *Nature* **345**, 716-8.

Mochida, S., Westenbroek, R. E., Yokoyama, C. T., Zhong, H., Myers, S. J., Scheuer, T., Itoh, K. and Catterall, W. A. (2003). Requirement for the synaptic protein interaction site for reconstitution of synaptic transmission by P/Q-type calcium channels. *Proc Natl Acad Sci U S A* **100**, 2819-24.

Morris, R. G. (2003). Long-term potentiation and memory. *Philos Trans R Soc Lond B Biol Sci* **358**, 643-7.

Moser, T. and Beutner, D. (2000). Kinetics of exocytosis and endocytosis at the cochlear inner hair cell afferent synapse of the mouse. *Proc Natl Acad Sci U S A* **97**, 883-8.

Mulkey, R. M., Endo, S., Shenolikar, S. and Malenka, R. C. (1994). Involvement of a calcineurin/inhibitor-1 phosphatase cascade in hippocampal long-term depression. *Nature* **369**, 486-8.

Murthy, V. N. and De Camilli, P. (2003). Cell biology of the presynaptic terminal. *Annu Rev Neurosci* **26**, 701-28.

Murthy, V. N., Sejnowski, T. J. and Stevens, C. F. (1997). Heterogeneous release properties of visualized individual hippocampal synapses. *Neuron* **18**, 599-612.

Nagy, G., Reim, K., Matti, U., Brose, N., Binz, T., Rettig, J., Neher, E. and Sorensen, J. B. (2004). Regulation of releasable vesicle pool sizes by protein kinase A-dependent phosphorylation of SNAP-25. *Neuron* **41**, 417-29.

Nakanishi, H., Obaishi, H., Satoh, A., Wada, M., Mandai, K., Satoh, K., Nishioka, H., Matsuura, Y., Mizoguchi, A. and Takai, Y. (1997). Neurabin: a novel neural tissue-specific actin filament-binding protein involved in neurite formation. *J Cell Biol* **139**, 951-61.

Nguyen, P. V. and Woo, N. H. (2003). Regulation of hippocampal synaptic plasticity by cyclic AMP-dependent protein kinases. *Prog Neurobiol* **71**, 401-37.

Nicoll, R. A. and Malenka, R. C. (1995). Contrasting properties of two forms of long-term potentiation in the hippocampus. *Nature* **377**, 115-8.

Niikura, Y., Abe, K. and Misawa, M. (2004). Involvement of L-type Ca2+ channels in the induction of long-term potentiation in the basolateral amygdala-dentate gyrus pathway of anesthetized rats. *Brain Res* **1017**, 218-21.

Nishizuka, Y. (1988). The molecular heterogeneity of protein kinase C and its implications for cellular regulation. *Nature* **334**, 661-5.

Ohtsuka, T., Takao-Rikitsu, E., Inoue, E., Inoue, M., Takeuchi, M., Matsubara, K., Deguchi-Tawarada, M., Satoh, K., Morimoto, K., Nakanishi, H. et al. (2002). Cast: a novel protein of the cytomatrix at the active zone of synapses that forms a ternary complex with RIM1 and munc13-1. *J Cell Biol* **158**, 577-90.

Oleskevich, S., Clements, J. and Walmsley, B. (2000). Release probability modulates short-term plasticity at a rat giant terminal. *J Physiol* **524 Pt 2**, 513-23.

Oliveria, S. F., Dell'Acqua, M. L. and Sather, W. A. (2007). AKAP79/150 anchoring of calcineurin controls neuronal L-type Ca2+ channel activity and nuclear signaling. *Neuron* **55**, 261-75.

Orita, S., Sasaki, T., Naito, A., Komuro, R., Ohtsuka, T., Maeda, M., Suzuki, H., Igarashi, H. and Takai, Y. (1995). Doc2: a novel brain protein having two repeated C2-like domains. *Biochem Biophys Res Commun* **206**, 439-48.

Ostrom, R. S. and Insel, P. A. (2004). The evolving role of lipid rafts and caveolae in G protein-coupled receptor signaling: implications for molecular pharmacology. *Br J Pharmacol* **143**, 235-45.

Otani, S., Auclair, N., Desce, J. M., Roisin, M. P. and Crepel, F. (1999). Dopamine receptors and groups I and II mGluRs cooperate for long-term depression induction in rat prefrontal cortex through converging postsynaptic activation of MAP kinases. *J Neurosci* **19**, 9788-802.

Otani, S., Daniel, H., Takita, M. and Crepel, F. (2002). Long-term depression induced by postsynaptic group II metabotropic glutamate receptors linked to phospholipase C and intracellular calcium rises in rat prefrontal cortex. *J Neurosci* **22**, 3434-44.

Ozaki, N., Shibasaki, T., Kashima, Y., Miki, T., Takahashi, K., Ueno, H., Sunaga, Y., Yano, H., Matsuura, Y., Iwanaga, T. et al. (2000). cAMP-GEFII is a direct target of cAMP in regulated exocytosis. *Nat Cell Biol* **2**, 805-11.

Pan, Z. H., Hu, H. J., Perring, P. and Andrade, R. (2001). T-type Ca(2+) channels mediate neurotransmitter release in retinal bipolar cells. *Neuron* **32**, 89-98.

Papez, J. W. (1937). A proposed mechanism of emotion. 1937. *J Neuropsychiatry Clin Neurosci* **7**, 103-12.

Pare, D., Quirk, G. J. and Ledoux, J. E. (2004). New vistas on amygdala networks in conditioned fear. *J Neurophysiol* **92**, 1-9.

Pare, D. and Smith, Y. (1993). Distribution of GABA immunoreactivity in the amygdaloid complex of the cat. *Neuroscience* **57**, 1061-76.

Pastalkova, E., Serrano, P., Pinkhasova, D., Wallace, E., Fenton, A. A. and Sacktor, T. C. (2006). Storage of spatial information by the maintenance mechanism of LTP. *Science* **313**, 1141-4.

Perez-Reyes, E. (2003). Molecular physiology of low-voltage-activated t-type calcium channels. *Physiol Rev* **83**, 117-61.

Peterson, B. Z., DeMaria, C. D., Adelman, J. P. and Yue, D. T. (1999). Calmodulin is the Ca2+ sensor for Ca2+ -dependent inactivation of L-type calcium channels. *Neuron* **22**, 549-58.

Pfenninger, K., Akert, K., Moor, H. and Sandri, C. (1972). The fine structure of freeze-fractured presynaptic membranes. *J Neurocytol* **1**, 129-49.

Phillips, G. R., Huang, J. K., Wang, Y., Tanaka, H., Shapiro, L., Zhang, W., Shan, W. S., Arndt, K., Frank, M., Gordon, R. E. et al. (2001). The presynaptic particle web: ultrastructure, composition, dissolution, and reconstitution. *Neuron* **32**, 63-77.

Pitkänen, A. (2000). Connectivity of the rat amygdaloid complex. In: The Amygdala: A Functional Analysis: Aggleton JP. Oxford UK: Oxford Univ. Press.

Pitkänen, A., Savander, V. and LeDoux, J. E. (1997). Organization of intra-amygdaloid circuitries in the rat: an emerging framework for understanding functions of the amygdala. *Trends Neurosci* **20**, 517-23.

Platzer, J., Engel, J., Schrott-Fischer, A., Stephan, K., Bova, S., Chen, H., Zheng, H. and Striessnig, J. (2000). Congenital deafness and sinoatrial node dysfunction in mice lacking class D L-type Ca2+ channels. *Cell* **102**, 89-97.

Poirier, M. A., Xiao, W., Macosko, J. C., Chan, C., Shin, Y. K. and Bennett, M. K. (1998). The synaptic SNARE complex is a parallel four-stranded helical bundle. *Nat Struct Biol* **5**, 765-9.

Powell, C. M., Schoch, S., Monteggia, L., Barrot, M., Matos, M. F., Feldmann, N., Sudhof, T. C. and Nestler, E. J. (2004). The presynaptic active zone protein RIM1alpha is critical for normal learning and memory. *Neuron* **42**, 143-53.

Purves, D., Augustine, G. J., Fitzpatrick, D., Katz, L. C., LaMantia, A.-S., McNamara, J. O. and Williams, S. M. (2001). Neuroscience, 2d ed: Sinauer Associates, Inc.

Qi, M., Zhuo, M., Skalhegg, B. S., Brandon, E. P., Kandel, E. R., McKnight, G. S. and Idzerda, R. L. (1996). Impaired hippocampal plasticity in mice lacking the Cbeta1 catalytic subunit of cAMP-dependent protein kinase. *Proc Natl Acad Sci U S A* **93**, 1571-6.

Quirk, G. J., Armony, J. L. and LeDoux, J. E. (1997). Fear conditioning enhances different temporal components of tone-evoked spike trains in auditory cortex and lateral amygdala. *Neuron* **19**, 613-24.

Rainnie, D. G., Asprodini, E. K. and Shinnick-Gallagher, P. (1993). Intracellular recordings from morphologically identified neurons of the basolateral amygdala. *J Neurophysiol* **69**, 1350-62.

Reid, C. A., Bekkers, J. M. and Clements, J. D. (2003). Presynaptic Ca2+ channels: a functional patchwork. *Trends Neurosci* **26**, 683-7.

Reid, C. A. and Clements, J. D. (1999). Postsynaptic expression of long-term potentiation in the rat dentate gyrus demonstrated by variance-mean analysis. *J Physiol* **518 (Pt 1)**, 121-30.

Reid, C. A., Dixon, D. B., Takahashi, M., Bliss, T. V. and Fine, A. (2004). Optical quantal analysis indicates that long-term potentiation at single hippocampal mossy fiber synapses is expressed through increased release probability, recruitment of new release sites, and activation of silent synapses. *J Neurosci* **24**, 3618-26.

Richmond, J. E., Weimer, R. M. and Jorgensen, E. M. (2001). An open form of syntaxin bypasses the requirement for UNC-13 in vesicle priming. *Nature* **412**, 338-41.

Riedel, G., Platt, B. and Micheau, J. (2003). Glutamate receptor function in learning and memory. *Behav Brain Res* **140**, 1-47.

Rizo, J., Chen, X. and Arac, D. (2006). Unraveling the mechanisms of synaptotagmin and SNARE function in neurotransmitter release. *Trends Cell Biol* **16**, 339-50.

Rizzoli, S. O. and Betz, W. J. (2005). Synaptic vesicle pools. *Nat Rev Neurosci* **6**, 57-69.

Robbe, D., Alonso, G., Chaumont, S., Bockaert, J. and Manzoni, O. J. (2002). Role of p/q-Ca2+ channels in metabotropic glutamate receptor 2/3-dependent presynaptic long-term depression at nucleus accumbens synapses. *J Neurosci* **22**, 4346-56.

Roberts, W. M., Jacobs, R. A. and Hudspeth, A. J. (1990). Colocalization of ion channels involved in frequency selectivity and synaptic transmission at presynaptic active zones of hair cells. *J Neurosci* **10**, 3664-84.

Robertson, D. and Paki, B. (2002). Role of L-type Ca2+ channels in transmitter release from mammalian inner hair cells. II. Single-neuron activity. *J Neurophysiol* **87**, 2734-40.

Rodrigues, S. M., Schafe, G. E. and LeDoux, J. E. (2004). Molecular mechanisms underlying emotional learning and memory in the lateral amygdala. *Neuron* **44**, 75-91.

Roesler, R., Schroder, N., Vianna, M. R., Quevedo, J., Bromberg, E., Kapczinski, F. and Ferreira, M. B. (2003). Differential involvement of hippocampal and amygdalar NMDA receptors in contextual and aversive aspects of inhibitory avoidance memory in rats. *Brain Res* **975**, 207-13.

Rogan, M. T., Staubli, U. V. and LeDoux, J. E. (1997). Fear conditioning induces associative long-term potentiation in the amygdala. *Nature* **390**, 604-7.

Rosenkranz, J. A. and Grace, A. A. (2002). Dopamine-mediated modulation of odour-evoked amygdala potentials during pavlovian conditioning. *Nature* **417**, 282-7.

Rosenkranz, J. A. and Grace, A. A. (2003). Affective conditioning in the basolateral amygdala of anesthetized rats is modulated by dopamine and prefrontal cortical inputs. *Ann N Y Acad Sci* **985**, 488-91.

Rosenmund, C., Clements, J. D. and Westbrook, G. L. (1993). Nonuniform probability of glutamate release at a hippocampal synapse. *Science* **262**, 754-7.

Rosenmund, C., Sigler, A., Augustin, I., Reim, K., Brose, N. and Rhee, J. S. (2002). Differential control of vesicle priming and short-term plasticity by Munc13 isoforms. *Neuron* **33**, 411-24.

Rosvold, H. E. and Delgado, J. M. (1956). The effect on delayed-alternation test performance of stimulating or destroying electrically structures within the frontal lobes of the monkey's brain. *J Comp Physiol Psychol* **49**, 365-72.

Rothman, J. E. (1994). Mechanisms of intracellular protein transport. *Nature* **372**, 55-63.

Rothstein, J. D., Martin, L., Levey, A. I., Dykes-Hoberg, M., Jin, L., Wu, D., Nash, N. and Kuncl, R. W. (1994). Localization of neuronal and glial glutamate transporters. *Neuron* **13**, 713-25.

Ruschenschmidt, C., Straub, H., Kohling, R., Siep, E., Gorji, A. and Speckmann, E. J. (2004). Reduction of human neocortical and guinea pig CA1-neuron A-type currents by organic calcium channel blockers. *Neurosci Lett* **368**, 57-62.

Sacktor, T. C., Osten, P., Valsamis, H., Jiang, X., Naik, M. U. and Sublette, E. (1993). Persistent activation of the zeta isoform of protein kinase C in the maintenance of long-term potentiation. *Proc Natl Acad Sci U S A* **90**, 8342-6.

Sah, P., Faber, E. S., Lopez De Armentia, M. and Power, J. (2003). The amygdaloid complex: anatomy and physiology. *Physiol Rev* **83**, 803-34.

Salin, P. A., Malenka, R. C. and Nicoll, R. A. (1996). Cyclic AMP mediates a presynaptic form of LTP at cerebellar parallel fiber synapses. *Neuron* **16**, 797-803.

Sastry, B. R., Goh, J. W. and Auyeung, A. (1986). Associative induction of posttetanic and long-term potentiation in CA1 neurons of rat hippocampus. *Science* **232**, 988-90.

Savonenko, A., Werka, T., Nikolaev, E., Zielinski, K. and Kaczmarek, L. (2003). Complex effects of NMDA receptor antagonist APV in the basolateral amygdala on acquisition of two-way avoidance reaction and long-term fear memory. *Learn Mem* **10**, 293-303.

Schafe, G. E. and LeDoux, J. E. (2000). Memory consolidation of auditory pavlovian fear conditioning requires protein synthesis and protein kinase A in the amygdala. *J Neurosci* **20**, RC96.

Scheuss, V. and Neher, E. (2001). Estimating synaptic parameters from mean, variance, and covariance in trains of synaptic responses. *Biophys J* **81**, 1970-89.

Scheuss, V., Schneggenburger, R. and Neher, E. (2002). Separation of presynaptic and postsynaptic contributions to depression by covariance analysis of successive EPSCs at the calyx of held synapse. *J Neurosci* **22**, 728-39.

Schiess, M. C., Asprodini, E. K., Rainnie, D. G. and Shinnick-Gallagher, P. (1993). The central nucleus of the rat amygdala: in vitro intracellular recordings. *Brain Res* **604**, 283-97.

Schluter, O. M., Schnell, E., Verhage, M., Tzonopoulos, T., Nicoll, R. A., Janz, R., Malenka, R. C., Geppert, M. and Sudhof, T. C. (1999). Rabphilin knock-out mice reveal

that rabphilin is not required for rab3 function in regulating neurotransmitter release. *J Neurosci* **19**, 5834-46.

Schoch, S., Castillo, P. E., Jo, T., Mukherjee, K., Geppert, M., Wang, Y., Schmitz, F., Malenka, R. C. and Sudhof, T. C. (2002). RIM1alpha forms a protein scaffold for regulating neurotransmitter release at the active zone. *Nature* **415**, 321-6.

Shaban, H., Humeau, Y., Herry, C., Cassasus, G., Shigemoto, R., Ciocchi, S., Barbieri, S., van der Putten, H., Kaupmann, K., Bettler, B. et al. (2006). Generalization of amygdala LTP and conditioned fear in the absence of presynaptic inhibition. *Nat Neurosci* **9**, 1028-35.

Sheng, Z. H., Westenbroek, R. E. and Catterall, W. A. (1998). Physical link and functional coupling of presynaptic calcium channels and the synaptic vesicle docking/fusion machinery. *J Bioenerg Biomembr* **30**, 335-45.

Shi, S. H., Hayashi, Y., Petralia, R. S., Zaman, S. H., Wenthold, R. J., Svoboda, K. and Malinow, R. (1999). Rapid spine delivery and redistribution of AMPA receptors after synaptic NMDA receptor activation. *Science* **284**, 1811-6.

Shibasaki, T., Sunaga, Y., Fujimoto, K., Kashima, Y. and Seino, S. (2004). Interaction of ATP sensor, cAMP sensor, Ca2+ sensor, and voltage-dependent Ca2+ channel in insulin granule exocytosis. *J Biol Chem* **279**, 7956-61.

Shinnick-Gallagher, P., McKernan, M. G., Xie, J. and Zinebi, F. (2003). L-type voltage-gated calcium channels are involved in the in vivo and in vitro expression of fear conditioning. *Ann N Y Acad Sci* **985**, 135-49.

Shirataki, H., Kaibuchi, K., Sakoda, T., Kishida, S., Yamaguchi, T., Wada, K., Miyazaki, M. and Takai, Y. (1993). Rabphilin-3A, a putative target protein for smg p25A/rab3A p25 small GTP-binding protein related to synaptotagmin. *Mol Cell Biol* **13**, 2061-8.

Silver, R. A. (2003). Estimation of nonuniform quantal parameters with multiple-probability fluctuation analysis: theory, application and limitations. *J Neurosci Methods* **130**, 127-41.

Silver, R. A., Momiyama, A. and Cull-Candy, S. G. (1998). Locus of frequency-dependent depression identified with multiple-probability fluctuation analysis at rat climbing fibre-Purkinje cell synapses. *J Physiol* **510 (Pt 3)**, 881-902.

Simsek-Duran, F., Linden, D. J. and Lonart, G. (2004). Adapter protein 14-3-3 is required for a presynaptic form of LTP in the cerebellum. *Nat Neurosci* **7**, 1296-8.

Singer, J. H. and Diamond, J. S. (2006). Vesicle depletion and synaptic depression at a mammalian ribbon synapse. *J Neurophysiol* **95**, 3191-8.

Sjostrom, P. J., Turrigiano, G. G. and Nelson, S. B. (2003). Neocortical LTD via coincident activation of presynaptic NMDA and cannabinoid receptors. *Neuron* **39**, 641-54.

Smith, Y. and Pare, D. (1994). Intra-amygdaloid projections of the lateral nucleus in the cat: PHA-L anterograde labeling combined with postembedding GABA and glutamate immunocytochemistry. *J Comp Neurol* **342**, 232-48.

Sosulina, L., Meis, S., Seifert, G., Steinhauser, C. and Pape, H. C. (2006). Classification of projection neurons and interneurons in the rat lateral amygdala based upon cluster analysis. *Mol Cell Neurosci* **33**, 57-67.

Spafford, J. D. and Zamponi, G. W. (2003). Functional interactions between presynaptic calcium channels and the neurotransmitter release machinery. *Curr Opin Neurobiol* **13**, 308-14.

Spassova, M., Eisen, M. D., Saunders, J. C. and Parsons, T. D. (2001). Chick cochlear hair cell exocytosis mediated by dihydropyridine-sensitive calcium channels. *J Physiol* **535**, 689-96.

Spillane, D. M., Rosahl, T. W., Sudhof, T. C. and Malenka, R. C. (1995). Long-term potentiation in mice lacking synapsins. *Neuropharmacology* **34**, 1573-9.

Stent, G. S. (1973). A physiological mechanism for Hebb's postulate of learning. *Proc Natl Acad Sci U S A* **70**, 997-1001.

Ster, J., De Bock, F., Guerineau, N. C., Janossy, A., Barrere-Lemaire, S., Bos, J. L., Bockaert, J. and Fagni, L. (2007). Exchange protein activated by cAMP (Epac) mediates cAMP activation of p38 MAPK and modulation of Ca2+-dependent K+ channels in cerebellar neurons. *Proc Natl Acad Sci U S A* **104**, 2519-24.

Stevens, D. R., Wu, Z. X., Matti, U., Junge, H. J., Schirra, C., Becherer, U., Wojcik, S. M., Brose, N. and Rettig, J. (2005). Identification of the minimal protein domain required for priming activity of Munc13-1. *Curr Biol* **15**, 2243-8.

Stotz, S. C. and Zamponi, G. W. (2001). Identification of inactivation determinants in the domain IIS6 region of high voltage-activated calcium channels. *J Biol Chem* **276**, 33001-10.

Stuart, G. J. and Sakmann, B. (1994). Active propagation of somatic action potentials into neocortical pyramidal cell dendrites. *Nature* **367**, 69-72.

Sudhof, T. C. (2004). The synaptic vesicle cycle. *Annu Rev Neurosci* **27**, 509-47.

Sudhof, T. C. and Rizo, J. (1996). Synaptotagmins: C2-domain proteins that regulate membrane traffic. *Neuron* **17**, 379-88.

Sugita, S., Johnson, S. W. and North, R. A. (1992). Synaptic inputs to GABAA and GABAB receptors originate from discrete afferent neurons. *Neurosci Lett* **134**, 207-11.

Sugita, S. and North, R. A. (1993). Opioid actions on neurons of rat lateral amygdala in vitro. *Brain Res* **612**, 151-5.

Sun, J. Y., Wu, X. S. and Wu, L. G. (2002). Single and multiple vesicle fusion induce different rates of endocytosis at a central synapse. *Nature* **417**, 555-9.

Sun, L., Bittner, M. A. and Holz, R. W. (2003). Rim, a component of the presynaptic active zone and modulator of exocytosis, binds 14-3-3 through its N terminus. *J Biol Chem* **278**, 38301-9.

Sunahara, R. K. and Taussig, R. (2002). Isoforms of mammalian adenylyl cyclase: multiplicities of signaling. *Mol Interv* **2**, 168-84.

Sutton, R. B., Fasshauer, D., Jahn, R. and Brunger, A. T. (1998). Crystal structure of a SNARE complex involved in synaptic exocytosis at 2.4 A resolution. *Nature* **395**, 347-53.

Tasken, K. and Aandahl, E. M. (2004). Localized effects of cAMP mediated by distinct routes of protein kinase A. *Physiol Rev* **84**, 137-67.

Tovar, K. R. and Westbrook, G. L. (2002). Mobile NMDA receptors at hippocampal synapses. *Neuron* **34**, 255-64.

Trisch, D., Chesnoy-Marchais, D. and Feltz, A. (1999). Physiologie du neurone ed Doin.

Tsien, R. W., Lipscombe, D., Madison, D. V., Bley, K. R. and Fox, A. P. (1988). Multiple types of neuronal calcium channels and their selective modulation. *Trends Neurosci* **11**, 431-8.

Tully, K., Li, Y., Tsvetkov, E. and Bolshakov, V. Y. (2007). Norepinephrine enables the induction of associative long-term potentiation at thalamo-amygdala synapses. *Proc Natl Acad Sci U S A* **104**, 14146-50.

Tzounopoulos, T., Janz, R., Sudhof, T. C., Nicoll, R. A. and Malenka, R. C. (1998). A role for cAMP in long-term depression at hippocampal mossy fiber synapses. *Neuron* **21**, 837-45.

Udagawa, R., Nakano, M. and Kato, N. (2006). Blocking L-type calcium channels enhances long-term depression induced by low-frequency stimulation at hippocampal CA1 synapses. *Brain Res* **1124**, 28-36.

Vaccarino, A. L., Olson, G. A., Olson, R. D. and Kastin, A. J. (1999). Endogenous opiates: 1998. *Peptides* **20**, 1527-74.

Varoqueaux, F., Sigler, A., Rhee, J. S., Brose, N., Enk, C., Reim, K. and Rosenmund, C. (2002). Total arrest of spontaneous and evoked synaptic transmission but normal synaptogenesis in the absence of Munc13-mediated vesicle priming. *Proc Natl Acad Sci U S A* **99**, 9037-42.

Vergara, R., Rick, C., Hernandez-Lopez, S., Laville, J. A., Guzman, J. N., Galarraga, E., Surmeier, D. J. and Bargas, J. (2003). Spontaneous voltage oscillations in striatal projection neurons in a rat corticostriatal slice. *J Physiol* **553**, 169-82.

Villacres, E. C., Wong, S. T., Chavkin, C. and Storm, D. R. (1998). Type I adenylyl cyclase mutant mice have impaired mossy fiber long-term potentiation. *J Neurosci* **18**, 3186-94.

Vogt, K. E. and Nicoll, R. A. (1999). Glutamate and gamma-aminobutyric acid mediate a heterosynaptic depression at mossy fiber synapses in the hippocampus. *Proc Natl Acad Sci U S A* **96**, 1118-22.

Walker, D. and De Waard, M. (1998). Subunit interaction sites in voltage-dependent Ca2+ channels: role in channel function. *Trends Neurosci* **21**, 148-54.

Walker, D. L. and Davis, M. (2002). The role of amygdala glutamate receptors in fear learning, fear-potentiated startle, and extinction. *Pharmacol Biochem Behav* **71**, 379-92.

Wang, H. and Storm, D. R. (2003). Calmodulin-regulated adenylyl cyclases: cross-talk and plasticity in the central nervous system. *Mol Pharmacol* **63**, 463-8.

Wang, M. C., Dolphin, A. and Kitmitto, A. (2004). L-type voltage-gated calcium channels: understanding function through structure. *FEBS Lett* **564**, 245-50.

Wang, Y., Liu, X., Biederer, T. and Sudhof, T. C. (2002). A family of RIM-binding proteins regulated by alternative splicing: Implications for the genesis of synaptic active zones. *Proc Natl Acad Sci U S A* **99**, 14464-9.

Wang, Y., Okamoto, M., Schmitz, F., Hofmann, K. and Sudhof, T. C. (1997). Rim is a putative Rab3 effector in regulating synaptic-vesicle fusion. *Nature* **388**, 593-8.

Wang, Y. and Sudhof, T. C. (2003). Genomic definition of RIM proteins: evolutionary amplification of a family of synaptic regulatory proteins(small star, filled). *Genomics* **81**, 126-37.

Wang, Y. T. and Linden, D. J. (2000). Expression of cerebellar long-term depression requires postsynaptic clathrin-mediated endocytosis. *Neuron* **25**, 635-47.

Washburn, M. S. and Moises, H. C. (1992). Electrophysiological and morphological properties of rat basolateral amygdaloid neurons in vitro. *J Neurosci* **12**, 4066-79.

Wayman, G. A., Impey, S., Wu, Z., Kindsvogel, W., Prichard, L. and Storm, D. R. (1994). Synergistic activation of the type I adenylyl cyclase by Ca2+ and Gs-coupled receptors in vivo. *J Biol Chem* **269**, 25400-5.

Weiskrantz, L. (1956). Behavioral changes associated with ablation of the amygdaloid complex in monkeys. *J Comp Physiol Psychol* **49**, 381-91.

Weisskopf, M. G., Bauer, E. P. and LeDoux, J. E. (1999). L-type voltage-gated calcium channels mediate NMDA-independent associative long-term potentiation at thalamic input synapses to the amygdala. *J Neurosci* **19**, 10512-9.

Weisskopf, M. G., Castillo, P. E., Zalutsky, R. A. and Nicoll, R. A. (1994). Mediation of hippocampal mossy fiber long-term potentiation by cyclic AMP. *Science* **265**, 1878-82.

Weisskopf, M. G. and Nicoll, R. A. (1995). Presynaptic changes during mossy fibre LTP revealed by NMDA receptor-mediated synaptic responses. *Nature* **376**, 256-9.

Westenbroek, R. E., Sakurai, T., Elliott, E. M., Hell, J. W., Starr, T. V., Snutch, T. P. and Catterall, W. A. (1995). Immunochemical identification and subcellular distribution of the alpha 1A subunits of brain calcium channels. *J Neurosci* **15**, 6403-18.

Whitlock, J. R., Heynen, A. J., Shuler, M. G. and Bear, M. F. (2006). Learning induces long-term potentiation in the hippocampus. *Science* **313**, 1093-7.

Wigstrom, H., Gustafsson, B., Huang, Y. Y. and Abraham, W. C. (1986). Hippocampal long-term potentiation is induced by pairing single afferent volleys with intracellularly injected depolarizing current pulses. *Acta Physiol Scand* **126**, 317-9.

Willoughby, D., Masada, N., Crossthwaite, A. J., Ciruela, A. and Cooper, D. M. (2005). Localized Na+/H+ exchanger 1 expression protects Ca2+-regulated adenylyl cyclases from changes in intracellular pH. *J Biol Chem* **280**, 30864-72.

Wilson, R. I. and Nicoll, R. A. (2001). Endogenous cannabinoids mediate retrograde signalling at hippocampal synapses. *Nature* **410**, 588-92.

Wong, S. T., Athos, J., Figueroa, X. A., Pineda, V. V., Schaefer, M. L., Chavkin, C. C., Muglia, L. J. and Storm, D. R. (1999). Calcium-stimulated adenylyl cyclase activity is critical for hippocampus-dependent long-term memory and late phase LTP. *Neuron* **23**, 787-98.

Wong, W. T. and Wong, R. O. (2000). Rapid dendritic movements during synapse formation and rearrangement. *Curr Opin Neurobiol* **10**, 118-24.

Woo, N. H., Duffy, S. N., Abel, T. and Nguyen, P. V. (2003). Temporal spacing of synaptic stimulation critically modulates the dependence of LTP on cyclic AMP-dependent protein kinase. *Hippocampus* **13**, 293-300.

Wu, L. G., Borst, J. G. and Sakmann, B. (1998). R-type Ca2+ currents evoke transmitter release at a rat central synapse. *Proc Natl Acad Sci U S A* **95**, 4720-5.

Yang, S. N., Tang, Y. G. and Zucker, R. S. (1999). Selective induction of LTP and LTD by postsynaptic [Ca2+]i elevation. *J Neurophysiol* **81**, 781-7.

Yao, J., Qi, J. and Chen, G. (2006). Actin-dependent activation of presynaptic silent synapses contributes to long-term synaptic plasticity in developing hippocampal neurons. *J Neurosci* **26**, 8137-47.

Yeckel, M. F., Kapur, A. and Johnston, D. (1999). Multiple forms of LTP in hippocampal CA3 neurons use a common postsynaptic mechanism. *Nat Neurosci* **2**, 625-33.

Yokoyama, C. T., Sheng, Z. H. and Catterall, W. A. (1997). Phosphorylation of the synaptic protein interaction site on N-type calcium channels inhibits interactions with SNARE proteins. *J Neurosci* **17**, 6929-38.

Yue, D. T., Herzig, S. and Marban, E. (1990). Beta-adrenergic stimulation of calcium channels occurs by potentiation of high-activity gating modes. *Proc Natl Acad Sci U S A* **87**, 753-7.

Yunker, A. M. and McEnery, M. W. (2003). Low-voltage-activated ("T-Type") calcium channels in review. *J Bioenerg Biomembr* **35**, 533-75.

Zakharenko, S. S., Patterson, S. L., Dragatsis, I., Zeitlin, S. O., Siegelbaum, S. A., Kandel, E. R. and Morozov, A. (2003). Presynaptic BDNF required for a presynaptic but not postsynaptic component of LTP at hippocampal CA1-CA3 synapses. *Neuron* **39**, 975-90.

Zakharenko, S. S., Zablow, L. and Siegelbaum, S. A. (2001). Visualization of changes in presynaptic function during long-term synaptic plasticity. *Nat Neurosci* **4**, 711-7.

Zalutsky, R. A. and Nicoll, R. A. (1990). Comparison of two forms of long-term potentiation in single hippocampal neurons. *Science* **248**, 1619-24.

Zamponi, G. W. (2003). Regulation of presynaptic calcium channels by synaptic proteins. *J Pharmacol Sci* **92**, 79-83.

Zamponi, G. W. and Snutch, T. P. (1998). Modulation of voltage-dependent calcium channels by G proteins. *Curr Opin Neurobiol* **8**, 351-6.

Zhao, J. P., Phillips, M. A. and Constantine-Paton, M. (2006). Long-term potentiation in the juvenile superior colliculus requires simultaneous activation of NMDA receptors and L-type Ca2+ channels and reflects addition of newly functional synapses. *J Neurosci* **26**, 12647-55.

Zhong, N. and Zucker, R. S. (2005). cAMP acts on exchange protein activated by cAMP/cAMP-regulated guanine nucleotide exchange protein to regulate transmitter release at the crayfish neuromuscular junction. *J Neurosci* **25**, 208-14.

Zhuravleva, S. O., Kostyuk, P. G. and Shuba, Y. M. (2001). Subtypes of low voltage-activated Ca2+ channels in laterodorsal thalamic neurons: possible localization and physiological roles. *Pflugers Arch* **441**, 832-9.

Ziv, N. E. and Garner, C. C. (2001). Principles of glutamatergic synapse formation: seeing the forest for the trees. *Curr Opin Neurobiol* **11**, 536-43.

Zucker, R. S. and Regehr, W. G. (2002). Short-term synaptic plasticity. *Annu Rev Physiol* **64**, 355-405.

Zuhlke, R. D., Pitt, G. S., Deisseroth, K., Tsien, R. W. and Reuter, H. (1999). Calmodulin supports both inactivation and facilitation of L-type calcium channels. *Nature* **399**, 159-62.

Elodie FOURCAUDOT
elodie.fourcaudot@fmi.ch

15 rue des glacières
67000 Strasbourg, France
+33-6-10-56-52-87

CURRICULUM VITÆ

Cursus :

2003 - 2007
PhD studies
- Faculté des sciences de la vie
  Université Louis Pasteur, Strasbourg, France
- Universität Basel, Switzerland

2002 - 2003
Diplôme d'Etudes Approfondies (fifth year diploma, master equivalent)
Neuroscience specialization
Faculté des sciences de la vie
Université Louis Pasteur, Strasbourg, France

2001 - 2002
Maîtrise de Biologie, Mention Biologie Cellulaire et Physiologie (fourth year diploma)
Physiology specialization
Options : Endocrinology and cellular neurobiology ; The brain
UFR Biologie et Sciences de la nature
Université Paris 7 - Denis Diderot, France

2000 - 2001
Licence de Biologie, Mention Biologie Cellulaire et Physiologie (third year diploma)
Physiology specialization
UFR Biologie et Sciences de la nature
Université Paris 7 - Denis Diderot
Mention : assez bien

1998 - 2000
DEUG de sciences de la vie (a two-year diploma)
UFR SNV (Sciences de la Nature et de la Vie)
Université Paris 7 - Denis Diderot

1997 - 1998
Baccalauréat série S (bachelor's degree, scientific series)
option : biology

Training courses :

july 2003 – december 2007
Laboratoire de Neurotransmission et Sécrétion Neuroendocrine – UPR 2356 – C. N. R. S. Strasbourg, France
Group leader : Bernard POULAIN
Friedrich Miescher Institute for Biomedical Research – Basel, Switzerland
Group leader : Andreas Lüthi
topic : Presynaptic mechanisms determining the dynamic range of neurotransmitter release in the Lateral Amygdala

septembre - july 2003
Laboratoire de Neurotransmission et Sécrétion Neuroendocrine – UPR 2356 – C.N.R.S Strasbourg
Frédéric DOUSSAU, Jean-Louis Bossu group leader : Bernard POULAIN
topic :

june - august 2001
Laboratoire de biologie cellulaire de la Synapse Normale et Pathologique – INSERM U 497 – E. N. S. Ulm, Paris, France
Sheela VYAS group leader : Antoine TRILLER
topic :Role of synaptic adhesion molecules in the life and death of neurons

june - july 1999
Institut Alfred Fessard - C . N . R . S . Gif sur Yvette, France
Eduardo DOMINGUEZ DEL TORO group leader : Jean CHAMPAGNAT
topic : study of the postnatal comportment of Kreisler -/- mutant mice

Articles :

L-type voltage-dependent Ca^{2+} channels mediate expression of RIM1α-dependent presynaptic LTP in amygdala
Fourcaudot E, Humeau Y, Casassus G, Poulain B, Lüthi A
The cerebellum 2006, vol 5, p. 243-256

Synaptic organization of the mouse cerebellar cortex in organotypic slice cultures
Dupont JL, Fourcaudot E, Beekenkamp H, Poulain B, Bossu JL
The cerebellum 2006, vol 5, p. 243-256

Dendritic spine heterogeneity determines afferent-specific Hebbian plasticity in the amygdala
Humeau Y, Herry C, Kemp N, Shaban H, Fourcaudot E, Bissiere S, Lüthi A
Neuron 2005, vol 45, p. 119-131

Talks :

December 2007 (Strasbourg, France): PhD defense
Presynaptic Mechanisms Determining the Dynamic Range of Neurotransmitter Release in the Lateral Amygdala

September 2007 (Grindelwald, Switzerland): FMI annual meeting
Presynaptic Mechanisms of Long-Term Synaptic Plasticity in the Amygdala

May 2006 (Giessbach, Switzerland)
Mechanisms of Presynaptic LTP at Cortico-Amygdala Afferents

January 2006 (Strasbourg, France)
Presynaptic Hebbian and Non-Hebbian Plasticities

Current research :

The amygdala is a central brain structure receiving sensory information from diverse regions of the central nervous system. Cortical and thalamic axons converge to the lateral amygdala (LA) which is thought to be the main site for fear-induced plasticity and associative learning. Several years ago, a new form of presynaptic long-term potentiation (LTP) was identified at the cortico-LA synapse. This heterosynaptic associative LTP (LTP_{HA}) is triggered by the activation of presynaptic NMDA receptors (NMDAR) at cortical presynaptic terminals, with the request of thalamic activation. However, nothing was known so far on the molecular mechanism involved. During my thesis, I could show that LTP_{HA} is mediated by an increase in the probability of vesicular release. Downstream to NMDAR opening, the activation of the adenylyl cyclase (AC) / protein kinase A (PKA) pathway recruits the synaptic protein Rim1α. The L-type voltage-dependent calcium channels (VDCCs) are also necessary for LTP_{HA} expression. The activation of PKA and the functional interaction between Rim1α and L-type VDCCs appear to be essential for the expression of presynaptic LTP, but could also play a role for baseline synaptic transmission in the amygdala.

The amygdala is a central brain structure receiving sensory information from diverse regions of the central nervous system. Cortical and thalamic axons converge to the lateral amygdala (LA) which is thought to be the main site for fear-induced plasticity and associative learning. Several years ago, a new form of presynaptic long-term potentiation (LTP) was identified at the cortico-LA synapse. This heterosynaptic associative LTP (LTP_{HA}) is triggered by the activation of presynaptic NMDA receptors (NMDAR) at cortical presynaptic terminals, with the request of thalamic activation. However, nothing was known so far on the molecular mechanism involved. During my thesis, I could show that LTP_{HA} is mediated by an increase in the probability of vesicular release. Downstream to NMDAR opening, the activation of the adenylyl cyclase (AC) / protein kinase A (PKA) pathway recruits the synaptic protein Rim1α. The L-type voltage-dependent calcium channels (VDCCs) are also necessary for LTP_{HA} expression. The activation of PKA and the functional interaction between Rim1α and L-type VDCCs appear to be essential for the expression of presynaptic LTP, but could also play a role for baseline synaptic transmission in the amygdala.

L'amygdale est une structure centrale recevant des informations sensorielles issues de diverses régions du système nerveux central. Des axones corticaux et thalamiques convergent au niveau de l'amygdale latérale (LA), qui est considérée comme étant le principal site de la plasticité et de l'apprentissage associatif induits par la peur. Une nouvelle forme de potentiation à long-terme (LTP) a été identifiée il y a quelques années à la synapse cortico-LA. Cette LTP hétérosynaptique et associative (LTP_{HA}) est déclenchée par l'activation de récepteurs NMDA présents au niveau des terminaisons corticales présynaptiques, cette activation nécessitant l'activation des fibres thalamiques. Pourtant, le mécanisme moléculaire impliqué n'était jusqu'à présent pas connu. Au cours de mon travail de thèse, j'ai pu montrer que la LTP_{HA} est médiée par une augmentation de la probabilité de libération vésiculaire. En aval de l'ouverture des récepteurs NMDA, l'activation de la voie adenylyl cyclase / protéine kinase A induit le recrutement de la protéine synaptique Rim1α. Les canaux calciques dépendents du voltage de type L (VDCCs de type L) sont également nécessaires à l'expression de la LTP_{HA}. L'activation de la PKA et une interaction fonctionnelle entre Rim1α et les VDCCs de type L semblent essentiels à l'expression de la LTP présynaptique, et ils pourraient également intervenir dans la transmission synaptique basale de l'amygdale.